36)

PHYSICO-CHEMICAL SPECIATION AND OCEAN FLUXES OF POLYCYCLIC AROMATIC HYDROCARBONS

by

ÖRJAN GUSTAFSSON

B.S. Chemistry, Slippery Rock University
(1990)

submitted in partial fullfillment of the requirements for the degree of

Doctor of Philosophy

at the

MASSACHUSETTS INSTITUTE OF TECHNOLOGY

and the

WOODS HOLE OCEANOGRAPHIC INSTITUTION

February 1997

©Massachusetts Institute of Technology 1997
All rights reserved

*Signature of Author*________________________________
Joint Program in Oceanography,
Massachusetts Institute of Tehnology,
Woods Hole Oceanographic Institution

*Certified by*________________________________
Dr. **Ken O. Buesseler**
Thesis co-supervisor

Dr. **Philip M. Gschwend**
Thesis co-supervisor

*Accepted by*________________________________
Dr. **Ed Boyle**, chair,
Joint Committee for Chemical Oceanography
Massachusetts Institute of Technology/
Woods Hole Oceanographic Institution

MASSACHUSETTS INSTITUTE
OF TECHNOLOGY

JAN 13 1997

LIBRARIES

Physico-Chemical Speciation and Ocean Fluxes of Polycyclic Aromatic Hydrocarbons

by

Örjan Gustafsson

Submitted to the Joint Committee for Chemical Oceanography, Massachusetts Institute of Technology and Woods Hole Oceanographic Institution, on January 13, 1997 in Partial Fulfillment of the Requirements for the Degree of Doctor of Philosophy in Oceanography

ABSTRACT

Partitioning of ecotoxicologically significant polycyclic aromatic hydrocarbons (PAHs) to non-aqueous, particularly colloidal and soot, phases results in a decrease in their, directly bioavailable, dissolved fractions. Functionally defining colloidal sorbents as *any constituents that provide a molecular milieu into and onto which chemicals can escape from the aqueous solution, and whose movement is not significantly affected by gravitational settling*, implies that not all macromolecules can act as sorbents, and thus, the colloidal sorbent pool can never be accurately isolated by any size-based filtration. Less invasive time-resolved fluorescence quenching was employed to directly quantify the ability of seawater colloids to bind methylperylene as a probe PAH. Extrapolation of these initial results to other PAHs through linear free energy relationships suggested that coastal colloids are a factor of five less good sorbents, on an organic-carbon basis, than sedimentary organic matter.

The hypothesis that soot may cause the elevated *in situ* PAH solid-water distribution coefficients was tested with development of an analytical technique quantifying the minor portion of sedimentary carbon that is pyrogenic. The spatial distributions of phenanthrene, pyrene, and benzo[a]pyrene concentrations in continental shelf surface sediments could be explained with the soot carbon concentrations ($r^2 = 0.97\text{-}0.99$) while they were not correlated with non-soot organic carbon at the 95% confidence level. Theoretically estimated soot-water partition coefficients, assuming sorbate-soot interaction is thermodynamically similar to sorbate fusion, agreed with published aqueous sorption coefficients to activated carbon, suggesting a soot sorption strength that, on a carbon basis, was a factor of 100 greater than for non-soot organic matter. Exponentially decreasing surface ocean fluxes of PAHs away from northeastern USA was demonstrated using ^{238}U-^{234}Th disequilibria. The first estimate of the annual flux of a PAH, pyrene, into the western North Atlantic corresponds to about 50% of the pyrene emissions from the coastal states in northeastern USA. Finally, insights about physico-chemical speciation and vertical fluxes were combined with estimates of horizontal dispersion and local PAH source functions in a box model for Portland Harbor, Casco Bay. As much benzo[a]pyrene as is locally deposited may be exported offshore.

Thesis Co-Supervisors:
Philip Gschwend, Professor of Civil and Environmental Engineering, MIT
Ken Buesseler, Research Scientist in Marine Chemistry and Geochemistry, WHOI

Acknowledgments

Numerous persons have contributed to the development of this thesis and its author. I am deeply grateful to my thesis co-advisors, Ken Buesseler and Phil Gschwend, for providing me innumerable professional experiences and a highly stimulating graduate career with the perfect balance between intellectual freedom and critical advise. Their scientific insights and constant enthusiasm and support is the solid foundation upon which this thesis is built. Brad Moran and John Farrington, members of the thesis committee, both provided challenging and constructive comments during many discussions. John Farrington is especially recognized for his contagious enthusiasm, for providing inspiring historical perspectives and scientific insights that kept the project well-oriented, and for fascilitating many professional contacts.

I am extremely fortunate, as a joint program student working at both institutions, to have had the opportunity to interact with scientists, colleagues, and friends in both Woods Hole and at MIT. The unique scientific community of WHOI has been inspiring and welcoming on every singly trip. The Parsons Lab family at MIT has been a productive and comfortable working environment. At WHOI, Tim and Lorraine Eglinton made sure I was off to a good start both scientifically and socially and have been supportive throughout my stay. Bill Martin kindly shared his insights while providing a summer-project in early sediment diagenesis, during which Alan Fleer and Mike Bacon provided advise and lab-space for radionuclide purification and analysis. The Café Thorium has constituted a welcoming, productive, cheerful and open-minded WHOI home-base. I am indebted to Hugh Livingston, John E Andrews III, Mary Hartman, Becky Belastock, and Larry Ball for their interest and constant willingness to lend a hand. The Fye lab has been equally welcoming and the site of many enlightening discussions with Jim Moffett, Tim Eglinton, Ed Sholkovitz, Neil Blough, Carl Johnson and other scientists. Many fellow joint program students and post-docs have provided a stimulating intellectual environment. In particular, inspiring discussions with Julian Sachs, Jean LéCorre, Kathy Barbeau, Anya Waite, and Melissa Bowen have both provided a broader perspective as well as helped me in thinking about the specific behavior of chemicals in the ocean.

At MIT, I have been fortunate to be a part of a dynamic research group consisting of people with quite varying expertise. To all Gschwendites (past and present) I am forever grateful for innumerable moments of sharing in plumbing advise, gas tanks and glassware loans, tons of frustration interspersed with some brief instances of success, laughs during hard and late work, and joint brainstorming sessions. I am particularly indebted to lab guru John MacFarlane, without whose broad technical expertise all of these exercises would have been so much harder to perform. Britt Holmén and Allison Mackay have been extremely good colleagues throughout, very helpful with technical details as well as providing many insightful discussions on the intricacies of sorption. Tom Ravens, Chris Swartz, Lukas Wick and many others have also shared their specific knowledge and friendship during these years. Many others at MIT and beyond, including François Morel, Mike Ernst, John Durant, John Hedges, Bob Eganhouse, Shige Takada, Johan Axelman, and Dag Broman have contributed with critical discussions on specific topics of this thesis. MIT enlarge, and Parsons lab in particular, has not only been an extremely interesting and productive place to conduct this graduate research, but has also provided a quite friendly environment. Hydros' soccer, table tennis, and water polo teams, as well as the Swedish unihoc league, have prevented me from developing the shape of an Erlenmeyer flask.

My mother Margareta, father Bernt, and sister Annika have always supported my endeavors while keeping me informed about the "home-front". Jonas and Marie have remained fantastic friends in spite of a decade of living on opposite sides of the ocean. The Hotchkiss family has been a great support for the past ten years. The "Scandinavian-Bostonian colony" has provided a rejuvenating source of strength on many joyous occasions. Finally, I thank my Cambridge housemates Robert Bock, Fernando Hesse, Tonya Putnam, and Hanspeter Pfister for years of friendship, provocative conversation, and liberal balance which have helped keep my view of the world somewhat in perspective.

Research funding has been provided by the Office of Naval Research, National Oceanic and Atmospheric Administration, the Environmental Protection Agency, the National Insititute of Environmental Health Sciences, and the Massachusetts Water Resources Administration. Acknowledgments of assistance with specific projects are given at the end of each chapter.

Table of Contents

Abstract 3
Acknowledgments 4
Table of Contents 6
List of Figures 11
List of Tables 14
Chapter One: General introduction 17
    Marine environmental organic chemistry 17
    PAHs in the ocean: Properties and anticipated behavior 19
    Previous work on the marine chemistry of PAHs 25
    Organization and contributions of this thesis 26
    References 28

Chapter Two: Aquatic colloids: Concepts, definitions, and current challenges 31
    Abstract 32
    Historical perspective 34
    Functional definition of aquatic colloids 41
    Delimiting the dissolved-colloidal boundary 44
    Delimiting colloidal from gravitoidal phases 45
    Illustrations of chem-centric phase speciation 47
    Conclusions and current challenges 54
    Acknowledgments 56
    References 57

Chapter Three: On the integrity of cross-flow filtration for collecting marine organic colloids 63
    Abstract 64
    Introduction 65
    Methods 68
    Results and discussion 79
        Blank and recovery assessment 79
        Colloid-membrane associations 83

Size cut-off....................97
CFF systems intercalibration....................101
Organic colloids in coastal Massachusetts sea water....................101
Use of CFF to assess HOCs....................110
Conclusions and recommendations....................110
Acknowledgments....................116
References....................117

Chapter Four: Time-resolved fluorescence quenching to quantify the ability of seawater colloids to bind hydrophobic compounds....................125
Introduction....................125
Experimental section....................129
Chemicals and solutions....................129
Ancillary measurements....................130
Fluorescence instrument....................130
Analog and photon-counting detection of steady state fluorescence....................131
Phase and modulation fluorescence lifetimes....................132
Factors that may influence the interpretation of fluorescence results....................133
Results and discussion....................134
Fluorescence of methylperylene and seawater....................134
Minimization of photodecomposition....................140
Quartz-wall sorption and fluorescence quenching....................146
Fluorescence lifetimes....................150
Colloid-water equilibrium partition coefficients....................164
References....................169

Chapter Five: Quantification of the dilute sedimentary soot-phase: Implications for PAH speciation and bioavailability....................173
Abstract....................174
Introduction....................174
Experimental section....................178
Background....................178
Removal of OC....................179

Removal of IC.. 180
CHN elemental analysis.. 180
Elucidation of optimal combustion temperature 181
Method testing with well-characterized matrices 181
Method application to natural sediments.. 182
Results and discussion 182
    Optimization of temperature conditions for SC-OC separation 182
    Method testing with well-characterized matrices 185
    Application to natural samples... 189
        Mystic Lake.. 189
        Boston Harbor.. 190
Acknowledgments 197
References 198

Chapter Six: Soot as a strong partition medium for planar aromatic molecules in aquatic system 201
    Abstract.. 202
    Introduction.. 202
    Methods 207
        Sediment sampling.. 207
        Quantification of sedimentary total organic and soot carbon............. 207
        Quantification of sedimentary PAHs.. 207
    Results and discussion 210
        Source-diagnostic PAH ratios.. 210
        The sedimentary distribution of organic and soot carbon 210
        Regression of PAHs with OC and SC... 211
        Physico-chemical properties of soot... 216
        Soot particles - formation and physical properties 216
        Soot particles - chemical properties... 217
        Soot-water partitioning of PAHs... 218
        Estimation of PAH soot-water partitioning 219
        Conclusions.. 223
        Acknowledgments 224

Literature cited 226

Chapter Seven: Using ^{234}Th disequilibria to estimate the vertical removal rates of polycyclic aromatic hydrocarbons from the surface ocean 231
Abstract 232
1. Introduction 232
2. Methods 234
2.1 HOC sampling and analysis 234
2.2 ^{234}Th and ^{238}U sampling and analysis 236
3. Results and discussion 237
3.1 Spatial trends in concentrations of PAHs, ^{234}Th, and ancillaries 237
3.2 PAH fluxes 238
3.3 Residence times of HOCs in the surface ocean 245
3.4 Global PAH mass balances 250
4. Conclusions 254
Acknowledgments 254
References 256

Chapter Eight: On the relative importance of horizontal and vertical transport of particle-reactive chemicals in the coastal ocean: Two-dimensional Th-234 modeling 263
Abstract 264
Introduction 265
Materials and methods 267
a. Sampling 267
b. Seawater ^{234}Th determination 270
c. Seawater ^{238}U determination 271
d. Sediment radionuclides determination 271
e. Estimation of horizontal transport parameters 272
Water column results 273
a. Seawater ^{234}Th 273
b. Seawater ^{238}U 275
Two-dimensional modeling of thorium-234 275
Sedimentary record of horizontal transport 282

Two-dimensional contaminant transport model 285
Conclusions 289
Acknowledgments 293
Appendix A: Scaling expression for tidal dispersion coefficients 294
References 295

Chapter Nine: Thesis distillation and a look to the future 303
General conclusions 303
Future work 305
References 308

List of Figures

Chapter One

fig. 1 Processes affecting the fate of PAHs in marine ecosystems................23

Chapter Two

fig. 1 Observed distributions between filter-retained and filter-passing ^{234}Th in marine surface waters of varying filter-collected solids concentrations...........39

fig. 2 Hypothetical curves of the distribution of solid mass among different particle size classes 43

fig. 3 Chem-centric speciation diagram 49

fig. 4 Effects of the chem-centric speciation on transformations of chemicals ..53

Chapter Three

fig. 1 Hydraulic permeate flux during marine CFF sampling 71

fig. 2 Schematic of the HOC/colloid size-fractionating sampling system 75

fig. 3 Organic carbon blank of CFF during both one-pass flushing and sampling mode cleaning 81

fig. 4 CFF integrity experiment with standard 3 kD DEXTRAN colloid 85

fig. 5 Recirculation-mode CFF integrity experiment with standard 10 kD DEXTRAN colloid 87

fig. 6 Batch membrane sorption experiment..89

fig. 7 Sampling-mode CFF integrity experiment with 70 kD DEXTRAN.......95

fig. 8 Recirculation-mode CFF integrity experiment with standard 70 kD DEXTRAN colloid 99

fig. 9 Size cut-off calibration curve for seawater colloids on Osmonics CFF membrane with a "1.0 kD" nominal cut-off 103

fig. 10 CFF organic carbon fractionation of coastal Massachusetts seawater ...109

fig. 11 Recirculation-mode CFF solute integrity experiment.....................113

Chapter Four

fig. 1 Corrected and blank-subtracted fluorescence emission spectra of methylperylene...137

fig. 2 Corrected fluorescence emission spectrum of Casco Bay seawater 139
fig. 3 Methylperylene photobleaching 143
fig. 4 Fluorescence quenching experiments of methylperylene sorption 149
fig. 5 Frequency spectrum of phase-shift and demodulation factors of methylperylene in artificial seawater 153
fig. 6 Phase and modulation based estimates of the average fluorescence lifetime at 2-200 MHz modulation frequencies of methylperylene in artificial seawater..... 157
fig. 7 Frequency spectrum of phase-shift and demodulation factors of filtered coastal seawater irradiated at 406 nm with a KV418 high band-pass emission filter..... 159
fig. 8 Phase and modulation based estimates of the average fluorescence lifetime at 2-200 MHz modulation frequencies of filtered coastal seawater irradiated at 406 nm with a 418KV high band-pass emission filter 161
fig. 9 Frequency spectrum of phase-shift and demodulation factors of methylperylene equilibrated with filtered coastal seawater......................... 163

Chapter Five

fig. 1 A. *In situ* PAH K_{oc}'s observed in several different types of environmental regimes. B. Calculated activated-carbon partition coefficients (K_{ac}) for a range of PAHs 177
fig. 2 Recoveries of soot C and humic acid organic C as a function of increasing oxidation temperature 187
fig. 3 Upper Mystic Lake profiles of (A) PAHs, and (B) soot carbon and organic carbon 193

Chapter Six

fig. 1 Enhanced organic-carbon normalized *in situ* partition coefficients $(K_{oc})_{obs}$ for PAHs observed in diverse environmental regimes 205
fig. 2 Locations of sediment sampling stations in the Gulf of Maine 209
fig. 3 PAH source-diagnostic ratios 213
fig. 4 Regressions between sedimentary concentrations of benzo[a]pyrene with organic carbon and soot carbon 215

Chapter Seven

fig. 1 Surface-ocean fluxes and area-integrated mass removal rates of PAHs...243
fig. 2 Literature-collated ocean pyrene fluxes 249
fig. 3 Receptor-based estimates of total pyrene and benzo[a]pyrene import to NW Atlantic Ocean 253

Chapter Eight

fig. 1 Map showing Gulf of Maine sampling stations...............................269
fig. 2 Comparison of the one- and two-dimensional model estimates of ^{234}Th scavenging flux 281
fig. 3 Two-dimensional box-models of pyrene and benzo[a]pyrene in Portland Harbor, Casco Bay 291

List of Tables

Chapter Three

Table 1 Comparison of equilibrium loss factors, retention coefficients, and e-folding times of standard colloids in CFF recirculation experiments 93
Table 2 Intercalibration of 1.0 kD nominal cut-off polysulfone membrane CFF systems 105

Chapter Four

Table 1 Photodegradation of methylperylene from a 300W Xe lamp 145
Table 2 Predicted PAH organic colloid - water partition coefficients 167

Chapter Five

Table 1 Results of testing the soot carbon method with matrices of known composition 183
Table 2 Different PAH partitioning models applied to Boston harbor sediments 195

Chapter Six

Table 1 Organic and soot carbon concentrations in Gulf of Maine sediments ... 211
Table 2 Correlations of PAHs with OC and SC in surface sediments 216
Table 3 Comparison of estimated K_{sw} with $K_{ac\text{-}w\text{-}}$ and K_{oc} values 223

Chapter Seven

Table 1 Concentrations of PAHs, ^{234}Th, ^{238}U, and POC in upper ocean regimes 239
Table 2 Estimated upper ocean fluxes of three PAHs in increasing hydrophobicity 241
Table 3 Comparison of vertical pyrene fluxes with literature reports 246
Table 4 Studies contributing pyrene flux data shown in figure 2 247

Chapter Eight

Table 1 Sampling dates, locations, surface water ancillary and radioisotope data 274
Table 2 Estimates and measurements of ^{238}U (dpm/kg) in size-fractionated Casco

Bay surface waters 276
Table 3 Two-dimensional box model of Casco Bay..................................278
Table 4 Sediment inventories, atmospheric and water-column sources of $^{210}Pb_{xs}$, ^{7}Be, and $^{234}Th_{xs}$ in the Gulf of Maine..284

Chapter 1

General Introduction

In many industrialized countries, the anthropogenic energy flow per unit area is ten times larger than the biotic, photosynthetic, energy flux (Stumm *et al.*, 1983). The related material flow, in particular the past several decades' exponential increases in production volumes of synthetic organic matter and combustion of fossil fuels, is leading to the introduction of many new, and unforeseen levels of "old", xenobiotic chemicals to the natural environment. These anthropogenic processes, deemed necessary for upholding our civilization and culture, are affecting the health of many organisms, notably humans, as well as the balance of whole ecosystems. It is one fundamental objective of environmental geochemistry to provide the basic understanding of the processes that govern the fates and effects of anthropogenic chemicals in order to optimize protection of human and ecosystem health. The goal of this thesis was to develop and test general concepts about the environmental behavior, specifically bioavailability and ocean fluxes, of a contaminant class of particularly high ecotoxicological significance, polycyclic aromatic hydrocarbons (PAHs). This general introduction will attempt to briefly outline the conceptual history and framework of environmental organic chemistry, with particular emphasis on PAHs in marine systems, as well as how this thesis contributes to the current state of the field.

Marine environmental organic chemistry

A growing awareness of adverse biological effects of many anthropogenic (mostly organic) chemicals have propelled "environmental problems" to a top priority of societies' agenda and have triggered the tremendous development seen in environmental organic chemistry over the past two decades. Effects of environmental contaminants range from highly visible and accute incidents (e.g., dead seabirds on beaches after accidental oil spills) to chronic toxic effects on specific organisms (e.g., elevated cancer rates in certain fish) to more subtle long-term impacts on whole ecosystems (e.g., changes in species composition). Widely publicized events such as the Exxon Valdez oil spill are, in spite of the local tragedies, limited in frequency, spatial impacts, and often transient with time (e.g., Wolfe *et al.*, 1994). The past ten years have witnessed many cases where adverse effects on individual species of marine organisms have been linked to specific organic pollutants. For example, physiological dysfunctions of some cetaceans are believed to be triggered by organochlorines such as polychlorinated biphenyls (PCBs) and dibenzo-p-dioxins (PCDDs) (e.g., Tanabe and Tatsukawa, 1992).

There has been less progress in assessing multi-species and multi-contaminant ecosystem-wide impacts of marine pollution; this is likely in part a result of the prohibitive complexity of evaluating intra- and inter-species interactions. However, given that marginal competitive advantages often control the species composition of an ecosystem (e.g., Tinbergen, 1970), an organism may be replaced and ecosystem balance shifted, in the presence of apparently trivial (but toxic) levels of a contaminant if the species is the most sensitive of the competitors. In addition to toxic effects, xenobiotic organic chemicals may interfere with other sociobiological life-support systems. For example, the presence of anthropogenic hydrocarbons in seawater interferes with chemotactic communication between certain algae (e.g., Derenbach and Gereck, 1980). In addition to the difficulty imposed by ecosystem complexity, another reason why environmental organic chemistry has not yet made larger strides in open ocean systems is the analytical challenge of accurately measuring *in situ* concentrations in specific reservoirs (e.g., DeLappe *et al.*, 1983, Farrington and Westall, 1986). Recently however, some reports of open ocean concentrations of PAHs obtained with "trace-organic clean" techniques (Petrick *et al.*, 1996; this thesis- chapter 7) raises some hope for our readiness to now embark on this line of research.

To rationally evaluate the risk of any anthropogenic organic chemical causing an adverse impact on marine systems, we need to develop general concepts about the compound-specific behavior under changing environmental conditions. Historically, there have been many reports on the identification and concentration of chemicals at various locations. Such monitoring yields only limited useful information for decribing the chemicals' fates and effects. Instead process-oriented studies on molecular-level interactions and macroscopic transport phenomena should be empasized (Blumer, 1975; Stumm *et al.*, 1983; Farrington and Westall, 1986; Gschwend and Schwarzenbach, 1992). To quantitatively describe, and *a priori* predict, the key transport and transformation processes, as well as the ultimate distribution and residual concentration (fugacity or activity), one requires in addition to a source function, a physico-chemical description of the system. Depending on the identity of the particular chemical, such a general assessment requires information about certain compound-specific properties (e.g., aqueous solubility, vapor pressure, octanol-water partition constant, Henry's law constant, acid dissociation constant, photolytic, chemical, and biological degradability) as well as certain environment-specific properties (e.g., temperature, salinity, particle composition, concentration, and settling rate, hydraulic advection and diffusion rates, light intensity, E_H, and pH). Such knowledge can greatly improve our ability to understand natural processes occuring in the ocean and to predict the distribution of organic chemicals on both the molecular and the macroscopic levels as illustrated in Gschwend and Schwarzenbach (1992) and more comprehensively in Schwarzenbach *et al.* (1993). Once sufficient understanding of anticipated key processes enables prediction of a chemical's distribution, it is of utmost importance that field measurements of its actual distribution and transport rates be performed in order to verify, and potentially revise, the model.

PAHs in the ocean: Properties and anticipated behavior

PAHs may be the class of anthropogenic compounds that are of highest ecotoxicological significance in aquatic systems, and this family of compounds have been the most intensely studied by marine environmental chemists. Yet, current distribution models are unable to correctly anticipate their *in situ* phase-distributions within an order of magnitude. In addition, no models exist to anticipate quantitatively their spatially varying fluxes and residence times in the ocean. The central role occupied by PAHs in chemical carcinogenesis is illustrated by the historical span and intensity of PAH research. In fact, the very first chemicals recognized as carcinogens were soot-assoicated PAHs (NAS, 1972). This discovery was made by the British physician Percival Pott in 1776, when he attributed the high incidence of scrotum cancer in chimney sweeps of London to their continual contact with PAH-carrying soot (NAS, 1972). Recently, modern DNA techniques with nucleotide resolution have revealed that the binding positions of benzo[a]pyrene diol epoxide adducts are the same as the major mutational loci in human lung cancer (Denissenko *et al.*, 1996), thus, providing a direct etiological link between a defined chemical carcinogen (a PAH) and human cancer.

Adverse effects of carcinogenic PAHs in environmental systems have similarly attracted concern for a long time (e.g., NAS, 1972, NRC, 1985, EPA, 1985, 1993). In fact, PAHs have been identified as the principal human cell mutagens in lipid extracts of natural sediments, not specifically or unusually contamined by PAHs (Durant *et al.*, 1994). Furthermore, in contrast to some other important contaminants (e.g., PCBs), large amounts of PAHs continue to be produced and released into the environment, primarily from combustion of fossil and wood fuel, but also from direct petroleum spills. These anthropogenic sources are overwhelming any natural sources such as forest fires and natural oil-seepages (e.g., Grimmer and Böhnke, 1975; Hites *et al.*, 1980; this thesis - Ch. 5-7).

An advantage of studying the environmental behavior of PAHs is that the post-sampling analytical methodology is well developed (e.g., see references in Ch. 7) and, many of their physico-chemical properties have been determined (e.g., summarized in Schwarzenbach *et al.*, 1993, p. 621). Following introduction to the ocean via atmospheric deposition, runoff, and/or spills, and given information of their compound-specific properties, we may start to anticipate some key behaviors affecting the spatial and temporal distribution of PAH concentrations (i.e., exposures) in the marine environment (Fig. 1). For PAHs and many other xenobiotic chemicals that are hydrophobic (the aqueous solubilities of 3-5 ringed PAHs are in the range of $10^{-4.5}$ - $10^{-6.5}$ M; from Schwarzenbach *et al.*, 1993, p. 621), one important process is the partitioning between dissolved and particle-bound pools. The resulting physico-chemical speciation affects the extent to which a given chemical may participate in any other transport and transformation processes. In the simplest sense, one may anticipate that there are truly dissolved molecules that may participate in homogeneous phase reactions (chemical, photochemical, and biochemical), while their counterparts sorbed to colloids and gravitoids (i.e., settling particles; Ch. 2) behave differently (e.g., are not so readily biodegraded; Guerin and Boyd, 1992, and may be differently amenable to photodegradation - Ch. 2). Similarly for transport, one may anticipate that dissolved and colloid-bound molecules are carried with the moving fluid while the gravitoid-bound fraction is removed vertically to a greater extent. Hence, one primary goal must be to assess the distribution between truly dissolved and sorbed to detrital and "living" (e.g., phytoplankton) particles of varying transport behavior (Fig. 1). Organic-matter based hydrophobic partition models (e.g., Karickhoff *et al.*, 1979; Chiou *et al.*, 1979) provide a starting point for evaluating the solid-solution distribution of hydrophobic organic compounds (HOCs):

$$K_d = f_{oc} \, K_{oc} \qquad (1)$$

Figure 1. Processes affecting the fate of PAHs in marine ecosystems.

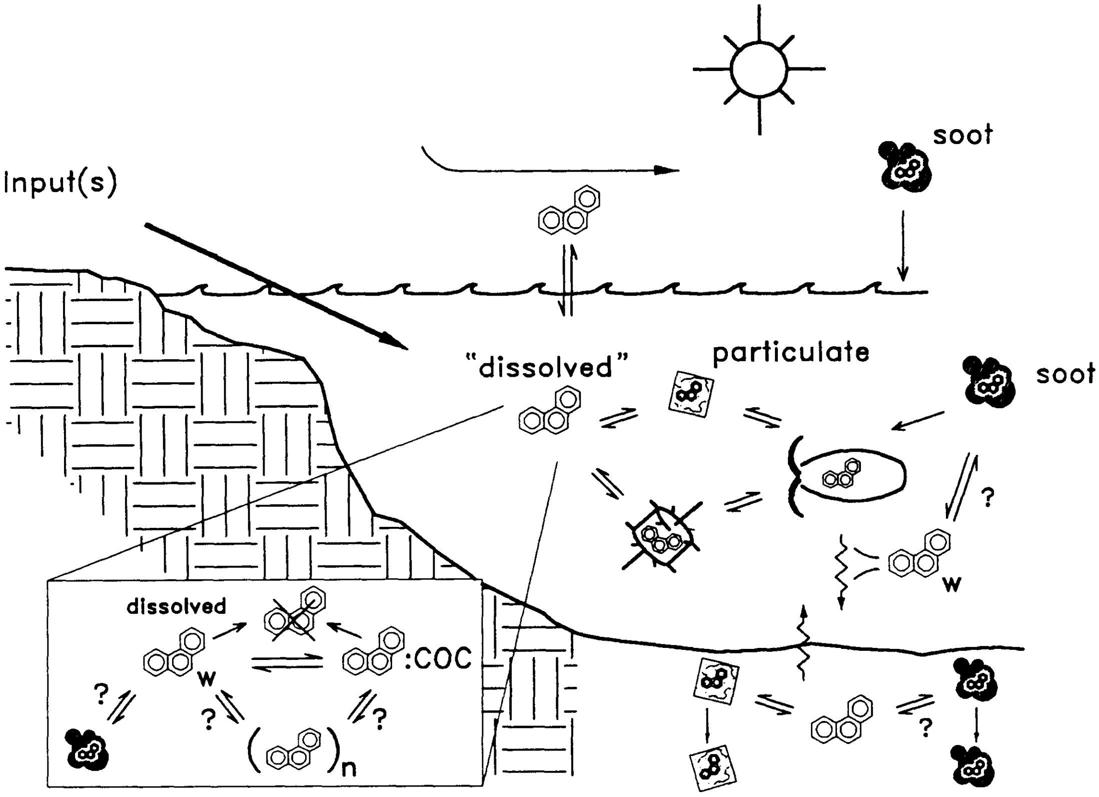
soot
Input(s)
"dissolved"
particulate
soot
?
w
dissolved
w
:COC
?
?
?
n
?

where K_d is the solid-solution distribution coefficient (mol kg^{-1} particles (mol L^{-1} water)$^{-1}$)), f_{oc} is the organic carbon fraction of the particles, and K_{oc} is the organic-carbon normalized solid-solution distribution coefficient (mol kg^{-1} particulate organic carbon (mol L^{-1} water)$^{-1}$)). f_{oc} is obviously an environment-specific property, whereas K_{oc} has been shown to be related through linear free energy relationships with such compound-specific properties as aqueous solubility (e.g., Karickhoff *et al.*, 1981). Hence, for the common PAH, benzo[a]pyrene (log K_{oc} of about 6.3; Karickhoff *et al.*, 1981), and typical coastal water levels of particulate organic carbon (POC; ≥ *ca* 0.7 µm) of 200 ug/L (17 uM carbon), this model predicts that twice as much of this compound is truly dissolved as is associated with filterable particles. The presence of filter-passing colloidal sorbents in seawater are also well known (e.g., Means and Wijayaratne, 1982, Whitehouse, 1985; Brownawell and Farrington, 1986; Chin and Gschwend, 1992). If we in a first order estimate may assume that a third of the filter-passing organic carbon (i.e., "DOC") is colloidal in nature (Whitehouse, 1985) and that its sorptivity on a carbon-basis is similar to other natural organic matter, then for a typical coastal seawater DOC of 2 mg/L (170 uM carbon), one would anticipate that 80% of the filter-passing benzo[a]pyrene, is associated with colloids. Such a scenario would significantly affect the prediction of toxicological exposure since it is believed that it is only the truly dissolved fraction that is available for direct biological uptake (e.g., Leversee *et al.*, 1983; McElroy *et al.*, 1989).

To anticipate doses of toxic compounds, information is required, not only bioavailable concentrations but also, on time of exposure. In order to understand and predict the longevity of PAHs in sensitive ecosystems such as the surface ocean, information is required on the fluxes of these contaminants through this reservoir. Hence, for sorptive chemicals such as PAHs, we need to quantify the particle-sorbent settling rates. One promising approach in this regard is the coupling of particle-bound concentrations with the surface water disequilibria between ^{238}U and highly particle-reactive ^{234}Th, as a measure of vertical particle export. Such flux estimates have been demonstrated for POC (e.g., Buesseler *et al.*, 1992) and seem applicable also to quantification of HOC fluxes.

Several other aspects of PAH behavior also need to be elucidated, such as the kinetics of seawater partitioning, in particular with "living" and combustion particles (Fig. 1). Sediment-water exchange and redistribution may significantly affect the water-column PAH concentrations, as may phase-specific photochemical reactions of these molecules of high electronic densities.

Previous work on the marine chemistry of PAHs

Polycyclic aromatic hydrocarbons have been studied in the environment for half a century (Kern, 1947). Numerous studies have reported concentrations of individual PAH compounds in sediments and several studies have assessed the spatial and historical pattern of sediment concentrations (summarized in Ch. 5-6). Such information has been useful in constraining the dominant sources of PAHs in modern regimes (fuel combustion) as well as realizing the recalcitrancy of these compounds in the environment.

A much smaller number of studies have attempted to elucidate aspects of transport and physico-chemical speciation of PAHs in the ocean. PAH concentrations in dated sediment cores and in sediment traps have been used to quantify their vertical fluxes at several sites (e.g., Gschwend and Hites, 1981; Broman *et al.*, 1988; Lipiatou *et al.*, 1993). Notably, one sediment-trap study proposed a quantitative model for the spatial distribution of PAH fluxes over coastal and continental shelf length scales (Näf *et al.*, 1992) .

The *in situ* distribution of individual PAHs between filterable and filter-passing reservoirs have been reported in a few studies (Readman *et al.*, 1987; Broman *et al.*, 1991; McGroddy and Farrington, 1995; Ko and Baker, 1996). Distribution ratios are typically significantly higher than anticipated from organic-matter based partition models. A role for soot in the phase distribution of PAHs have been proposed in several studies (Prahl and Carpenter, 1979; Farrington *et al.*, 1983; Broman *et al.*, 1990; McGroddy and Farrington, 1995) but soot has never been simultaneously measured quantitatively. Whitehouse (1984) verified the "salting out" effect (Setchenow, 1889) on the aqueous solubilites of several PAHs in seawater. Solubility enhancement experiments showed that seawater with colloids can accomodate PAHs in suspension at higher levels than in seawater which had been photooxidized (Whitehouse, 1985). Another laboratory partition experiment on the distribution of spiked pyrene between sediment porewater colloids and seawater reported a K_{oc} of similar magnitude as expected from the existing partition model (Chin and Gschwend, 1992).

Organization and contributions of this thesis

It is the overriding objective of this thesis to contribute a better understanding of processes affecting the fate and effects of PAHs in the ocean. In light of the anticipated behavior of PAHs from their compound-specific properties, the specific properties of the ocean environment, and available process-driven field studies, the goal was to quantitatively comprehend (1) the solid - water distribution and (2) the horizontal and vertical water column fluxes of PAHs. The thesis may conceptually be divided into three parts. The first section relates to the role of colloids in the physico-chemical speciation of PAHs (chapters 2-4). This is followed by a second speciation portion where soot as a partition medium for PAHs is evaluated (chapters 5-6). The final part of this thesis utlilizes ^{234}Th-derived PAH fluxes to develop some concepts about the speciation-dependent vertical and horizontal transport of PAHs in the ocean (chapter 7-8).

Based on results from the type of exploratory speciation calculation mentioned above for benzo[a]pyrene and the limited data available on colloid-seawater partitioning (Whitehouse, 1985; Chin and Gschwend, 1992), we recognized the urgent need to elucidate the quantitative role that colloidal sorbents may play in affecting the cycling of individual PAHs. The current challenges facing researchers attempting to study the role of colloids in trace chemical speciation is reviewed in chapter 2. A functionally-based definition of colloidal sorbents is offered based on thermodynamical reasoning (lower end) and hydrodynamic arguments (upper end). In chapter 3, I explore the (f)utility of cross-flow filtration for accurately isolating marine organic colloids for evaluation of HOC speciation. Preliminary time-resolved flourescence-quenching experiments are introduced in chapter 4 to investigate the hydrophobic sorbent characteristics of surface seawater colloids.

An analytical method to measure the minor portion of sedimentary carbon that is of pyrogenic origin was developed to evaluate quantitatively whether soot sorption is causing the elevated *in situ* distribution coefficents observed for PAHs (chapter 5). Individual PAH compounds, total organic and soot carbon were simultaneously quantified in surface sediments from the New England continental shelf to assess the governing PAH speciation (chapter 6). A theoretical model for the molecular interaction between PAH molecules and the soot matrix is also forwarded (chapter 6).

Chapter 7 explores the spatially varying upper ocean fluxes of PAHs. Vertical export estimates are obtained from coastal to pelagic sites by coupling the mixed layer particulate PAH inventory with the radioactive disequilibrium of ^{238}U-^{234}Th, a technique based on direct measurements of mixed layer properties. A mathematical description of the bi-exponentially decreasing flux away from the continental source is used to provide the first receptor-based estimate of the Northwest Atlantic PAH sink. The process-insight developed in the earlier chapters (speciation and vertical flux estimation) was finally applied to construct a PAH mass-balance cycling model for Portland Harbor-Casco Bay, Gulf of Maine, to estimate the current spatial fate and surface residence times (doses) of such ecotoxicologically significant compounds (chapter 8). Particularly, the relative importance of horizontal and vertical exports of hydrophobic chemicals were assessed. The model also provides a measure of the current status of our knowledge and enables anticipation of future fates and exposure under changing conditions.

Finally, in chapter 9, the overall conclusions of the thesis are reviewed and the specific implications for dispersal and bioavailability (exposure) are discussed. Directions are proposed for future investigations of PAH speciation and transport. Chapters 2, 3, 5, 6, 7, and 8 are presented in the format of journal articles and were co-authored with my thesis advisors, Dr. Philip M. Gschwend and Dr. Ken O Buesseler; chapters 5 and 8 also have other collaborators as co-authors (see these chapters).

References

Blumer, M. *Angew. Chem. Int. Ed. Engl.* **1975,** *8,* 507.

Broman, D., A. Colmsjö, B. Ganning, C. Näf and Y. Zebühr. *Environ. Sci. Technol.***1988**, *22*, 1219.

Broman, D; C. Näf; M. Wik; I. Renberg. *Chemosphere,* **1990,** *21,* 69.

Broman, D; C. Näf; C. Rolff; Y. Zebühr. *Environ. Sci. Technol*. **1991**, *25,* 1850.

Brownawell, B. J; J. W. Farrington, *Geochim. Cosmochim. Acta,* **1986,** *50,* 157.

Buesseler, K. O., M. P. Bacon, J. K. Cochran, H. D. Livingston. *Deep-Sea Res.,* **1992**, *39*, 1115.

Chin, Y.-P.; Gschwend, P. M., *Environ. Sci. Technol.* **1992,** *26,* 1621.

Chiou, C. T; P. E. Porter; D. W. Schmedding, *Science* **1979,** *206,* 831.

DeLappe, B. W.; Risebrough, R. W.; Walker, W. *Canad. J. Fish. Aq. Sci.* **1983**, *40(S2)*, 322.

Denissenko, M. F; A. Pao; M-S. Tang; G. P. Pfeifer. *Science,* **1996,** *274,* 430.

Derenbach, J. B; M. V. J. Gereck. *J. exp. mar. Biol. Ecol.* **1980,** *44,* 61.

Durant, J. L.; W. G. Thilly; H. F. Hemond; A. L. Lafleur. *Environ. Sci. Technol.* **1994**, *28*, 2033.

EPA, 1985. Evaluation and Estimation of Potential Carcinogenic Risks of Polynuclear Aromatic Hydrocarbons. Office of Health and Environmental Assessment, Office of Research and Development, US Environmental Protection Agency, Washington, DC.

EPA, 1993. Sediment Quality Criteria for the Protection of Benthic Organisms: Fluoranthene; EPA 822-R-93-012; Offices of Water, Research, and Development and, Science and Technology; U.S. Environmental Protection Agency, Washington, DC.

Farrington, J. W; E. D. Goldberg; R. W. Risebrough; J. H. Martin; V. T. Bowen, *Environ. Sci. Technol.* **1983,** *17,* 490.

Farrington, J. W.; Westall, J. **1986** In: The Role of the Oceans as a Waste Disposal Option. Kullenberg, G. (Ed.), Reidel: Dortmund.

Grimmer, G; H. Böhnke, *Cancer. Lett.* **1975,** *1,* 75.

Gschwend, P. M, R. A. Hites; *Geochim. Cosmochim. Acta.* **1981,** *45,* 2359.

Gschwend, P. M; R. P. Schwarzenbach, *Mar. Chem.* **1992,** *39,* 187.

Guerin, W. F.; Boyd, S. A., *Appl. Environ. Microbiol.* **1992,** *58*, 1142.

Hites, R. A; R. E. LaFlamme; J. G. Jr, Windsor; J. W. Farrington; W. G. Deuser. *Geochim. Cosmochim. Acta* **1980,** *44,* 873.

Karickhoff, S. W; D. S. Brown; T. A. Scott. *Water Research,* **1979,** *13,* 241.

Kern, W. *Helv. Chim. Acta,* **1947**, *30,* 1595.

Ko, F. -C.; Baker, J. E. *Mar. Chem.*, **1996,** *49*, 171.

Leversee, G. J.; Landrum, P. F.; Giery, J. P.; Fannin, T., *Canad. J. Fish. Aq. Sci.* **1983**, *40(S2)*, 63.

Lipiatou, E., Marty, J. -C. and A. Saliot. *Mar. Chem.*, **1993**, *44:*, 43.

McElroy, A. E.; Farrington, J. W.; Teal, J. M., **1989**, In: Metabolism of Polycyclic Aromatic Hydrocarbons in the Aquatic Environment. Varanasi, U. (Ed.), CRC Press: Boca Raton, FL., 1-39.

McGroddy, S. E.; Farrington, J. W., *Environ. Sci. Technol.* **1995**, *30*, 172.

Means, J. C.; Wijayaratne, R., *Science*, **1982**, *215*, 968.

Näf, C., D. Broman, H. Pettersen, C. Roff and Y. Zebühr. *Environ. Sci. Technol.* **1992**, *26*, 1444.

NAS, **1972**. Particulate Polycyclic Organic Matter. National Academy of Sciences, Washington, DC.

NRC, **1985**. Oil in the Sea: Inputs, Fates, and Effects. National Research Council, Washington, DC.

Petrick, G., D. E. Schulz-Bull, V. Martens, K. Scholz, and J. C. Duinker. *Mar. Chem.*, **1996,** 54, 97.

Prahl, F. G; R. Carpenter, *Geochim. Cosmochim. Acta* **1979,** *43*, 1959.

Readman, J. W; R. F. C. Mantoura; M. M. Rhead, *Sci. Total. Environ,* **1987,** *66,* 73.

Schwarzenbach, R. P., P. M. Gschwend and D. M. Imboden. **1993**. Environmental Organic Chemistry, Wiley, New York, 681 pp.

Setchenow, J. *Z. Phys. Chem.,Vierter Band* , **1889**,*1*, 117.

Stumm, W; R. Schwarzenbach; L. Sigg. *Angew. Chem. Int.. Ed.Engl.* **1983**, *22*, 380.

Tanabe, S; Tatsukawa, R. **1992,** In: Persistent Pollutants in Marine Ecosystems. Walker, C. H. and Livingstone, D. R. (Eds.), Pergamon: Oxford, England.

Tinbergen, N. **1970**, Signals for Survival, Clarendon Press: Oxford.

Whitehouse, B. *Mar. Chem.*, **1984**, *14*, 319.

Whitehouse, B. *Estuar. Coastal Shelf Sci.*, **1985**, *20,* 393.

Wolfe, D. A.; M. J. Hameed; J. A. Galt; G. Watabayashi; J. Short; C. O'Claire; S. Rice; J. Michel; J. R. Payne, J; J. Braddock; S. Hanna; D. Sale. *Environ. Sci. Technol,* **1994**, *13,* 561.

Chapter 2

Aquatic colloids: Concepts, definitions, and current challenges

Örjan Gustafsson and Philip M. Gschwend
R. M. Parsons Laboratory, MIT 48-415,
Massachusetts Institute of Technology,
Cambridge, MA 02139

submitted
Limnology & Oceanography

Abstract

Colloidal phases in natural waters may be important to various environmental questions, especially those concerning the cycling of vital and toxic trace chemicals. Current treatments of the role of colloids in chemical speciation largely rely on operational definitions of phases such as 1000 D ultrafilter and 0.45-µm filter cut-offs. Defining chemical phases exclusively by a physical parameter such as size is contributing to a situation where the observed filterable vs. unfilterable distribution coefficients, D, are not well-predicted from thermodynamically derived sorbed vs. solute equilibrium constants, K. Achieving the goal of relating the natural distributions of chemicals to theoretical expectations is contingent upon progress in development of a functionally meaningful colloid definition and interpretation of observed distributions of trace substances in terms of the relevant physico-chemical properties of the system.

We assess the phase status of typical components in natural waters from a "chem-centric" point of view (i.e., one whose motivation is to understand the cycling of trace chemicals in the environment). As a result, we define colloids so as to provide a thermodynamic grounding for evaluating chemical speciation and a hydrodynamic framework distinguishing phases that is transported with the solution from those that are not. These constraints lead one to define an aquatic colloid as *any constituent that provides a molecular milieu into and onto which chemicals can escape from the aqueous solution, and whose movement is not significantly affected by gravitational settling.* Such a definition allows development of mass balance equations, suited to assessing chemical fates, which reflect processes uniquely acting on dissolved, colloidal, or settling particle phases.

For aquatic scientists concerned with the behavior and effects of trace chemicals, one important process is the partitioning of those trace constituents between the dissolved and bound pools. The resulting speciation affects the extent to which the chemical participates in various transport and transformation processes. For example, one may anticipate that the truly dissolved trace molecules may participate in homogeneous solution phase reactions, while this is not true for their counterparts sorbed to *colloids* (particles "immune to gravity", Graham 1861) or settling particles (henceforth referred to as *gravitoids*). Such sorbed species may be less bioavailable and may exhibit different photoreactivity than their solution-phase counterparts. Likewise, for transport processes, one may anticipate that dissolved and colloid-bound molecules are carried with the moving fluid (e.g., in sediment pore-water irrigation), while the gravitoid fraction may fall out of a mixed water body to loci below. Distinguishing among these functionally distinct forms is essential if we are to elucidate the cycling and effects of trace chemicals in natural waters.

Recently, efforts to quantify the roles of colloids in the cycling of trace compounds have been confounded by the realization that results obtained by the most common sampling technique, cross-flow ultrafiltration (CFF), are operator- and equipment-dependent (Buesseler et al. 1996). CFF also appears to cause undesired fractionation of colloidal components (Gustafsson et al. 1996). Nevertheless, continuing efforts to elucidate the applicability of CFF to collecting natural water colloids, along with development of new approaches for investigating these elusive components, guarantee that the current momentum of colloid studies will be maintained in the near future.

In this paper, we focus on how colloids may influence the cycling of trace compounds in natural waters (i.e., a chem-centric view). In particular, we attempt to constrain how colloidal entities may affect trace chemical speciation. We especially highlight the difference between operational distribution coefficients, hereafter designated with the symbol D, derived from the ratio of filterable-to-nonfilterable concentrations, from thermodynamically-based equilibrium constants, hereafter designated by K, which quantify the relation between a single, truly dissolved species and a single, bound counterpart. Thus, after we briefly review the history of colloid-related studies, especially those pertinent to partitioning and scavenging processes in natural waters, we offer a definition of colloids based on our chem-centric point of view. This definition is then used to discuss whether various constituents of natural waters should be considered colloidal from the chem-centric point of view and to illustrate how colloid associations might influence chemical cycling.

Historical perspective

The current picture of speciation and physical states of chemicals in natural waters is a result of a series of historical developments and conceptual formulations involving measures of the abundance of various suspended phases and inferences regarding the modes whereby trace chemicals interact with these phases. By the 1930s, aquatic scientists already worked to separate particulate, colloidal, and dissolved organic carbon phases (POC, COC, DOC). For example, Krogh and Lange (1931) size-fractionated lakewater with "plankton-filters" and "ultrafilters". These ultrafilters were reportedly manufactured by impregnating paper-filters with certain "colloidal suspensions under varying conditions" (Zsigmondy and Bachman 1918; Zsigmondy 1926) and were calibrated with macromolecular dyes, colloidal gold of increasing size, and egg albumin (45 kD). Using a home-built "archea-HTCO" organic carbon analyzer, based on catalytic oxidation with cupric oxide at "red-glowing" high temperature, Krogh (1930) determined that POC made up 20% and COC about 15% of the total organic carbon in lake waters - values within the range of recent observations for natural waters using modern CFF and HTCO methods!

Today's distinction between dissolved and particulate phases in geochemistry can be traced back to the application of 0.5-μm cellulose acetate membrane filters to ocean waters by Goldberg et al. (1952). Goldberg (1954) also introduced the concept of "marine distribution coefficient", D, as the ratio of an element in such filter-collected solid phases to that in the filter-passing media. In the first natural water application of stirred-cell ultrafiltration techniques (reported 0.003-μm cutoff), Sharp (1973) demonstrated for seawater that most filter-passing organic matter actually could be colloidal. Nearly a quarter-century ago, Sharp called for relinquishing the misleading delineation of particulate and dissolved phases at about 0.5 μm which by then had become firmly established.

Reports that colloids influence the speciation of low-solubility chemicals in fresh and marine waters appeared in the mid-1970s. For example, Boehm and Quinn (1973) observed that the apparent seawater solubilities of n-alkane and isoprenoid hydrocarbons decreased when colloidal fulvic acid was removed. Likewise, Sholkovitz (1976) demonstrated the association of inorganic constituents such as Fe, Mn, Al, and P with colloid-sized humic substances, resulting in their co-flocculation during simulated estuarine mixing. Eventually, field studies also supported the idea that colloids could have an important impact on the speciation and fate of trace chemicals, such as when colloids were shown to affect PCB cycling in the Laurentian Great Lakes (Baker et al. 1986) and in sediment pore-waters of New Bedford Harbor (Brownawell and Farrington 1986).

On the theoretical side, Sillén (1961) proposed a thermodynamically based framework using chemical solubilities for interpreting partitioning and scavenging observations. This idea triggered the development of surface complexation models (SCMs) to interpret aqueous-solid partitioning phenomena for charged constituents (Schindler and Kamber 1968; Stumm et al. 1970; Schindler and Gamsjager 1972; Dzombak and Morel 1990). SCMs consider the free energy of solid-water adsorption to be a combination of both the intrinsic strength of the actual sorbate-sorbent bond and the electrostatic energy involved in moving the charged sorbate to the charged surface. Taking the saturated sorbed concentration to reflect unit activity in the solid phase and 1 M to be unit activity in the solution phase, we find

$$K_{SCM} = \frac{\sigma A}{1M} \exp(-(\Delta G_{chem} + zF\Psi)/RT) \qquad (1)$$

where K_{SCM} (mol kg^{-1} (mol liter^{-1})$^{-1}$) is the solid-water adsorption constant, σ is the concentration of one type of reactive site per solid surface area (mol sites m^{-2}), A is the area of particle surface per mass of solid (m^{2} kg^{-1}), ΔG_{chem} reflects the intrinsic contribution of the energy of bond formation for a chemical distributing itself between a liter of solution and a specific charged site on a kilogram of solids, z is the charge of the chemical, F is the Faraday constant, Ψ is the surface potential relative to the bulk solution, R the molar gas constant, and T the absolute temperature.

A hydrophobic partition model (HPM) was also developed for predicting the equilibrium phase distributions of nonionic and hydrophobic organic compounds, HOCs (Karickhoff et al. 1979; Chiou et al. 1979). The natural organic matter in particles offers a relatively nonpolar environment into which HOCs may dissolve. Hence, association of HOCs with the organic matter content of natural particles reflects the difference in excess free energies of HOCs dissolving in natural organic matter vs. dissolving in aqueous solutions (Chiou et al. 1979; Schwarzenbach et al. 1993). As a result, the HPM allows prediction of nonionic compound sorption on the basis of the organic matter content of the particles and the relative solvophilicity of the chemical. Taking unit activity in the solid phase as the (liquid) compound's solubility in the organic matrix (C_{om}^{sat}; units: mol kg^{-1} organic matter (om)) and in the solution as the (liquid) compound's aqueous solubility (C_w^{sat}; units: mol $liter^{-1}$ water (w)), one may derive a thermodynamic expression:

$$K_{HPM} = \frac{f_{om}\, C_{om}^{sat}}{C_w^{sat}} \exp(-\Delta G_{om}/RT) \qquad (2)$$

where K_{HPM} (mol kg^{-1} (mol $liter^{-1})^{-1}$) is the solid-water absorption constant, f_{om} is the organic matter fraction of the sorbent particles ($kg_{om}\ kg^{-1}{}_{solid}$), and ΔG_{om} reflects the free energy of sorbate exchange between a kilogram of natural organic matter and a liter of water.

A major geochemical inconsistency with these sorption models was reported and widely discussed in the 1980s. Distribution coefficients, D values, for numerous trace chemicals (e.g., Co, DDT) were observed to change as a function of the concentration of the solids in the suspensions studied (e.g., O'Connor and Connolly 1980). Observations of the distribution of ^{234}Th between filterable and unfilterable phases are typical (Fig. 1). At low solids concentrations ($\leq$ 3 mg $liter^{-1}$), the D(^{234}Th) is seen to be nearly constant at a relatively high value (i.e., ~ 10^6). However, at increasing solids concentrations, the observed distribution coefficient decreases steadily. Such data are not consistent with expectations for K(trace chemicals) put forth by SCM and HPM models (and assuming other properties of the solution like pH do not change.) A unifying quality of these thermodynamic models is that they predict constant K values for trace chemicals, no matter what the sorbent:solution ratio.

These discrepancies between D and K values are due to a combination of factors. First, conventionally nonfilterable media are now recognized to include colloidal sorbent phases in the apparently dissolved phase (Gschwend and Wu 1985). Additionally, situations with high solids concentrations, resulting in rapid removal of colloids and gravitoids (e.g., rapid coagulation and settling or rapid phytoplankton growth and grazing), may not allow sufficient solid-water contact for sorptive

Fig. 1. Observed distributions (D) between filter-retained and filter-passing ^{234}Th in marine surface waters of varying filter-collected solids concentrations. A trend of decreasing D at solids concentrations greater than approximately D^{-1} is indicative of the presence of ^{234}Th adsorbed to particles passing through the filters (the Particle-concentration-effect). (Δ - Baskaran et al. 1992; **o** - Coale and Bruland 1985; × - Wei and Murray 1992; ◇ - Moran and Buesseler 1993; ● - McKee et al. 1984; ❑ - McKee et al. 1986)

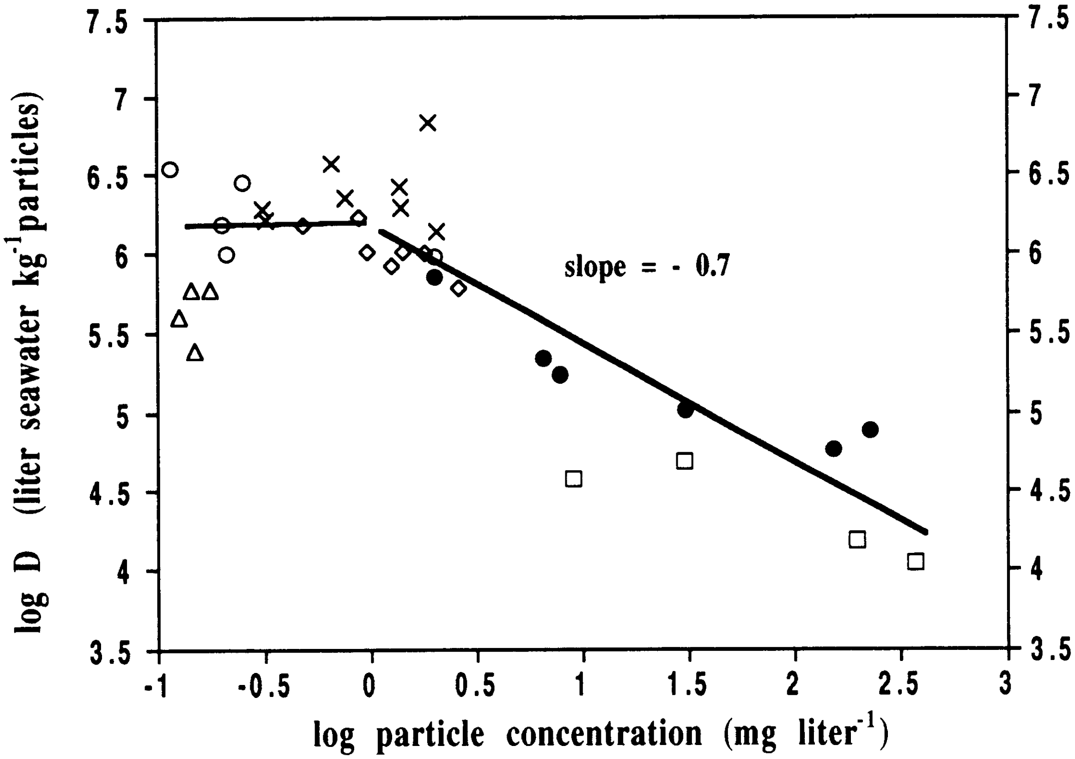

7.5
7
6.5
6
5.5
5
4.5
4
3.5
-1
-0.5
0
0.5
1
1.5
2
2.5
3
slope = - 0.7
log D (liter seawater kg^{-1}particles)
log particle concentration (mg liter^{-1})

equilibrium to be achieved. Hence, observations of solid-water partitioning in these cases may not reflect chemical equilibria (Wu and Gschwend 1988; Honeyman et al. 1988; Swackhammer and Skoglund 1993.)

In addition to sorption, the other group of processes central to scavenging trace constituents from natural waters involves the removal of sorbent phases from the water column. Both physically and biologically coupled models have been developed to describe colloid coagulation and gravitoid sedimentation. Physical treatment of particle dynamics normally involves Smoluchowski's coagulation theory (1917) coupled with particle removal mechanisms. Good treatments are available of the fundamental factors that govern coagulation: the encounter rate of particles, η , and the fraction of the collisions that result in aggregation, α (e.g., Friedlander 1977; O'Melia 1987; Israelachvili 1992). Several studies have also observed that colloids are both produced and taken up by microbial and planktonic food webs (e.g., Johnson and Kepkay 1992; Tranvik et al. 1993; Amon and Benner 1994). Biologically coupled aggregation models are hybrids of the thermodynamically based coagulation theory and empirical descriptions of, for example, bloom dynamics. In recent versions, the smallest, primary, particles in such models are 1 μm (Jackson 1990; Hill 1992), which obviously means that the colloids are largely ignored.

Stoke's law for gravity-driven settling, ranging from 0.1 to 100 m d^{-1} for 1-100-μm spherical particles, is commonly used to yield a kinetic expression of particulate matter removal (e.g., Lerman 1979). However, porous aggregates, like marine snow, exhibit such a low specific density and non-spherical geometries (e.g., Alldredge and Silver, 1988; Lick et al. 1993), that development of formulations for collision functions and settling rates that considers their hydrodynamic effects is required (e.g., Stolzenbach 1993; Johnson et al. 1996). A complementary scavenging mechanism to gravitational settling in shallow systems may involve vertical mixing coupled with collection of both gravitoids and colloids at the bed surface (Stolzenbach et al. 1992).

An important feature of both physical and biological models of particle dynamics is that colloids and gravitoids are all part of the same dynamic aggregation-breakup continuum. Net coagulation rates are expected to be a function of the total solids concentration. No matter if coagulation is taken to be physical or biological, particle aggregation can better compete with vertical particle removal in situations of higher solids concentration, and hence a greater fraction of the total particles can be sustained in larger size classes at steady state at higher total solids concentrations (shown schematically in Figure 2A). Particle size classes, which are lower in mass concentration than smaller particle classes from which they are being formed, may be interpreted as the critical sizes where a net responsiveness to gravitational removal becomes important. Particle size distribution data down through the submicrometer range, required to verify the concepts illustrated in Fig. 2A, are scarce. However, recently Buffle and Leppard (1995) have demonstrated that the predicted particle size distribution curves are seen down to particle sizes of 10s of nanometers in groundwater, lake water, and seawater despite neglecting many solid properties in model calculations (e.g., density, shape).

A ramification of the hypothetical size distributions depicted in Fig. 2A is that it is not straightforward to estimate colloid concentrations from filterable solid loads. One should expect a nonlinear relation between colloid and gravitoid concentrations (shown schematically in Fig. 2B). In suspensions with higher solids concentrations, where the rate of coagulative formation of large particles should be enhanced, greater contamination of the gravitoid fraction by the colloidal particles in conventionally filtered samples may be expected (Fig. 2). Thus, colloid-gravitoid relationships based on ratios of solids retained by and passing through filters (Gschwend and Wu 1985; Moran and Moore 1989; Honeyman and Santschi 1989) seem doomed to inaccuracy because they do not try to account for the critical particle size in the water mass under study.

Functional definition of aquatic colloids

To better characterize the chem-centric roles of colloids, a definition of what qualifies as a colloid would be useful. In much current work, nonfilterable versus filterable particulate phases is still used to distinguish colloids and gravitoids; this practical approach does not allow us to anticipate accurately many trace chemical behaviors in environmental systems. We suggest that it would be beneficial to adopt a distinction between dissolved versus colloid-associated species based on the nature of trace chemicals' specific molecular interactions and their corresponding thermodynamics descriptors, K's. And then, since we are also interested in trace chemical transport, we

Fig. 2. Hypothetical curves reflecting particle size distributions based on models such as that of Farley and Morel (1986). Concentrations refer to filterable solids concentrations. **A**. Steady-state particle-size distributions (mass-based) for three aquatic regimes with widely different total solids concentrations. The points where the curves are changing slopes may be interpreted as the functional, chem-centric, distinctions between colloids and gravitoids, which are seen to be a function of the total solids levels. The hatched regions indicate the traditional, operational, distinctions between dissolved-small (colloidal) particles (left) and small-large particles (right). **B**. Schematic representation (deduced from panel **A**) of the effect of total solids concentrations on the relative distribution of mass between filter-defined small and large particle sizes, indicating a non-linear relationship. The decreasing value of the slope, inserted in the figure, is an outcome of a greater fraction of the total solid mass residing in the large particle class as a result of coagulation becoming more important with respect to sedimentation at increasing total solids concentrations.

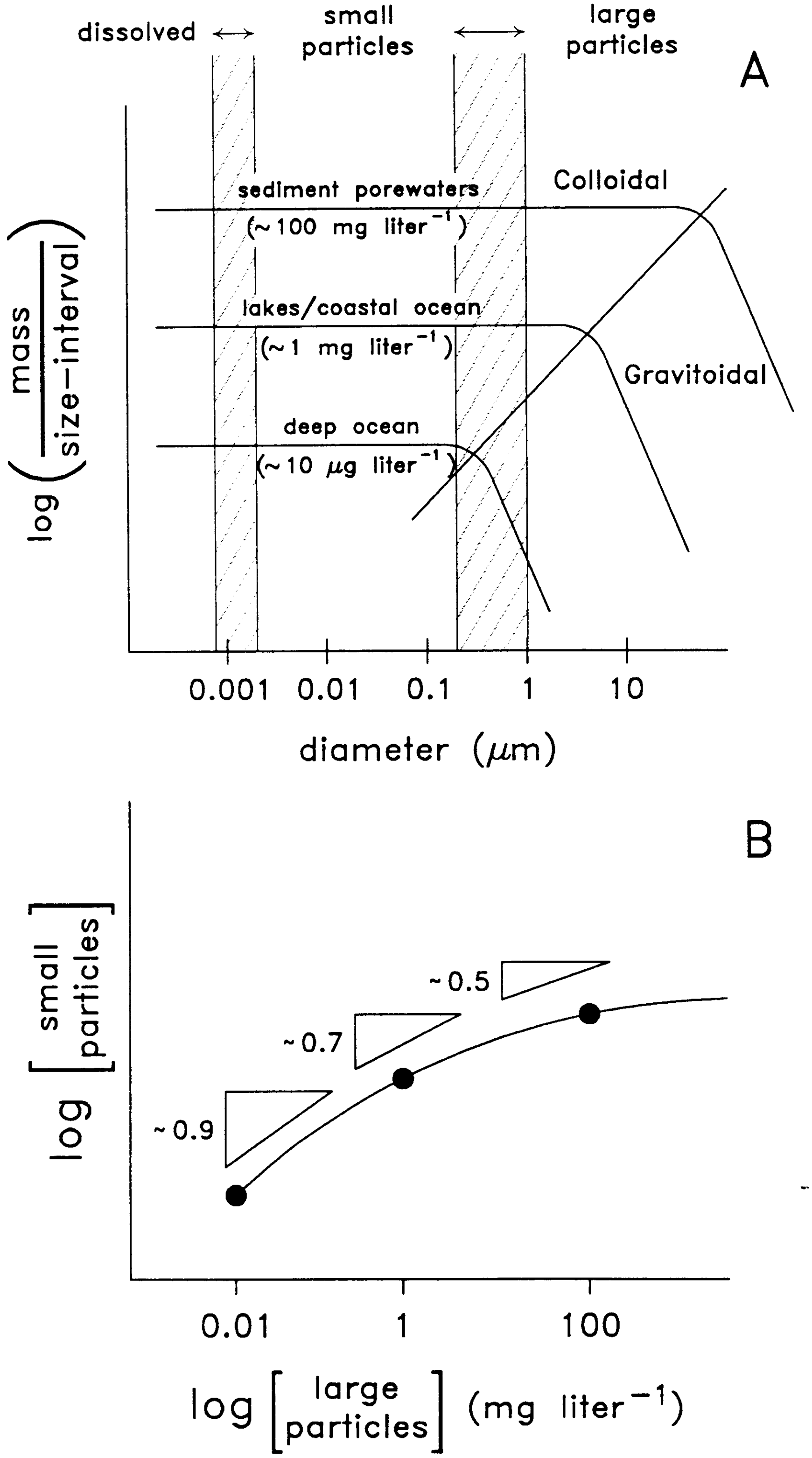
dissolved
small particles
large particles
A
sediment porewaters
(~100 mg liter^{-1})
lakes/coastal ocean
(~1 mg liter^{-1})
deep ocean
(~10 μg liter^{-1})
Colloidal
Gravitoidal
log (mass / size−interval)
0.001
0.01
0.1
1
10
diameter (μm)
B
~0.5
~0.7
~0.9
log [small particles]
0.01
1
100
log [large particles] (mg liter^{-1})

should distinguish between nonaqueous media whose own cycles are dominated by coagulative versus settling removal mechanisms. Motivated by the need to anticipate the behavior of trace chemicals in natural waters, we attempt a chem-centric definition of freshwater and marine colloidal sorbents below.

Delimiting the dissolved-colloidal boundary

Since our ultimate goal is to better understand the cycling of chemical compounds in natural waters, the first critical question is: when is some entity large enough to provide an opportunity for trace compounds to move out of the aqueous solution phase and into (absorption) or onto (adsorption) this new medium? The answer yields the chem-centrically relevant distinction between solution species and colloidal ones.

The chem-centric view requires us to consider materials of at least nanometer dimensions. For example, phenanthrene is a polycyclic aromatic hydrocarbon (PAH) of molecular mass 178 D and extending about 0.7 nm across its longest dimension. Thus, a colloidal medium relevant to phenanthrene must be at least this size. Consequently, if one assumes a lower limit size for colloids consistent with 1-2-nm diameter spherical particles, then molecular masses of organic macromolecules would have to be larger than ~ 300-2000 D. This size is in the range reported for riverine fulvic acids (Aiken and Malcolm 1987) and lacustrine and marine sediment pore-water organic macromolecules (Chin and Gschwend 1991).

Next, the chem-centric view suggests that a new phase must also offer trace constituents some volumetric or interfacial microenvironment in which the spatially and temporally averaged bulk properties of the medium are distinguished from those of the aqueous solution. For example, since intermolecular forces are electrostatic in nature, one important bulk property is a medium's dielectric constant (a measure of the medium's ability to transmit polar interactions). One example of a microvolume with clearly different dielectric property from water is a micelle built from about 60 dodecyl sulfate molecules (micellar weight of ~18,000 D and about 4 nm in diameter). The interior of such molecular aggregates provides a nonpolar microenvironment into which HOC molecules like phenanthrene can partition. That this microvolume exhibits a different dielectric nature than the surrounding aqueous solution can be seen in the changed light absorption by incorporated chromophores; for example, vibrionic bands of PAHs shift to longer wavelengths when these compounds exist in nonpolar media like micelles rather than water (Chandar et al. 1987). Given the common perception of humic substances as natural micelle-like macromolecules (e.g., Wershaw 1986), one may reasonably imagine that these complex organic constituents provide microenvironments within their interior where there are substantially different bulk properties (like dielectric constants) than exist in the exterior solution phase.

A second necessary trait for an entity to be large enough to be a colloid is the presence of an interfacial region with properties varying from those of the aqueous phase to those of the colloidal phase. For example, if the exterior of the medium includes ionized moieties spaced close enough to influence one another so as not to be well represented by isolated point charges, then a surface potential will exist. A diffuse double layer of counterions will accumulate in a region between the solution and such a colloidal phase. Said another way, to qualify chem-centrically as colloids, oligoelectrolytic macromolecules or inorganic precipitates need to be large enough and structured so that one should consider the presence of an electrostatic field around them. As discussed by Bartschat et al. (1992), by considering humic substances of molecular mass near 1000 D to have such particle-like charging, one may greatly improve our ability to predict the ionic interactions of charged species like Cu^{2+} with these organic macromolecules.

In sum, macromolecular entities should be considered colloidal when they require property descriptions which average bond-scale effects to yield medium properties important to the trace constituents of concern. In general, this criterion translates into nanometer or larger scales, but such a requirement does not necessarily mean that all entities larger than a nanometer are colloids. For example polyelectrolytes, which assume an extended conformation in water and whose charged moieties do not substantially influence one another, would not be colloidal with the chem-centric view espoused above.

Delimiting colloidal from gravitoidal phases

There is no upper size limitation to sorbents affecting chemicals on the molecular level. Consequently, a characteristic other than the ability to contribute to phase-partitioning of chemicals must be chosen to distinguish colloidal and larger particulate phases. Because our concern lies with the overall behavior of trace chemicals, we suggest that the delimiter for colloid-bound species vs. gravitoid-bound forms be based on distinguishing environmental transport mechanisms. Thus, colloids should be distinguished from larger sorbents based on their predominant transport with the water, without substantial removal by settling.

Therefore, to functionally distinguish colloids from gravitoids one must consider the conditions and the timescales relevant to natural waters. Particle size distributions (Fig. 2A) result from the kinetic competition between coagulation (of colloids) and sedimentation (of gravitoids). Conceptually, these distinct fates of sorbent mass are reflected by the breakpoint in the solid distribution curves (Fig. 2A, diagonal line). Although the time it takes for a given particle to sink out from the surface layer is independent of overall solid concentrations, the coagulative conversion rate of the same particle is proportional to the abundance of aggregating solids.

The implication is that the distinction between gravitoids and colloids is a function of total solids concentration. The effect of any filterability-based separation is apparent in the idealized size distribution curves (Fig. 2A: hatched regions). For example, at modest concentrations of particles as in the coastal ocean, the typical size-based distinction between gravitoids (particulate) and colloids may no longer coincide with the critical solid size at which settling starts to outcompete coagulation. The current upper-end colloid definition (Fig. 2A, right hatched region), set around 0.5 μm, is wanting since the functional distinction between particles dominated by either coagulation or settling is not constant (Fig. 2A, diagonal line). In this context it is of less significance that some biological and physical formulations of coagulation and settling yield slightly different absolute values of the critical coagulation-to-settling breakpoint at a given site. Instead, the important concept is that the sorbent-transport-based colloid-gravitoid distinction will vary between sites (Fig. 2A, diagonal line), dependent on the regime-specific coagulation vs settling rates.

The breakpoint defining particles that predominantly settle is not only a function of total solid levels but a function of the hydrodynamics and particle surfaces of the water body of interest. The depth of the well-mixed layer sets the environmental timescale over which settling must compete with coagulative removal of solid mass from a given size bin. Hence deeper, well-mixed, water systems should exhibit reduced settling importance and consequently comprise even larger colloidal sizes. It is also known that the process of coagulation is a function of particle and aqueous solution properties. For instance, because of differences in solution charge-shielding, particle coagulation in seawater should be more efficient than in freshwater. Hence, all other things equal (e.g., particle composition and concentration, mixed layer depth), seawater colloids should be larger than their freshwater counterparts.

In light of this discussion, it is informative to assess some observations attempting to distinguish between suspended and settling particles. Weilenmann et al. (1989) studied particle transport in two Swiss lakes throughout an annual cycle. Lake Zürich had an enhanced coagulation rate, due to relatively lower levels of colloid-stabilizing humic substances (giving a higher sticking coefficient, α). Particles suspended in the epilimnion of this lake were dominated by a narrow size-distribution centered around 8 μm. A bimodal size distribution was observed in the Lake Sempach surface waters. A 20-30-μm size fraction was due to bacterial colonies, whereas a 5-μm centered pool of largely nonliving particles was consistent with the higher levels of stabilizing organic macromolecules in this lake. Based on estimated settling velocities from settling fluxes and solids concentrations, Baker et al. (1991) predicted that settling particles in oligotrophic Lake Superior are roughly 12 μm in size. From these natural water observations, we conclude that colloidal sorbents corresponding to a particle-size near 10 μm (to be contrasted with old 0.5 μm definition) may be retained at steady state in surface water suspension of large lakes through an apparent neutral buoyancy arising from coagulative formation outcompeting settling removal.

Thus, from a chem-centric point of view, we propose that *an aquatic colloid is any constituent that provides a molecular milieu into and onto which chemicals can escape from the aqueous solution and whose environmental fate is predominantly affected by coagulation-breakup mechanisms, as opposed to removal by settling.*

Illustrations of chem-centric phase speciation

To illustrate how a chem-centric colloid definition differentiates between phases, we consider the speciation of two trace chemicals - copper and phenanthrene (Fig. 3). Although both dissolved and colloidal constituents may associate with these trace substances, we distinguish colloidal phases as those which exhibit medium properties (e.g., nonpolar medium, surface potential). Further, we separate gravitoidal phases based on their propensity to settle (i.e., large, favorable shape, and dense enough). It is apparent that dissolved, colloidal, and gravitoidal phases overlap one another on a size

Fig. 3. A chem-centric speciation diagram. Two trace substances, phenanthrene and copper, are used to illustrate how such chemicals' interactions with various constituents may affect their functional speciation.

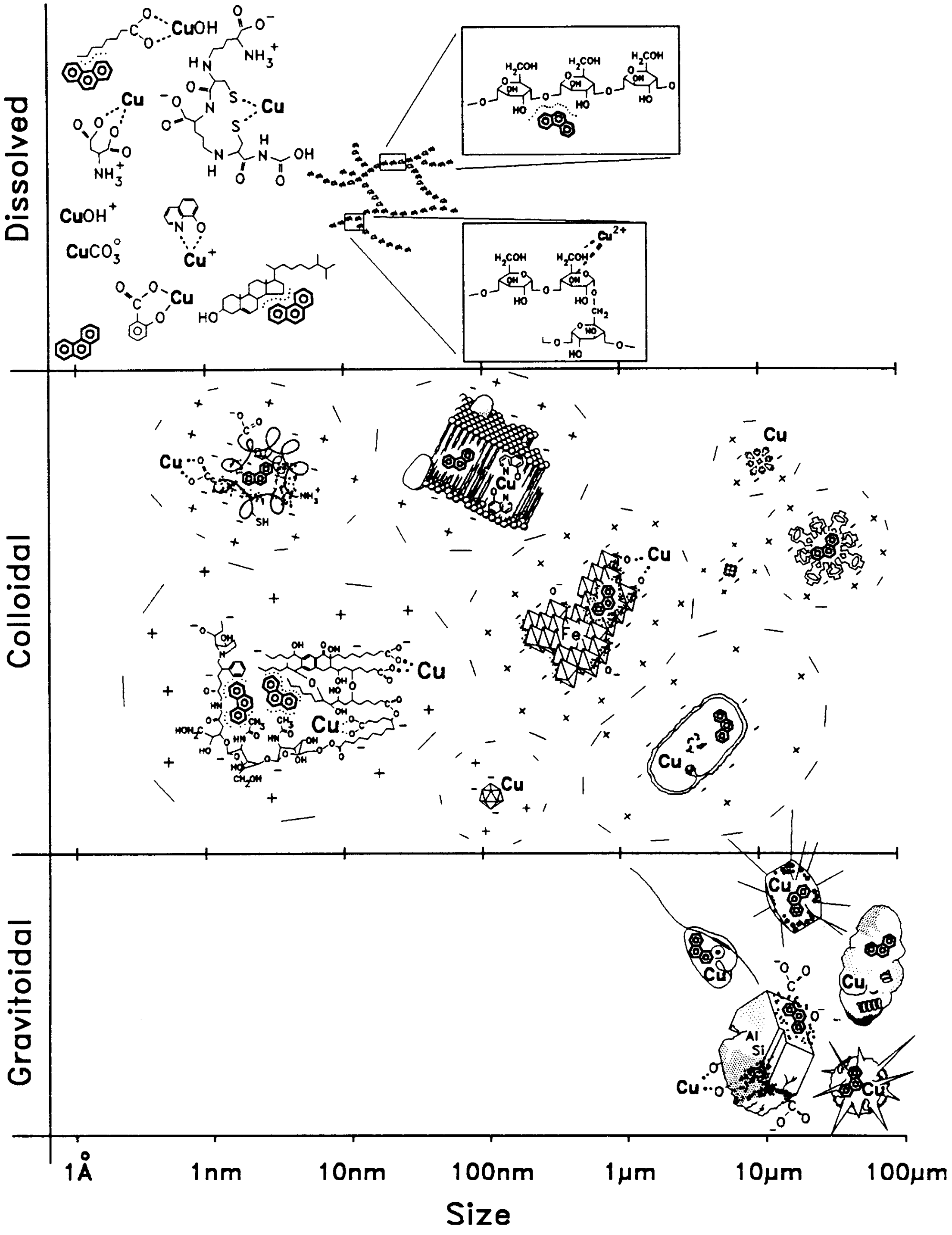
Dissolved
Colloidal
Gravitoidal
CuOH
CuOH⁺
CuCO₃°
Cu
Cu⁺
Cu²⁺
Fe
Al
Si
1Å
1nm
10nm
100nm
1µm
10µm
100µm
Size

axis. One sees that traditional dissolved species include complexes (e.g., $CuCO_3$), and that the relevant ligands (i.e., CO_3^{2-}) do not exhibit bulk properties (e.g., surface potential) differentiating them from the aqueous phase. Notably, this implies that elongate organic macromolecules which are well mixed with the water solvent do not constitute colloidal phases from our chem-centric point of view. Although very high in molecular-weight, extended, long-chain carbohydrates and nonglobular proteins may be considered to be in the dissolved phase, from the functional perspective of the forces acting on the trace chemical. This view is supported by the finding of Garbarini and Lion (1986) that cellulose (mol. wt. ~1,000,000 D), despite its large size, is unable to sorb hydrophobic compounds to an appreciable extent.

Another implication of a functional chem-centric definition of a colloid is that its state is not limited to solids, but may equally well include liquid sorbents. Examples include micelles and other aggregates of amphiphiles such as phospholipids of fragmented membranes (Fig. 3). A chem-centric colloid definition would also include in the colloidal pool such entities as coiled proteins and humic substances if they include hydrophobic interiors or interacting exterior charges best treated with double layer theories. Biological particles such as viruses and nonmotile bacteria should be considered colloids. Also, sufficiently small (i.e., coagulation more important than settling) aggregates such as organically coated, mineral particles (e.g., iron oxyhydroxides or aluminosilicates) would fall in the chem-centrically defined colloid class. Supermicrometer-sized aggregates of marine snow might be considered predominantly colloidal since their near-neutral bouyancies cause coagulation-disaggregation to be more frequent than settling removal.

Finally, gravitoids are those materials which, like colloids provide substances such as copper and phenanthrene alternative media to aqueous solution. But unlike colloids, gravitoids are separated from the aqueous suspension primarily through gravitational settling due to their own traits (including size and particle density) and environmental situation (e.g., solids concentration, fluid density, solution ionic strength, mixed depth). Hence, larger minerals with associated finer materials or biologically produced aggregates such as 100 μm fecal pellets may not qualify as colloids (Fig. 3). Plankton including diatoms, foraminifera, and radiolaria, to name a few, would not be included as colloids unless one believes their water column fates are predominantly set by predation-driven coagulation (i.e., grazing).

The specific merit of the proposed conceptual framework is that it is consistent with the needs of trace chemical cycling studies. Additionally, a functional description of natural water entitites may contribute a useful framework for assessing the physicochemical phase-distribution and transport of major components such as total solid mass and elements such as carbon and nitrogen. One implication would be that most of surface water POM is probably colloidal, from a hydrodynamic perspective.. In describing the fates of substances such as copper or phenanthrene, one must recognize the influence of the environmental milieu in the immediate vicinity of the substance of interest on the rates of various transformations. For example, phenanthrene in an aqueous carbohydrate suspension will be as available to incident light as would a completely aqueous phenanthrene solution (Fig. 4A). However, phenanthrene molecules contained within humic media would likely not experience the same photointensity (Fig. 4B). Photons may be absorbed by humic chromophores, and the light reaching any phenanthrene molecules in the interior may thus be altered. Further, the phenanthrene absorption within humic media may shift to longer wavelengths due to the more nonpolar local environment. Because natural light is more abundant at longer wavelengths, this may contribute to an enhanced rate of light absorption for the humic-associated species relative to the same molecule absorbing light when it is surrounded by water. Thus, compensating factors may cause the direct photolysis of phenanthrene to be either more or less significant for the molecules located in the interior volume of the colloidal humic macromolecule.

In contrast, one may expect that the relative concentrations of reactive transients (e.g., singlet oxygen ($^1O_2$), triplet DOM, ROO·, HO·) are elevated in the colloidal organic phase. For example, since molecular oxygen has a higher solubility in organic phases than in water (e.g., Lee and Rodgers 1983), and since organic chromophores have been implicated as sensitizers forming $^1O_2$ (Haag and Hoigné 1986), one might expect more $^1O_2$ to be formed in suspended organic phases. As a result, indirect photochemical transformations (Fig. 4B) such as the phenanthrene endo-peroxide formation after reaction with $^1O_2$ and the reduction of copper(II) to copper(I) resulting from reactions within the humic microenvironment may require explicit consideration of the relevant colloidally bound species.

The transport fate of chemicals such as phenanthrene and copper is also dependent on their propensity to be transferred into settling phases. Santschi and others

Fig. 4. Effects of the chem-centric speciation on transformations of chemicals. The interaction of trace chemicals with dissolved macromolecules (**A**), respectively in/on colloidal macromolecules (**B**) are providing significantly different surrounding media. Such differences in molecular-scale environment are likely to have implications for the fate of trace chemicals in general as illustrated here by the speciation-dependent processing of the hypothetical probes copper and phenanthrene.

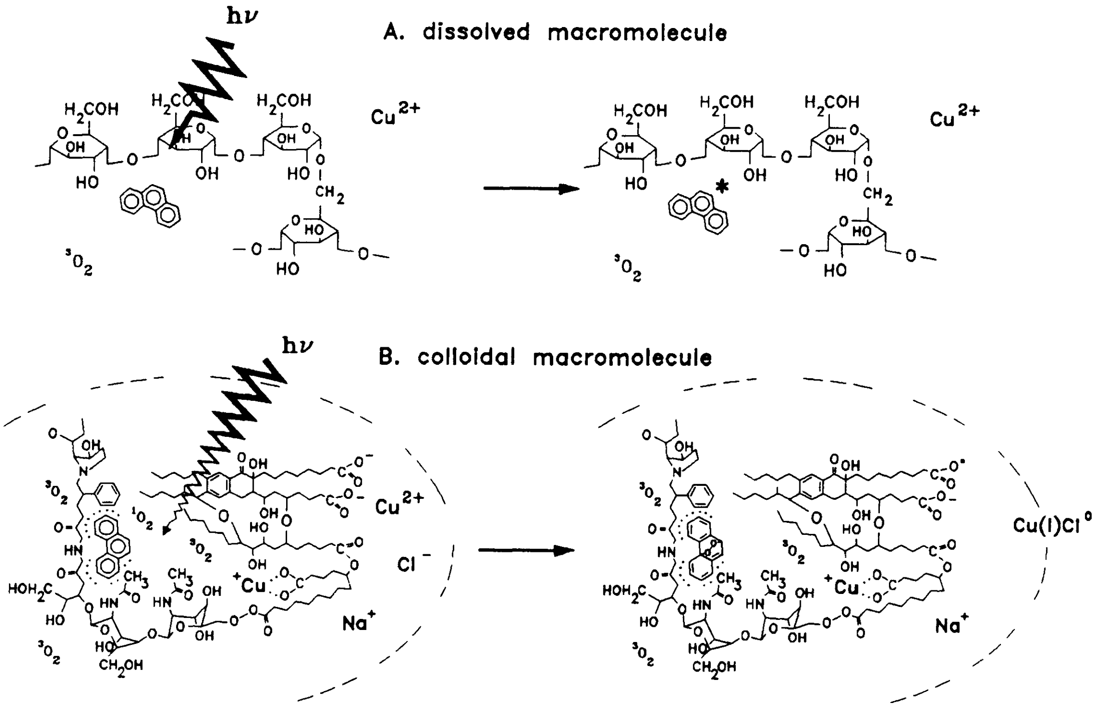
hν
A. dissolved macromolecule
H₂COH
Cu²⁺
OH
HO
CH₂
³O₂
*
hν
B. colloidal macromolecule
³O₂
¹O₂
Cu²⁺
Cl⁻
⁺Cu
Na⁺
HN
CH₃
HOH₂C
CH₂OH
Cu(I)Cl°

(e.g., Santschi et al. 1986; Honeyman and Santschi 1991) have shown that metals such as copper are first sorbed to colloidal phases, before coagulation of these small sorbents results in the accumulation of the sorbate (e.g., copper) with larger (and therefore potentially settling) solids. Thus, the relative tendency of the chemicals to be transported up the particle-size spectrum via piggy-backing is a function of the colloids with which they associate (McCarthy et al. 1993; Gu et al. 1995).

Another significant practical implication of the conceptual chem-centric colloid framework is that a traditional, filtration-based, definition will never succeed in distinguishing species that, in large part, behave independently of size. Hence, to make practical progress towards anticipating the environmental behavior of trace chemicals, analytical approaches that recognize their speciation, such as studies of the light processing abilities of chemicals of interest, are required to probe the physico-chemical distribution and behavior of the colloids and sorbing chemicals of interest. Similarly, to separate functionally between colloidal and gravitoidal sorbents, analytical techniques based on the (functional) sedimentation process such as centrifugation and split-flow thin cells (SPLITT; e.g., Giddings, 1988) should be further explored. An important consideration in the functional colloid-gravitoid distinction is that their boundary condition is dynamic and set by the environment-specific time-scale on which the coagulation and sedimentation processes occur for the specific solid phases present. With knowledge of the mixed layer depth and sizes and wet densitites of the particles, the relative importance of coagulation and sedimentation may be anticipated (e.g., Farley and Morel, 1986). From the chem-centric view of the researche interested in the gravitoid-bound vertical flux of a trace chemical, coupling of particulate inventories of the trace chemical with that of ^{234}Th and the total ^{238}U-^{234}Th disequilibrium may provide an indirect estimate of this process (see chapter 7).

Conclusions and current challenges

Studies of aquatic colloids, and in particular those addressing their role in affecting chemical speciation, have accelerated over the past ten years. However, only limited progress has been made in relating empirical distribution data to thermodynamically-based surface complexation and hydrophobic partitioning models. Enough is now frequently known about the physico-chemical system parameters that govern colloid partitioning in natural waters to attempt rationalization of the observed chemical distributions in terms of these well established theoretical frameworks.

One current challenge complicating the successful application of such an approach is selective assessment of only the organic macromolecules that are able to interact with, and thus change the speciation of, trace chemicals in natural waters. This challenge is especially difficult because, by our definition, not all macromolecules are colloids (i.e., offering an alternative phase to chemicals of interest). Currently used filter-size-based colloidal sorbent definitions constitute a severe limitation to such progress. Ultrafilters do not distinguish between colloidal and noncolloidal macromolecules. Also, filters with approximately micrometer-sized pores are not comprehensively applicable to distinguish between particles that experience significant settling removal from those that do not (e.g., marine snow), especially when applied statically with the same cutoff to environments of different particle dynamics (i.e., Fig. 2A).

Generation of yet more chemical distribution ratios between filter-based gravitoidal, colloidal, and dissolved fractions will do little to further our understanding of chemical speciation and cycling in lake and ocean waters. Real progress is more likely to come from investigations selectively probing the functional colloid-dissolved partitioning through relatively noninvasive techniques such as time-resolving fluorescence quenching spectroscopy and competitive-ligand titrations coupled with ion-selective electrodes. Such colloid partitioning results need to be accompanied by an increased effort to obtain necessary ancillary system parameters to enable interpretation of these observed D values in terms of the corresponding theoretical K values. Further, efforts to assess the fraction of sorbing media participating in settling transport are needed. Separation techniques based on specific density should prove useful in this regard, such as analytical ultracentrifugation (e.g., Sipos et al. 1972) and split-flow thin (SPLITT) cells (e.g., Giddings 1988; Fuh et al. 1992).

An aquatic colloid definition is suggested, based on whether the molecular-level interactions of a chemical with a particular entity result in that compound's involvement in colloidal processes (i.e., presence in a nonaqueous environment; participation in coagulation, but not settling). Thus, *an aquatic colloid is any constituent that provides a molecular milieu into and onto which chemicals can escape from the bulk aqueous solution, while its vertical movement is not significantly affected by gravitational settling.*

Acknowledgments

We gratefully acknowledge the constructive comments on this manuscript by K. Barbeau, K. Buesseler, and E. Sholkovitz. Funding was provided from the Office of Naval Research (grant # NOOO14-93-1-0883) and by a grant from the National Oceanic and Atmospheric Administration pursuant to Award No. NA36RM044-UM-S242. The views expressed herein are those of the authors and do not necessarily reflect the views of NOAA or any of its subagencies.

References

AIKEN, G. R., AND R. L. MALCOLM. 1987. Molecular weight of aquatic fulvic acids by vapor pressure osmometry. Geochim. Cosmochim. Acta 51: 2177-2185.

ALLDREDGE, A. L., AND M. W. SILVER. 1988. Characteristics, dynamics and significance of marine snow. Prog. Oceanogr. 20: 41-82.

AMON, R. M. W., AND R. BENNER. 1994. Rapid cycling of high-molecular-weight dissolved organic matter in the ocean. Nature 369: 549-552.

BAKER, J. E., P. D. CAPEL, AND S. J. EISENREICH. 1986. Influence of colloids on sediment-water partition coefficients of polychlorobiphenyl congeners in natural waters. Environ. Sci. Technol. 20: 1136-1143.

BAKER, J. E., S. J. EISENREICH, AND B. J. EADIE. 1991. Sediment trap fluxes and benthic recycling of organic carbon, polycyclic aromatic hydrocarbons, and polychlorobiphenyl congeners in Lake Superior. Environ. Sci. Technol. 25: 500-509.

BARTSCHAT, B. M., S. E. CABANISS, AND F. M. M. MOREL. 1992. Oligoelectrolyte model for cation binding by humic substances. Environ. Sci. Technol. 26: 284-294.

BASKARAN, M., P. H. SANTSCHI, G. BENOIT, AND B. D. HONEYMAN. 1992. Scavenging of thorium isotopes by colloids in seawater of the Gulf of Mexico. Geochim. Cosmochim. Acta 56: 3375-3388.

BOEHM, P. D., AND J. G. QUINN 1973. Solubilization of hydrocarbons by the dissolved organic matter in sea water. Geochim. Cosmochim. Acta 37: 2459-2477.

BROWNAWELL, B. J., AND J. W. FARRINGTON. 1986. Biogeochemistry of PCBs in interstitial waters of a coastal marine sediment. Geochim. Cosmochim. Acta 50: 157-169.

BUESSELER, K. O. AND OTHERS. 1996. An intercomparison of cross-flow filtration techniques used for sampling marine colloids: Overview and organic carbon results. Mar. Chem. 55: 1-31.

BUFFLE, J., AND G. LEPPARD. 1995. Characterization of aquatic collids and macromolecules. 1. Structure and behavior of colloidal material. Environ. Sci. Technol. 29: 2169-2175.

CHANDAR, P., P. SOMASUNDARAN, AND N. J. TURRO. 1987. Fluorescence probe studies on the structure of the adsorbed layer of dodecyl sulfate at the alumina-water interface. J. Colloid. Interface Sci. 117: 31-46.

CHIN, Y-. P., AND P. M. GSCHWEND. 1991. The abundance, distribution, and configuration of porewater organic colloids in recent sediments. Geochim. Cosmochim. Acta 55: 1309-1317.

CHIOU, C. T., L. J. PETERS, AND V. H. FREED. 1979. A physical concept of soil-water equilibria for nonionic organic compounds. Science 206: 831-832.

COALE, K. H., AND K. W. BRULAND. 1985. ^{234}Th:^{238}U disequilibria within the California Current. Limnol. Oceanogr. 30: 22-33.

DZOMBAK, D. A., AND F. M. M. MOREL. 1990. Surface complexation modeling: Hydrous ferric oxide. Wiley-Interscience.

FARLEY, K. J., AND F. M. M. MOREL. 1986. Role of coagulation in the kinetics of sedimentation. Environ. Sci. Technol. 20: 187-195.

FUH, C. B., M. N. MYERS, AND J. C. GIDDNGS. 1992. Analytical SPLITT fractionation: Rapid particle size analysis and measurement of oversized particles. Anal. Chem. 64: 3125-3132.

FRIEDLANDER, S. K. 1977. Smoke, dust and haze: Fundamentals of aerosol behavior. Wiley-Interscience.

GARBARINI, D. R., AND L. W. LION. 1986. Influence of the nature of soil organics on the sorption of toluene and trichloroethylene. Environ. Sci. Technol. 20: 1263-1269.

GIDDINGS, J. C. 1988. Continuous separation in split-flow thin (SPLITT) cells: Potential applications to biological materials. Separation. Sci. Technol. 23: 931-943.

GOLDBERG, E. D. 1954. Marine geochemistry 1. Chemical scavengers of the sea. J. Geol. 62: 249-265.

GOLDBERG, E. D., M. BAKER, AND D. L. FOX. 1952. Microfiltration in oceanographic research I. marine sampling with the molecular filter. J. Mar. Res. 11: 194-203.

GRAHAM, T. 1861. Liquid diffusion applied to analysis. Trans. Roy. Soc. (London) 151: 183-224.

GSCHWEND, P. M., AND S.-C. WU. 1985. On the constancy of sediment-water partition coefficients of hydrophobic organic pollutants. Environ. Sci. Tech. 19: 90-96.

GU, B., J. SCHMITT, Z. CHEN, L. LIANG, AND J. F. MCCARTHY. 1995. Adsorption and desorption of different organic matter fractions on iron oxide. Geochim. Cosmochim. Acta 59: 219-229.

GUSTAFSSON, Ö., K. O. BUESSELER, AND P. M. GSCHWEND. 1996. On the integrity of cross-flow filtration for collecting marine organic colloids. Mar. Chem. submitted.

HAAG, W. R., AND J. HOIGNÉ. 1986. Singlet oxygen in surface waters. 3. Photochemical formation and steady-state concentrations in various types of waters. Environ. Sci. Technol. 20: 341-348.

HILL, P. S. 1992. Reconciling aggregation theory with observed vertical fluxes following phytoplankton blooms. J. Geophys. Res. 97: 2295-2308.

HONEYMAN, B. D., L. S. BALLISTRIERI, AND J. W. MURRAY. 1988. Oceanic trace metal scavenging: the importance of particle concentration. Deep-Sea Res. 35: 227-246.

HONEYMAN, B. D., AND P. H. SANTSCHI. 1989. A Brownian-pumping model for oceanic trace metal scavenging: Evidence from Th isotopes. J. Mar. Res. 47: 951-992.

HONEYMAN, B. D., AND P. H. SANTSCHI. 1991. Coupling adsorption and particle aggregation: Laboratory studies of "colloidal pumping" using 59Fe-labeled hematite. Environ. Sci. Technol. 25: 1739-1747.

ISRAELACHVILI, J. 1992. Intermolecular and surface forces 2nd ed. Academic.

JACKSON, G. A. 1990. A model of the formation of marine algal flocs by physical coagulation prcesses. Deep-Sea Res. 37: 1197-1211.

JOHNSON, B. D., AND P. E. KEPKAY. 1992. Colloid transport and bacterial utilization of oceanic DOC. Deep-Sea Res. 39: 855-869.

JOHNSON, C. P., X. LI, AND B. E. LOGAN. 1996. Settling velocities of fractal aggregates. Environ. Sci. Technol. 30: 1911-1918.

KARICKHOFF, S. W., D. S. BROWN, AND T. A. SCOTT. 1979. Sorption of hydrophobic pollutants on a natural sediment. Water. Res. 13: 241-248.

KROGH, A. 1930. Eine Mikromethode für die organische Verbrennungsanalyse, besonders von gelösten Substanzen. Biochem. Z. 221: 247-263.

KROGH, A., AND E. LANGE. 1931. Quantitative Untersuchungen über Plankton, Kolloide und gelöste organische und anorganische Substanzen in dem Furesee. Int. Rev. Ges. Hydrobiol. 26: 20-53.

LEE, P. C., AND M. A. J. RODGERS. 1983. Singlet molecular oxygen in micellar systems. 1. Distribution equilbiria between hydrophobic and hydrophilic compartments. J. Phys. Chem. 87: 4894-4898.

LERMAN, A. 1979. Geochemical Processes Wiley.

McCARTHY, J. F., AND OTHERS. 1993. Mobility of natural organic matter in a sandy aquifers. Environ. Sci. Technol. 27: 667-676.

MCKEE, B., D. J. DEMASTER, AND C. A. NITTROUER. 1984. The use of ^{234}Th/^{238}U disequilibrium to examine the fate of particle-reactive species on the Yangtze continental shelf. Earrth Planet. Sci. Lett. 68: 431-442.

MCKEE, B., D. J. DEMASTER, AND C. A. NITTROUER. 1984. Temporal variability in the partitioning of thrium between dissolved and particulate phases on the Amazon shelf: implications for the scavenging of particle-reactive species. Cont. Shelf Res. 6: 87-106.

MORAN, S. B., AND K. O. BUESSELER. 1993. Size-fractionated ^{234}Th in continental shelf waters off New England: implications for the role of colloids in oceanic trace metal scavenging. J. Mar. Res. 51: 893-922.

MORAN, S. B., AND R. M. MOORE. 1989. The distribution of colloidal aluminum and organic carbon in coastal and open ocean waters of Nova Scotia. Geochim. Cosmochim. Acta 53: 2519-2527.

MOREL, F. M. M., AND P. M. GSCHWEND 1987. The role of colloids in the partitioning of solutes in natural waters, p. 405-422. In W Stumm [ed.], Aquatic surface chemistry. Wiley-Interscience.

O'CONNOR, D. J., AND J. P. CONNOLLY. 1980. The effect of concentration of adsorbing solids on the partition coefficient. Water. Res. 14: 1517-1523.

O'MELIA, C. R. 1987. Particle-particle interactions, p. 385-403. In W Stunm [ed.], Aquatic surface chemistry. Wiley-Interscience.

SANTSCHI, P. H., U. P. NYFELLER, Y. -H. LI, AND P. O'HARA. 1986. Radionuclide cycling in natural waters: relevance of scavenging kinetics, p. 183-191. P. G. Sly [ed.] In Sediments and water interactions. Springer.

SCHINDLER, P. W., AND H. GAMSJAGER. 1972. Acid-base reactions of the

TiO2 (Anatase)-water interface and the point of zero charge of TiO2 suspensions. Kolloid Z. Z. Pollymere 250: 759-763.

SCHINDLER, P. W., AND H. R. KAMBER. 1968. Die Acidität von Silanolgruppen. Helv. Chim. Acta 51: 1781-1786.

SCHWARZENBACH, R. P., P. M. GSCHWEND, AND D. M. IMBODEN. 1993. Environmental Organic Chemistry. Wiley-Interscience.

SHARP, J. H. 1973. Size classes of organic carbon in seawater. Limnol. Oceanogr. 18: 441-447.

SHOLKOVITZ, E. R. 1976. Flocculation of dissolved organic and inorganic matter during the mixing of river water and seawater. Geochim. Cosmochim. Acta 40: 831-845.

SILLÉN, L. G. 1961. The physical chemistry of seawater, p. 549-581. In M. Sears [Ed.] Oceanography. American Association for the Advancement of Science.

SIPOS, S., I. DÉKANY, F. SZANTO, AND É. SIPOS. 1972. Investigation of humic acids and metal humates with analytical ultracentrifuge. Acta Phys. Chem. 18: 253-257.

SMOLUCHOWSKI, M. 1917. Versuch einer matematischen Theorie der Koagulationskinetik kolloider Lösungen. Z. Phys. Chem. 92: 129-168.

STOLZENBACH, K. D. 1993. Scavenging of small particles by fast-sinking porous aggregates. Deep-Sea Res. 40: 359-369.

STOLZENBACH, K. D., K. A. NEWMAN, AND C. S. WONG. 1992. Aggregation of fine particles at the sediment-water interface. J. Geophys. Res. 97: 17,889-17,898.

STUMM, W., C. P. HUANG, AND S. R. JENKINS. 1970. Specific chemical interactions affecting the stability of dispersed systems. Croat. Chem. Acta 42: 223-244.

SWACKHAMMER, D. L., AND R. S. SKOGLUND. 1993. Bioaccumulation of PCBs by algae: Kinetics versus equilibrium. Environ. Toxicol. Chem. 12: 831-838.

TRANVIK, L. 1993. Effects of colloidal organic matter on the growth of bacteria and protists in lake water. Limnol. Oceanogr. 39: 1276-1285.

WEI, C. -L., AND J. W. MURRAY. 1992. Temporal variations of 234Th activity in the water column of Dabob Bay: Particle scavenging. Limnol. Oceanogr. 37: 296-

314.

WEILENMANN, U., C. R. O'MELIA, AND W. STUMM. 1989. Particle transport in lakes: Models and measurements. Limnol. Oceanogr. 34: 1-18.

WERSHAW, R. L. 1986. A new model for humic materials and their interactions with hydrophobic organic chemicals in soil-water or sediment-water systems. J. Contam. Hydrol. 1: 29-45.

WU, S.-H., AND P. M. GSCHWEND. 1988. Numerical modeling of sorption kinetics of organic compunds to soil and sediment particles. Water Resour. Res. 24: 1373-1383.

ZSIGMONDY, R. 1926. Über feinporige Filter und neue Ultrafilter. Biochem. Z. 171: 198-203.

ZSIGMONDY, R., AND W. BACHMAN. 1918. Über neue Filter. Z. Anorg. Allg. Chem. 103: 119-128.

Chapter 3

ON THE INTEGRITY OF CROSS-FLOW FILTRATION FOR COLLECTING MARINE ORGANIC COLLOIDS

Örjan Gustafsson[1,2], Ken O. Buesseler[2], and Philip M. Gschwend[1]

1: R. M. Parsons Laboratory for Water Resources and Hydrodynamics, MIT 48-415,
Dept. of Civil and Environmental Engineering, Massachusetts Institute of Technology.
Cambridge, MA 02139
2: Dept. of Marine Chemistry and Geochemistry, Woods Hole Oceanographic Institution.
Woods Hole, MA 02543

submitted
Marine Chemistry

ABSTRACT

The application of cross-flow filtration (CFF) to separate organic colloids with their sorbed load from dissolved components in seawater has been tested. Investigations have aimed at deconvoluting and quantifying several aspects of seawater CFF integrity: organic carbon blanks, membrane interactions (for both organic colloids and trace organic constituents), and the effective filter cut-off. A dynamic feed, permeate, and retentate sampling protocol during regular CFF fractionation of coastal seawater organic carbon and macromolecular standards was used to gain diagnostic information about sampling integrity.

The organic carbon blank of the membrane module was significant. Large amounts of low-C water were required to flush the system to attain acceptable levels in what appears to be a diffusion-limited conditioning process. Observed decreasing permeate flux as a function of concentration factor (*cf*) was shown to be directly correlated with CFF colloid-fouling. A series of experiments were performed with a set of standard macromolecules, added at realistic seawater concentrations, to distinguish colloidal losses to the membrane from breakthrough. It was found that large fractions of carbohydrate, proteinaceous, and synthetic amphiphilic macromolecules became associated with the Osmonics PT1 (polysulfone, nominal cut-off 1.0 kD) CFF all-glass-and-stainless-steel system while partitioning between the seawater suspension and the membrane slowly reached steady state. Without further losses to the membrane, the retention coefficients for the colloid standards were determined, and an inherent seawater colloidal suspension cut-off at about 50 kD was found. Comparisons with the membrane science literature and theoretical calculations are presented to rationalize the observed artifacts and to direct optimization schemes.

INTRODUCTION

The pivotal role of marine colloids in both major element and trace constituent cycling processes has been recognized for some time. Recently, attention has been given to the function of colloidal organic matter (COM) in the marine carbon cycle, not only because COM constitutes a large portion of the total reduced carbon in the ocean, but also because it appears to be a highly dynamic pool (e.g., Amon and Benner, 1994). Another important environmental process is sorption of metal and organic solutes to colloidal carrier-phases, affecting the physical speciation of trace chemicals and thereby controling their fates, toxicity, and bioavailability (e.g., Morel and Gschwend, 1987). The interaction of colloids may lead to aggregation into larger particles, which in turn may eventually settle. As a consequence, colloidally mediated "scavenging" results in removal of both bulk matter as well as associated trace components. While a physically-based functional definition of marine colloids would be preferable, so far in oceanography, colloids have been described operationally as the material that is collected between two sequential filters. In this paper, we shall adhere to an exclusively size-based definition, which normally entails a lower nominal cut-off around 1.0 or 10 kD, while the upper cut-off may range from 0.2-1.0 μm.

Representative sampling of marine colloids is complicated by several factors. Aquatic colloids inherently tend to coagulate with each other or with other surfaces throughout the collection device. Artifacts leading to either peptization (Gibbs, 1981) or coagulation (Leppard, 1986) during colloid sampling have been reported. Isolating enough dilute-ocean colloidal material to allow quantification of its characteristics and composition, while not suffering substantial fractionation, represents a special challenge to the sampling protocol.

Our long-term scientific objective concerning marine colloids is to quantify and understand their role in (i) the physical speciation of hydrophobic organic compounds (HOCs), and (ii) the solid-phase dynamics and relevance to the transport of HOCs in the ocean. As one approach, we sought to use CFF. Since CFF has also become the overall dominant technique for collecting marine colloids, the objective of this study was to systematically investigate the integrity of cross-flow filtration of organic colloids. Aspects of marine CFF integrity that required assessment were: (a) the system blank (both for bulk organic carbon and trace organic constituents), (b) membrane interactions (of both colloids and dissolved species), (c) effective size cut-off in seawater, and (d) retentate dynamics. Secondary aspects that influence the above concerns include the choice of equipment and operating conditions.

A variety of techniques have been employed to separate colloids from natural water matrices; for example, stirred-cell ultrafiltration (e.g., Sharp, 1973; Carlson *et al.*, 1985), ultracentrifugation (e.g., Sipos *et al.*, 1972; Buffle *et al.*, 1978; Wells and Goldberg, 1992), centrifugal ultrafiltration ("Centricon" microconcentrators; e.g., Chin and Gschwend, 1991), gel chromatography or high-pressure size-exclusion chromatography (e.g., Mantoura and Riley, 1975; Buffle *et al.*, 1978; Chin and Gschwend, 1991), resin-adsorption (XAD: Riley and Taylor, 1969; Stuermer and Harvey, 1977; Ehrhardt, 1983, CHROMOSORB T: Yunker *et al.*, 1989, C_{18}: Mills and Quinn, 1981; Mills *et al.*, 1987; Donat *et al.*, 1986; Amador *et al.*, 1990), imbedding suspensions in resins for electron microscopy (Perrett *et al.*, 1991), dialysis (e.g., Dawson and Duursma, 1974; Salbu *et al.*, 1985), field-flow fractionation (e.g., Giddings, 1981; Caldwell, 1988), and cross-flow filtration (e.g., Whitehouse *et al.*, 1986; accompanying papers in this issue).

Of these techniques, only resin-adsorption and cross-flow filtration are able to sample in a reasonable time the large volume of seawater commonly required to meet detection limits for the detailed characterization of the diverse colloidal materials. Since the resin-adsorption techniques extract materials based on their affinity for the solid phase, they recover some chemically-defined portion of both dissolved and colloidal substances, as opposed to a size-defined colloidal yield. Consequently, the past few years have seen an accelerated application of CFF to the study of the role of colloids in a variety of marine processes (Whitehouse *et al.*, 1989; Baskaran *et al.*, 1992; Benner *et al.*, 1992; Moran and Buesseler, 1992, 1993; Amon and Benner, 1994; Guo *et al.*, 1994; Sempére *et al.*, 1994).

In CFF the main retentate flow direction is parallel to the filter surface. After penetrating the depth-type membrane, the permeate also flows along the filter plane. While this flow design decreases concentration polarization artifacts common to conventional filters, thereby making higher fluxes with smaller pores possible, it has been long recognized that polarization and other membrane-fouling artifacts are still prevalent in the CFF separation method (e.g., Blatt *et al.*, 1970; Colton *et al.*, 1972; Fane *et al.*, 1983; Michelena *et al.*, 1994; Philp *et al.*, 1994). Recent reports in the membrane science literature have focused on modeling the observed processes which lead to incomplete recoveries and sample fractionation (e.g., Dharmappa *et al.*, 1992; Stamatakis and Tien, 1993; Song and Elimelech, 1995). This improved understanding of CFF artifacts has lead to new and improved designs, including pulsed flow through baffled tubular channels and novel inorganic membrane materials (e.g., Wang *et al.*, 1994; Sempéré *et al.*, 1994).

Some integrity testing of ultrafiltration membranes has been conducted in freshwater applications. Buffle *et al.* (1978), operating Amicon systems, reported that humic substances may adsorb to the membrane. This adsorption not only changes the apparent pore size, but it also modifies the filter characteristics by giving rise to charge repulsion of anionic solutes. Varying operational conditions yielded significantly different fractionation results. Buffle *et al.* (1978) recommended that the final concentration factor be less than 10 to avoid colloid aggregation and breakthrough. Also using Amicon systems, and humic-acid-like standard colloids, Aiken (1984) found that the actual membrane cut-off deviated by up to an order of magnitude from that specified by the manufacturer. Salbu *et al.* (1985) reported metal adsorption to a neutral membrane during lake-water colloid fractionation.

Some indirect indications of compromised integrity may also be found in the marine literature. The simplest performance test is to measure the permeate flow rate throughout a sampling run. With no other alterations to the operating conditions, the permeate flux, Ψ_{perm} (flow rate normalized to two-dimensional membrane surface area), is inversely proportional to the hydraulic resistances exerted by the CFF system (Song and Elimelech, 1995):

$$\Psi_{perm} \propto \frac{1}{R_{memb}} + \frac{1}{R_{pol}} + \frac{1}{R_{cake}} \qquad (1)$$

where R_{memb} is the inherent resistance to transmembrane flow of the membrane itself, R_{pol} is the resistance to flow resulting from a polarization layer of retained colloids near the membrane surface, and R_{cake} is the resistance that would be added if a filtration cake would form. While some level of concentration polarization is always taking place in any filtration procedure, cake formation would be unlikely to occur under CFF of relatively dilute natural water suspensions. In the absence of cake formation, any changes in permeate flux must be ascribed to changes in R_{memb} or R_{pol}, and these, in turn, must be due to retained colloids. Fane *et al.* (1981) proposed that R_{memb} is inversely proportional to the square of the pore-radius, r_p^2, which decreases as colloids clog these channels through the membrane.

In previous permeate rate measurements with Millipore systems (Whitehouse *et al.*, 1986, 1990; Moran, 1991), as well as in our study on an Osmonics CFF, there is a slow continuous decrease in Ψ_{perm} throughout the sampling runs (Figure 1). Furthermore, in the two runs with highest Ψ_{perm}, this is proceeded by a more rapid decrease over the first 50 L. According to Eq. 1, a decreasing permeate flux is indicative of an increasing resistance to flow throughout the run. No matter which mechanism is responsible, the decreasing Ψ_{perm} is direct evidence of losses of colloids from the matrix to the system. This "clogging" effect has also been reported widely in the membrane literature (e.g., Fane *et al.*, 1981; Philp *et al.*, 1994). This problem of decreasing Ψ_{perm} and its implications have also been noted elsewhere (Brownawell, 1991; Benner, 1991).

A second indication of compromised CFF integrity is the report by Benner (1991) that increased recoveries of marine colloids may be realized by rapid recirculation of the retentate with the permeate line closed at the end of a sampling session. This enhanced recovery has also been observed in our experiments (data not shown). These observations imply that the increased shear tends to decrease the thickness of the membrane polarization layer (suggesting significant colloid accumulation in a near-membrane layer, as opposed to within the membrane itself).

The goal of the present study was to investigate the integrity of using CFF to process seawater samples. Our technical approach was to conduct process-oriented experiments using a combination of natural analytes and standard organic colloids in coastal seawater. We employed a dynamic on-line sampling protocol of feed, retentate, and permeate solutions as a function of increasing time and concentration factor; and we continuously monitored mass balances for various organic colloids examined.

METHODS

In order to develop a seawater sampling system suited for HOC/colloid studies, the equipment design needed to meet several criteria. First, individual HOC occur at trace

Figure 1. Hydraulic permeate flux throughout marine CFF sampling (● = Scotian Shelf, Whitehouse (1990); = "seawater", Moran (1991); ♦ = Baltic Sea, Whitehouse *et al.* (1986); o = coastal MA, this study). A 1.0 kD nominal cut-off Osmonics CFF was used in this work, whereas 10.0 kD Millipore CFFs were used in the earlier studies.

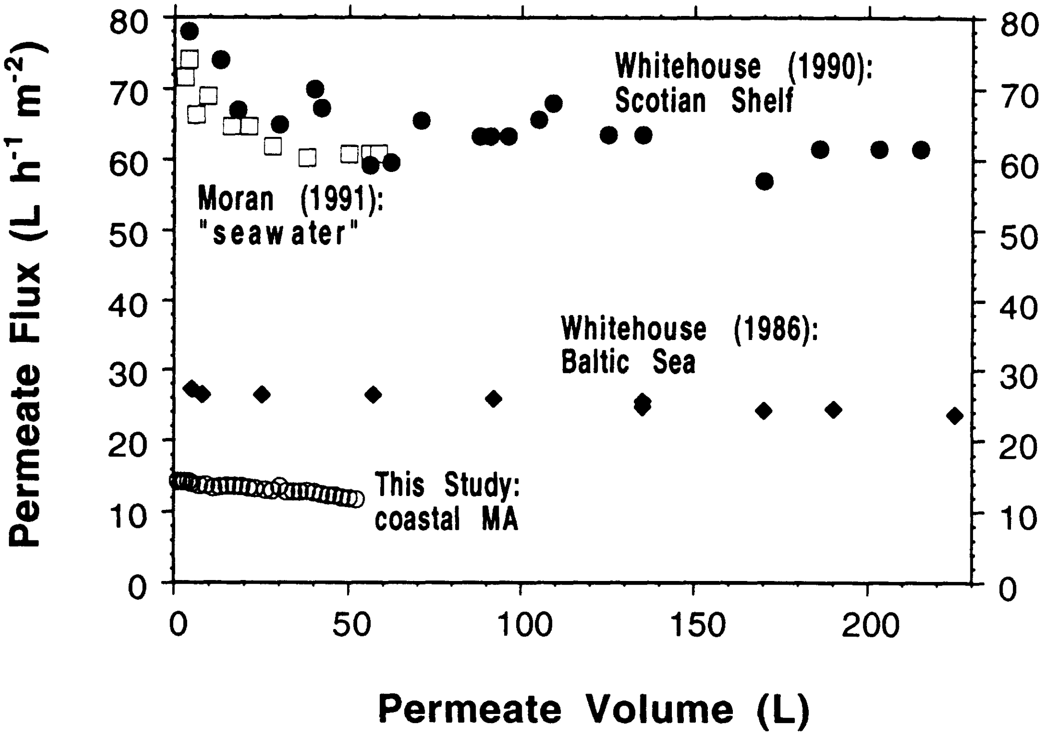
Permeate Flux (L h^{-1} m^{-2})
Permeate Volume (L)
0
10
20
30
40
50
60
70
80
0
50
100
150
200
Whitehouse (1990): Scotian Shelf
Moran (1991): "seawater"
Whitehouse (1986): Baltic Sea
This Study: coastal MA

levels (e.g., aM-fM; Gustafsson *et al.*, submitted), so the system requires correspondingly low blanks. Next, the HOCs exhibit high sorptive tendencies (aqueous activity coefficients to 10^{11}); thus construction material must minimally attract HOCs from solution. Our CFF system (Fig. 2) was constructed around a nominal 1.0 kD spiral-wound, polysulfone membrane (OSMO-112-PT1 "full fit", with about 1.0 m^2 filter area; OSMONICS Inc., Minnetonka, MN). The polymer used in our membrane was poly(oxy-1,4-phenylenesulfonyl-1,4-phenyleneoxy-1,4-phenylene(1-methylethylidene)-1,4-phenylene), a neutral copolyether-sulfone with a significant degree of conjugation. To minimize hydrophobic organic compound sorption to the surface materials, the permeate tube was constructed from 316 stainless steel. The polypropylene binder that normally covers the exterior of the membrane was removed ("full-fit" design; OSMONICS Inc.), and the spiral CFF was contained in a stainless steel filter housing. All tubing, valves, and holders throughout the system were high-grade 316 SS; these were replaced, if corroded, and thoroughly cleaned prior to each sampling event. A non-greased impeller-type pump of 316 SS and with a Teflon pump-house membrane (Prominent Fluid Controls, Pittsburgh, PA) continuously recirculated the retentate through the CFF module at 1.2 L/min from a specially fitted 4-L amber-glass retentate reservoir. Pressure was monitored throughout the system, and sampling ports were installed for frequent on-line sampling of feed, retentate, and permeate solution (Fig. 2). The system was operated with a transmembrane pressure of 8-12 psi yielding a permeate flow rate of 200-280 mL/min.

Coastal Massachusetts seawater (pre-filtered through GF/F filters ; Whatman Inc.) was used as the matrix in these exercises. In light of Chapter 2, this pre-filtration did not separate functionally between gravitoids and colloids. If not ultrafiltered right away, the seawater was stored in the dark at 6 °C and then refiltered (GF/F) preceeding experiments. The organic carbon (OC) content of the pre-filtered seawater remained constant (110-130 ±10 μM) during storage. For cleaning and blank-analysis, we used doubly-distilled RO water (≈ 30 μM OC), which hereafter will be referred to as "clean" water. Seawater was stored and introduced to the CFF system from glass carboys. The OC measurements of seawater and "clean" water were performed on a modified Ionics 555 HTCO instrument (Ionics Inc., Watertown, MA). Thirty milliliter samples for OC analyses were immediately acidified with 200 uL 50% H_3PO_4 and analyzed within hours,

Figure 2. Schematic of the HOC/colloid size fractionating sampling system. Fultz pump refers to *in situ* pumping system used for shipboard operations. In integrity experiments, the seawater was instead introduced from glass carboys.

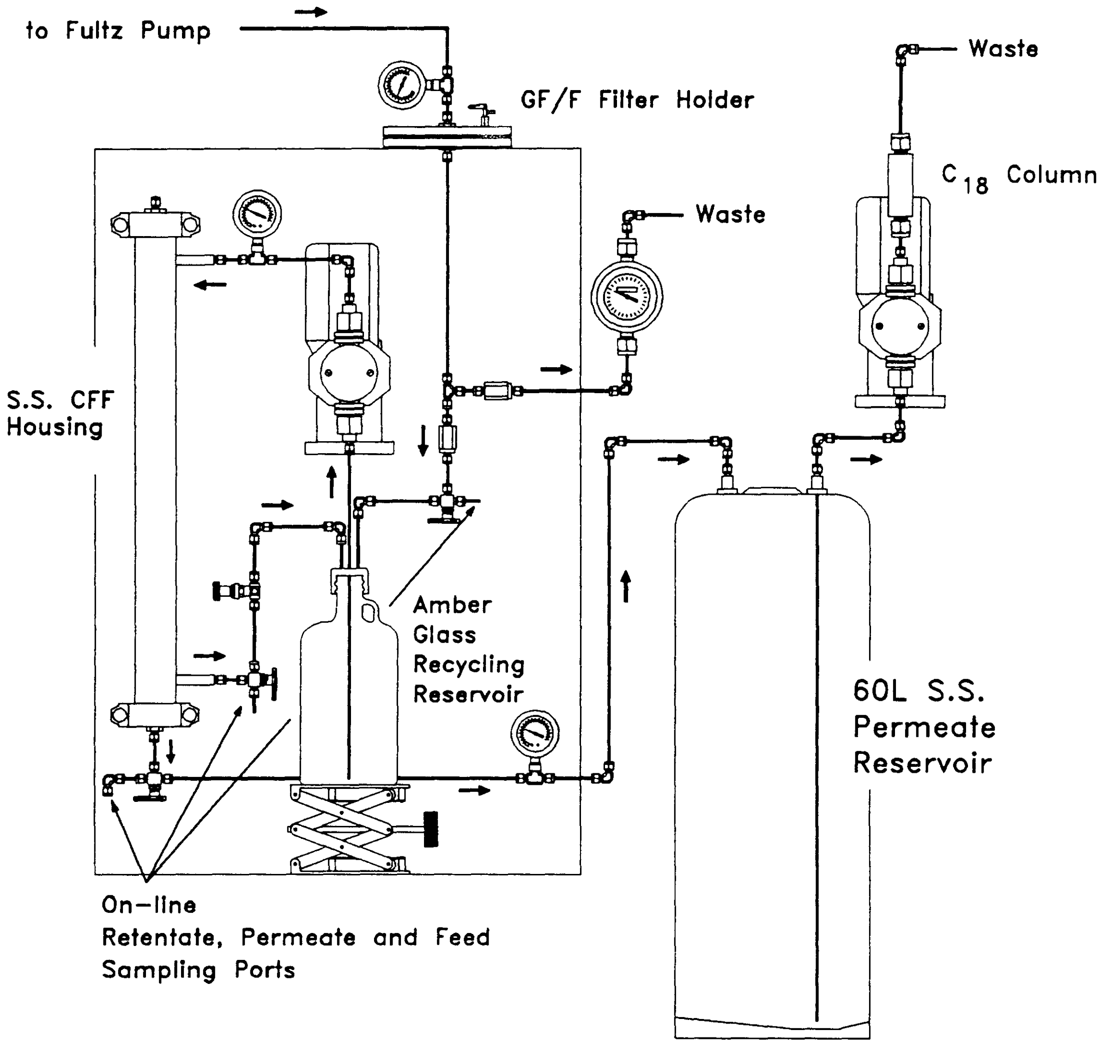
to Fultz Pump
GF/F Filter Holder
Waste
C18 Column
Waste
S.S. CFF Housing
Amber Glass Recycling Reservoir
60L S.S. Permeate Reservoir
On-line Retentate, Permeate and Feed Sampling Ports

in triplicate, after purging with N_2. Samples from the Pacific ocean and low-C water, provided by Ed Peltzer (WHOI, Woods Hole, MA), were used to verify our method. Agreement within 4% was obtained.

We used standard organic colloids to assess the CFF. Colloid standards were added to seawater at levels consistent with those reported for chemically comparable organic macromolecules in seawater (e.g., Lee and Bada, 1977; less than few-10s μM "OC"-equivalents), because it is known that the effective cut-off of CFFs is sensitive to the total colloid concentration. A range of standard organic colloids, representing the major marine organic colloid functionalities and spanning nearly two orders of magnitude in size, were used: polystyrene sulfonates, PSS, (1.8 kD MW, polydispersity of 1.25; Polyscience, Warrington, PA), dextran carbohydrates, DEX (3.0, 10.0, 40, and 70 kD MW, polydispersities of 1.3-1.6; Molecular Probes, Eugene, OR), polyethyleneglycol, PEG, (3.4 kD, polydispersity of 1.05; Shearwater Polymers, Huntsville, AL), and lactalbumin proteins, LAC, (14.8 kD; Molecular Probes, Eugene, OR). PSS was analyzed with a UV absorption spectrometer (DU 640, Beckman Instruments Inc., Fullerton, CA) at a wavelength of 225 nm. Fluorescein-conjugated derivates of DEX, PEG, and LAC were used (ca. 1 fluorescein/colloid; Molecular Probes, Eugene, OR). In this manner, micromolar OC-equivalent colloid levels could be quantified by fluorescence spectroscopy using 494 nm excitation (5 nm band width) and 524 nm emission (10 nm band width) wavelengths (PE LS 50B; PerkinElmer Ltd., Beaconsfield, Buckinghampshire, UK).

The applicability of the selected colloid standards was considered in detail. Dextran carbohydrates and polyethylene glycol, with or without a conjugated fluorescein, as well as polystyrene sulfonates, have all shown wide stability and applicability in various submicron size-exclusion studies, including both biological (e.g., Liang *et al.*, 1988; Pepperkok *et al.*, 1988; Rosemberg and Korenstein, 1990) and manufactured (e.g., Bottino *et al.*, 1984; Staub *et al.*, 1984; Chin and Gschwend, 1991; Sémperé *et al.*, 1994) membranes. The biologically unusual α-1,6-polyglucose linkages of the cross-linked dextran polysaccharides render these highly resistant to bio-enzymatic degradation. Furthermore, the conjugation of a succinimidyl ester derivative of fluorescein with an amino dextran, the synthetic path employed by Molecular Probes (Eugene, OR), results in the formation of highly stable amide linkages in these high purity fluorescent colloid standards (Haugland, 1992). These particular fluorescently tagged macromolecules have also proven effective in another seawater application (Carlson, 1991). A thin-layer chromatography (Baker-flex Silica Gel IB-F, J.T. Baker Inc., Phillipsburg, NJ) method was used by us to check the purity and solubility behavior of the fluorescein-labelled Dextran standard. Fluorescein, fluorescein-conjugated dextran, and free dextran were developed in parallell using a tertiary solvent system consisting of $CHCl_3$/ CH_3OH/CH_3COOH (91:6:3). The free fluorescein was mobilized ("R_f" = 0.8), whereas both the fluorescein-conjugated dextran and free dextran remained at the origin ("R_f" < 0.05) and showed no free fluorescein contamination. The fluorescent standard thus behaved like the non-conjugated form and was found to be of high purity. The conjugate also exhibited complete stability in seawater during storage for several days.

A batch sorption experiment to assess the association of 10kD-DEX with dissected CFF membrane in seawater was also performed. Three 250-mL glass bottles filled with seawater, one without any membrane (control), and two others with different masses of membrane, were spiked with DEX colloid standard and agitated on a wrist-action shaker in the dark. Repeated sampling of the suspension and analysis of the fluorescent DEX indicated when an apparent equilibrium distribution was achieved. Sorbed DEX was deduced by difference using the control.

Hydrophobic solutes were also tested for their tendency to sorb to the polysulfone membrane. We employed a set of standards spanning a range of well-known physico-chemical properties: toluene, n-propyl-benzene, naphthalene, and 1-methyl-naphthalene. These organic compounds were added to seawater and recirculated through the CFF system. Samples of retentate were withdrawn at intervals and analyzed by gas chromatography with flame ionization detection (GC-FID; Carlo Erba Strumentazione, Milan, Italy) through making direct aqueous injections following the method of MacFarlane and Gschwend (1987).

Different set-ups of the CFF system were required. In the standard configuration (referred to as the "sampling mode"), glass carboys with 20 L of freshly pre-filtered coastal seawater were positioned in place of the GF/F-filter holder (Fig. 2), and sample was continuously fed into the retentate reservoir. In the "one-pass mode", the retentate sampling port is left open to flush out non-desirable (e.g., cleaning) solutions. In the "recirculation mode" both the retentate and the permeate were fed back into the retentate reservoir. At times we would also bypass the actual CFF housing with supplemental tubing to differentiate interactions with the membrane from that to the rest of the system ("system-minus-membrane recirculation mode"). The feed, retentate, and permeate of the standard colloid-in-seawater solutions were sampled frequently throughout each run and analyzed within minutes.

For long-term storage, the CFF membranes were kept in a 10% methanol - 1% formaldehyde aqueous solution at the manufacturer's recommendation. The leaching protocol between samples began by rinsing any remnant seawater with a few liters of "clean" water. The CFF was subsequently cleaned by recirculating two solutions, each followed by "clean" water rinses. First, 0.01 M NaOH was recirculated for 15 minutes (PT1 Polysulfone recommended pH range is 1-13; Osmonics Inc.) with the objective of solubilizing fouling humic substances. This alkaline solution was immediately followed by one-pass, and then sampling mode, "clean" water until pH was near neutral. The second 15-min recirculation used an acidified (pH 2) 25% methanol aqueous solution, meant to solubilize metals and lipids. Finally, up to 60 L "clean" water were applied until a low organic carbon blank was achieved. Immediately prior to collection of a CFF sample, the system was conditioned in sampling mode with about 20 liters of 1 μm-filtered seawater.

At the Colloid Intercomparison Workshop on Hawaii, a colloid standard experiment was conducted to compare several different nominally 1 kD cut-off polysulfone CFF systems currently utilized throughout the oceanographic community to isolate marine colloids. Prefiltered intermediate Pacific seawater (water properties described in Sansone *et al.*, 1988) was spiked to a common 400 nM OC-equivalents of 3 kD DEX colloid standard. The spiked retentate was sampled before the start and at the conclusion of the experiment, while the permeate was sampled at *cf*=2 and at the conclusion (*cf*, concentration factor, is the ratio of total volume processed to the isolated volume retentate). Samples were collected in 40 mL amber vials, stored at 4°C and in darkness, and analyzed within a few hours using a Hitachi F-3010 fluorescence spectrometer, blank-corrected for the fluorescence of the 600 m seawater used. Intercalibrated 1 kD nominal cut-off CFF systems are described in greater detail in the overview paper of this volume (Buesseler *et al.*, 1996).

RESULTS and DISCUSSION

Blank and Recovery Assessment

Large volumes of "clean" water and, notably, significant time, were required to counter an initially high organic carbon blank (Figs. 3a and 3b). While a low OC blank eventually was achieved, >50 liters of "clean" water were required. The increase in the OC blank observed after the CFF had been in idle for several hours indicated that the cleaning was diffusion-limited. Hence, this CFF blank "memory effect" (Errede *et al.*, 1984) emphasizes the importance of performing the cleaning immediately prior to sampling (Fig. 3). This process may also explain many of the high initial blanks recorded at the Colloid Workshops, which could not be traced to organic-solution-stored CFFs (Buesseler *et al.*, 1996, this volume).

The blanks of individual HOCs were determined through both controlled recirculation exercises and through mass balances in samples and leachates from the field. Using the "recirculation mode", 3 L of "clean" water was processed through both the permeate and retentate for 1 hour. At the end of this time, samples were collected for direct aqueous injection on GC-FID. Five detectable peaks eluting in the 190-210 °C range were found, corresponding to a total mass of about 20 μM carbon. Hence, at least a portion of the OC blank consists of relatively low-molecular-weight nonpolar compounds.

It does not appear feasible to background-correct CFF data for OC because of the existing difficulty to isolate a true blank value. The "clean" water type CFF blanks described above and reported elsewhere (e.g., Whitehouse *et al.*, 1986, 1989, 1990; Sémpére *et al.*, 1994; Buesseler *et al.*, 1996) are not at realistic seawater pH and ionic strength, and consequently may not reflect the true blank during seawater operation. However, the inherently low background of such "clean" water matrices simplifies any blank quantification since simultaneous losses of monitored chemicals from solution is thus avoided. UV-irradiated deep ocean seawater may serve as a better blank solution. Because of its low background, such low-C seawater could only have very small losses to the system and would consequently provide a higher signal-to-noise blank sensitivity. In addition to bulk matter (e.g., OC), the background levels of analytes of specific interest (e.g., trace metals and organic compounds) as well as potentially interfering chemicals (e.g., paramagnetic Fe in NMR analyses) could ideally be quantified.

Figure 3. Organic carbon blank of CFF during **(a)** one-pass flushing followed by **(b)** sampling mode cleaning, performed with repetitive 15-20 L batches of "clean" water spaced over time (Δ = permeate, ● = retentate, and = feed solution). Times in parentheses represent time since start of first flushing (a batch of one-pass and sampling mode cleaning takes 15 and 80 min., respectively).

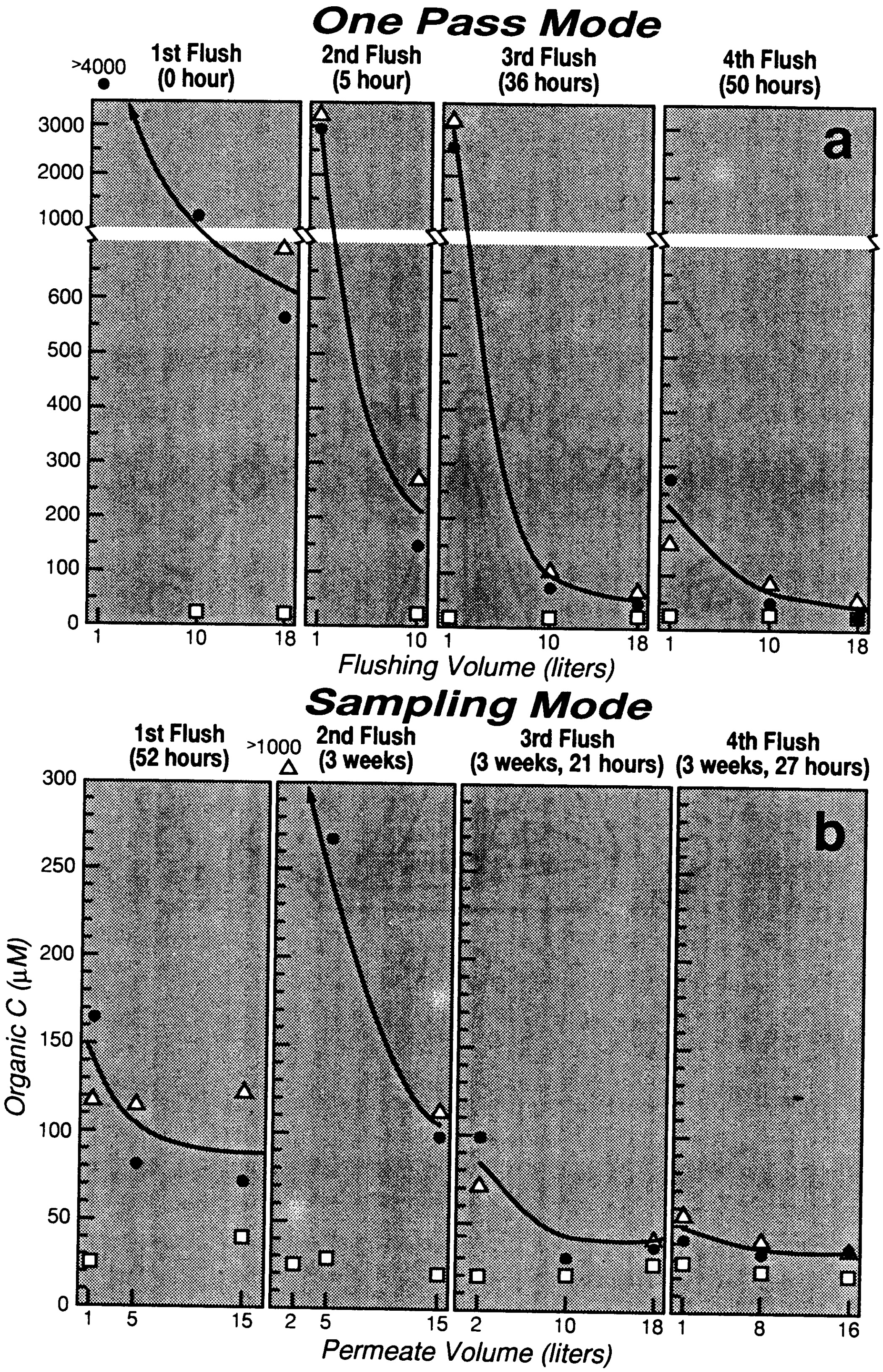
One Pass Mode
>4000
1st Flush
(0 hour)
2nd Flush
(5 hour)
3rd Flush
(36 hours)
4th Flush
(50 hours)
a
3000
2000
1000
600
500
400
300
200
100
0
1
10
18
1
10
1
10
18
1
10
18
Flushing Volume (liters)
Sampling Mode
1st Flush
(52 hours)
>1000
2nd Flush
(3 weeks)
3rd Flush
(3 weeks, 21 hours)
4th Flush
(3 weeks, 27 hours)
b
300
250
200
150
100
50
0
Organic C (µM)
1
5
15
2
5
15
2
10
18
1
8
16
Permeate Volume (liters)

Another approach to addressing blanks and losses of substances during CFF is to look at the apparent recovery, R%, at the conclusion of a seawater sampling run (e.g., Whitehouse *et al.*, 1986, 1990; Benner *et al.*, 1992; Guo *et al.*, 1994). For instance, one may sum the OC in the *cf*-corrected retentate (=[coll]) and permeate (=[diss]) and contrast them with the OC of the influent (=[feed]):

$$\mathbf{R\% = 100 \frac{[Coll] + [Diss]}{[Feed]}} \qquad (2)$$

While this approach uses the OC in seawater itself and provides a useful initial indicator of gross contamination, it also has a number of limitations. Most importantly, examination of R% does not separate the two simultaneously occurring processes: contamination by the system and losses to the system. For instance, if R% < 100%, one may only conclude that losses are greater than contamination, whereas for R% > 100%, one sees that contamination is greater than losses to the system. Whitehouse *et al.* (1990) have pointed out that R% is insensitive to actual colloid recovery unless the colloidal fraction is very high. This situation is exacerbated because the deviation of R% from 100% is highly sensitive to a correct (i.e., < few μM OC) analytical blank subtraction (Sharp *et al.*, 1995). This becomes particularly problematic when working with low carbon waters. Recent intercomparison results of OC analysis have highlighted the existing uncertainty and sensitivity of the correct assessment and subtraction of this analytical blank (Sharp *et al.*, 1995).

Sorptive losses to the large CFF membrane is likely to occur in response to the physical chemical properties of the system. In the Gulf of Maine, a dominant portion of some hydrophobic compounds (PAHs, PCBs) were lost to the CFF system and were recoverable in the base and methanol leachates (Gustafsson and Gschwend, unpublished results). Similar substantial losses have been reported also for other low-solubility chemicals such as ^{234}Th (Baskaran *et al.*, 1992), Fe for all CFF systems in the Colloid Workshop (Reitmeyer *et al.*, this volume), and certain other trace metals (Wen *et al.*, this volume). Consequently, leaching is necessary to quantify such losses and to mitigate carry-over between samples. It is very difficult to determine whether these recoverable substances originally were dissolved or associated with colloids. Clearly, such losses raise concern about organic matter fractionation during CFF. We do not believe that it is currently possible to assign them to either of these fractions.

Colloid-Membrane Associations

The first aspect of CFF sampling integrity that was possible to address by applying standard organic colloids was the extent to which macromolecules associated with the CFF membrane. In an initial CFF colloid integrity test with our 1 kD cut-off system, pre-filtered seawater in the retentate reservoir was spiked with 3kD-DEX and 12 L permeate was obtained in regular sampling mode (Fig. 4). This standard colloid disappeared almost completely from the retentate solution, while 25% was accounted for in the permeate. Hence, about 70% was lost to the system in this experiment. Clearly, two non-desirable processes were occurring simultaneously: colloid losses to the CFF system and colloid breakthrough to the permeate side.

To deconvolute losses to the membrane from colloid breakthrough, we examined both the retentate and permeate contents throughout experiments conducted by recirculating the colloid-spiked seawater. This "recirculation mode" allows quantification of the "loss capacity" of the system towards the tested standard colloid types (Fig. 5). When the membrane was bypassed, no losses resulted. Hence, the interaction was with the CFF membrane, as opposed to with any other part of the system. It appears that the observed interaction eventually resulted in a steady-state distribution of the colloid, where the forward and reverse rates of exchange were equal (Fig. 5). The fraction of colloid lost from the seawater to the CFF membrane, once this steady state was established, may be defined as:

$$F_{loss} = \frac{C_0 - C_f}{C_0} \tag{3}$$

where C_0 is the starting seawater colloid concentration and C_f is the concentration when no more loss occurs. F_{loss} for the 10kD-DEX carbohydrate (Fig. 5) was 0.95. While the data are reminiscent of that from sorption kinetics, the lack of direct evidence prevents us from concluding that the interaction was sorptive in nature as opposed to a physical, or hydraulic, effect (see below).

Batch sorption experiments of 10kD-DEX with dissected membrane material suspended in seawater also resulted in substantial colloid losses from solution (Fig. 6). While the DEX in the control remained at a constant level, the DEX concentrations decreased in proportion to the amount of membrane present, indicating a sorptive interaction between the colloid and the membrane. The resulting sorptive distribution

Figure 4. Initial CFF integrity experiment where retentate reservoir was spiked with standard 3 kD DEXTRAN colloid (● = retentate and Δ = permeate).

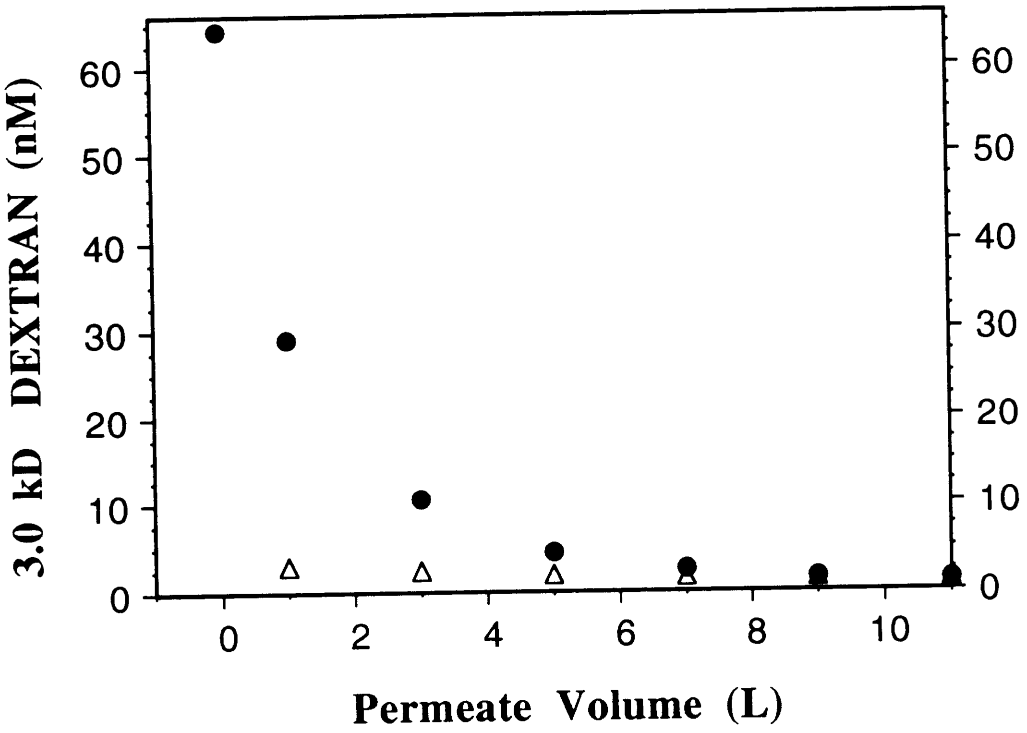
3.0 kD DEXTRAN (nM)
Permeate Volume (L)
0
10
20
30
40
50
60
0
2
4
6
8
10
0
10
20
30
40
50
60

Figure 5. Recirculation-mode CFF integrity experiment where retentate reservoir was spiked with standard 10 kD DEXTRAN colloid. The *open circles* (**o**) represent the result with the membrane by-passed (starting conc. 7 nM), whereas the *filled in circles* (●) was the level in the retentate during CFF recirculation (starting concentration 20.5 nM).

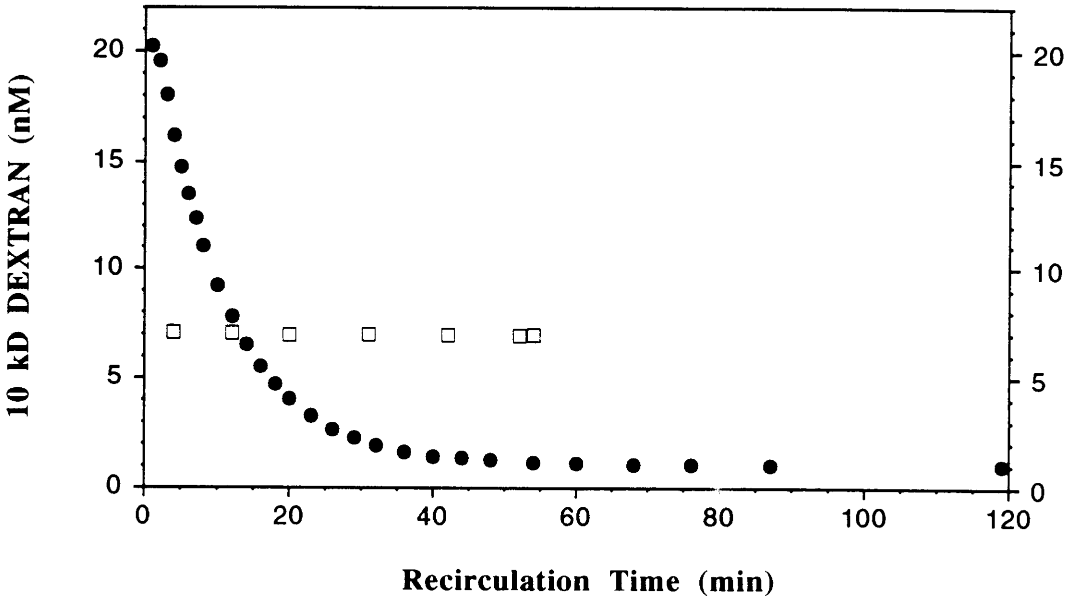
10 kD DEXTRAN (nM)
Recirculation Time (min)
0
20
40
60
80
100
120
0
5
10
15
20

Figure 6. Batch sorption experiment. Concentration of 10-kD DEXTRAN colloid in agitated seawater with suspended CFF membrane pieces (performed in the dark).

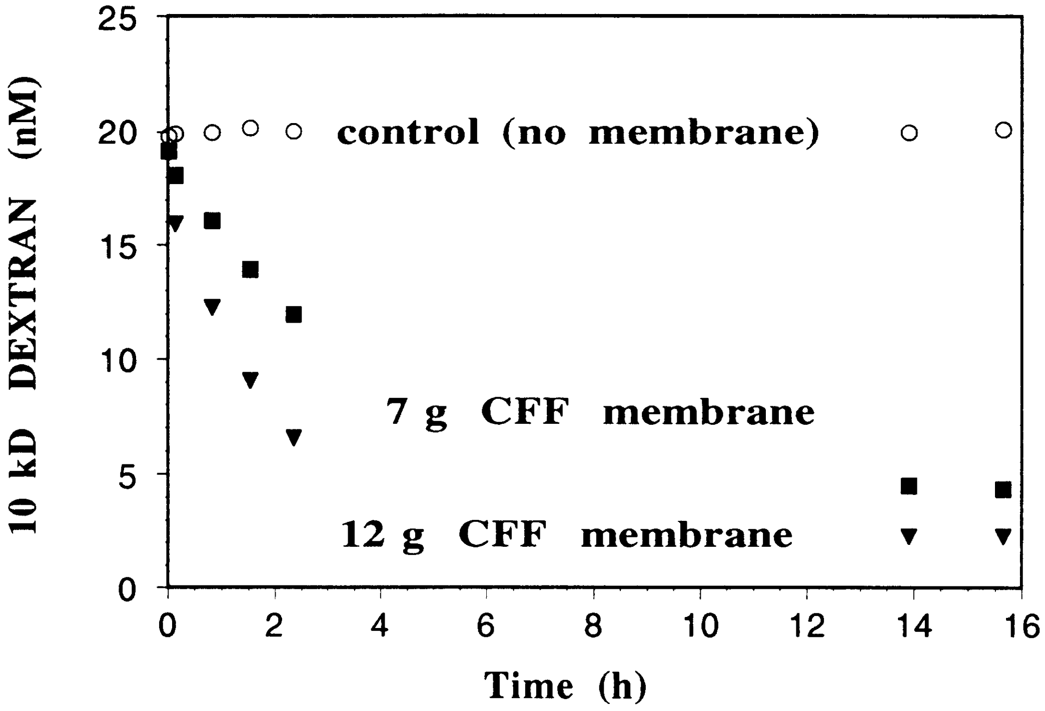
10 kD DEXTRAN (nM)
25
20
15
10
5
0
0
2
4
6
8
10
12
14
16
Time (h)
control (no membrane)
7 g CFF membrane
12 g CFF membrane

coefficient for DEX between the CFF membrane and seawater was about 100 L_{sw}/kg_{memb}. This would correspond to a F_{loss}= 0.9 for the membrane-seawater ratios found in the intact CFF system. Hence, this sorption result can explain the bulk of the losses found for the intact CFF system (Fig. 5).

F_{loss} results for all the colloid standards, obtained under identical conditions, were in the range 0.91-0.97 (Table 1). The macromolecular standards varied significantly in terms of their functional groups and size, yet a dominant fraction of all colloids tested eventually became associated with the membrane. However, the rate at which this equilibrium distribution was achieved decreased for larger colloid molecules (Table 1). A number of these experiments were repeated on a second identical system (data not shown), yielding very similar results. These results suggest that a mass transfer process characterizes the loss mechanism. More importantly, such differential behavior further suggests the likelihood of colloid fractionation by CFF.

The scope of this initial study did not include optimizing operational protocols. However, repeating the 40kD-DEX experiment with the permeate flow rate reduced to 25% of normal flux, yielded an intriguing outcome (Table 1). Both the loss rate was decreased and the total colloidal material lost to the CFF membrane in the end was much less. Furthermore, a significantly larger fraction of the colloid remained in the retentate pool. This result suggests that colloid losses may not simply be sorptive in nature.

Recovery of colloidal macromolecules was a function of time when CFF was utilized in the regular sampling mode. In the same experiment that a decreasing hydraulic permeate flux was noted as a function of *cf* (Fig. 1), the pre-filtered seawater was spiked with a 70kD-DEX colloid standard, and the feed, retentate, and permeate levels were analyzed throughout the run (Fig. 7). The concentrations of 70 kD-DEX in both the feed and the permeate stayed constant throughout the run. The retentate contents increased linearly as a function of concentration factor. However, mass balance calculations indicate that a continual loss (≈ 75%) of this carbohydrate standard occured throughout the entire filtration process. While colloids were continuously being concentrated, the slope of the retentate did not approach that predicted for no losses (upper solid line in Fig. 7), indicating that the loss mechanism was not saturated throughout the 52 L of seawater processed. F^*_{loss}, the fraction of colloid standard lost in this sampling mode test, may be calculated analogous to the equilibrium loss-factor, F_{loss} (Eqn. 3). While significant membrane associations were also taking place in the regular sampling mode, three times as much colloids stayed in suspension compared to in the recirculation mode experiment [i.e., $(1-F^{*}_{loss}) = 3\,(1-F_{loss})$]. Hence, the loss process did not appear to reach partition equilibrium for this 70kD standard during a regular sampling run. F_{loss} may be better viewed as a measure of the thermodynamic loss potential of a given colloid in the system.

It is necessary to discern the processes causing the observed colloid losses in order to mitigate them. In the present study, similar F_{loss} values were observed for a 10kD-DEX colloid standard in both recirculation (Fig. 5) and batch (Fig. 6) experiments, indicating a chemically driven sorption interaction. On the other hand, nearly identical CFF-recirculation F_{loss} results for many different colloid functionalities and sizes (Table 1) suggested that the colloid chemical properties were not determining factors in the loss process. This view is also supported by the variations in F_{loss} observed for a 40kD-DEX when a varying permeate flux was used (Table 1). Different CFF systems, with presumably similar 1kD polysulfone membrane material, but operated under varying flow and pressure conditions, differed greatly in recorded losses (test performed at the Colloid Intercomparison Workshop, see below); a result which also is difficult to rationalize with a single chemical sorption process. Hence, while some results clearly point towards a sorptive loss mechanism, other results support a physical loss mechanism.

In this section we examine if a hydraulically-induced loss process can be responsible for the observed behavior. It has been shown that some colloid loss to CFF membranes is dependent on the hydrodynamics of the system (e.g., Suki *et al.*, 1984). The dependency of F_{loss} on transmembrane pressure documented above, is consistent with a physically driven loss process.

Mass balance of colloidal substances in the CFF system requires that:

$$\mathbf{C_f V_{sw} = C_0 V_{sw} - M_p A_{memb}} \qquad (4)$$

where V_{sw} is the volume of colloid-spiked seawater equilibrated with the system in a recirculation experiment (m^3), M_p is the membrane surface concentration of polarized colloids (mol/m^2), and A_{memb} is the membrane surface area (m^2). Song and Elimelech (1995) have developed a general theory for concentration polarization in cross-flow

TABLE 1 Comparison of equilibrium loss factors, retention coefficients, and e-folding times[a] of standard colloids in CFF recirculation experiment

Colloid Standard	F_{loss}	RC	e-time (min)
Polystyrene Sulfonate (1.8 kD)	0.94	0.036	6.5
Polyethylene Glycol (3.4 kD)	0.96	0.061	12
Dextran (10 kD)	0.95	0.11	13
Lactalbumin (14.8 kD)	0.93	0.14	11
Dextran (40 kD)	0.97	0.34	28
Dextran (70 kD)	0.91	0.80	52
Dextran[b] (40 kD)	0.83	0.79	97

[a] Time to reach e^{-1} of initial concentration.

[b] The permeate flow rate was reduced to 25% compared to all the other experiments.

Figure 7. Sampling-mode CFF integrity experiment with 70 kD DEXTRAN spiked into 52 L seawater (● = retentate, Δ = permeate, and = feed solution). The *solid lines* represent the predicted evolution of colloid concentration in the retentate and the permeate, respectively, expected from the equilibrium RC of 0.80 if no net losses would have occurred (Table 1). Note that these permeate levels were easily detected.

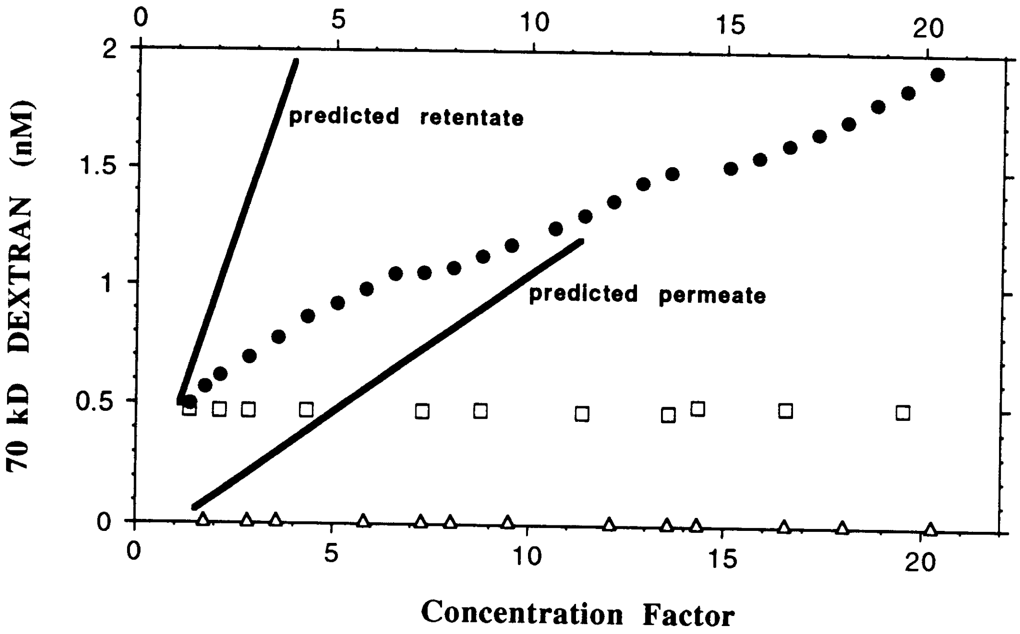
0
5
10
15
20
2
1.5
1
0.5
0
predicted retentate
predicted permeate
70 kD DEXTRAN (nM)
0
5
10
15
20
Concentration Factor

filtration based on the hydrodynamics of the system. These investigators have shown that the abundance of colloids, focused in a boundary layer near the CFF membrane, can be described by:

$$M_p = \frac{C_0}{D\,\gamma}\, v_{perm}\,(u_0 - u)\,B \qquad (5)$$

where D is the colloid aqueous diffusivity ($m^2\,s^{-1}$), γ is the longitudinal shear rate (s^{-1}), v_{perm} is the permeate linear velocity ($m\,s^{-1}$), u_0 and u are the longitudinal retentate channel velocities ($m\,s^{-1}$) at the inlet and at the outlet of the CFF cartridge, respectively, and B is the retentate channel width (m). A theoretical formulation of F_{loss}, termed F'_{loss}, describing the accumulation of colloids on the CFF system that results from concentration polarization, may be derived by inserting Eq. (5) into Eq. (4) and rearranging for F'_{loss}.

$$F'_{loss} = \frac{A_{memb}\, v_{perm}\,(u_0 - u)\,B}{V_{sw}\, D\,\gamma} \qquad (6)$$

The magnitude of F'_{loss}, representing only physically-induced colloid loss, may thus be estimated *a priori* for any CFF system, given information about the flow and operating conditions used. An aqueous diffusivity of $D = 1.3 \times 10^{-10}\ m^2\,s^{-1}$ for the 10 kD carbohydrate colloid was estimated following the approach of Chin *et al.* (1991). The one parameter in the above expression that is the least understood is the CFF shear rate. The longitudinal shear rate in a flow system of parallel plates may simply be approximated by (Schlichting, 1968):

$$\gamma \approx \frac{u'}{\delta} \qquad (7)$$

where u' in our case equals $(u_0+u)/2$, and where δ is the boundary layer thickness. Using the theory of flow field-flow fractionation developed in Beckett *et al.* (1987), the thickness of the colloid cloud accumulated at a membrane with cross-flow, can be estimated by the ratio of the aqueous colloid diffusivity and permeate (cross-flow) linear velocity:

$$\delta \approx \frac{D}{v_{perm}} \qquad (8)$$

For our CFF application we estimated a boundary layer thickness of 37 μm and a resulting shear rate on the order of 400 s^{-1}. With the dimensions and operating conditions of our Osmonics CFF system outlined above (and $u' = 1.5 \times 10^{-2}$ m s^{-1}, $B = 1.3 \times 10^{-3}$ m) and the calculated values for D and γ, we use Eq. (6) to estimate that concentration polarization can account for a significant part of our colloid loss ($F'_{loss} = 0.14$ for the 10 kD Dextran). Furthermore, if we use the typical shear rate suggested by Song and Elimelech (1995) for CFF systems ($\gamma = 100$ s^{-1}), then the F'_{loss} becomes 0.56. Also, consistent with the data, Eq. (6) predicts less colloid losses with decreasing v_{perm}; a result observed for the 40kD-DEX when the permeate flow was reduced (Table 1). The batch sorption experiments, along with this theoretical concentration polarization calculation, show that both chemical and physical loss mechanisms are plausible to account for the observed colloid-CFF associations.

Size Cut-off

The second CFF property that was quantified with dilute seawater suspensions of standard organic colloids was the membrane size cut-off. At the asymptotic plateau in a recirculation experiment, the concentrations of the colloids remained constant in both the retentate and the permeate (Fig. 8). Due to this steady state condition where net colloid losses to the membrane have stopped, one may solve for the retention coefficient, RC:

$$RC = \frac{[ret] - [perm]}{5/6[ret] + 1/6[perm]} \qquad (9)$$

where RC is the retention coefficient of a colloid and [perm] and [ret] are the concentrations of colloid standard in the permeate and retentate outlets, respectively, at the time when steady-state partitioning has been achieved. The denominator represents the mixed feed solution that is recirculated through the CFF, taking the relative flows into consideration (1.0 L/min retentate and 0.2 L/min permeate). As expected, RC values increased with the size of the standard colloids (Table 1). Since a range of colloid sizes was used, this data set could be employed to calibrate the CFF cut-off in a seawater

Figure 8. Recirculation-mode CFF integrity experiment where retentate reservoir was spiked with standard 70-kD DEXTRAN colloid (● = retentate and Δ = permeate).

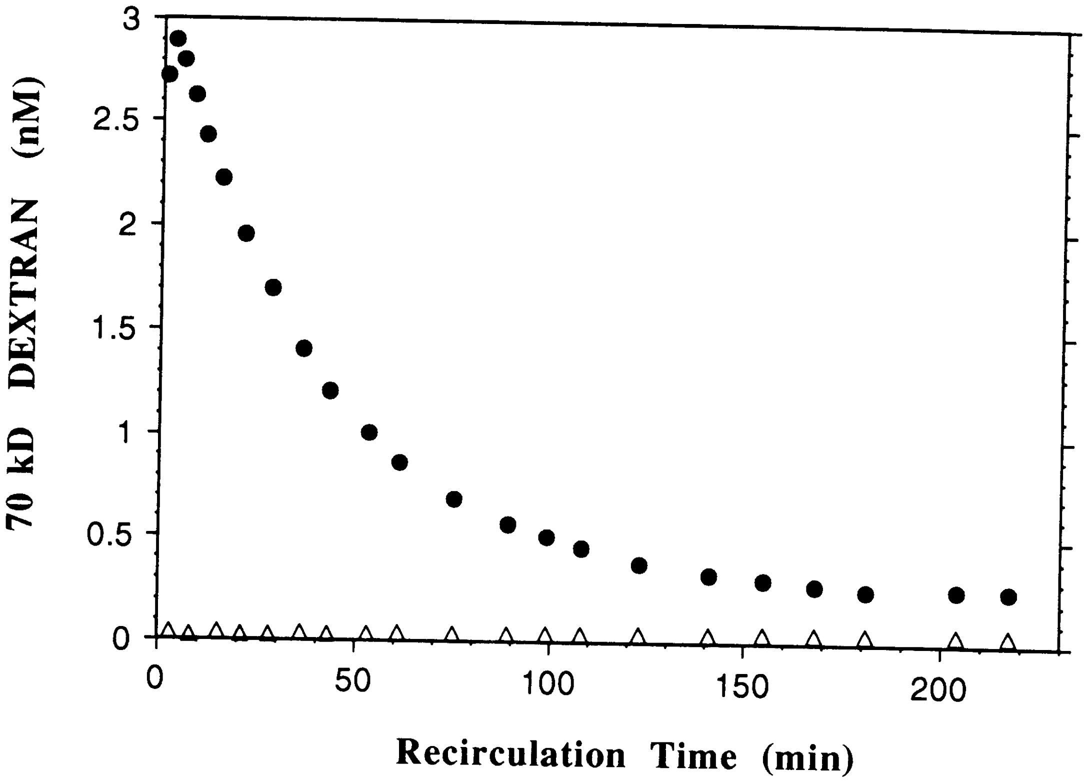
3
2.5
2
1.5
1
0.5
0
0
50
100
150
200
70 kD DEXTRAN (nM)
Recirculation Time (min)

matrix with realistic nanomolar concentrations of colloids (Fig. 9). A much larger inherent cut-off (ca. 50 kD; defined as 50% retention) was obtained than that expected based on manufacturer calibration (1.0 kD). The result of calculating an apparent RC, RC*, when net losses of colloids during membrane penetration are still occurring leads to an artificially low value for [perm] in the regular sampling mode and consequently an overestimation of RC. This is evident for the 70 kD-DEX run in both "recirculate" (no net losses at large times) and "regular sampling" (continuous losses). The inherent RC was 0.80 (Table 1 and Fig. 8), while the RC* from the latter test was > 0.97 (Fig. 7). Such loss-affected "apparent" RCs (i.e., RC*) may result in a conclusion of a smaller CFF cut-off than we determined here.

The discrepancy between the CFF cut-off observed in dilute colloidal suspensions of seawater and that specified by the manufacturer need to be understood. Commonly, the protocols used in manufacturer CFF calibration involve a suite of size-standards and conditions designed to mimic industrial applications, where colloid concentrations are typically in the order of g/L. This is obviously quite unrealistic for marine conditions. Cut-off calibration of CFF membranes, such as the ones we used, involves using a series of dextrans at an aqueous concentration of 3 g/L (Brian Rudie, Osmonics Inc., pers. comm.). Their experiences with several CFF brands have shown a clear relationship between the level of colloid standard used and the nominal cut-off obtained. When a nominal 1.0 kD membrane (as determined at 3 g/L) had been tested with 100 mg/L standard solutions, the cut-off realized was about 10 kD (Rudie, pers. comm.). The apparently decreasing cut-off with increasing colloid concentration was coincident with loss of dextran (and protein) standards, implying fouling of membrane surfaces. The dependency of retention behavior and effective cut-off on colloid characteristics and adsorption has also been reported in the membrane literature (e.g., Fane *et al.*, 1983; Bottino *et al.*, 1984). The observations of increasing rejection (apparently decreasing cut-off) and decreasing flow-rate have been shown to result directly from colloid adsorption on the membrane (e.g., Fane *et al.*, 1983; Suki *et al.*, 1984; Philp *et al.*, 1994). As pointed out above, a pre-requisite for obtaining a non-biased RC is that there are no more net losses of colloids to the CFF, as this would lead to an artifactually low permeate level and consequently an overestimation of the RC. As would be expected for any kinetically influenced process, membrane losses, as well as apparent cut-off, are both highly influenced by the operating conditions. An implication of these results is that the CFF cut-off needs to be calibrated by the user for each specific application.

CFF Systems Intercalibration

At the Hawaii Colloid Intercomparison Workshop, a group effort was made to initiate **intercalibration** of several CFF 1 kD polysulfone systems utilized for marine research. Taking the mean of the two permeate samples collected at *cf* = 2 and *cf* = final as representative of the colloid level in the permeate, the distribution of the 3.0 kD DEX carbohydrate standard between the retentate, permeate, and inferred losses to the CFF system, was calculated (Table 2). General trends among the different manufacturer CFF systems were apparent. The Membrex vortex flow filtration (system X1) had an apparent seawater cut-off that was much larger than the manufacturer-specified 1.0 kD, although almost none of the 3.0 kD DEX was lost to this type of system. The two Filtron CFF systems (F1 and F3) both retained about one-fifth of the 3 kD colloid, with the remainder being split between the permeate and CFF losses. The three Osmonics CFF systems (O1, O2, and O3) all recorded about a 70% loss, with about an equal distribution of the remainder between retentate and permeate. The two Amicon systems exhibited results that deviated markedly from each other. One Amicon system operated with a small *cf* (system A5), retained a large portion of standard colloid in the retentate (74%), while still losing 22% to the system surfaces. The other Amicon system (A4) used a higher *cf* and retained only one-third of the colloids in the retentate, while two-thirds of the colloids were accounted for in the permeate. Suprisingly, no colloids were reported lost in this system. It should be noted that system A4 was tested independently after the conclusion of the official workshop and its results may, therefore, not be directly comparable to the others. While different CFF systems behaved differently, this preliminary intercalibration of marine colloid sampling showed that all CFF systems exhibit serious macromolecule losses and do not really have cut-offs as small as advertised.

Organic Colloids in Coastal Massachusetts Seawater

Cross-flow filtration of pre-filtered coastal Massachusetts seawater illustrated the usefulness of dynamic sampling of feed, retentate, and permeate to elucidate the integrity of a CFF-fractionated sample. The general features of this test: (1) [perm] was less than [feed], (2) both [perm] and [feed] were constant with time, and (3) [ret] increased

Figure 9. Size cut-off calibration curve for seawater colloids on Osmonics CFF membrane with a "1.0 kD" nominal cut-off. ♦ represents various standard colloids of differing size (see Table 1).

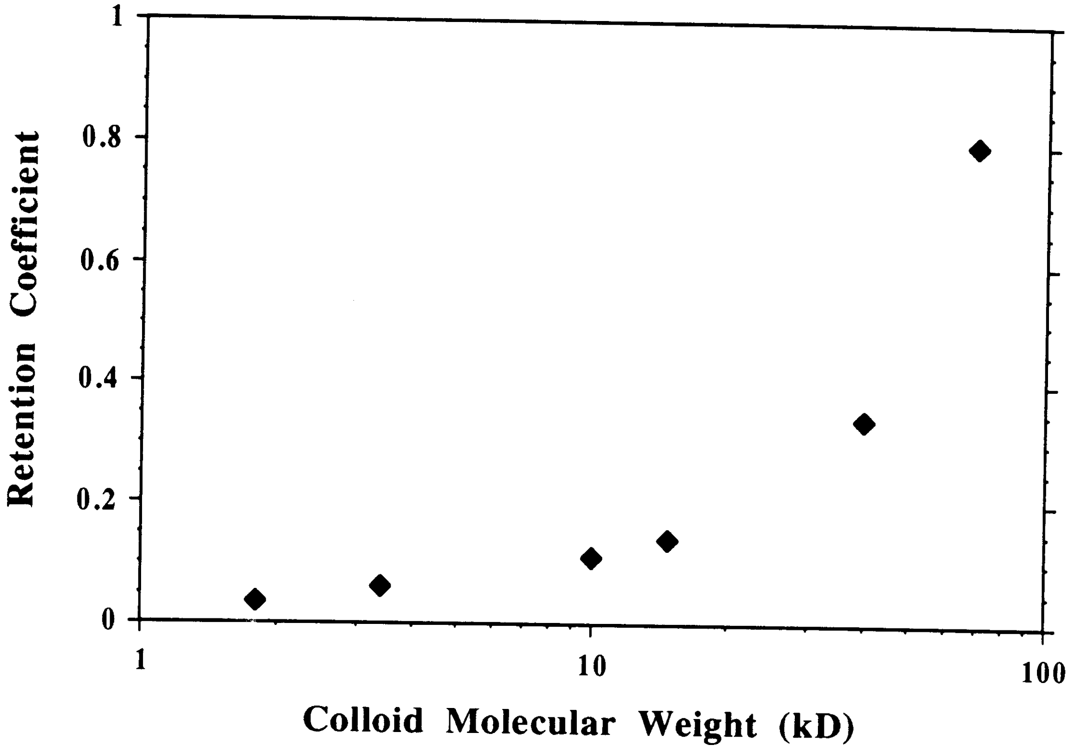

Retention Coefficient
1
0.8
0.6
0.4
0.2
0
1
10
100
Colloid Molecular Weight (kD)

TABLE 2

Intercalibration of 1.0 kD nominal cut-off polysulfone membrane CFF systems with ≈ 400 nM OC-equivalents of a 3.0 kD Dextran colloid standard in Pacific thermocline-base seawater

CFF System	*cf*	Retentate	Permeate	Losses[a]
Membrex (X1)	19	5%	93%	2%
Filtron (F1)	12	16%	62%	22%
Filtron (F3)	7.7	25%	33%	42%
Osmonics (O1)	5.2	12%	13%	75%
Osmonics (O2)	4.0	12%	18%	70%
Osmonics (O3)	3.0	18%	13%	69%
Amicon (A4)[b]	16	30%	70%	-
Amicon (A5)	3.5	74%	4%	22%

[a] The losses to the CFF system were inferred from difference in mass balance.

[b] System A4 was tested independently at several orders of magnitude lower colloid level after the completion of the official workshop.

linearly, indicated an apparently successful run (Fig. 10). The bulk recovery parameter, R%, using only the final measured values, indicated an "acceptable" 97% recovery of total organic carbon. However, utilizing the mean feed (118±10 μM) and permeate (100±7 μM) values throughout the entire run from the complete data set showed that the recovery was only 90%. Since the colloidal organic carbon which we concentrated using our ~ 50 kD inherent cut-off membrane was a relatively small fraction of the total OC (6%), the lost carbon pool (≈ 10%) is nearly twice as large as the isolated colloidal carbon. If one uses the difference between mean feed and mean permeate as the colloidal concentration, one may predict how the retentate should develop, were there no losses (Fig. 10). Clearly, such a typical data set, with apparently favorable features and an apparently good final bulk recovery, is of dubious value with respect to COC quantification. This is without considering exacerbating and potentially coinciding OC contamination and an inherently large cut-off size! This analysis underscores the importance of contrasting the lost (or added contaminating) organic carbon quantities to the collected colloidal pool size, as opposed to the total OC.

An important implication of incomplete recovery is the potential for fractionation of the natural colloids. Since colloid calibration of our CFF system indicated an actual cut-off on the order of 50 kD, the obtained %COC (6%) must be a large underestimation of the *in situ* colloidal fraction. Aiken and Malcolm (1987) reported from vapor pressure osmometry studies that aquatic fulvic acids were near 1 kD in size. Chin and Gschwend (1991) found, using high-pressure size-exclusion chromatography, that the mean MW of marine porewater organic colloids was 2 kD or 9 kD, depending on which tertiary configuration was presumed. If one assumes that the mean, MW-based, seawater colloid has a size somewhere between the 3 and 10 kD standards used, one might be able to estimate the true %COC, based on a combination of the magnitude of the isolated colloid fraction and the realized retention coefficient for those colloid sizes (Table 1). Such a calculation would predict that about 75% of all organic carbon in coastal seawater is colloidal (i.e., > 1 kD)! This indirect approach to estimate %COC is obviously poorly constrained and should simply be viewed as an illustration of the magnitude of the uncertainties that we are facing (i.e., true %COC could be anywhere in the range 6 to 75%).

Figure 10. CFF organic carbon fractionation of coastal Massachusetts seawater (● = retentate, Δ = permeate, and = feed solution). The *error bars* represent one standard deviation of the propagated uncertainty. The *thin lines* highlight the pattern of the dynamically collected data. The single *thick line* represents the predicted retentate based on the difference between feed and permeate, assuming no losses.

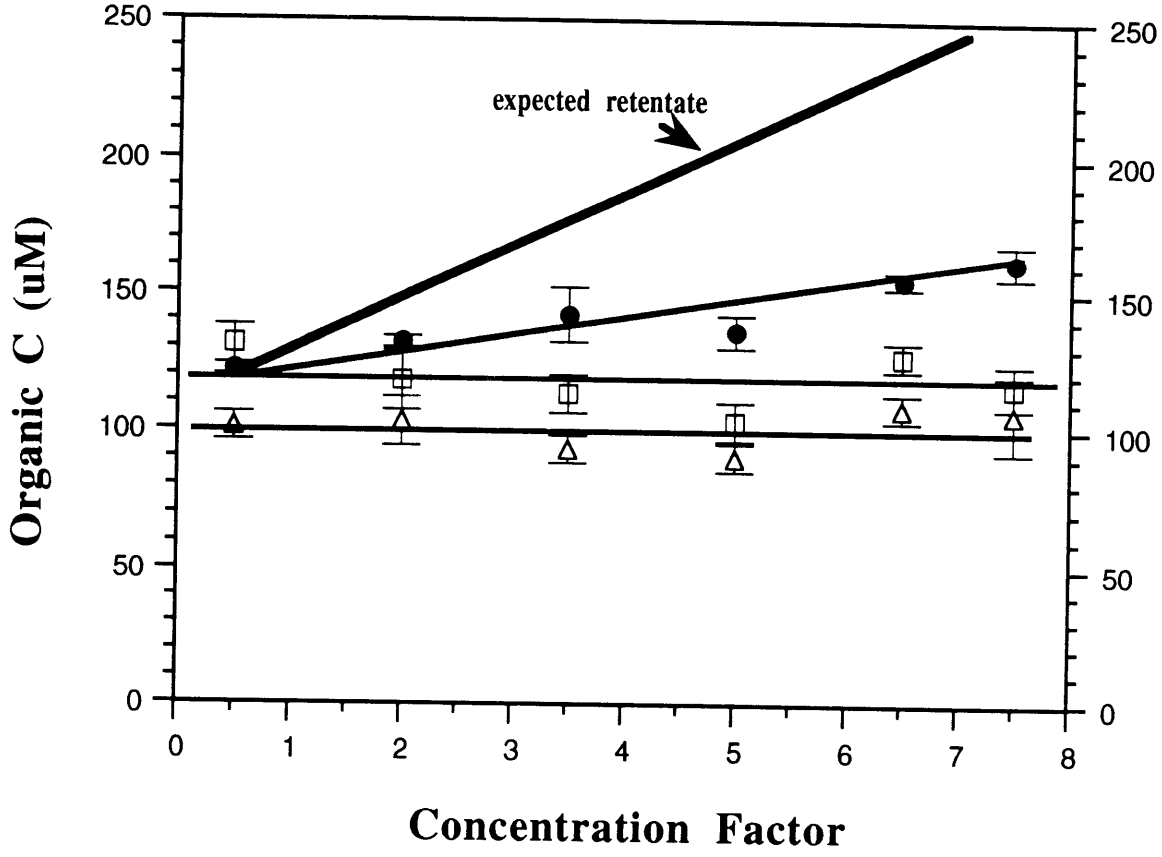
expected retentate
Organic C (uM)
Concentration Factor
0
50
100
150
200
250
0
1
2
3
4
5
6
7
8

Use of CFF to Assess HOCs

Recirculation experiments using a set of hydrocarbon standards showed substantial losses of such HOCs when manipulated with our CFF system. In the CFF by-pass mode, brief initial (<4 min) decreases in concentrations followed the trend in Henry's Law constants and was likely due to equilibration with the gas-phase in the recirculating reservoir headspace (ca. 0.5 L). In contrast, in the CFF recirculation experiment (Fig. 11), the initial gas-phase losses were followed by extensive losses of all hydrocarbons throughout the experiment, presumably to the CFF membrane. The most hydrophobic solute tested, 1-methyl-naphthalene, had the largest losses (over 96% lost after 1 h), whereas the least hydrophobic compound (toluene) had the smallest losses (Fig. 11). Hence, in the case of this type of organic solute, the intrinsic CFF loss mechanism may involve hydrophobic sorption. Such a non-specific interaction should be anticipated when the CFF membrane is of a relatively nonpolar material like our copolyether-sulfone (solubility parameter, $\delta' = 10.5$ cal$^{1/2}$ cm$^{3/2}$; Barton, 1990). These compounds ($\delta' = 8$ to 9 cal$^{1/2}$ cm$^{3/2}$) would be much more compatible with the polysulfone membrane than with seawater (water $\delta' = 21$ cal$^{1/2}$ cm$^{3/2}$). Since many other natural and anthropogenic organic compounds of interest to us and present in seawater (e.g., fatty acid esters, alkenones, phthalate esters, PAHs, PCBs) may possess solubility parameters in the range 7-10 cal$^{1/2}$ cm$^{3/2}$ (Seymour and Carraher, 1981), it should be expected that their affinity towards the large mass of nonpolar organic material in existing CFFs, would lead to significant sorptive losses during CFF processing. In this aspect, a CFF membrane of regenerated cellulose (cellulose $\delta' = 15$-16 cal$^{1/2}$ cm$^{3/2}$; Seymour and Carraher, 1981) instead of polysulfone would appear advantageous.

CONCLUSIONS AND RECOMMENDATIONS

The integrity of cross-flow filtration for sampling marine organic colloids has been assessed. While these results may be applicable also to other types of systems, our findings are specifically concern spiral-wound configurations with polysulfone membranes currently used in marine science (Buesseler *et al.*, 1996). First, organic carbon contamination was found to be problematic unless extensive, and long-lasting,

Figure 11. Recirculation-mode CFF solute integrity experiment showing chemical concentration (C) normalized to the initial concentration (C_0) as a function of time for Toluene ( ), n-propyl-Benzene (x), Naphthalene (◊), and 1-methyl-Naphthalene (▼); all initially at an aqueous concentration of 10-100 μM.

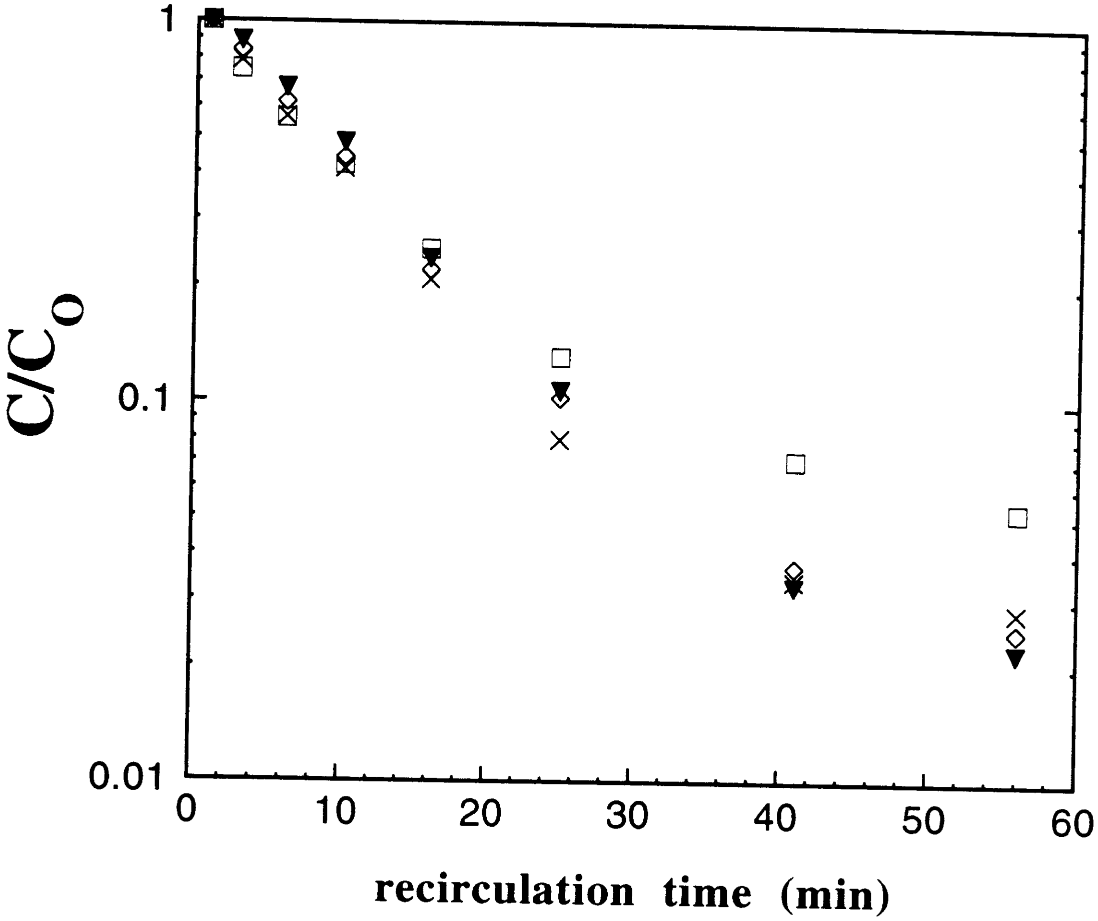
C/C$_o$
1
0.1
0.01
0
10
20
30
40
50
60
recirculation time (min)

leaching was performed. Our OC blank results indicate that it is crucial that CFF conditioning takes place immediately before sampling. Currently applied "clean" water blanks and apparent mass balance approaches are not providing a reliable blank assessment. A poorly constrained blank may lead to an erroneous representation of marine colloids and associated trace constituents. Contamination may also interfere with certain analyses (e.g., Fe in NMR and plasticizers in GC-FID/MS). We propose that low-C seawater should be used to quantify any contamination.

This study has demonstrated the feasibility of applying organic colloid standards in a seawater matrix to test the applicability of CFF to marine colloid sampling. Nanomolar seawater concentrations of a set of organic macromolecules were used here, facilitated by molecular level spectroscopic analyses. These levels are consistent with those of comparable macromolecules in seawater (e.g., Lee and Bada, 1977). It is important to recognize that elements cycle in the ocean in molecular forms as opposed to as "bulk-atoms". Hence, CFF testing requires molecular-scale tracers.

Two co-occuring artifacts of marine CFF have been identified, separated, and quantified: (1) large losses to the polysulfone membrane of standard protein, carbohydrate, and humic-analogue macromolecules, and (2) appearance in the permeate of a series of colloid standards significantly larger than the manufacturer-specified cut-off. To elucidate the nature of these colloid losses and breakthrough observations, several CFF experimental protocols were combined with separate studies of colloid sorption with dissected membrane components and theoretical calculations of physical processes affecting colloid distribution. Chemical sorption and hydraulically-induced concentration polarization are likely to combine to produce the observed colloid losses. While the polysulfone membranes employed were specified by the manufacturer to have a 1.0 kD nominal cut-off (Osmonics Inc.), our calibration with dilute colloid standards in seawater yielded a broad and much larger inherent cut-off centered around 50 kD. The equilibrium colloid loss fractions (F_{loss}) and retention coefficients (RC) should be regarded as inherent properties of the CFF system. These properties were quantitatively different than the kinetically-limited operational values obtained during regular sampling. Continual decrease in permeate flux, parallelling standard carbohydrate colloid loss during sampling of 52 L seawater, indicated that there is little hope for some simple pre-conditioning scheme to be successful. Losses of standard colloids and colloid breakthrough were also observed for all types of CFF systems tested at the Hawaii Intercomparison Workshop.

Like colloids in natural waters, dissolved organic molecules were found to associate with the membrane to a significant extent. The loss trend of a suite of hydrocarbons largely followed their relative hydrophobicities. Hence, fractionation of the characteristics of the dissolved pool must also be expected in currently used CFF systems. Solute and colloid losses may not constitute much of a limitation in traditional CFF applications like industrial processes, where water is separated from some other fluid, or for a biologist only interested in harvesting one particular cell-type from a suspension. In contrast, such losses, with associated fractionation and poorly constrained effective cut-offs, can be detrimental to the mass balance requirements of marine chemists interested in describing some aspect of a dilute assembly of natural colloids.

There currently appears to exist a large inconsistency between marine colloid studies using CFF. For instance, at the Colloid Workshop, the fraction of organic carbon in Pacific intermediate water that different CFF operators found in the colloidal fraction ranged from <2% to 54%. Similarly, the reported colloidal fraction of ^{234}Th in coastal waters range from a few percent (Moran and Buesseler, 1993) up to 78% (Baskaran *et al.*, 1992), both studies employing 10kD CFF systems. However, such a range has been observed through a single plankton bloom (Niven *et al.*, 1995) and may thus also be a result of natural variability. The serious artifacts associated with CFF of seawater that have been discussed in our study may be central to our eventual understanding of the current poor constraints of marine colloid behavior.

To make progress towards CFF characterization of colloids in the ocean, we recommend the following: (1) studies employing CFF should document applicability and integrity of their CFF system for the conditions under investigation. At a minimum, this entails system testing and calibration with standard colloids, relevant to the geochemical entities under investigation, in association with reliable contamination and recovery assessments. (2) To refine our understanding of seawater CFF, there is a need to continue the mechanistic studies of the CFF process introduced in this paper. The development of a such physico-chemical understanding will, not only lead to quantification of exposed artifacts, but also will serve to guide optimization of design and operating conditions. While optimization was not within the scope of this initial investigation, the presented theoretical treatment relating solute polarization in CFF to measurable system parameters (Eqn. 6) may serve as a useful guide to such subsequent studies. For example, we did find that lowering of the permeate flux resulted in a decrease in colloid loss to the membrane, consistent with this theoretical prediction. Similarly, comparison of typical solubility parameters of organic solutes and colloids with those of membrane materials, predicts that less sorptive losses would be experienced with regenerated cellulose than with the most commonly used copolyether-sulfone membrane.

Continual refinement of CFF technology to sampling of marine colloids could, in several instances, be favorably complimented by non-phase separating methods (e.g., photon correlation spectrososcopy, fluorescence quenching, and electrochemical techniques). Such approaches would not only provide independent verification tests of CFF results, but they would also directly contribute to the collective understanding of the multi-facetted characteristics and roles of colloids in marine chemistry.

ACKNOWLEDGMENTS

We are grateful to L. Song and M. Elimelech for sharing a pre-publication manuscript with us. C.C. Mei contributed insights on boundary-layer theory and C. Colton shared his experience of ultrafiltration engineering . Ed Peltzer kindly provided analytical advice and samples for OC analysis, while Charmaine Chan assisted with some of these analyses. Chris Long is thanked for help at the WHOI Workshop. John MacFarlane produced Fig. 2 and is acknowledged for general support and technical advise throughout this project. The manuscript benefitted from constructive comments by Ed Sholkovitz, acting guest editor, Bruce Brownawell and two anonymous reviewers. This study was funded by the Office of Naval Research (grant # NOO014-93-1-0883) and by a grant from the National Oceanic and Atmospheric Administration, pursuant to Award No. NA36RM044. The views expressed herein are those of the authors and do not necessarily reflect the views of NOAA or any of its sub-agencies. Funds for the Colloid Intercomparison Workshops were provided by DOE/NSF/ONR. This is contribution #XXXX from the Woods Hole Oceanographic Institution.

REFERENCES

Aiken, G.R., 1984. Evaluation of ultrafiltration for determining molecular weight of fulvic acid. Environ. Sci. Technol., 18: 978-981.

Aiken, G.R. and Malcolm, R.L., 1987. Molecular weight of aquatic fulvic acids by vapor pressure osmometry. Geochim. Cosmochim. Acta 51: 2177-2187.

Amador, J.A., Milne, P.J., Moore, C.A. and Zika, R.G., 1990. Extraction of chromophoric humic substances from seawater. Mar. Chem., 29: 1-17.

Amon, R.M.W. and Benner, R., 1994. Rapid cycling of high-molecular-weight dissolved organic matter in the ocean. Nature, 369: 549-552.

Barton, A.F.M., 1990. CRC Handbook of Polymer-Liquid Interaction Parameters and Solubility Parameters. CRC Press, Boca Raton, FL, pp.52-53.

Baskaran, M., Santschi, P.H., Benoit, G. and Honeyman, B.D., 1992. Scavenging of thorium isotopes by colloids in seawater of the Gulf of Mexico. Geochim. Cosmochim. Acta, 56: 3375-3388.

Beckett, R., Jue, Z. and Giddings, J.C., 1987. Determination of molecular weight distributions of fulvic and humic acids using flow field-flow fractionation. Environ. Sci. Technol., 21: 289-295.

Benner, R., 1991. Ultra-filtration for the concentration of bacteria, viruses, and dissolved organic matter. In: D.C. Hurd and D.W. Spencer (Editors), Marine Particles: Analysis and Characterization. Geophys. Monogr. 63 American Geophysical Union, Washington DC, pp. 275-280.

Benner, R., Pakulski, D.J., McCarthy, M., Hedges, J.I. and Hatcher, P.G., 1992. Bulk chemical characteristics of dissolved organic matter in the ocean. Science, 255: 1561-1564.

Blatt, W.F., Dravid, A., Michaels, A.S. and Nelsen, L., 1970. Solute polarization and cake formation in membrane ultrafiltration. In: J.E. Flinn (Editor), Membrane Science and Technology. Plenum Press, New York, p. 47

Bottino, A., Capannelli, G., Imperato, A. and Munari, S., 1984. Ultrafiltration of hydrosoluble polymers: Effect of operating conditions on the performance of the membrane. J. Memb. Sci., 21: 247-267.

Brownawell, B.J., 1991. Methods for isolating colloidal organic matter from seawater: General considerations and recommendations. In: D.C. Hurd and D.W. Spencer

(Editors), Marine Particles: Analysis and Characterization. Geophys. Monogr. 63 American Geophysical Union, Washington DC, pp. 275-280.

Buesseler, K.O., Bauer, J., Chen, R., Eglinton, T., Gustafsson, Ö., Landing, W., Mopper, K., Moran, S.B., Santschi, P., VernonClark, R. and Wells, M., 1995. Sampling marine colloids using cross-flow filtration: Overview and results from an intercomparison study. Mar. Chem., submitted.

Buffle, J., Deladoey, P. and Haerdi, W., 1978. The use of ultrafiltration for the separation and fractionation of organic ligands in fresh waters. Anal. Chim. Acta, 101: 339-357.

Buffle, J., Perret, D. and Newman, M., 1992. The use of filtration and ultrafiltration for size fractionation of aquatic particles, colloids, and macromolecules. In: J. Buffle and H. P. van Leeuwen (Editors), Environmental Particles (Vol. 1). Lewis, Boca Raton, pp. 171-230.

Caldwell, K. D., 1988. Field-flow fractionation. Anal. Chem., 60: 959A-971A.

Carlson, D.J., Brann, M.L., Mague, T.H. and Mayer, L.M., 1985. Molecular weight distribution of dissolved organic materials in seawater determined by ultrafiltration: a re-examination. Mar. Chem., 16: 155-171.

Carlson, D.J., 1991. In situ exploration of macromolecules and particulate materials in seawater. In: D.C. Hurd and D.W. Spencer (Editors), Marine Particles: Analysis and Characterization. Geophys. Monogr. 63 American Geophysical Union, Washington, D.C., pp. 195-198.

Chin, Y.-P. and Gschwend, P.M., 1991. The abundance, distribution, and configuration of porewater organic colloids in recent sediments. Geochim. Cosmochim. Acta, 55: 1309-1317.

Chin, Y.-P., McNichol, A.P. and Gschwend, P.M., 1991. Quantification and characterization of pore-water organic colloids. In: R. A. Baker (Editor), Organic Substances and Sediments inWater. Lewis Publishers, Chelsea, MI., pp. 107-126.

Colton, C.K., Friedman, S., Wilson, D.E. and Lees, R.S., 1972. Ultrafiltration of lipoprotein through a synthetic membrane: implications for the filtration theory of atherogenesis. J. Clin. Invest., 51: 2472-2481.

Dawson, R. and Duursma, E.K., 1974. Distribution of radioisotopes between phytoplankton, sediment, and seawater in a dialysis compartment system. Neth. J. Sea Res., 8: 339-353.

Dharmappa, H.B., Verink, J., Ben Aim, R., Yamamoto, K. and Vigneswaran, S., 1992. A comprehensive model for cross-flow filtration incorporating polydispersity of the influent. J. Memb. Sci., 65: 173-185.

Donat, J.R., Statham, P.J. and Bruland, K.W., 1986. An evaluation of a C-18 solid phase extraction technique for isolating metal-organic complexes from central north Pacific Ocean waters. Mar. Chem., 18: 85-99.

Ehrhardt, M., 1983. Preparation of lipophilic organic seawater concentrates. In: K. Grasshoff, M. Ehrhardt and K. Kremling (Editors), Methods of Seawater Analysis. Verlag Chemie, Weinheim, pp. 276-281.

Errede, L.A., 1984. Effect of molecular adsorption on water permeability of microporous membranes. J. Memb. Sci., 20: 45-61.

Fane, A.G., Fell, C.J.D. and Waters, A.G., 1981. The relationship between surface pore characteristics and flux for ultrafiltration membranes. J. Memb. Sci., 9: 245-262.

Fane, A.G., Fell, C.J.D. and Waters, A.G., 1983. Ultrafiltration of protein solutions through partially permeable membranes - The effect of adsorption and solution environment. J. Memb. Sci., 16: 211-224.

Feng, Z., Mopper, K. and Chen, R.F., 1995. Effects of cross-flow filtration on the absorbance of and fluorescence properties of seawater. Mar. Chem., submitted.

Gibbs, R.J., 1981. Floc breakage by pumps. J. Sed. Pet., 51: 670-672.

Giddings, J.C., 1981. Field flow fractionation: a versatile method for the characterization of macromolecular and particulate materials. Anal. Chem., 53: 1170A-1178A.

Guo, L., Coleman Jr, C.H. and Santschi, P.H., 1994. The distribution of colloidal and dissolved organic carbon in the Gulf of Mexico. Mar. Chem., 45: 105-119.

Guo, L., Santschi, P. H., 1995. Evaluation of the cross-flow ultrafiltration technique for sampling of colloidal organic carbon in seawater. Mar. Chem., submitted.

Gustafsson, Ö., Gschwend, P.M. and Buesseler, K.O., 1995. Fluxes of PAHs through the upper ocean derived from coupling with an isotopic "clock". submitted.

Haugland, P., 1992. Handbook of fluorescent probes and research chemicals, 5th ed. Molecular Probes, Eugene, OR pp. 195-198.

Lee, C. and Bada, J.L., 1977. Dissolved amino acids in the equatorial Pacific, Sargasso Sea, and Biscayne Bay. Limnol. Oceanogr., 22: 502-510.

Leppard, G.G., 1986. The fibrillar matrix component of lacustrine biofilms. Wat. Res., 20: 697-702.

Liang, H., Purucker, W.J., Stenger, D.A., Kubinec, R.T. and Hui, S.W., 1988. Uptake of fluorescence-labeled dextrans by 10T 1/2 fibroplasts following permeation by rectangular and exponential-decay electric field pulses. BioTechniques, 6: 550-558.

MacFarlane, J.K. and Gschwend, P.M., 1987. Field analysis of groundwater for volatile organic compounds using on-column aqueous injection capillary gas chromatography. MIT-EL Report 87-007. Energy Laboratory, Massachusetts Institute of Technology.

Mantoura, R.F.C. and Riley, J.P., 1975. The use of gel filtration in the study of metal binding by humic acids and related compounds. Anal. Chim. Acta, 78: 193-200.

Michelena, G., Bell, A. and Rivas, E.M., 1994. Fractionation of dextran solutions by cross-flow filtration. Acta Biotechnol., 14: 293-298.

Mills, G.L. and Quinn, J.G., 1981. Isolation of dissolved organic matter and copper-organic complexes from estuarine waters using reverse-phase liquid chromatography. Mar. Chem., 10: 93-102.

Mills, G.L., McFadden, E. and Quinn, J.G., 1987. Chromatographic studies of dissolved organic matter and copper-organic complexes isolated from estuarine waters. Mar. Chem., 20: 313-325.

Moran, S.B., 1991. The application of cross-flow filtration to the collection of colloids and their associated metals in seawater. In: D.C. Hurd and D.W. Spencer (Editors), Marine Particles: Analysis and Characterization. Geophys. Monogr. 63 American Geophysical Union, Washington DC, pp. 275-280.

Moran, S.B. and Buesseler, K.O., 1992. Short residence time of colloids in the upper ocean estimated from ^{238}U-^{234}Th disequilibria. Nature, 359: 221-223.

Moran, S.B. and Buesseler, K.O., 1993. Size-fractionated ^{234}Th in continental shelf waters off New England: Implications for the role of colloids in oceanic trace metal scavenging. J. Mar. Res., 51: 893-922.

Morel, F.M.M. and Gschwend, P.M., 1987. The role of colloids in the partitioning of solutes in natural waters. In: W. Stumm (Editor), Aquatic Surface Chemistry. Wiley, New York, pp. 405-422.

Niven, S. E. H., Kepkay, P. E. and Boraie, A., 1995. Colloidal organic carbon and colloidal ^{234}Th dynamics during a coastal phytoplankton bloom. Deep-Sea Res., 42: 257-273.

Pepperkok, R., Schneider, C., Philipson, L. and Ansorge W., 1988. Single cell assay with an automated capillary microinjection system. Exp. Cell Res., 178: 369-376.

Perrett, D., Leppard, G.G., Müller, M., Belzile, N., De Vitre, R. and Buffle, J., 1991. Electron microscopy of aquatic colloids: non-perturbing preparation of specimens in the field. Wat. Res., 25: 1333-1343.

Philp, J.L., Jaffrin, M.Y. and Ding, L., 1994. Protein adsorption and trapping during steady state and pulsed flow plasma cross-flow filtration. J. Memb. Sci., 88: 197-209.

Reitmeyer, Powell, Measures and Landing 1995. Colloidal Al and Fe in seawater: An intercomparison between various cross-flow ultrafiltration systems. Mar. Chem., submitted.

Riley, J.P. and Taylor, D., 1969. The analytical concentration of traces of dissolved organic materials from sea water with Amberlite XAD-1 resin. Anal. Chim. Acta, 46: 307-309.

Rosemberg, Y. and Korenstein, R., 1990. Electroporation of the photosynthetic membrane: A study by intrinsic and external optical probes. Biophys. J., 58: 823-832.

Salbu, B., Bjørnstad, H.E., Lindstrøm, N.S., Lydersen, E., Brevik, E.M., Rambaek, J.P. and Paus, P.E., 1985. Size fractionation techniques in the determination of elements associated with particulate or colloidal material in natural fresh waters. Talanta, 32: 907-913.

Sansone, F.J., Smith, S.V., Price, J.M., Walsh, T.W., Daniel, T.H. and Andrews. C.C., 1988. Long-term variation in seawater composition at the base of the thermocline. Nature, 332: 714-717.

Schlichting, H., 1968. Boundary-Layer Theory, 6th ed. McGraw-Hill, New-York, 747 pp.

Sempére, R., Cauwet, G. and Randon, J., 1994. Ultrafiltration of seawater with a zirconium and aluminum oxide tubular membrane: Application to the study of colloidal organic carbon distribution in an estuarine bottom nepheloid layer. Mar. Chem., 46: 49-60.

Seymour, R.B. and Carraher, C.E., 1981. Polymer Chemistry. Marcel Dekker, New York, NY, 564 pp.

Sharp, J.H., 1973. Size classes of organic carbon in seawater. Limnol. Oceanogr., 18: 441-447.

Sharp, J.H., Benner, R., Bennett, L., Carlson, C.A., Fitzwater, S.E., Peltzer, E.T. and Tupas, L.M., 1995. Analyses of dissolved organic carbon in seawater: the JGOFS EqPac methods comparison. Mar. Chem., 48: 91-108.

Sipos, S., Dékány I., Szántó, F. and Sipos, É., 1972. Investigation of humic acids and metal humates with analytical ultracentrifuge. Acta Phys. Chem., 18: 253-257.

Song, L. and Elimelech, M., 1995. Theory of concentration polarization in cross-flow filtration. J. Chem. Soc. Faraday Trans., 91: 3389-3398.

Suki, A., Fane, A.G. and Fell, C.J.D., 1984. Flux decline in protein ultrafiltration. J. Memb. Sci., 21: 269-283.

Stamatakis, K. and Tien, C., 1993. A simple model of cross-flow filtration based on particle adhesion. AIChE Journal, 39: 1292-1302.

Staub, C., Buffle, J. and Haerdi, W., 1984. Measurement of complexation properties of metal ions in natural conditions by ultrafiltration: Influence of various factors on the retention of metals and ligands by neutral and negatively charged membranes. Anal. Chem., 56: 2843-2849.

Stuermer, D.H. and Harvey, G.R., 1977. The isolation of humic substances and alcohol-soluble organic matter from seawater. Deep-Sea Res., 24: 303-309.

Wang, Y., Howell, J.A., Field, R.W. and Wu, D., 1994. Simulation of cross-flow filtration for baffled tubular channels and pulsatile flow. J. Memb. Sci., 95: 243-258.

Wells, M.W. and Goldberg, E.W., 1992. Marine submicron particles. Mar. Chem., 40: 5-18.

Wen, L-S., Stordal, M. C., Tang, D., Gill, G. A. and Santschi, P. H., 1995. An ultraclean cross-flow ultrafiltration technique for the study of trace metal phase speciation in seawater. Mar. Chem., submitted.

Whitehouse, B.G., Petrick, G. and Ehrhardt, M., 1986. Crossflow filtration of colloids from Baltic Sea water. Wat. Res., 20: 1599-1601.

Whitehouse, B.G., Macdonald, R.W., Iseki, K., Yunker, M.B. and McLaughlin, F., 1989. Organic carbon and colloids in the Mackenzie River and Beaufort Sea. Mar. Chem., 26: 371-378.

Whitehouse, B.G., Yeats, P.A. and Strain, P.M., 1990. Cross-flow filtration of colloids from aquatic environments. Limnol. Oceanogr., 35: 1368-1375.

Yunker, M.B., McLaughlin, F.A., Macdonald, R.W., Cretney, W.J., Fowler, B.R. and Smyth, T.R., 1989. Measurement of natural trace dissolved hydrocarbons by in situ column extraction: An intercomparison of two adsorption resins. Anal. Chem., 61: 1333-1343.

Chapter 4

Time-resolved fluorescence quenching to quantify the ability of seawater colloids to bind hydrophobic compounds

Introduction

The important role of colloids in affecting the physical speciation of hydrophobic organic pollutants is well recognized (e.g., Boehm and Quinn, 1973; Means and Wijayaratne, 1982; Carter and Suffet, 1982; Landrum *et al.*, 1984; Whitehouse, 1985; Gschwend and Wu, 1985; Baker *et al.* 1986; Brownawell and Farrington, 1986; Chiou *et al.*, 1986; Chin and Gschwend, 1992). This phase-distribution is a major control on the direct exposure to biota as well as on the ability of the chemical to participate in other transport and transformation processes, determining the ultimate fate of the pollutant (e.g., see chapters 1 and 2 of this thesis). Since one important goal of environmental chemistry is to quantify the fraction of a given chemical that is in a bioavailable form, it is worth underlining that toxic compounds such as benzo[a]pyrene have been seen to be rendered "unavailable" to cause toxic effects on zooplankton when associated with colloids (Leversee *et al.*, 1983).

Recently, the colloidal samples obtained from cross-flow filtration (CFF) of seawater have been shown to be significantly operator- and equipment-dependent (Buesseler *et al.*, 1996: chapter 3 of this thesis). CFF has also been shown to cause undesired fractionation of both major and minor organic components of the colloids (chapter 3 of this thesis). Filtration-based approaches to colloid speciation will never succeed in distinguishing colloidal sorbents that behave independently of size (chapter 2 of this thesis). For example, humic and fulvic acids of about 10^3 D molecular weight have been shown to sorb hydrophobic organic compounds, HOCs, (e.g., Boehm and Quinn, 1973; Chiou *et al.*, 1986), whereas much larger carbohydrates (about 10^6 D), possibly attaining an extended tertiary configuration in aqueous solution, may not sorb HOCs (e.g., Garbarini and Lion, 1986). In light of the continuing need to understand the phase-associations of hydrophobic pollutants, analytical approaches are required that can assess the chemical speciation *in situ* without physically separating the phases. Time-resolved fluorescence quenching of strongly fluorescing PAH probes may offer, in addition to eliminating phase-separation artifacts, other potential advantages including rapidity, high precision and reproducibility, and inherent sensitivity at very low pollutant concentration.

Gauthier established fluorescence quenching as a technique to study PAH-colloid binding in aquatic systems (Gauthier *et al.*, 1986, 1987). The technique is based on the observation that the fluorescence of a PAH probe is quenched on association with aquatic organic colloids (e.g., Gauthier *et al.*, 1986, 1987; Backhus and Gschwend, 1990; Morra *et al.*, 1990). Whereas other quenchers certainly also exist in natural waters (e.g., hydrogen peroxide, oxygen, xenon, bromate, iodide, amines, nitrous oxide, and certain metals; e.g., Lakowicz, 1983), these are believed to be of lesser significance than the high electron density aromatic systems of colloidal sorbent macromolecules. Furthermore, some dissolved quenchers may be easily removed (i.e., gases such as oxygen, xenon, nitrous oxide may be purged) and/or accounted for by using a similar matrix in the reference as in the sample.

Fluorescence quenching is defined as any process that decreases the fluorescence intensity of a fluorophore such as excited state reactions, energy transfers, complex formations, and collisional quenching (e.g., Lakowicz, 1983). Based on the specific mechanism, fluorescence quenching may be divided into two groups: static or dynamic. In static quenching, a nonfluorescing ground-state (dark) complex between the fluorophore and the quencher is formed. In the case of static quenching, the fluorescence quantum yield of the colloid-bound fluorophore (ϕ_{coll}) is very near zero and thus the PAH fluorophore concentrations may be substituted with the fluorescence intensities to derive an expression for the colloid binding constant:

$$K_{coll} = \frac{[\text{PAH-Coll}]}{[\text{PAH}]\,[\text{Coll}]} = \frac{F_0 - F}{F} \qquad (1)$$

where PAH is the probe, "Coll" is the colloidal quencher, F_0 is the probe fluorescence in the absence of colloids, and F is the probe fluorescence in the presence of quencher. This expression may be rearranged into the familiar Stern-Volmer equation (e.g., Lakowicz, 1983):

$$\frac{F_o}{F} = 1 + K_{sv}\,[\mathrm{Coll}] \qquad (2)$$

where $K_{coll} = K_{SV}$ [Coll]. Hence, in the case of static quenching, the Stern-Volmer quenching constant (K_{sv}) is equal to the bound-to-free distribution ratio.

In dynamic, or collisional, quenching, a diffusional collision of the fluorophore and quencher results in nonradiative relaxation during the lifetime of the excited state. For dynamic quenching, the Stern-Volmer quenching constant is equal to the product of the bimolecular quenchng constant, k_q, and the (intrinsic) lifetime of the fluorophore in the absence of the dynamic quencher, in this case presumed to be colloids (τ_o):

$$\frac{F_o}{F} = 1 + k_q\,\tau_o\,[\mathrm{Coll}] \qquad (3)$$

When the quenching interaction between colloids and PAH fluorophores are dynamic in nature, ϕ_{coll} has a value between zero and the PAH's fluorescence quantum yield in the aqueous solution. In the dynamic case, the observed fluorescence intensities are thus not proportional to the ratio of bound and free fluorophore as the bound component contributes to the observed overall fluorescence. Since k_q is a function of the temperature and viscosity of the solution as well as the concentration of quencher and fluorophore, greater caution must be exercised when interpreting dynamic quenching in terms of colloid binding. However, given a single fluorophore and constant conditions, results from dynamic quenching may also be used to derive distribution ratios (e.g., Lakowicz, 1983). The temperature and viscosity dependence of quenching can be used to discern whether static or dynamic quenching is dominant. However, the measurement of fluorescence lifetimes is the most definitive means to distinguish between the two quenching mechanisms, and in the case of dynamic quenching, to quantify the extent of fluorescence from the bound fluorophore (Lakowicz, 1983).

Most fluorescence quenching studies of PAH binding, using natural colloids, assume a static mechanism, but the predominance of static vs dynamic quenching of PAHs in aquatic systems is currently debated (e.g., Backhus and Gschwend, 1990; Puchalski *et al.*, 1992, Chin and Gschwend, 1992; Chen *et al.*, 1994, Danielsen *et al.*, 1995; Green and Blough, 1996). By far most of the existing studies have been performed using steady state fluorescence techniques and the near absence of simultaneous lifetime measurements complicates the resolution of this issue.

PAH fluorescence quenching studies of natural colloids have typically been performed on humic acid isolates of natural soils reconstituted into distilled water (Gauthier *et al.*, 1986, 1987, Morra *et al.*, 1990, Puchalski *et al.*, 1991, 1992; Schlautman and Morgan, 1993a,b; Chen *et al.*, 1994; Danielsen *et al.*, 1995). The isolation and concentration steps of the humic acid fraction may change the character of these complex macromolecules and the final product likely represents only a select portion of all the colloidal sorbents present in the sampling environment. Chin and Gshwend (1992), while using colloids from whole water samples, used ultrafiltration to concentrate their sediment porewater colloids. While potentially providing a more complete picture of HOC sorption to natural colloids, their results do contain the uncertain influence of ultrafiltration artifacts (e.g., Aiken, 1984; Buffle *et al.*, 1992; chapter 3 of this thesis). Notably, in one study of PAH binding to groundwater colloids, the anoxic experiments were performed with whole water samples and without any preconcentration steps (Backhus and Gschwend, 1990). Nevertheless, existing fluorescence quenching results suggest that, on an organic-carbon basis, humic acids as well as groundwater and marine sediment porewater colloids, are nearly as efficient sorbents as large sediment and soil particles (e.g., Gauthier *et al.*, 1986; Backhus and Gschwend, 1990; Chin and Gshwend, 1992; Schlautman and Morgan, 1993b). This may not be surprising since the molecular composition of soil humic acids and porewater organic colloids could be expected to be relatively similar to the surrounding organic matter associated with the bulk solid. However, solubility enhancement studies have shown that colloidal size and composition does have a discernible effect on the HOC sorption by humic and fulvic acids (Chiou *et al.*, 1986).

The sorbent effectiveness of colloids present in the surface ocean is largely unknown but may be expected to be lower than for sedimentary constituents. Several studies have shown that increasing polarity (e.g., as reflected in C/O ratios) leads to decreasing organic-carbon normalized parition coefficients (K_{oc}), reflecting lower sorbent abilities toward nonpolar HOCs (e.g., Chiou *et al.*, 1986; Garbarini and Lion, 1986; Gauthier *et al.*, 1987; Chin and Weber, 1989). Since the polarity of organic matter is known to decrease during diagenesis (e.g., Tissot and Welte, 1978) and since the fresh colloidal organic matter in surface waters is believed to contain large amounts of carbohydrates (e.g., Benner *et al.*, 1992), it may be anticipated that seawater colloids have a relatively low sorbent "quality".

The objectives of this chapter are (1) to develop a non-invasive time-resolved fluorescence quenching technique for studying colloid-water partitioning of hydrophobic compounds, and (2) to demonstrate the technique by quantifying the organic-carbon normalized sorbent efficiency of coastal surface water colloids towards PAHs. Fulfillment of the second objective would greatly contribute to our understanding of the bioavailabilities of such HOCs to planktonic and nektonic organisms. It would also provide speciation information relevant to evaluate the availability of PAHs to participate in photochemical reactions (e.g., a different wavelength spectrum and intensity of light may be available to the colloid-partitioned species).

Experimental Section

Chemicals and Solutions

The seawater sampling is described in detail in chapter 7 of this thesis. Briefly, an all stainless steel system is used to obtain "HOC-clean" ocean samples. An immersible low-internal volume pump (Fultz Inc., Lewistown, PA) was positioned in the surface layer, and water was pumped onboard through high-grade 316 stainless steel tubing through a pre-combusted (450 °C for 24 h) 293 mm GF/F glass-fiber filter (ca. 0.7 um cut-off; Whatman Inc.) held in a stainless steel filter holder with a Teflon O-ring (Microfiltration Systems Inc., Dublin, CA). Filtrates for fluorescence quenching studies were collected on-line into pre-combusted 150 mL amber glass bottles with Teflon-lined screw caps and kept in the dark at 4 °C until further use. The filter back-pressure was closely monitored using on-line pressure gauges and kept below 20 psi to minimize breakage of biological cells. The surface seawater utilized in this initial study was collected in Inner Casco Bay (outer Portland, ME harbor) on July 10, 1996. it was filtered (GF/F; Whatman Inc.) and stored in the cold and in darkness, for the 4-5 months prior to these experiments, in order to improve preservation. Analysis of normalized fluorescence and DOC was performed after this storage to make sure that the used sample exhibited properties typical of coastal seawater.

Artificial seawater was prepared in low-carbon water from an Aries clean water system (Vaponics Inc.) by adding NaCl to attain an ionic strength of 0.7 M and by adjusting the pH to 8.0 by adding the appropriate phosphate buffer system.

Methylperylene (provided by R. J. Liukkonen, Dept. of Chem., Univ. of Minnesota, Duluth, MN; mp 386 °C; >95% purity as determined by GC-FID, GC-MS) was synthesized following Peake *et al.* (1983). Methylperylene has an aqueous solubility (4 ug/L) which is an order of magnitude higher than perylene, yet the methyl substitution causes it to be more sorptive than perylene (aqueous activity coefficient of methylperylene, log $\gamma_w = 8.7$, compared to 8.1 for perylene; Backhus, 1990). These properties, in addition to high extinction coefficient and fluorescence quantum yield expectations from structural similarity with perylene, makes methylperylene an ideal candidate as a fluorescent probe for investigation of hydrophobic sorption with dilute suspensions of seawater colloids. A solution of methylperylene in de-aerated methanol was prepared and kept in the dark in a glove box filled with nitrogen gas. An exact volume (in the range 40-60 uL) of this stock was transferred using a stainless steel and glass syringe to 3.0 mL of the de-aerated aqueous matrices in quartz cuvettes immediately preceeding an experiment to yield aqueous concentrations around one-fourth of methylperylene solubility.

A liquid quantum counter was prepared by adding 8 ug Rhodamine B (Sigma Chemicals, St. Louis, MO) per liter ethylene glycol (Sigma Chemicals, St. Louis, MO). This solution was added to a triangular cuvette placed in front of a red filter (2mm RG-630) in the reference light path in order to correct steady state spectra for variations in the excitation light intensity. As a lifetime scatter reference ($\tau = 0$ sec) we daily prepared fresh aqueous solutions of glycogen.

Ancillary measurements

Absorbance measurements were obtained on a Beckman DU-640 UV/VIS spectrophotometer. Total organic carbon measurements were obtained after H_3PO_4 acidification and nitrogen purging with a high-temperature catalytic oxidation instrument (Shimadzu TOC 5000). Response factors were obtained by running a series of dodecyl sulfate standards and method blanks were obtained using the clean water described above. Dissolved oxygen concentrations in the samples were estimated from clean water batches treated in parallel with the samples using a colorimetric method (Chemets Inc.).

Fluorescence Instrument

All fluorescence intensity and lifetime measurements were obtained with an ISS K2-Digital multifrequency cross-correlation phase and modulation fluorometer (ISS Inc., Champaign, IL) equipped with a 300-W Xe lamp, operated at 18A. The cuvette compartment was always temperature-controlled to 25 °C by recirculating water from an auxiliary water bath (Neslab Inc.) through the brass water-jacketed cuvette holder base. The sample compartment was constantly purged with nitrogen gas to create an atmosphere devoid of oxygen.

Analog and photon-counting detection of steady state fluorescence

To collect steady state spectra and single-wavelength intensity data for fluorescence quenching, the photomultiplier tubes (PMT) were operated in either analog or photon-counting mode. In the less sensitive analog mode, the individual pulses are averaged creating a mean anode current that is amplified. In the photon-counting mode, each individual anode pulse is detected and counted, resulting in much increased sensitivity which is beneficial when working with low signal levels commonly found in seawater samples. In the photon counting mode, the PMT was cooled to -8°C to decrease the dark counts using an auxiliary Peltier system coupled with an additional heat dissipation system (Neslab Inc.).

For characterization of the native seawater fluorophores, emission spectra were acquired with excitation at 355 nm (Hoge *et al.*, 1993). Methylperylene emission spectra were acquired with excitation at 406 nm and with a KV 418 high-pass filter inserted in the emission path. The effective band-pass at full-width half-maximum (fwhm) for the excitation monochromator was 16 nm and for the emission monochromator 8 nm. For kinetic studies of methylperylene, intensity at 442 nm (same excitation and emission filters as for spectral analysis) was integrated for 4 sec for each reading.

In both spectra and single wavelength acquisition, the fluorescence intensity from a blank cuvette containing the current matrix, but without methylperylene probe, was subtracted from the sample fluorescence. The fluorescence intensity was also normalized to the wavelength-dependent variations in irradiation intensity recorded with the quantum counter in the reference path (excitation correction). The wavelength dependent response of the detection system was corrected by applying the appropriate emission correction files, developed by the manufacturer using a spectral irradiance standard lamp, provided in the ISSPC software package (ISS Inc., Champaign, IL).

Phase and modulation fluorescence lifetimes

The K2-Digital instrument employed to estimate fluorescence lifetimes utilizes the variable-frequency phase and modulation technique (Gratton and Limkeman, 1983; Gratton *et al.*, 1984). Advantages of phase-modulation methods over laser-pulse techniques to obtain fluorescence lifetimes include shorter acquisition times and the ability to resolve shorter lifetime components (e.g., Lakowicz, 1983). In phase-modulation measurements, the sample is excited with light whose intensity is sinusoidally modulated. The finite time lag between absorption and emission results in a phase delay (ϕ) and demodulation factor (m) of the emitted light relative to excitation. From these measurable quantities one may calculate phase (τ_p) and modulation (τ_m) based estimates of the observed fluorescence lifetimes (Lakowicz, 1983):

$$\tan \phi = \omega \tau_p, \qquad \tau_p = \omega^{-1} \tan \phi \tag{4}$$

$$m = [1 + \omega^2 \tau_m{}^2]^{-1/2}, \qquad \tau_m = \omega^{-1} [(1/m^2) - 1]^{1/2} \tag{5}$$

where ω is the circular frequency ($\omega = 2\pi$ freq.) of the modulation.

In the case of methylperylene, 406 nm excitation light (16 nm fwhm) was modulated over 16 logarithmically-spaced frequencies in the range 2 -200 MHz. Phase-shifts and demodulation factors were collected using a cross-correlation frequency of 80 Hz. The emitted light was filtered through a KV 418 high-band pass filter, and Raleigh scatter from a freshly prepared aqueous glycogen solution was assigned a reference lifetime of 0 ns. Results were averaged for six alternate positions of the sample-reference cuvettes at each frequency. Stop and analysis maximum error criteria were for phase 0.2 and modulation 0.004 relative standard deviations and the maximum integration time was 40 sec. The collected phase and modulation data were analyzed with ISS187 decay analysis software (ISS Inc., Champaigne, IL) using a Marquardt-Levenburg least-squares minimization algorithm to derive estimates of different components' lifetime distributions.

Factors that may influence the interpretation of fluorescence results

In addition to the need of resolving whether static or dynamic quenching is occuring, one need to address also other factors that may affect the results such as quenching by oxygen, sorption to the cuvette wall, self-absorption of the medium (inner filter effect), and photodegradation of either the probe or the native fluorophore sorbents.

It is well known that oxygen is an efficient dynamic quencher of PAH fluorescence (e.g., Ware, 1962; Geiger and Turro, 1975). It is also clear that PAHs such as pyrene ($\tau_o = 200$ ns in water, $\tau_o = 373$ ns in ethanol; Liu *et al.*, 1993) are more likely to collide diffusionally with oxygen during their excited stage than shorter-lived molecules such as perylene ($\tau_o = 6.0$ ns in ethanol; Liu *et al.*, 1993). Larger attention to such environmental factors is required when dealing with very long-lived excited states such as that of pyrene (e.g., Eaton, 1988; Green and Blough, 1996). While we expected oxygen quenching to be less significant for methylperylene, we decided to operate under deoxygenated conditions. Hence, the methanol used to prepare the methylperylene spike solution was bubbled with argon and the solution was stored in a glove box filled with nitrogen. The artificial seawater was similarly deoxygenated. Since we feared that bubbling of seawater would induce colloid coagulation of surface-active organic species, these samples were instead exposed to the nitrogen atmosphere in the glove box until the oxygen content was reduced to below the detection limit of the colorimetric method used to quantify dissolved oxygen (< 0.3 uM).

Initial studies revealed the need to consider photodegradation of methylperylene at the irradiation levels of this instrument. The intensity as a function of time and wavelength of irradiation, with and without oxygen, was quantified in both seawater and artificial seawater solutions.

Optically-dense solutions may absorb a significant fraction of either the exciting or the emitted light and thus affect the obtained fluorescence quenching results. Such an inner filter effect becomes significant at optical densities greater than 0.05 (Lakowicz, 1983, p.45). The absorbance of the seawater was obtained at both 406 and 442 nm (excitation/emission wavelengths used for methylperylene) to, if necessary, be able to correct for the inner filter effect (e.g., Gauthier *et al.*, 1986; Puchalski *et al.*, 1991).

Finally, losses of highly hydrophobic PAHs to quartz cuvette walls have previously been seen (Backhus and Gschwend, 1990; Schlautman and Morgan, 1994). We desired to account for the differential losses of methylperylene to the quartz surfaces in the seawater relative to in the artificial seawater. The quartz cuvettes were always prepared by soaking in chromic-sulfuric acid ("Chromerge"; Fisher Scientific Inc.), followed by thorough rinsing in clean water (Aries; Vaponics Inc.). The surface protonation was controlled by rinsing in pH 8 phosphate-buffered artificial seawater. Exactly 3.0 mL of the aqueous matrix to be investigated was glass-pipetted into the 1x1 cm cuvettes inside the nitrogen-containing glove-box followed by capping the cuvettes. The sample was then transferred to the continuously nitrogen-purged sample compartment of the instrument. Immediately prior to start of data acquisition, about 50 uL of methylperylene in a deoxygenated methanol carrier was spiked directly into the cuvette. The decrease in fluorescence intensity at steady state yielded information about the wall-solution partition constant for methylperylene.

In order to assess whether dynamic quenching was important, the fluorescence lifetime of methylperylene in seawater was compared to that in artificial seawater. If a significant portion of the fluorescence quenching in seawater is collisional, then the lifetime of the probe would be correspondingly decreased.

Results and discussion

Fluorescence of methylperylene and seawater

Corrected and blank-subtracted emission spectra of methylperylene in both seawater and artificial seawater exhibit maxima at 442 and 466 nm (Fig. 1). The structure, relative intensity and position of the two methylperylene peaks appear to be virtually identical in these two matrices. Based on this characteristic spectrum, quantification of single wavelength emission intensity in the following fluorescence quenching experiments was performed at 442 nm since the Raman peak of water ($(\lambda_x)_{max}$ = 406 nm) was overlapping with the 466 nm peak.

The filtered coastal seawater was irradiated at 355 nm and the fluorescence emission spectrum was obtained (Fig. 2). Hoge *et al.* (1993) have proposed a standardized protocol for determination of colored dissolved organic matter (CDOM) by normalizing the fluorescence at 450 nm (λ_x= 355 nm) to the Raman peak of water as an internal radiometric standard. The value of this normalized fluorescence, $F_n(355)$, of the filtered Inner Casco Bay seawater was 0.683, which is in the range reported for similar coastal sites such as Delaware Bight and off Cape Hatteras by Hoge *et al.* (1993). The DOC of this filtrate was 179 ± 4 uM. The "typical" coastal values obtained for $F_n(355)$

Figure 1. Corrected and blank-subtracted fluorescence emission spectra of methylperylene in coastal seawater (dark line) and in artificial seawater (dashed line). Excitation wavelength was 406 nm and a KV418 high band-pass filter was placed in the emission path. Note that these two samples had not been subjected to the same conditions prior to spectrum acquisition and no interpretation should be made of their relative intensities.

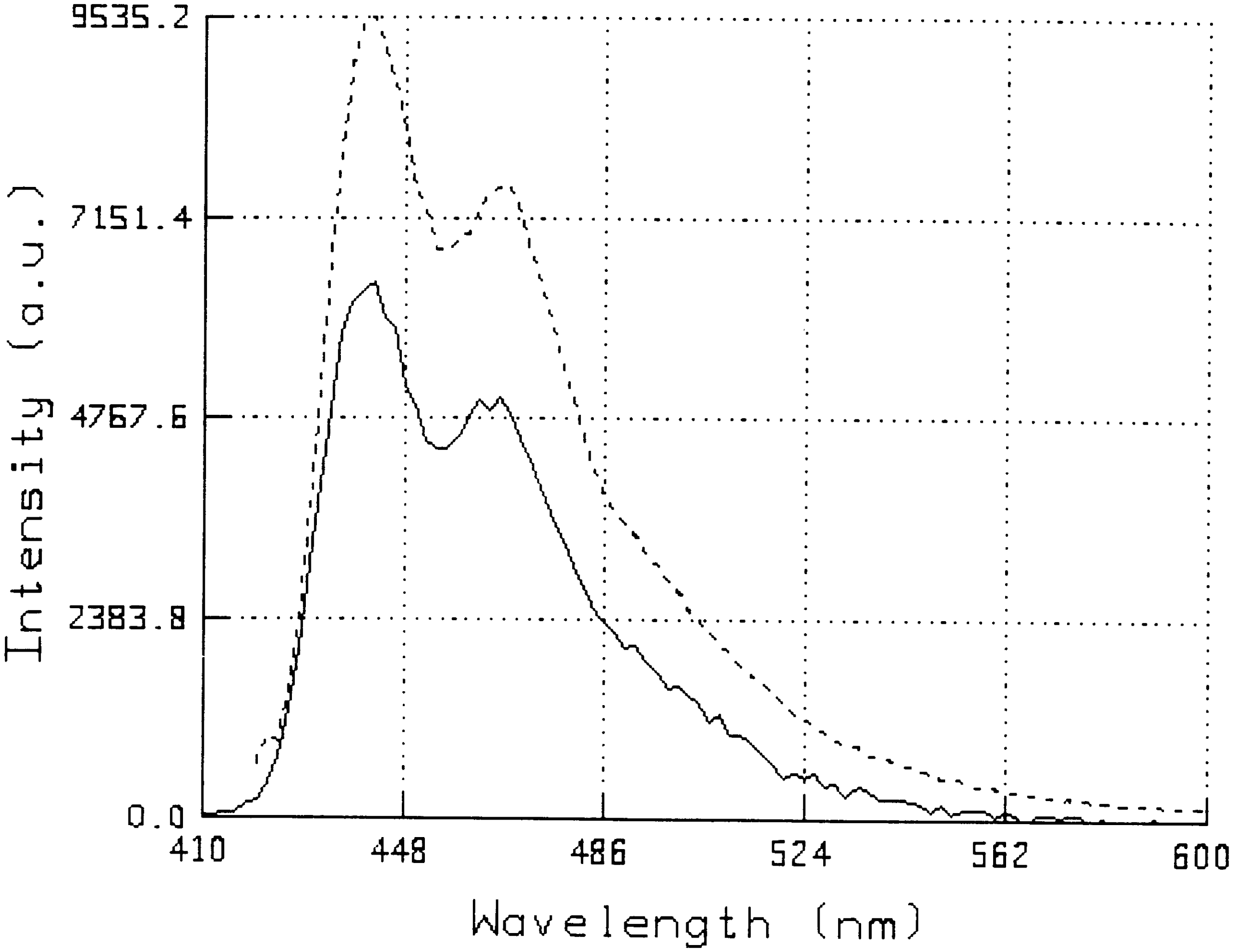
9535.2
7151.4
4767.6
2383.8
0.0
Intensity (a.u.)
410
448
486
524
562
600
Wavelength (nm)

Figure 2. Corrected fluorescence emission spectrum of filtered inner Casco Bay seawater excited at 355 nm.

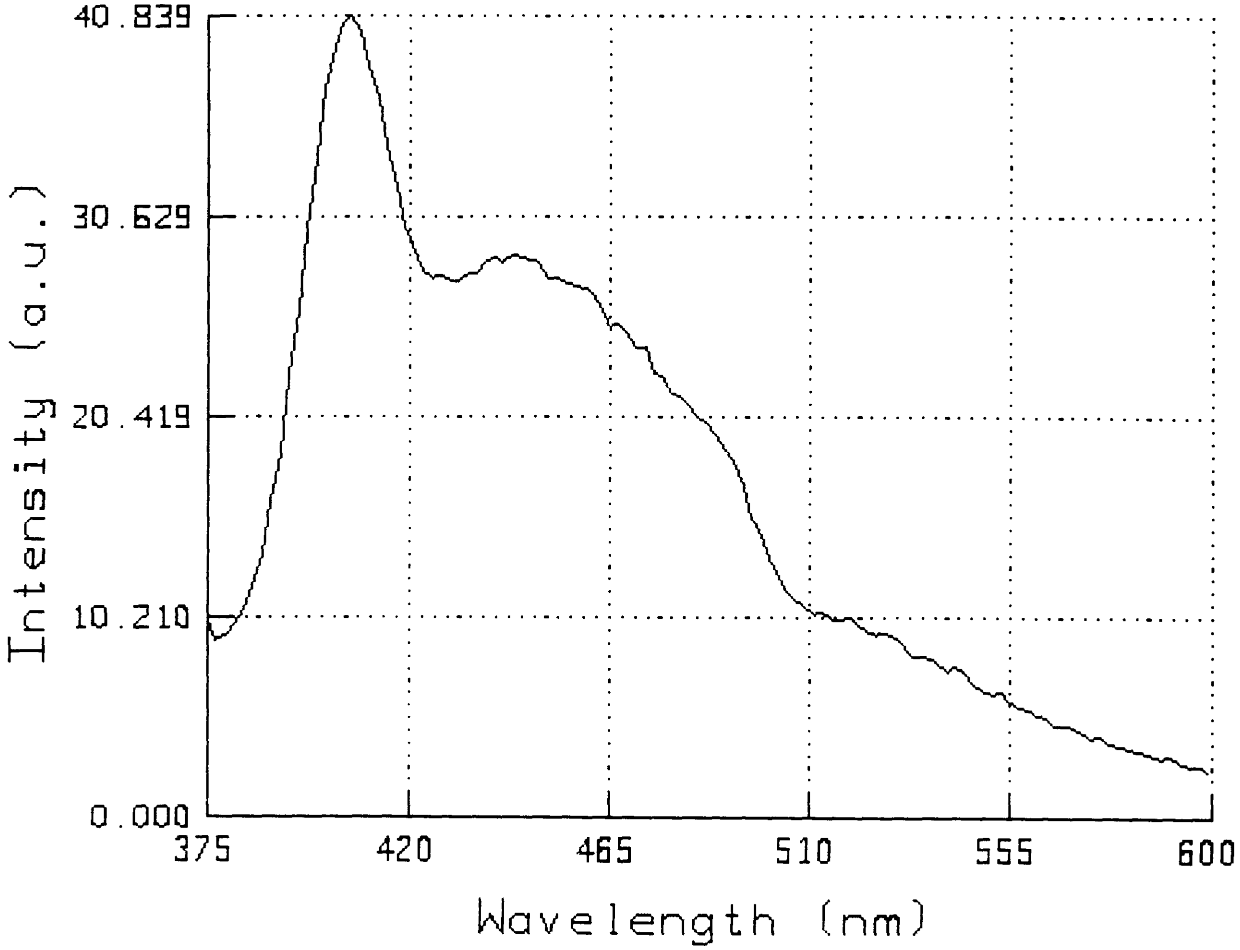

40.839
30.629
20.419
10.210
0.000
375
420
465
510
555
600
Intensity (a.u.)
Wavelength (nm)

and DOC of this filtrate suggests that its colloidal organic matter were decently preserved during storage. Ideally, the quenching experiments should be performed immediately on unfiltered samples. When run under the conditions used for analysis of methylperene, the intensity of the seawater's native fluorescence was about 25% of the total fluorescence of methylperylene-spiked seawater, and this signal was automatically blank-subtracted. The UV/VIS absorption spectrum of this seawater revealed optical densities (OD) of the sample matrix at the employed excitation (λ_x= 406 nm) and emission (λ_m= 442 nm) wavelengths of 0.0302 and 0.0293, respectively. These ODs were so low that any inner filter effects were small (≤ 3%) in this study (Lakowicz, 1983; Gauthier *et al.*, 1986).

Minimization of photodecomposition

To optimize design of the fluorescence quenching experiments and to accurately interpret their results, we assessed the potential for influence of methylperylene photodegradation. The choice of irradiation wavelength and dissolved oxygen level had large effects on the rate of methylperylene dissappearance (Fig. 3). Initial rates appeared linear in all cases, indicating a first-order removal mechanism such as photodegradation. That photolysis was the removal mechanism was further supported by the larger removal rates at shorter wavelengths (Table 1). Lower oxygen content resulted in significantly lowered rates of methylperylene removal; at 7 uM O_2, no losses were observed in the artificial seawater during 1 hour of constant irradiation. The loss rate in seawater was similarly much decreased when the oxygen content was lowered to 10 uM. However, the decrease in rate did not appear to be simply proportional to the decrease in oxygen content, indicating that the mechanism is more complex in the presence of natural components of seawater. In response to these findings, the fluorescence quenching experiments were performed with the solutions further deoxygenated (< 0.3 uM O_2). Furthermore, in the single wavelength quenching experiments, data points were only acquired during short pulses (4 sec integration) of intermittent 406 nm irradiation. In addition to removal of oxygen from the solutions, the intensity modulation in the lifetime experiments yields lower average levels of excitation light. The order of the frequencies at which phase and modulation data were acquired was scrambled so that any decrease in methylperylene fluorescence would be averaged over the whole range of possible lifetimes. Indicative of the fact that the detected fluorophore population remained unchanged even when significant photodegradation occured, the photobleached seawater-

Figure 3. Effect of matrix, dissolved oxygen levels, and excitation wavelength on the rate of decrease of methylperylene fluorescence at 442 nm during constant illumination. Filled symbols represent results from experiments in filtered seawater and open symbols were in artificial seawater. Triangles represent experiments of 278 nm irradiation of air equilibrated solutions. Irradiations at 406 nm were performed with solutions either fully air-equilibrated (squares) or with the dissolved O_2 concentrations decreased to about 10 uM (air equilibrated seawater is about 200 uM O_2; circles).

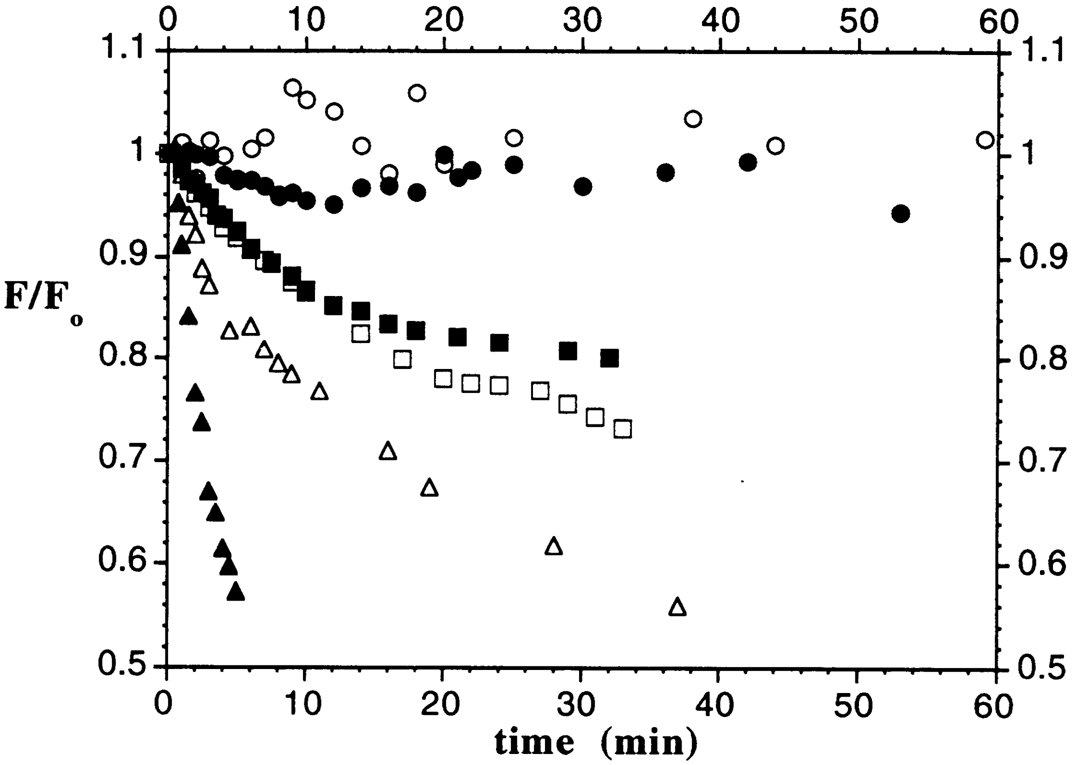
F/F$_o$
time (min)
0
10
20
30
40
50
60
0.5
0.6
0.7
0.8
0.9
1
1.1

TABLE 1. Photodegradation of methylperylene from a 300W Xe lamp

matrix	λ_x	$[O_2]$ (uM)	k_o^{app} (h^{-1})[a]
seawater	406	>200	0.88
seawater	278	>200	7.2
seawater	406	10	0.24
artificial seawater	406	>200	0.71
artificial seawater	278	>200	3.2
artificial seawater	406	7	0

[a] Since the mechanism of the degradation process is unknown, the initial first-order rate constant observed as a decrease of the 442 nm emission (KV 418 filtered) includes any edduct concentration in addition to the intrinsic reaction rate.

methylperylene spectrum was qualitatively unchanged relative to methylperylene in artificial seawater (Figure 1).

Quartz-wall sorption and fluorescence quenching

Methylperylene was found to sorb appreciably both to seawater colloids and to the walls of the quartz cuvette. A slower initial decrease in fluorescence was observed in the artificial seawater than in the seawater-methylperylene system (Fig. 4). This was interpreted as partitioning onto the quartz surface. Very rapid initial decrease in methylperylene fluorescence for the seawater system, spiked to the same starting level, indicated that colloid-seawater partitioning was simultaneously occuring andequilibrium was established on the timescale of 1 minute (Fig. 4). This was followed by a second and slower process causing continued fluorescence decrease (ca. 10 minutes), indicative of partitioning onto the quartz wall.

The rate of inferred quartz wall sorption in this study is in agreement with reports on this process from previous workers (Backhus and Gschwend, 1990; Schlautman and Morgan, 1994). Similarly, results of other investigators also indicate that colloid-water equilibration of HOCs is extremely rapid and occurs on timescales of 1 minute (e.g., Landrum *et al.*, 1984; McCarty and Jimenez, 1985; Gauthier *et al.*, 1986; Backhus and Gschwend, 1990).

The probe partitioning onto the quartz walls of the cuvette can be quantified from the artificial seawater results (Backhus and Gschwend, 1990):

$$K_{qtz} = \frac{[PAH_{wall}]}{[PAH_{aq}]\ (SA/V)} = \frac{(F_{o\text{-}start} - F_{o\text{-}end})}{F_{o\text{-}end}} \qquad (6)$$

where K_{qtz} (mL/cm^2) is the wall-water equilibrium partition coefficient, $[PAH_{wall}]$ (mol/cm^2) and $[PAH_{aq}]$ (mol/mL) are the concentrations of PAH associated with the wall and the aqueous solution, respectively. SA is the surface area of the 1 cm squared cuvette that is in contact with the water (13 cm^2) and V is the volume of water (3.0 mL). $F_{o,start}$ and $F_{o,end}$ are the original and equilibrium fluorescence of methylperylene in the artificial seawater solution. Assuming that the kinetics of wall sorption is a first-order process, the data in Fig. 4 may be fitted to:

$$F_o(t) = F_{o\text{-}end} + (F_{o\text{-}start} - F_{o\text{-}end})\ \exp(-k_{wall}\ t) \qquad (7)$$

Figure 4. Fluorescence quenching experiments of methylperylene sorption to quartz cuvette wall (artificial seawater: open circles) and cuvette wall in addition to seawater colloids (filtered seawater: closed circles).

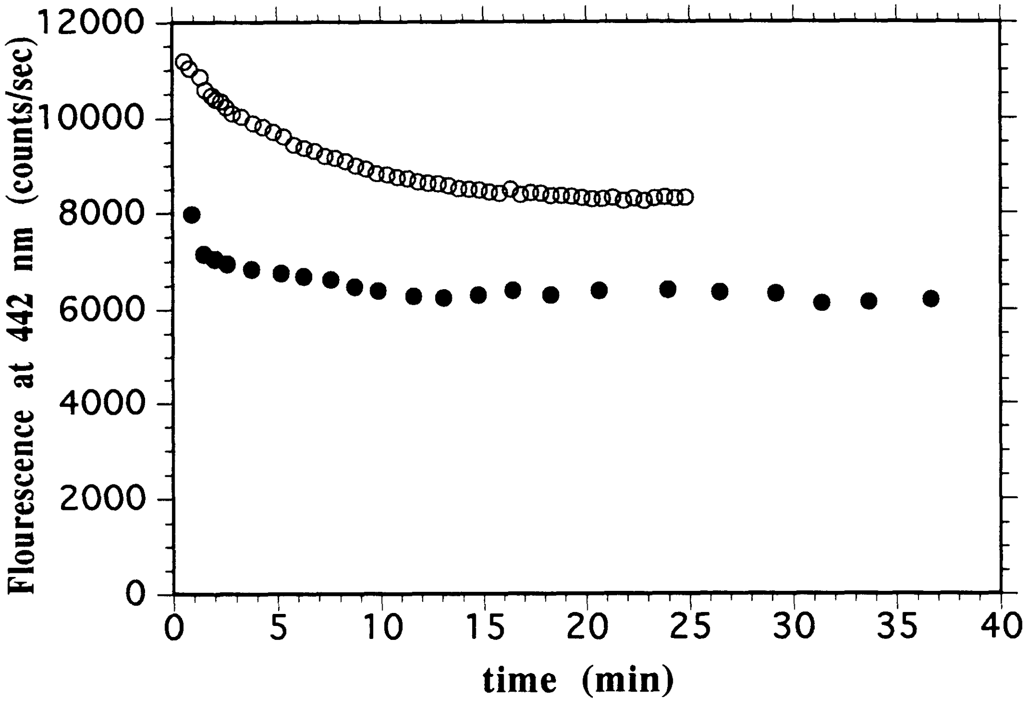

Flourescence at 442 nm (counts/sec)
12000
10000
8000
6000
4000
2000
0
0
5
10
15
20
25
30
35
40
time (min)

where $F_o(t)$ is the fluorescence of methylperylene in artificial seawater at time t (min), and k_{wall} (min^{-1}) is the rate of wall sorption. This yielded $F_{o,start}$ = 11360 ± 30 photon-counts/sec, $F_{o,end}$ = 8200 ± 20 photon-counts/sec,and k_{wall} = 0.163 ± 0.003 min^{-1} (R^2 = 0.997). This experiment thus suggested a K_{qtz} of methylperylene of 0.089 cm^2/mL. This experiment was repeated two additional times giving results of 0.080 and 0.10 cm^2/mL. Backhus (1990) reported a K_{silica} of methylperylene of 0.6 cm^2/mL from batch sorption experiments with a set of borosilicate glass containers with varying SA/V values. The discrepancy between the results from the two studies may be a result of differences in both the identity of, and PAH interactions with, surface cations as well as different SA/V values. Borosilicate may exhibit a different cationic surface than quartz which may better sorb PAHs of high electron densities. Backhus' (1990) systems also had larger SA/V values; hydrophobic PAHs are likely to partition onto this interface to decrease their interfacial energies (e.g., Goss, 1994).

The steady-state fluorescence in the seawater system when equilibrium was established (F_{end}) was lower that in the artificial seawater cuvette, indicating that there was additional quenching of methylperylene in addition to wall sorption. The quenching ratio $F_{o,end}$ to F_{end} (or F_o/F) was 1.32 in the above experiment (Fig. 4). A value of 1.28 was similarly obtained in an early test with solutions that were not deoxygenated (data not shown). This additional quenching, inferred to contain information about colloid-sorption, is difficult to interpret in the absence of knowledge regarding dynamic or static quenching. Furthermore, the fraction of methylperylene that was lost to the wall was expected to be lower in seawater due to colloid mediated "solubility enhancement". Hence, before developing a mathematical framework to derive a colloidal binding coefficient, it is necessary to analyze the lifetime distribution of methylperylene in the absence and presence of colloidal quenchers.

Fluorescence lifetimes

Measurement of fluorescence lifetimes is considered the most convincing method to elucidate whether dynamic quenching is occuring (e.g., Lakowicz, 1983; Chen *et al.*, 1994; Green and Blough, 1996). In the wall-equilibrated artificial seawater system, the smooth pattern in phase-shift and demodulation factors over the analyzed frequency range indicate that only one or a few fluorophores were contributing to the overall fluorescence (Fig. 5). A crossover frequency in the range of 120-130 MHz was suggestive of the

Figure 5. Frequency spectrum of phase-shift (crosses) and demodulation factors (squares) of methylperylene in artificial seawater.

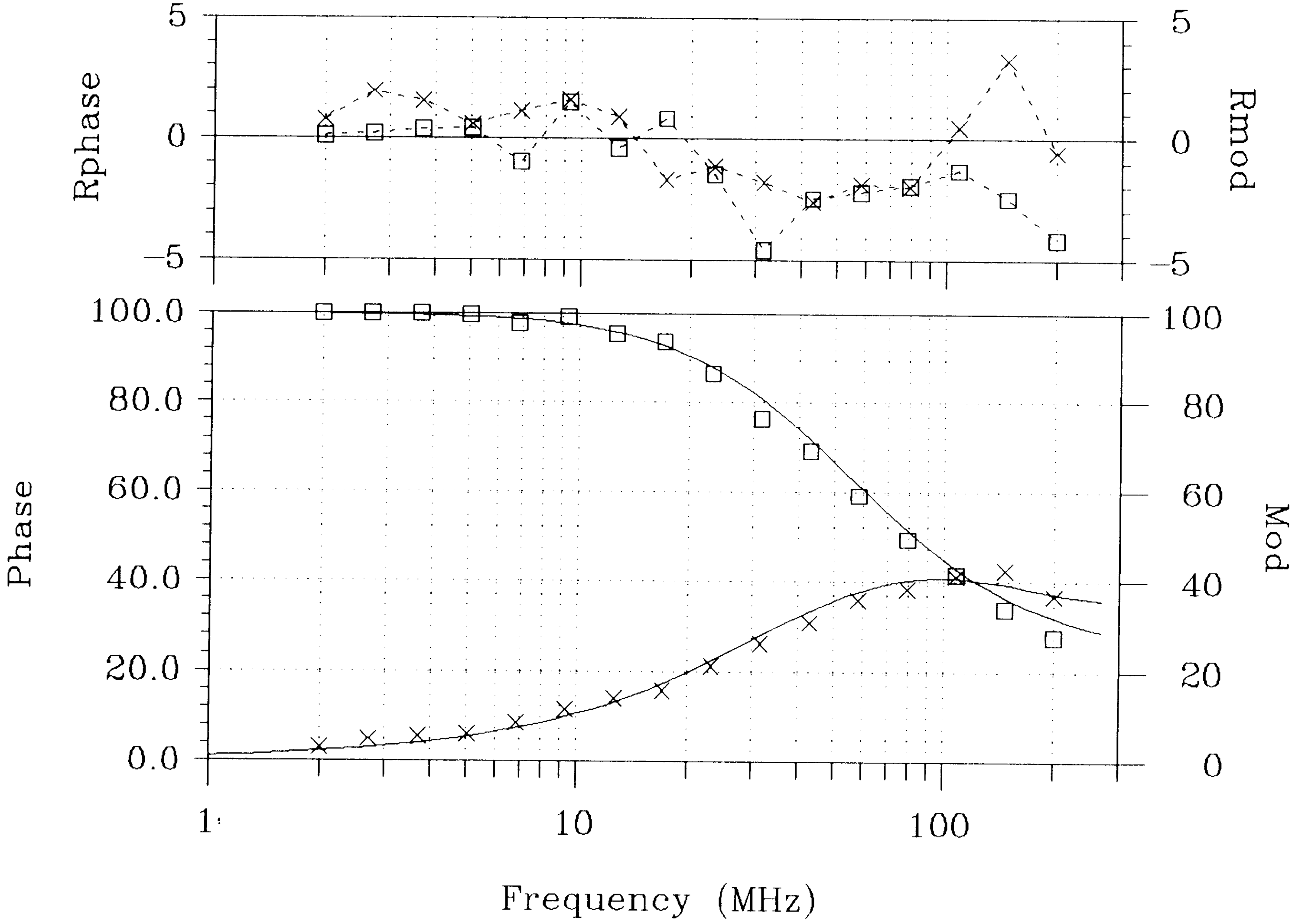
Rphase
Rmod
5
0
−5
Phase
Mod
100.0
80.0
60.0
40.0
20.0
0.0
100
80
60
40
20
0
1
10
100
Frequency (MHz)

dominance of fluorophore components with lifetimes of a few to several nanoseconds. Lifetimes calculated at each frequency with the ISS187 software suggested values between 0 and 5 nsec (Fig. 6). Unconstrained least-squares regression for two discrete components resulted in $\tau_1 = 3.85 \pm 0.23$ nsec (73% of total intensity) and $\tau_2 = 0.14 \pm 0.06$ nsec (23%). Since we knew that scatter was detected under these conditions (Rayleigh in the range of 415- 425 nm and Raman around 465 nm), we explored the effect of fixing the shorter-lived component at an instrument-limited measurable lifetime of scatter at 4 psec. However, this did not change the χ^2 of the fit (about 29) and did not significantly change the resolved lifetime of the first component ($\tau_1 = 3.61 \pm 0.30$ nsec; 80%). The determined lifetime of methylperylene in deoxygenated artificial seawater of 3.8 nsec is in the range of the lifetime of perylene at 6 nsec reported in a variety of solvents (e.g., Liu *et al.*, 1993).

In the unspiked, deoxygenated, seawater, the fluorescence lifetime distribution indicated the complete absence of the 3.8 nsec component (Fig. 7 and 8). Only a single short-lived component at 64 ± 8 psec could be resolved ($\chi^2 = 3.5$). Attempting to fit the phase and modulation data with two discrete components and/or with fixing the short -lived component at a scatter lifetime (4 psec) resulted in worse fits. It is interesting to note that the chloroplasts of green algae exhibit a fast lifetime component in the range 50-80 ps (e.g., Holzwarth *et al.*, 1985).

The lifetime distributions of the methylperylene in deoxygenated seawater system suggest the absence of a dynamically-quenched methylperylene species. Smaller phase-shifts and demodulation factors than in artificial seawater (Fig. 9) were indicative of the more dominant presence of a shorter-lived species than in the artificial seawater system (Fig. 5). However, demodulation and phase-shifts were recorded at the same frequencies as for methylperylene in artificial seawater. Unconstrained least-squares regression of the data with two discrete components resulted in $\tau_1 = 4.18 \pm 0.45$ nsec (23% of total intensity) and $\tau_2 = 0.085 \pm 0.017$ nsec (73%) with a χ^2 of 15. Fixing the shorter-lived component at 64 psec, as had been determined for the unspiked seawater matrix, resulted in an equally good fit of the data and a $\tau_1 = 3.86 \pm 0.42$ nsec (24%). Increasing the number of components on subsequent regressions did not improve the χ^2, indicating that no shorter-lived, potentially dynamically-quenched methylperylene components, were significantly contributing to the overall fluorescence. The identical lifetime of methylperylene (3.9 nsec) with or without quencher present was furthermore supported

Figure 6. Phase (crosses) and modulation (squares) based estimates of the average fluoresescence lifetime at 2- 200 MHz modulation frequencies of a solution of methylperylene in artificial seawater.

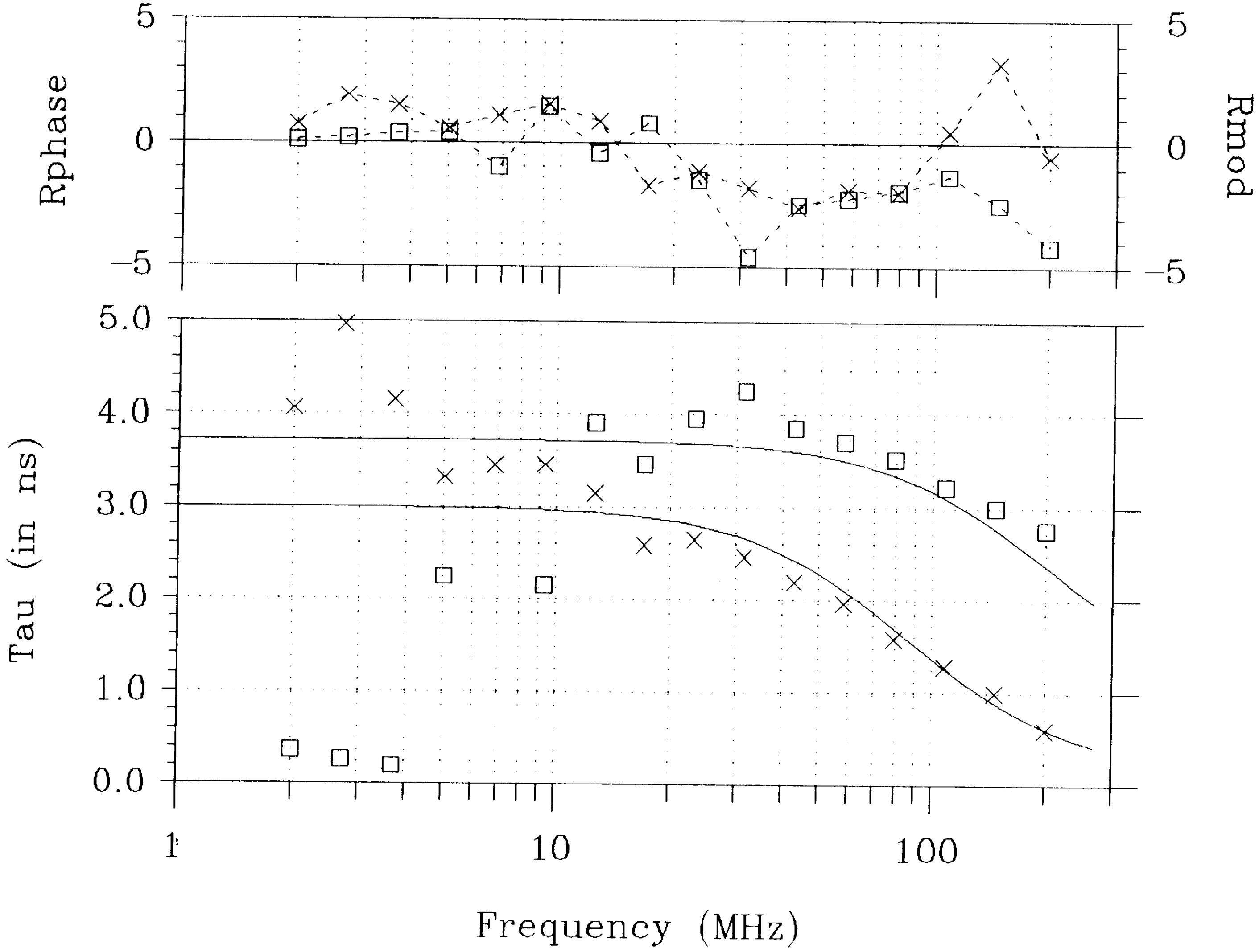
Rphase
Rmod
5
0
−5
Tau (in ns)
5.0
4.0
3.0
2.0
1.0
0.0
1
10
100
Frequency (MHz)

Figure 7. Frequency spectrum of phase-shift (crosses) and demodulation factors (squares) of filtered coastal seawater irradiated at 406 nm with a KV418 high band-pass emission filter.

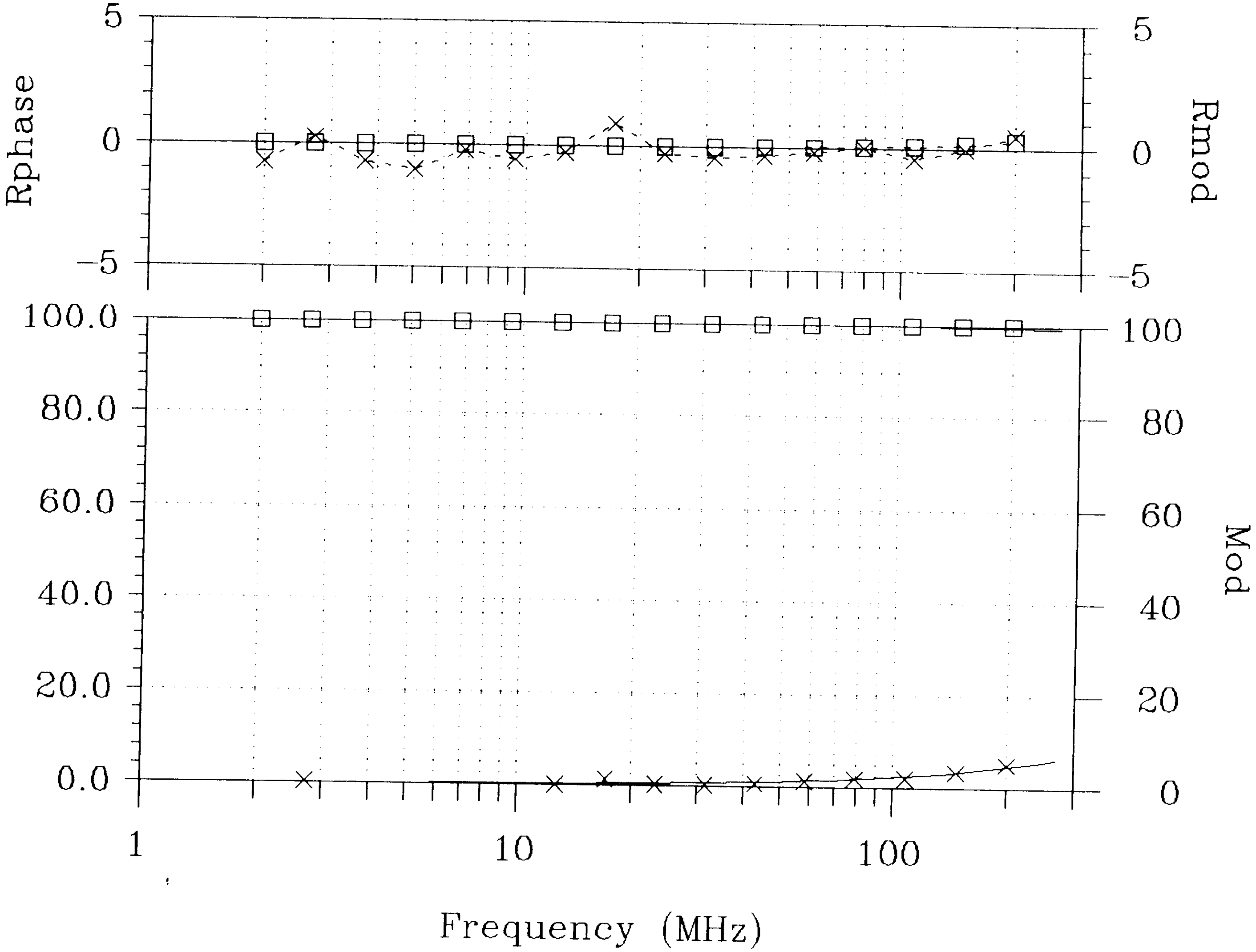
Rphase
5
0
−5
Rmod
5
0
−5
Phase
100.0
80.0
60.0
40.0
20.0
0.0
Mod
100
80
60
40
20
0
1
10
100
Frequency (MHz)

Figure 8. Phase (crosses) and modulation (squares) based estimates of the average fluoresescence lifetime at 2- 200 MHz modulation frequencies of filtered coastal seawater irradiated at 406 nm with a KV418 high band-pass emission filter.

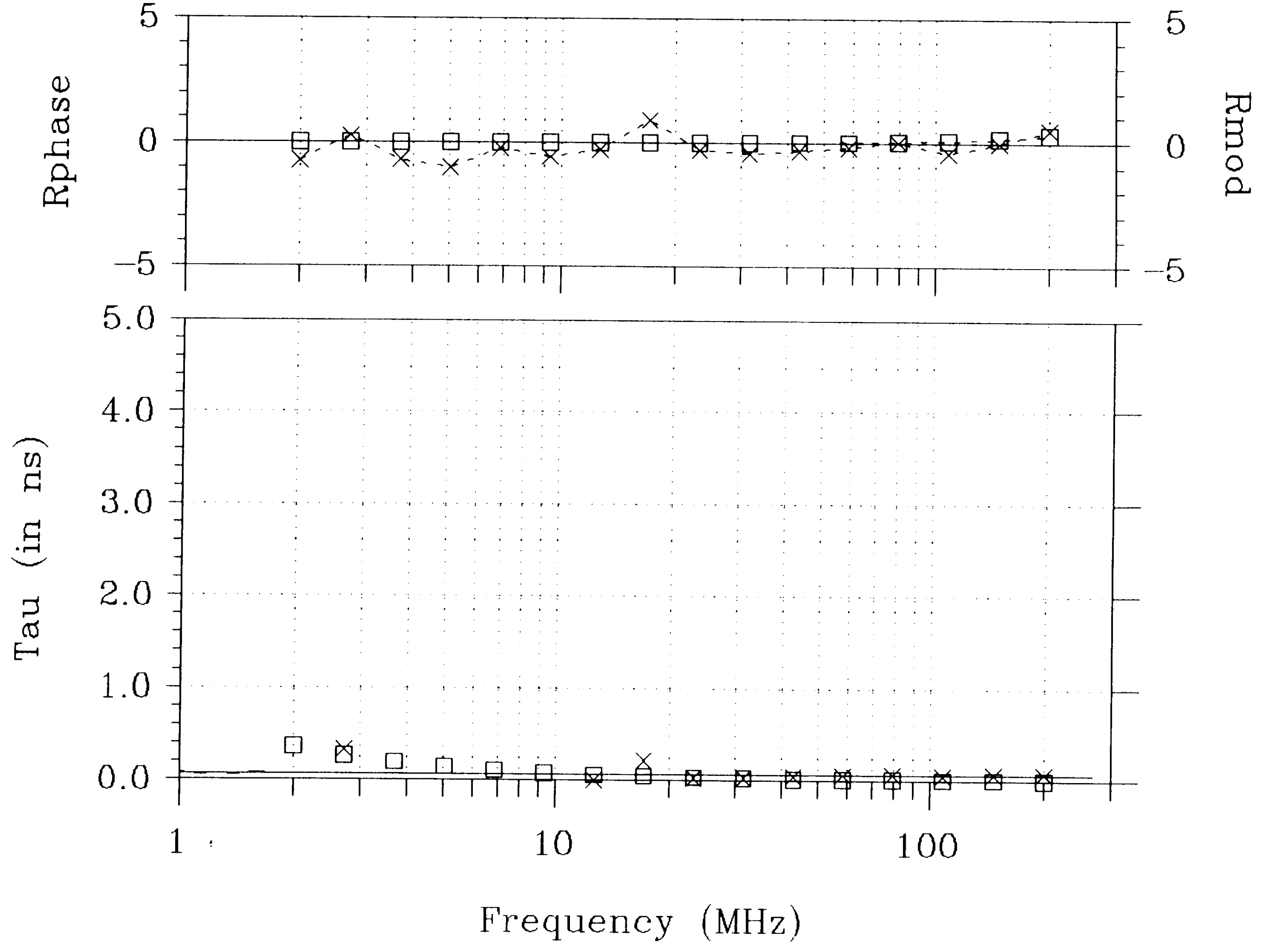
Rphase
Rmod
5
0
−5
5
0
−5
Tau (in ns)
5.0
4.0
3.0
2.0
1.0
0.0
1
10
100
Frequency (MHz)

Figure 9. Frequency spectrum of phase-shift (crosses) and demodulation factors (squares) of methylperylene equilibrated with filtered coastal seawater.

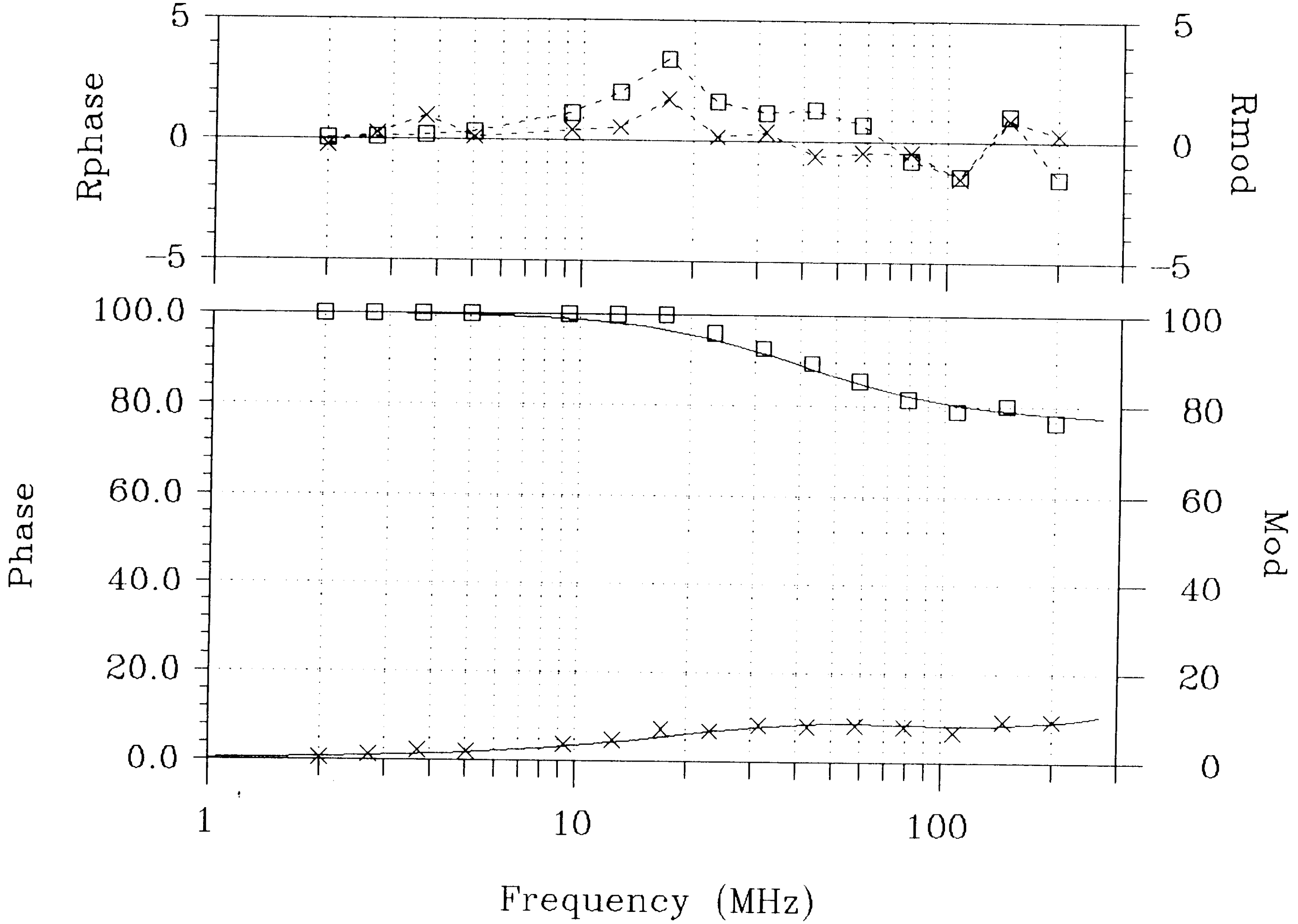
5
0
-5
Rphase
5
0
-5
Rmod
100.0
80.0
60.0
40.0
20.0
0.0
Phase
100
80
60
40
20
0
Mod
1
10
100
Frequency (MHz)

by the results from a very similar initial experiment performed with air-equilibrated samples. The inferred single lifetime of methylperylene in both those two oxygen-containing systems was 3.77 ± 0.20 nsec. Another observation suggesting that there is no significant dynamic quenching in the seawater-methylperylene system is the unchanged wavelength position and relative ratios of the two maxima in the methylperylene spectra in artificial vs. natural seawater (Fig. 1). Dynamically-quenched PAHs, such as pyrene associating with micellar systems, have been observed to exhibit a red-shift in emission as well as changing intensity of the different emission bands (Chandar *et al.*, 1987). The absence of a shorter-lived methylperylene fluorescence component in the presence of seawater colloids is strongly suggestive of a static mechanism dominating the seawater colloid quenching of PAHs. Furthermore, the identical lifetime recorded for the dissolved methylperylene fluorescence in artificial and natural seawater indicates that there is no significant quenching due to dissolved seawater species.

Colloid-water equilibrium partition coefficients

Given that all the PAH fluorescence was from the dissolved state (complete static quenching of colloid-associated methylperylene), it is possible to derive a wall-loss corrected colloidal binding constant for PAHs. The fluorescence quenching observed in the artificial seawater system can be described by (Backhus and Gschwend, 1990):

$$\frac{F_{o\text{-start}}}{F_{o\text{-end}}} = \frac{[PAH_{tot}]}{[PAH_{o\text{-aq}}]} = 1 + K_{qtz}(SA/V) \qquad (8)$$

For the seawater system, the addition of colloid-binding yields:

$$\frac{F_{start}}{F_{end}} = \frac{[PAH_{tot}]}{[PAH_{aq}]} = 1 + K_{qtz}(SA/V) + K_{DOC}[DOC] \qquad (9)$$

where K_{DOC} is the colloid-water distribution coefficient normalized to the DOC in the filtrate (in absence of accurate techniques to obtain colloidal organic carbon; see chapter 3 of this thesis). Since the initial losses in fluorescence were rapid (Fig. 4), the extrapolated initial values of fluorescences do include some uncertainty. Thus instead, equations 8 and 9 may be solved for $F_{o\text{-start}}$ and F_{start} (being equal), equated and rearranged to isolate the DOC-normalized binding coefficient without using the initial estimates:

$$K_{DOC} = \frac{\left((1 + K_{qtz}(SA/V))\left(\frac{F_{o\text{-}end}}{F_{end}} - 1\right)\right)}{[DOC]} \tag{10}$$

A value for F_{end} was obtained by fitting the portion of the seawater system data in Fig.4 that was believed to represent the wall sorption (all data points but the first) to Eqn. 7. This resulted in $F'_{start} = 7410 \pm 110$ photon-counts/sec, $F'_{end} = 6260 \pm 30$ photon-counts/sec, and $k'_{wall} = 0.18 \pm 0.03$ min^{-1} ($R^2 = 0.96$). With all these parameters quantified ($K_{qtz} = 0.10$ cm^2/mL, SA = 13 cm^2, V = 3.0 mL, $F_{o\text{-}end} = 8200$ photon-counts/sec, $F_{end} = 6260$ photon-counts/sec, and [DOC] = 179 uM), this expression yields a log K_{DOC} for methylperylene of 5.32 L_{sw}/kg_{DOC} (liter seawater per kg dissolved organic carbon).

The K_{DOC} may also be estimated using an alternative approach that is based on the apparent decrease in wall sorption in the seawater system relative to in the artificial seawater; a result of colloid-mediated solubility enhancement in the former solution. This competitive-sorbent titration (wall vs colloid sorption) was only possible because the binding to the wall and to the colloids were of similar magnitude. The apparent wall sorption coefficient ($(K_{wall})_{app}$) in the seawater system can be described by:

$$(K_{wall})_{app} = \frac{[PAH_{wall}]}{[PAH_{aq}] + [PAH_{coll}]} \tag{11}$$

Inverting and substituting for $[PAH_{wall}]$ from Eq. 6, yields:

$$\frac{1}{(K_{wall})_{app}} = \frac{1}{K_{qtz}} + \frac{[PAH_{coll}]}{[PAH_{aq}]\ K_{qtz}(SA/V)} \tag{12}$$

This equation may be solved for the colloid-water distribution constant, which may be normalized to the DOC content:

$$K_{coll} = \frac{\left(\frac{K_{qtz}}{(K_{wall})_{app}} - 1\right)}{[DOC]} \qquad (13)$$

Calculation of $(K_{wall})_{app}$, following Eq. 6, yielded a value of 0.044 mL/cm^2. This identical experiment had been performed once earlier, under aerobic conditions, yielding a $(K_{wall})_{app}$ of 0.042 mL/cm^2. The competitive-sorbent titration approach results in a log K_{DOC} for methylperylene of 5.77 L_{SW}/kg$_{DOC}$, which is within a factor of three of the K_{DOC} calculated above. Since I believe there is less uncertainty in the fluorescence quenching partition coefficient (based on equilibrium fluorescence levels and not the extrapolated initial values), log K_{DOC} of methylperylene was set to 5.3.

In the Inner Casco Bay seawater, one-third of a compound in the filtrate, with a similar hydrophobicity as methylperylene (log K_{DOC} = 5.3), would be predicted to be associated with colloids (Table 2). Using an aqueous activity coefficient for methylperylene of log γ_w = 8.7 (mol-based; Backhus, 1990), current partition models would predict a log K_{oc} of 6.60 for this compound (Karickhoff, 1981). There are several potential explanations to the much lower partitioning to organic carbon in seawater filtrate compared to previously explored natural organic matter from soils, sediments and porewater colloids. As discussed in detail in chapter 2, to qualify as a colloidal sorbent an organic macromolecule must be large enough to accomodate a hydrophobic solute. With total surface areas of 3-5 ringed PAHs of around 2 nm^2, this criterium translates into macromolecular weights of 1-10,000 D. Hence, smaller molecules and macromolecules with extended configuration without an interior "core" of such dimensions, may not sorb PAHs (chapter 2). Since whether a macromolecule acts colloidally is partially independent of its size, size-based speciation attempts to fractionate colloidal sorbents are difficult to reconcile with this view. Nevertheless, if one accepts that the two-thirds of the TOC that frequently is found to pass through 1000 D ultrafilters (e.g., Benner *et al.*, 1992; Guo *et al.*, 1994) is too small to sorb PAHs, the organic-carbon normalized partition coefficient of the remainder would be increased by a factor of three (0.5 log units) compared to the K_{DOC} listed in Table 2. Affecting the predictions in the opposite direction, "salting out" of solutes in seawater (e.g., May, 1980; Whitehouse, 1984) results in 0.2 log units higher estimates of log K_{oc} than the K_{DOC} listed in Table 2. Clearly, seawater colloids appear less efficient sorbents for HOCs than predicted from existing models. However, these low colloid partition coefficients are in agreement with solubility enhancement studies of benzo[a]pyrene where log K_{DOC}'s were found in the range of 5.0 - 5.3 using seawater

TABLE 2. Predicted PAH organic colloid - water partition coefficients

				K_{OC}-predicted	
compound	**log K_{DOC} (L_{sw}/kg_{DOC})**	**f_{aq}**	**f_{coll}**	**log K_{oc}[a] (L_w/kg_{oc})**	**f_{aq}**
methylperylene	5.3	0.70	0.30	6.6	0.10
benzo[a]pyrene	5.1	0.79	0.21	6.4	0.17
perylene	4.5	0.94	0.06	5.6	0.52
pyrene	4.1	0.97	0.03	5.1	0.78
phenanthrene	3.4	0.99	0.006	4.3	0.96

[a]The organic-carbon normalized partition constants were estimated from the compounds' solubilities (Miller *et al.*, 1985, except methylperylene: Backhus, 1990) using the linear free energy relationship for aromatic hydrocarbons in Karickhoff (1981).

from coastal, shelf, and pelagic surface regimes (Whitehouse, 1985). Furthermore, Chiou *et al.* (1986) have shown that colloidal aquatic fulvic acids may have a log K_{oc} of similarly hydrophobic DDT that is 0.7 units lower than when tested with larger and more nonpolar soil humic acids. The "quality" of the organic matter may make a significant difference to the sorbent characteristics of colloidal particles.

The low sorption efficiency of surface seawater colloidal organic matter must be related to its structure and hence its ability to interact intermolecularly with PAHs. Macromolecules in seawater have been shown to have a very high turnover rate (Amon and Benner, 1994), resulting from the high carbohydrate content of this filter-defined pool (Benner *et al.*, 1992). Many carbohydrate macromolecules are known to attain an extended tertiary configuration that would not provide an interior phase for HOCs to partition into (see further chapter 2). This has been succinctly illustrated by the inability of cellulose to sorb PCBs (Garbarini and Lion, 1986). Furthermore, Chen and co-workers have shown that the organic-carbon normalized total fluorescence in marine sediment porewater is at least an order of magnitude higher than in the overlying seawater (Chen *et al.*, 1993; Chen and Bada, 1994). Given that the fluorescence is largely indicative of aromatic moieties, which could be expected to have a higher sorptive affinity for PAHs, this indicates that diagenetically altered macromolecular organic matter may constitute better sorbents for HOCs.

Using the relationship for methylperylene between the found log K_{DOC} and the predicted log K_{oc} (log $K_{DOC} \approx 0.80$ log K_{oc}), similar colloid-water partition coefficients for several other PAHs were estimated from their respective log K_{oc} values (Table 2). The relatively weak interactions for PAHs with these seawater colloids resulted in the prediction that the dominant fraction of filter-passsing PAHs are truly dissolved. The colloidal fraction ranges from 0.6% for phenanthrene to 21% for benzo[a]pyrene (Table 2). One significant implication of this discovery of "poor" sorbent properties of surface seawater colloids is that the bioavailable fraction of filter-passing hydrophobic pollutants is much higher than predicted from organic-matter based partition models (e.g.; Karickhoff, 1981) and estimates of the colloidal organic carbon levels.

References

Aiken, G.R., 1984. Environ. Sci. Technol., 18: 978-981.

Amon, R.M.W. and Benner, R., 1994. Nature, 369: 549-552.

Backhus, D. A. Ph.D. Dissertation, Massachusetts Institute of Technology, 1990.

Backhus, D. A., and P. M. Gschwend. 1990. Environ. Sci. Technol., 24: 1214-1223.

Baker, J. E., P. D. Capel, and S. J. Eisenreich. 1986. Environ. Sci. Technol. 20: 1136-1143.

Benner, R., Pakulski, D.J., McCarthy, M., Hedges, J.I. and Hatcher, P.G., 1992. Science, 255: 1561-1564.

Boehm, P. D., and J. G. Quinn 1973. Geochim. Cosmochim. Acta 37: 2459-2477.

Brownawell, B. J., and J. W. Farrington. 1986. Geochim. Cosmochim. Acta 50: 157-169.

Buesseler, K.O., Bauer, J., Chen, R., Eglinton, T., Gustafsson, Ö., Landing, W., Mopper, K., Moran, S.B., Santschi, P., VernonClark, R. and Wells, M., 1996. Mar. Chem. 55: 1-31.

Buffle, J., Perret, D. and Newman, M., 1992. In: J. Buffle and H. P. van Leeuwen (Editors), Environmental Particles (Vol. 1). Lewis, Boca Raton, pp. 171-230.

Carter, C.W., and I. H. Suffet. 1982. Environ. Sci. Technol. 16: 735-740.

Chandar, P., P. Somasundaran, and N. J. Turro. 1987. J. Colloid. Interface Sci. 117: 31-46.

Chen, R. F., J. L. Bada, and Y. Suzuki. 1993. Geochim. Cosmochim. Acta 57: 2149-2153.

Chen, R. F., J. L. Bada. 1994. Mar. Chem. 45: 31-42.

Chen, S., W. P. Inskeep, S. A. Williams, and P. R. Callis. 1994. Environ. Sci. Technol. 28: 1582-1588.

Chin, Y.-P., and P. M. Gschwend. 1992. Environ. Sci. Technol. 26: 1621-1626.

Chin, Y.-P., and W. Weber. 1989. Environ. Sci. Technol. 23: 978-984.

Chiou, C. T., L. J. Peters, and V. H. Freed. 1979. Science 206: 831-832.

Chiou, C. T., R. L. Malcolm, T. I. Brinton, and D. E. Kile. 1986. Environ. Sci. Technol. 20: 502-508.

Danielsen, K. M., Y.-P. Chin, J. S. Butterbaugh, T. L Gustafson, and S. J. Traina. 1995. Environ. Sci. Technol. 29: 2162-2165.

Eaton, D. F. 1988. Pure Appl. Chem. 60: 1107-1114.

Garbarini, D. R., and L. W. Lion. 1986. Environ. Sci. Technol. 20: 1263-1269.

Gauthier, T. D., E.C. Shane, W. F. Guerin, W. R. Seitz, and C. L. Grant. 1986. Environ. Sci. Technol. 20: 1162-1166.

Gauthier, T. D., W. R. Seitz, and C. L. Grant. 1987. Environ. Sci. Technol. 21: 243-248.

Geiger, M. W., and N. J. Turro. 1975. Photochem. Photobiol. 22: 273-290.

Goss. K.-U. 1994. Environ. Sci. Technol. 28: 640-645.

Gratton, E., and M. Limkeman. 1983. Biophys. J. 44: 315-324.

Gratton, E., D. M. Jameson, N. Rosato, and G. Weber. 1984. Rev. Sci. Instrum. 55: 486-494.

Green, S. A., and N. V. Blough. 1996. Environ. Sci. Tech. 30: 1407-1408.

Gschwend, P. M., and S.-C. Wu. 1985. Environ. Sci. Tech. 19: 90-96.

Guo, L., Coleman Jr, C.H. and Santschi, P.H., 1994. Mar. Chem., 45: 105-119.

Haag, W. R., and J. Hoigné. 1986. Environ. Sci. Technol. 20: 341-348.

Hoge, F. E., A. Vodacek, and N. V. Blough. 1993. Limnol. Oceanogr. 38: 1394-1402.

Holzwarth, A. R., J. Wendler, W. Haehnel. 1985. Biochim. Biophys. 807: 155-167.

Karickhoff, S. W., D. S. Brown, and T. A. Scott. 1979. Water. Res. 13: 241-248.

Lakowicz, J. R. Principles of Fluorescence Spectroscopy. Plenum Press, New York, 1983, 496 pp.

Landrum, P., S. R. Nihart, B. E. Eadie, and W. S. Gardner. 1984. Environ. Sci. Technol. 18: 187-192.

Leversee, G. J., P. Landrum, J. Giesy, T. Fannin. 1983. Ca. J. Fish. Aq. Sci., 40(S2): 63-69.

Liu, Y. S., P. de Mayo, and W. R. Ware. 1993. J. Phys. Chem. 97: 5987-5994.

May, W. E. In: Petroleum in the Marine Environment, L. Petrakis and F. T. Weiss (Eds.), Ch.7, Advances n Chemistry Series No. 185, American Chemical Society, Washington, DC, 1980, pp. 143-192.

McCarty, J. F., and B. D. Jimenez. 1985. Environ. Sci. Technol. 19: 1072-1076.

Means, J. C., and R. Wijayaratne. 1982. Science 215: 968-970.

Miller, M. M., S. P. Wassik, G.-L. Huang, W.-Y. Shiu, and D. Mackay. 1985. Environ. Sci. Technol. 19: 522-531.

Morra, M. J., M. O. Corapcioglu, R. M. A. von Wandruszka, D. B. Marshall, and K. Topper. 1990. Soil Sci. Soc. Am. J. 54:1283-1289.

Peake, D. A., A. R. Oyler, H. E. Heikkila, R. J. Liukkonen, E. C. Engroff, and R. M. Carlson. 1983. Synth. Commun. 13: 21-26.

Puchalski, M. M., M. J. Morra, and R. von Wandruszka. 1991. Fresenius J. Anal. Chem. 340: 341-344.

Puchalski, M. M., M. J. Morra, and R. von Wandruszka. 1992. Environ. Sci. Technol. 26: 2787-792.

Schlautman. M. A., and J. J. Morgan. 1993a. Environ. Sci. Technol. 27: 2523-2532.

Schlautman. M. A., and J. J. Morgan. 1993b. Environ. Sci. Technol. 27: 961-969.

Schlautman, M. A., and J. J. Morgan. 1994. Environ. Sci. Technol. 28: 2184-2190.

Tissot, B. P., and D. H. Welte. Petroleum Formation and Occurence. Springer-Verlag: New York, 1978.

Ware, W. R. 1962. J. Chem. Phys. 66: 455-458.

Whitehouse, B. G. 1984. Mar. Chem. 14: 319-332.

Whitehouse, B. G. 1985. Estuar. Coastal Shelf Sci. 20: 393-402.

Chapter 5

Quantification of the Dilute Sedimentary Soot-Phase: Implications for PAH Speciation and Bioavailability

Örjan Gustafsson, Farnaz Haghseta, Charmaine Chan,
John MacFarlane, and Philip M. Gschwend*
R. M. Parsons Laboratory, MIT 48-415
Department of Civil and Environmental Engineering
Massachusetts Institute of Technology
Cambridge, MA 02139

submitted
Environmental Science and Technology

Abstract

Existing field data indicate that soot may significantly affect the environmental speciation of polycyclic aromatic hydrocarbons, PAHs. To expand hydrophobic partition models to include soot partitioning, we need to quantify f_{SC}, the soot fraction of the solid matrix, and K_{SC}, the soot-carbon normalized partition coefficient. To this end, we have developed a method that allows quantification of soot carbon in dilute and complex sedimentary matrices. Non-soot organic carbon is removed by thermal oxidation and inorganic carbonates by acidification, followed by CHN elemental analysis of the residual soot carbon. The selectivity of the soot carbon method was confirmed in tests with matrices of known composition.

The soot quantification technique was applied to two sets of natural sediments, both previously analyzed for PAHs. The input histories of PAHs and soot recorded in a lacustrine sediment core followed the same general trends and we thus infer a coupling between the two. Our measures of f_{SC} and calculations of K_{SC}, approximated from studies of PAH sorption onto activated carbon (1), were applied to rationalize previously generated *in situ* K_{OC}'s (2-3). Intriguingly, we find that the elevated PAH K_d's of two marine sediment-porewater systems are now quantitatively explainable through the extended, soot-partioning inclusive, distribution model. The importance of the soot-phase for PAHs in the environment has implications for how we perceive (and should test) *in situ* bioavailability and consequently also for the development of sediment quality criteria.

Introduction

There are numerous indications in existing field data that soot-like phases may significantly affect the environmental PAH speciation. Socha and Carpenter (4) were not able to detect any porewater PAHs at a site contaminated by pyrogenic sources, despite expectations from $f_{oc}K_{oc}$ calculations (f_{oc}, the organic carbon fraction of the solid matrix, and K_{oc}, the organic-carbon normalized partition coefficient: ref. 5-7) of considerable porewater PAHs. They attributed this to the association of PAHs with soot. Several recent field investigations have reported K_{oc}'s for PAHs that are much larger than predictions based on organic matter partitioning models (5-7) (Figure 1a). These studies were performed in many different settings, including lake (8), estuarine (9), and marine (10) surface waters, sediment pore-waters (2-3), and rain-water (11). These results suggest the presence of a particulate phase like soot, to which PAHs are significantly more strongly associated than with natural organic matter. Since these data still indicate an influence of sorbate hydrophobicity (e.g., K_{ow}) on the reported K_{oc}'s, it may be concluded that an exchange between the "super-sorbent" and solution phases is taking place. In contrast, field-obtained K_{oc}'s for similarly hydrophobic polychlorinated biphenyls (PCBs) are typically lower and agree better with the organic-matter-based partition-model predictions (2, 3, 8, 11, 14).

In order to rationalize the elevated K_d's commonly observed for PAHs from the field, we suggest that the hydrophobic partitioning framework be expanded to also include partitioning with (mostly anthropogenic) soot phases:

$$\mathbf{K_d = f_{oc}\ K_{oc} + f_{sc}\ K_{sc}} \qquad (1)$$

where f_{sc} is the soot carbon fraction of the solid matrix (g soot carbon/g solid) and K_{sc} is the soot-carbon normalized partition coefficient [(mol/g soot) x (mol/ mL solution)$^{-1}$]. Hence, to model accurately the environmental fate of compounds like PAHs which appear to exhibit high affinities for soot, two new parameters, f_{sc} and K_{sc}, may need to be constrained. While we know of no controlled investigations on soot-water partitioning of PAHs, sorption studies onto activated carbon have been reported (Figure 1b) (1, 15). Mass-normalized activated carbon-aqueous solution partition coefficients, K_{ac}, for PAHs, calculated from such studies, resemble the elevated partition coëfficients observed in the environment for combustion-derived compounds like PAHs. If we thus may assume that K_{sc} can be reasonably approximated by the K_{ac}'s derived in Figure 1b, then the only other parameter required to investigate quantitatively the importance of soot partitioning for PAH speciation is the environmental soot abundance, f_{sc}.

FIGURE 1. (a) *In situ* PAH K_{OC}'s observed in several different types of environmental regimes: estuarine (dotted open circles = ref. 9), lacustrine (open squares = ref. 8) and marine (filled circles = ref. 10) surface waters, rain water (open triangles = ref. 11), and sediment pore-water (crosses = ref. 2-3).
(b) Calculated activated-carbon partition coefficients (K_{ac}) for a range of PAHs. (open squares = ref. 15; filled circles = ref. 1). The K_{ac} values from ref. 1 were calculated using the linearized Langmuir equation for the low equilibrium PAH concentration range; this case appear most applicable to environmental levels and Walters and Luthy (1) found this form to best represent their isotherm data. K_{ow} values for both (a) and (b) are from (5, 12-13, 16).

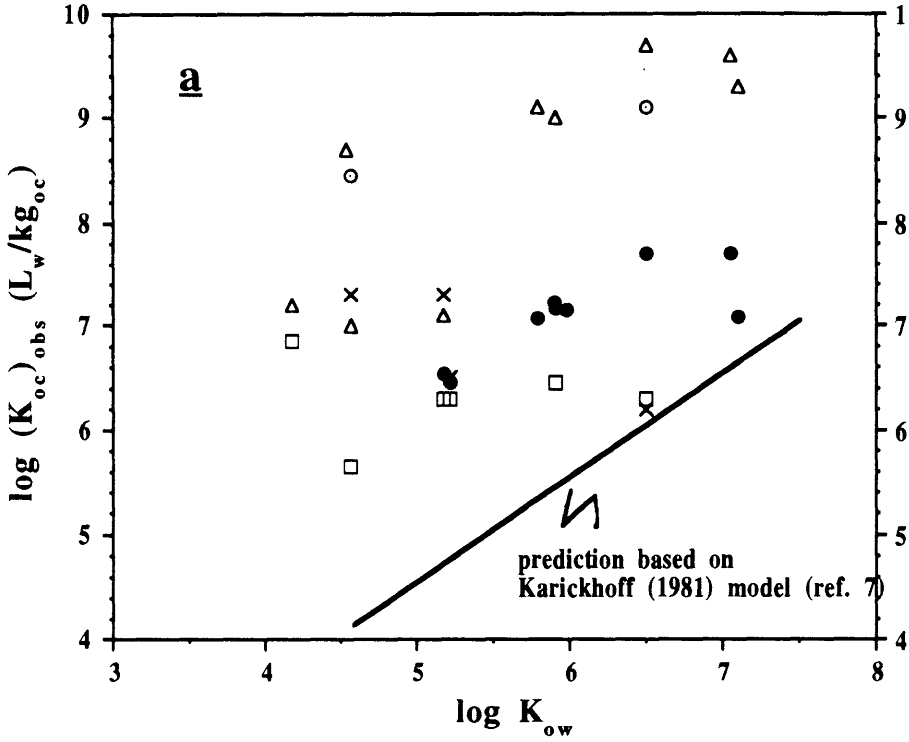
a
log $(K_{oc})_{obs}$ (L_w/kg_{oc})
log K_{ow}
prediction based on Karickhoff (1981) model (ref. 7)
10
9
8
7
6
5
4
3
4
5
6
7
8

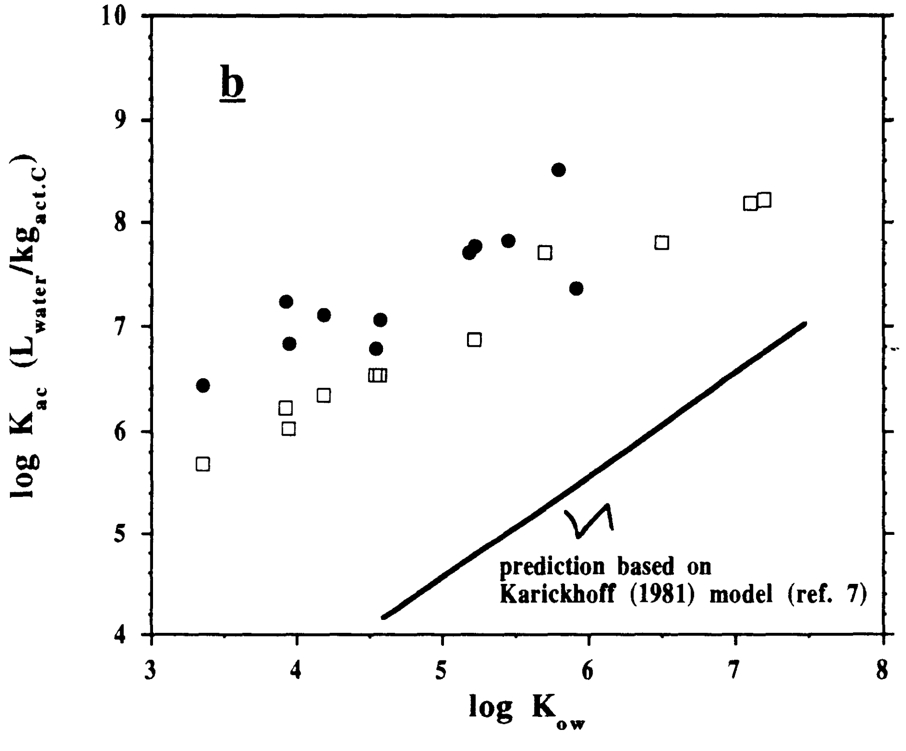
b
log K_{ac} $(L_{water}/kg_{act.C})$
log K_{ow}
prediction based on Karickhoff (1981) model (ref. 7)
10
9
8
7
6
5
4
3
4
5
6
7
8

It is the primary objective of this paper to describe a method that allows quantitative estimation of this dilute soot-phase in complex environmental matrices. We then apply this method to natural sediments and demonstrate the potential importance of a soot sorbent phase to estimating the environmental behavior and effects of combustion-derived contaminants like PAHs.

Experimental Section

Background

As pointed out by Ed Goldberg in his book, *Black Carbon in the Environment*, there is no unambigious definition of the highly condensed carbonaceous residue from incomplete combustion processes (17). The myriad of existing descriptors: soot, smoke, black carbon, carbon black, charcoal, spheroidal carbonaceous particles, elemental carbon, graphitic carbon, and charred particles, reflect either the functional processes studied or the operational techniques and definitions employed by different investigators. With the present objective of understanding PAH speciation, a method is warranted that quantitatively recovers the total mass of PAH-carrying soot carbon from dilute environmental matrices like sediments without inclusion of carbon from carbonates and biogenic organic matter.

Previous analytical approaches may be divided into three broad categories: (i) particle counting of dilute sedimentary soot , (ii) thermal carbon determination of abundant atmospheric soot, and (iii) spectroscopical structural investigation of pure soot. Sedimentary soot studies characteristically involve an acid-digestion and oxidation treatment, followed by microscopical soot particle counting (18-21). Using this approach, Goldberg and co-workers have recreated the historical "charcoal" record of forest fires in cores from Lake Michigan and the pelagic ocean (18, 22). The spatial and temporal history of anthropogenic fossil fuel combustion has similarly also been investigated (21-23). In the only previous study to have investigated directly the importance of soot on PAH distribution in natural waters, a correlation between the particulate concentration of individual PAHs and the abundance of such large "spheroidal carbonaceous particles" was indeed found in an urban estuary (24). However, these microscopy-based methods are commonly limited to soot-particles >5-10 μm. Since it has been shown that most soot particles in the atmosphere are smaller than a few microns (25), only analyzing the coarse fraction of soot prevents quantitative interpretation of such studies in terms of a PAH partition model.

The atmospheric soot methods are typically based on identifying the temperature conditions where organic carbon, OC, is thermally destabilized, while the soot carbon, SC, is still intact (26-27). While a selective thermal approach may recover a substantial fraction of the whole SC mass, the current methods, developed primarily for atmospheric particles and forest fire residues, are not directly applicable to a complex sedimentary matrix. It is important to consider the differences between soot-laden atmospheric particles and dilute sedimentary samples. Atmospheric particles contain high levels of SC, and the organic fraction is comprised primarily of sorbed low-molecular-weight molecules, which are easy to thermally degrade. To determine accurately dilute SC in sediments using a thermal approach, the method needs to be developed and tested for its suitability in the presence of recalcitrant macromolecular organic matter, physically large solids, and large abundance of carbonate minerals (see Table 1, below).

Spectroscopical investigations of soot have been aimed at obtaining qualitative structural information (28-29). Such techniques might reveal properties of the exterior of SC. They do not yield quantitative measures needed for the present investigation.

The approach taken in this study to determine the dilute sedimentary soot-phase is based on thermal oxidation of OC, followed by release of inorganic carbonates (IC) via *in situ* acidification. The residual SC is then quantified by CHN elemental analysis.

Removal of OC

Samples were dried in covered containers at 60°C and ground to <500 μm individual particle size. About 50 mg of each sample was weighed into pre-tared porcelain crucibles with a silica glaze surface (Coors Ceramics, Golden, CO). A rack of up to eight crucibles, covered with pre-combusted aluminum foil, was placed inside a muffle furnace (Thermolyne model F-A1730 equipped with an auxiliary temperature controller Thermolyne Furnatrol 133, Sybron Corp., Dubuque, Iowa). All samples were oxidized at 375°C for 24 h in the presence of excess oxygen (air).

Removal of IC

The cooled samples were subsampled and weighed (1-10 mg, depending on availability of residue and expected C content) into pre-tared Ag capsules (D2029, 8x5 mm; Elemental Microanalysis Ltd., Manchester, NH) using an electrical microbalance (Cahn 25 Automatic Electrobalance; Ventron Corp., Cerritos, CA). Throughout the acidification procedure, the Ag capsules were kept in a home-built Al tray with 32 positions. Several method blanks and standards (acetanilide) were included in each batch of samples. A micro-dispenser with a glass capillary tube was used in adding low-C water (Aries Vaponics, Vaponics Corp., Rockland, MA) and acid for the *in situ* removal of IC. After wetting each sample with 25 µl water, 25 µl of 1 M HCl was added into each Ag capsule. Then, the samples were allowed to sit for 1 hour at room temperature covered with clean Al foil. When the capsules had cooled, another 50 µl of 1 M HCl was added, followed by 30 min of cooling. The Al tray with samples was then placed in an oven and dried at 60°C. The last three steps were repeated until effervescence upon acid-addition ceased, indicating complete removal of carbonates. As pointed out by Nieuwenhuize *et al.* (30), this type of carbon determination, using *in situ* acidification, is advantageous in that it eliminates reweighing procedures, consumes only about 10 mg sample per analysis and, importantly, avoids losses of acid-soluble organic material to transitory containers.

CHN Elemental Analysis

The composition of the prepared samples was determined using a PE 2400 CHN Elemental Analyzer (Perkin Elmer Corp., Norwalk, CT). The detection limit of the analyzer (i.e., instrument blank) was about 4 µg C. Response factors were determined using an acetanilide standard (relative standard deviation within batches was ca. 0.3%). Sample preparation blanks were determined with each batch (for entire project: 9.6±4.4 µg C, n=19) and subtracted from raw sample data. Tests in which temperature and duration of combustion were varied verified that the same set of standard operating procedures could be used for quantitative C determination of all samples, irrespective of the soot content. Quantitative oxidation of soot by this instrumental method was indicated by a yield of 82% C upon analysis of weighed standard soot (Table 1), well within the 75-90% range commonly found on soot particles (31).

Elucidation of Optimal Combustion Temperature

The first analytical objective was to constrain the temperature where natural organic matter was thermally unstable, while soot mass was preserved intact. For SC, we employed National Institute of Standards & Technology (NIST) Standard Reference Material 1650: diesel particulate matter (NIST, Gaithersburg, MD). Initial characterization of this soot standard using photon correlation spectroscopy (N4 submicron particle analyzer, Coulter Electronics; Hialeah, FL) yielded an average soot size in sonicated ethanol suspensions of 180±20 nm. Scanning electron microscopy (SEM) of this standard indicated a primary particle size of 30 nm, with aggregates up to 400 nm. To represent natural OC, we used Humic Acid (Aldrich Chem. Co.; Milwaukee, WI). Based on the recoveries of these two standards, the optimal temperature selectivity was elucidated through a set of runs where the combustion temperature was systematically varied, while keeping all other parameters constant.

Method Testing with Well-Characterized Matrices

The suitability of the method to sedimentary SC quantification was validated through testing with several rather well-characterized substances, which could be considered as representing different components of complex sedimentary organic matter or anthropogenic combustion "phases" (see Table 1). Two organic polymers, polystyrene and polyethylene, were obtained by fine-shredding of a coffee-cup and a milk-bottle, respectively. Fine dust of oak wood was similarly prepared from a cleaned piece of lumber. Starchy and waxy corn pollen were from Carolina Biological Supply (Burlington, NC). Fuel oil (Diesel #2) and crude oil (Gullfax field, North Sea) were both tested. We also analyzed an unused car-tire (vulcanized rubber) sample containing 30±2% carbon black (Bernard Chien, Cooper Tire, Findlay, OH, personal communication). A number of coal matrices of increasing thermal maturity were tested. Two well-studied kerogens, Green River shale and Kimberlite (e.g., ref. 32), were analyzed. Three samples were also tested from the well-characterised Argonne National Laboratory's premium Coal Series: Beulah-Zap (a lignite), Pittsburgh seam, and Pocahontas (an anthracite). As an indicator of the maturity of the coal, the vitrinite reflectances of these samples were 0.28, 0.81, and 1.42, respectively (Users' Handbook for Argonnne Premium Coals; L. Eglinton, Woods Hole Oceanographic Institution, Woods Hole, MA, pers. comm.). Finally, we analyzed the OC-SC distribution of four activated carbon samples of decreasing particle size: mesh 4-12, 12-20, 20-40 (Darco®; Aldrich Chem. Co., Milwaukee, WI) and mesh 100+ (Norit A®; Aldrich Chem. Co., Milwaukee, WI).

Method Application to Natural Sediments

As a final test of the the soot quantification technique, we applied the method to two sets of natural sediments, both previously analyzed for PAHs. First, SC was determined in two Boston Harbor sediment subsamples (0-2 cm near Spectacle Island at 42°20'N 71°00'W and 7-9 cm of Fort Point Channel at 42°21'N 71°03'W), in which McGroddy and co-workers (2-3) had previously found peculiarly elevated PAH partition coefficients (Fig. 1a). Second, a profile of sedimentary SC was obtained from an Upper Mystic Lake, MA (42°26'N 71°06'W) sediment core, which has been radiometrically dated (33) and for which we have measured individual PAHs. For PAH analysis, 5-10 g of the extruded wet sediment were spiked with deuterated PAH recovery standards. The recoveries were: d_{10}-phenanthrene 96±20%, d_{14}-terphenyl 101±30%, and d_{12}-perylene 80±26%. Following a 1 h CH_3OH soak in the soxhlet, the sediment was soxhlet-extracted for 24 h in 90:10 CH_2Cl_2-CH_3OH, followed by 24 h in pure CH_2Cl_2. The concentrated and combined extracts were eluted on gravity columns containing $NaSO_4$ (anh.) and neutral alumina. The PAHs were eluted in the second fraction with 50 mL hexane-CH_2Cl_2 and quantified by GCMS (HP 5995B).

In response to the potential interference of pollen (Table 1), independent quantification of pollen and spores in the sediment samples was conducted by Richard Orson (Environmental Consulting, Branford, CT). Pollen analysis (sediment digestion, mounting, counting, and identification) followed published methods (34, 35).

Results and Discussion

Optimization of Temperature Conditions for SC-OC Separation

The combustion temperature with optimal selectivity between OC and SC was found by comparing the recovered C mass in samples of NIST "soot" or Aldrich humic acid over the temperature range 275-450 °C. The humic acid OC was found to be

TABLE 1 Results of Testing the Soot Carbon Method with Matrices of Known Composition

sample	OC + SC (g C/g sample)	SC (g C/g sample)	$\frac{SC}{OC + SC}$
NIST diesel particulate matter	0.822±0.019	0.777±0.031	0.95
humic acid	0.455±0.014	0.00069±0.00025	0.0015
acetanilide	0.715±0.003	no residue	<0.0001
polystyrene	0.914±0.007	no residue	<0.0001
polyethylene	0.862±0.005	no residue	<0.0001
oak	0.466±0.013	0.00008±0.00006	0.0002
fuel oil, diesel#2	(0.8) ?	no residue	<0.0001
crude oil, Gullfax North Sea	(0.8) ?	no residue	<0.0001
corn pollen, starchy	0.344±0.016	0.28	0.82
corn pollen, waxy	0.37	0.10	0.28
Green River Shale kerogen	0.75	no residue	<0.0001
Kimberlite kerogen	0.65	<0.0001	<0.0002
Beulah-Zap lignite Argonne Nat'l Lab Coal #8 vitrinite reflectance 0.28	0.535±0.003	0.00016	0.00031
Pittsburgh seam coal Argonne Nat'l Lab Coal #4 vitrinite reflectance 0.81	0.712±0.036	0.0028	0.0039
Pocahontas anthracite	0.762±0.052	0.0034	0.0045

Argonne Nat'l Lab Coal #5 vitrinite reflectance 1.42			
Activated carbon (mesh 4-12)	0.67	0.068	0.10
Activated carbon (mesh 12-20)	0.82±0.05	0.14	0.17
Activated carbon (mesh 20-40)	0.66±0.03	0.35	0.53
Activated carbon (100+ mesh)	0.899±0.004	0.54±0.04	0.60
car tire (Cooper: 30±2% carbon black)	0.862±0.003	0.33±0.3	0.38

significantly more labile than SC (Figure 2). For the humic acid, only a fifth of the OC was preserved at 275 °C and a mere 0.15% of the carbon mass was recovered at 375 °C. The soot was significantly more recalcitrant with 95% preserved at 375 °C, and 84% still remaining at 425 °C. SC was only quantitatively oxidized at 450 °C (0.06% recovered C). Based on these results, we chose to use 375 °C to distinguish between OC and SC. While a very small amount of OC still may be included in this operational SC (≈0.15% of humic OC preserved) and a small amount of soot-matrix carbon may be excluded (≈5% of NIST diesel particle C lost), these conditions appear suitable to minimize interference of OC matrices on SC, while giving an estimate of SC applicable to investigation of its role in PAH speciation. A similar temperature, 340 °C, was found in a previous study to be suitable for the oxidative thermal separation of OC from "black carbon" in residues of forest fires (27).

Method Testing with Well-Characterized Matrices

Due to the complexity of aquatic sediments, and the interference potential of some of their constituents, the method was tested with several known matrices (Table 1). These samples may be divided into two categories. First, samples whose reduced carbon content may be classified as exclusively OC; in addition to humic acid and acetanilide, this group includes plastic polymers, oak wood, pollens, oils, and coals. Second, samples which contain carbon of soot-like structure; in addition to the NIST diesel particulate matter, this includes the activated carbon samples and the car tire (containing a significant amount of carbon black). In Table 1, the results are presented for each sample's total reduced carbon content prior to the thermal treatment (i.e., OC+SC) as well as after the complete pre-treatment procedure (i.e., SC). The ratio SC/(OC+SC) reflects the potential of a component of the natural organic matter category to be included in the SC pool. For the OC samples, this "interference potential" would also indicate if an organic matter matrix was significantly "charred" by the method to produce SC.

The precision of the data was typically in the range 1-3% (expressed as the relative standard deviation). For the organic matter samples, interference potentials were 0-0.5% (except for pollen; see discussion below). This result is quite sufficient since we find that SC/OC in coastal marine sediments is about 10% and in a historical lacustrine sediment 2-6% (see Results below).

FIGURE. 2. Recoveries of soot C (dark circles) and humic acid organic C (open squares) as a function of increasing oxidation temperature.

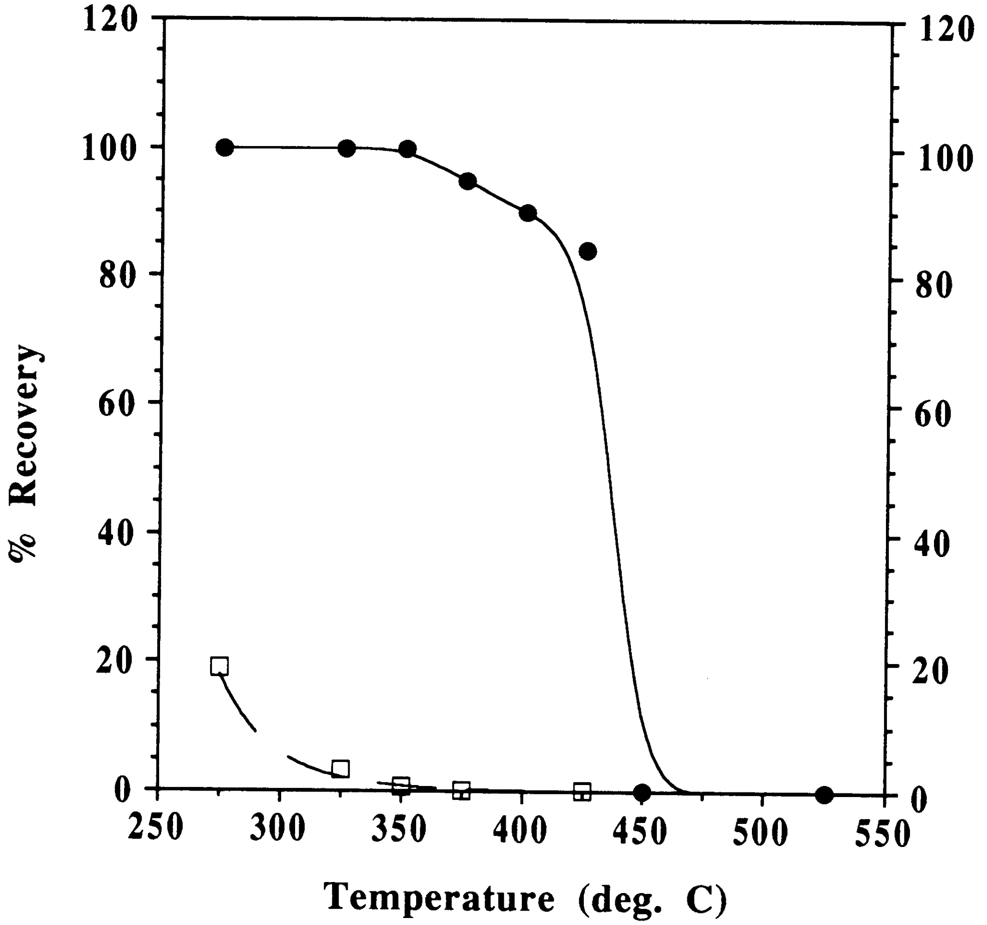
120
100
80
60
40
20
0
% Recovery
250
300
350
400
450
500
550
Temperature (deg. C)
120
100
80
60
40
20
0

The significant interference potential of corn pollen inspired us to obtain an independent estimate of pollen abundance in the natural sediments where we were measuring SC in order to evaluate whether such results could be compromised by pollen. The recalcitrancy of pollen observed over geological time-scales has been traced to sporopollenin, currently believed to be biopolymers of predominantly aromatic structures, present in the pollen-wall (36). The 48-50 cm depth Mystic Lake sediment sample was found to contain 87,000 pollen grains per gram dry weight. Dominant species were oak, birch, pine, fern, and ambrosia, with an average upper diameter of 35 μm. Using the measured carbon-content of corn pollen (ca. 35%), a specific gravity of pollen at 1.4 (ref. 35), and assuming a spherical shape, we can estimate that this lacustrine sediment contain about 0.0010 g pollen C in each gram dry sediment. Assuming that half of the pollen C may be quantified as SC (Table 1), we estimate that such pollen levels may account for one-quarter to one-tenth of the SC measured in Mystic Lake (see Results below). Thus, we conclude that the presence of pollen does not appear to compromise appreciably the dilute SC quantification at this lacustrine site. In the 7-9 cm Fort Point Channel sediment (Boston Harbor), two samples gave pollen counts of 23,000 and 22,000 grains per gram dry sediment, respectively. This represents over an order of magnitude lower pollen-C than SC concentrations in this marine sediment and thus no risk of interference from pollen on the SC findings.

Analysis of the five coal samples with our methodology yielded an insignificant return of SC but did indicate an influence of coal maturity on the SC results. Consistent with their degree of condensation, as indicated by increasing vitrinite reflectances, the lignitic samples produced the lowest apparent SC recovery and the anthracite the highest (Table 1).

The activated carbon sample series also provided a notable trend. While these samples contained both OC and SC, the smaller the grain size, the higher the relative soot content. If charring were occuring, as a result of reaction-limiting diffusional transport of oxygen during our thermal treatment, the opposite trend would have been expected; larger grain sizes with smaller surface-area-to-volume ratios would have resulted in incomplete OC oxidation/volatilization. We found the opposite trend and interpret it to be related to how the activated carbon is produced. In activated carbon manufacturing, some woody tissues (e.g., coconut shells) are fragmented and pyrolyzed. It is likely that there will be more complete conversion to SC for smaller fragments (larger the mesh number) as a result of larger surface-area-to-volume ratios. Hence, the activated carbon results suggest that charring is insignificant with our method and that to simulate soot partitioning using activated carbon sorbents, the smallest particle size should be employed.

In sum, testing of our method with substances representative of complex sedimentary components demonstrate that our SC measurements are likely free of significant interference from either charring or recalcitrant OC. These results with well-characterized matrices lends credence to the suitability of this method for quantifying dilute soot in natural regimes.

Application to Natural Samples

The developed soot method was used to investigate two natural sediments with previously determined (a) historical PAH input (Mystic Lake) and (b) PAH partitioning behavior (Boston Harbor).

Mystic Lake

The PAH depositional history, as recorded in the Mystic Lake core (Figure 3a), is temporally similar to previous sediment core observations of historical PAH loadings (37-40). The concentrations of individual PAHs ranges from a maximum around 10 μg/g to less than 10 ng/g at the core bottom. The relative compound abundances are indicative of combustion being the dominant source throughout the core. For example, the (methylfluoranthenes+methylpyrenes)/fluoranthene ratio was relatively consistent at 0.29±0.06. A value for this ratio of 0.24 has been measured on pure soot (41). In contrast, this ratio would be expected to be above unity if the source was direct petroleum contamination (42-43).

Using the deposition rates derived in this and a parallel core from radionuclide data and knowledge of local industrial events (33), the historical variations in PAH input were assessed (Fig. 3a). The deepest section of our core analyzed for PAHs represents approximately the turn-of-the-century. The very low fluxes at this time, prior to onset of heavy industrialization and the associated fossil-fuel combustion, may be indicative of PAHs from natural processes such as forest fires, as well as residential and agricultural wood-burning. In fact, the downcore ratio of 1,7-dimethylphenanthrene to 2,6-

dimethylphenanthrene (1,7-DMP/2,6-DMP; Fig. 3a), an indicator of the relative contribution to pyrogenic PAH from woody vs fossil fuel combustion (44), suggests that wood/forest burning may have been a dominant PAH contributor to the deepest core sections. However, such sources appear to become less significant at shallower depths in this core, as the dramatic increase in PAH fluxes likely reflects the rapid acceleration of industrial activities in this part of the world during the first half of the 1900s. Consistent with results from the aforementioned four studies (37-40), the dramatic increase of sedimentary PAH-flux reached a maximum around 1960, after which a slight decrease followed. This may reflect the switchover from coal as the primary energy source to gas and oil, which occured in the United States during this period (45). While the total energy consumption was increasing, widespread switchover to oil and gas which produce less PAHs per BTU than coal (46), apparently resulted in a net decrease in PAH production during this transitory period.

We used our SC method to develop a corresponding profile of soot input to the Mystic Lake (Figure 3b). The dilute sedimentary soot was found in the concentration range 0.002-0.007 (g SC/g dry sed.), corresponding to a maximum SC flux of 2.3 (g m^{-2} yr^{-1}). The soot profile was found to mimic the combustion-derived PAH profiles described above. While the SC abundances were only several percent of the OC levels (0.11±0.02 g OC/g dry sed.), the SC and OC profiles were completely decoupled (OC showed no clear trend with depth; Fig. 3b), further supporting the contention that interferences from pollen or charring are negligible. The increasing value of 1,7-DMP/2,6-DMP in the deeper sections (Fig. 3a) indicates that soot may have different sources and properties (e.g., PAH content) over time. Our quantitative historical record of total soot input exhibits the same qualitative temporal trend as the microscopy-counted Lake Michigan sedimentary charcoal record (18, 20). The PAH-soot coupling recorded in this sediment core adds confidence to the applicability of the proposed method for quantifying dilute soot in such complex sedimentary environments.

Boston Harbor

Finally, we applied our soot method to two Boston Harbor sediment samples, in which anomalously elevated *in situ* PAH partition coefficients have been found (2-3). While the OC contents of these marine sediments (0.04-0.05 g OC/g dry sed.) were lower than in the Mystic Lake sediments, the SC contents were similar (see footnotes of Table 2). This resulted in SC/OC ratios near 0.10 in this anthropogenically-influenced urban harbor. An important finding of McGroddy and co-workers in the aforementioned work was that the environmental PAH speciation deduced by measuring the actual *in situ* phase-distribution did not comply with the expectations from existing sorption models (i.e., 5-7). These workers observed K_d's several orders of magnitude above the predictions from such a commonly applied hydrophobic partition framework (Table 2), which is based on the presumption of natural organic matter being the sole (or dominant) sorbent for hydrophobic compounds in the environment. To explain the elevated K_d's, McGroddy *et al.* (2-3) hypothesized that the PAHs were existing in an apparent disequilibrium due to a significant fraction of the bound PAHs being sequestered in a physical-chemical form (e.g., soot), making them unavailable for equilibrium partitioning on the decadal timescale of these accreting sediments. An alternative, or further development of the above interpretation is that the inferred soot is a much stronger PAH sorbent than natural organic matter and thus causes equilibrium *in situ* K_d's to be elevated compared to the simple organic matter partitioning scenario. Our ability to quantify the dilute sedimentary soot-phase makes it possible to now investigate whether such a sorbent is present in sufficient amounts to explain the elevated partition coefficients observed. Using our measures of f_{sc} and calculating K_{sc} from ref. 1 (Fig. 1b), the extended hydrophobic partitioning framework (Eqn. 1) was applied to rationalize the *in situ* PAH speciation (Table 2). It is seen that the K_d predictions of the product $f_{oc}K_{oc}$, are orders of magnitude lower than the K_d's actually observed. In contrast, the extended framework, which includes a term for soot-partitioning, appears successful in predicting the actual PAH distribution (Table 2). Of course, we should emphasize that it is possible that some fraction of the soot-associated PAHs are held within the aromatic planes of the soot structure (28-29, 48) such that they may not desorb to reach equilibrium with the surrounding water on timescales of interest for certain processes. However, the good agreement between total (gas adsorption) and external (electron microscopy) surface area (48) suggests that soot has very limited internal pore structures to occlude PAHs.

The implications of an association between PAH and soot in natural sediments are intriguing. These findings quantitatively support the inclusion of specific combustion phases in environmental speciation models of hydropohobic contaminants (i.e., Eqn. 2). The large number of studies reporting peculiarly elevated partition coefficients for PAHs

FIGURE. 3. (a) Upper Mystic Lake profiles of pyrene (dark circles), benzo[a]pyrene (dark inverted triangles), and the ratio of the 1,7- to 2,6-dimethylphenanthrene isomers (open squares). (b) Mystic Lake profile of soot carbon (dark circles) and organic carbon (open squares).

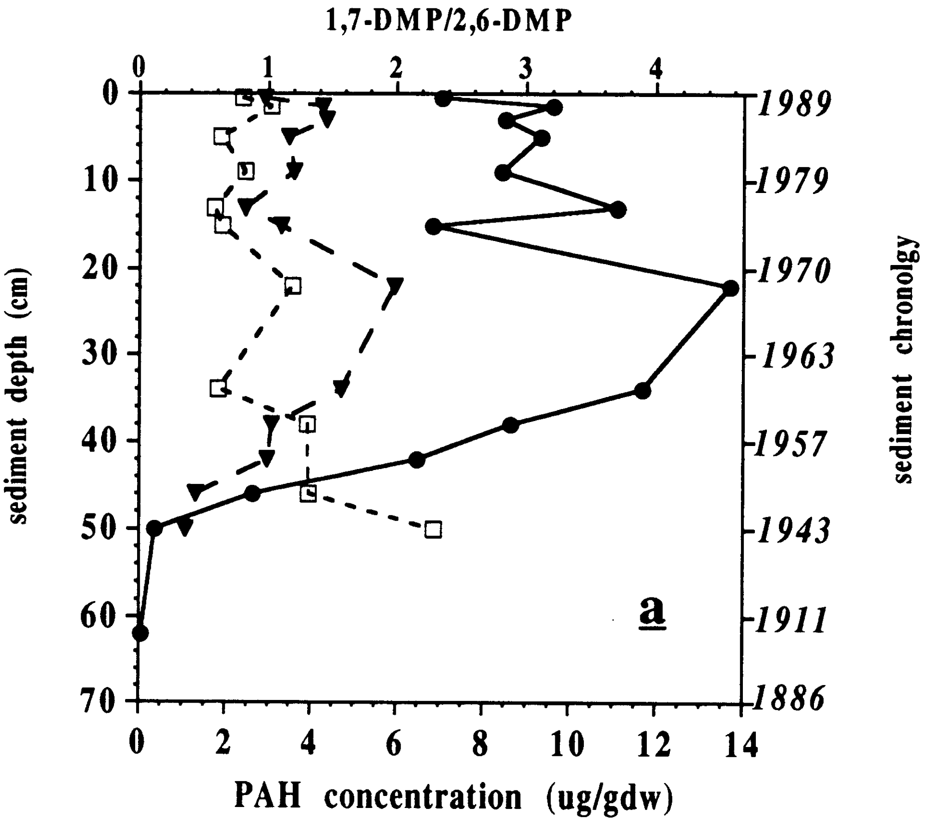
1,7-DMP/2,6-DMP
0
1
2
3
4
sediment depth (cm)
0
10
20
30
40
50
60
70
0
2
4
6
8
10
12
14
PAH concentration (ug/gdw)
a
sediment chronolgy
1989
1979
1970
1963
1957
1943
1911
1886

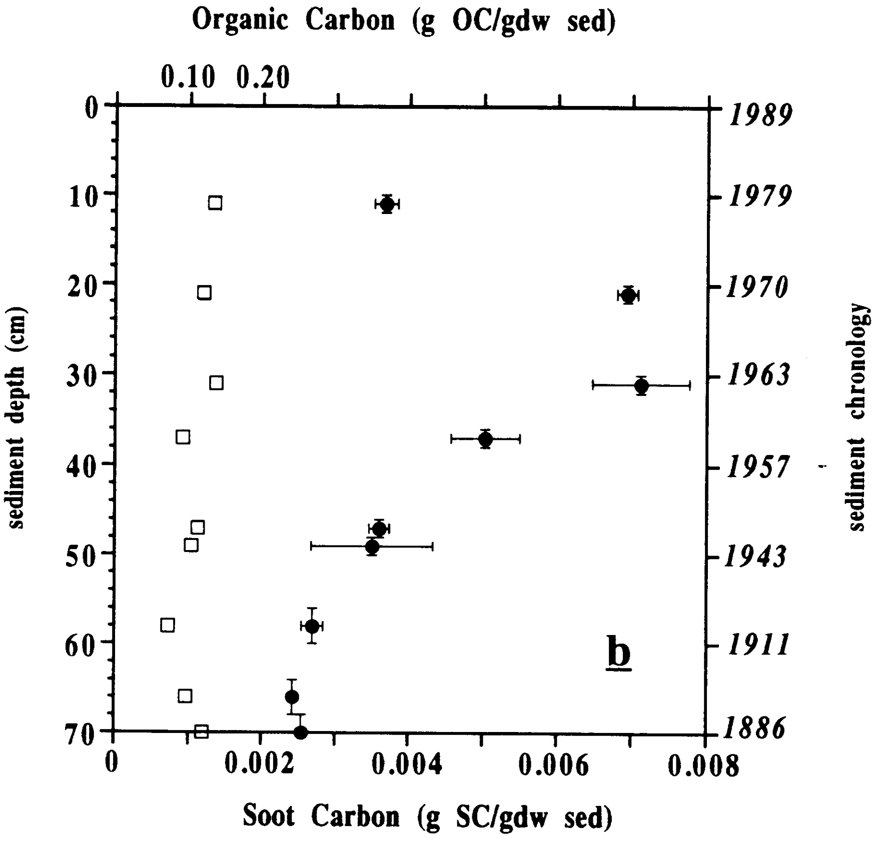
Organic Carbon (g OC/gdw sed)
0.10
0.20
sediment depth (cm)
0
10
20
30
40
50
60
70
0
0.002
0.004
0.006
0.008
Soot Carbon (g SC/gdw sed)
b
sediment chronology
1989
1979
1970
1963
1957
1943
1911
1886

TABLE 2
Different PAH Partitioning Models Applied to Boston Harbor Sediments

	log K_d ($L_{pore\text{-}water}/kg_{dry\text{-}sed.}$)	
Fort Point Channel (7-9cm)[a]	Phenanthrene	Fluoranthene
Actual distributions measured *in situ* (ref. 2)	5.0	5.4
Distributions predicted from ($K_d = f_{oc}K_{oc}$)[b]	2.9	3.6
Distributions predicted when including a soot-phase[c] (Eqn. 1)	4.9	5.6
Spectacle Island (0-2cm)[d]		
Actual distributions measured *in situ* (ref. 2)	5.9[e]	5.2
Distributions predicted from ($K_d = f_{oc}K_{oc}$)[b]	2.8	3.4
Distributions predicted when including a soot-phase[c] (Eqn. 1)	4.5	5.2

[a] The f_{oc} was 0.0547 gOC/gdw (2) and the soot content, f_{sc}, of this sediment was determined to be 0.0066±0.0008 gSC/gdw. [b] We used log K_{oc} values for phenanthrene and fluoranthene of 4.12 and 4.79, calculated from log K_{ow} values in (12) using the relationship of (7). [c] Soot-partition coefficients were calculated from data in ref. 1 (shown in Fig. 1b) and the log K_{sc} were for phenanthrene 7.1 and for fluoranthene 7.8. [d] The f_{oc} was 0.0406 gOC/gdw (2) and the f_{sc} was determined to be 0.0027±0.0004 gSC/gdw. [e] This reported value (2) deviates from the commonly observed trend of hydrophobicity-driven *in situ* K_d's. Since this surficial sediment sample is well-oxidized, it is possible that this value reflects biodegradation of porewater phenanthrene being faster than desorption (i.e., non-equilibrium) as significant biotransformation rates of spiked phenanthrene to oxidized Boston Harbor sediments have been observed (47).

(e.g., Fig. 1a), but not for PCBs, may now be explained by the presence of anthropogenic soot controlling the PAH distribution. Soot particles appear to consist of a highly conjugated and condensed carbonaceous matrix, and their structure may be thought of as a multi-layered macro-PAH (28-29, 48-49). Hence, it may be expected that strong π-π interactions are established between the often co-introduced flat PAH molecules and the soot particles. Interestingly, it was recently reported that coplanar PCBs exhibited 0.5 log-units elevated affinities to urban aerosols compared to predictions from their vapor pressures while this was not seen for congeners of larger dihedral angles (51). Dioxins and other planar aromatic molecules may similarly establish favorable dispersion interactions with soot, which could affect their environmental speciation. The present results suggest that the chemical exchange of PAHs between these strongly sorbing, but dilute, anthropogenic phases and the surrounding aqueous solution may be at or near equilibrium (at least in this decade-old sediment-porewater system initially evaluated).

Our results support the hypothesis forwarded by Farrington and co-workers in reflection of the results from the US Mussel Watch Survey (52) that, unlike petroleum-spilled PAHs, pyrogenic PAHs may be less available for biological uptake as a result of presumed strong associations with combustion particles. This finding is particularly important as recently elucidated geographical fall-out pattern and relative compound abundances of PAH fluxes into the northwestern Atlantic suggest that pyrogenic sources are dominating the PAH input to the ocean (53). The tremendous influence of PAH-soot associations on the bioavailable fraction should be taken into account in the establishment of sediment quality criteria (SQC), currently being developed by the U.S. EPA (e.g., ref. 54). The basis of these SQCs is to ensure that the porewater concentration, in *equilibrium* with the sediment, is not exceeding the final chronic water quality criteria values (FCV). Since the soot phase may be dominating the environmental PAH speciation, we propose that the SQC may need to be redefined as:

$$\mathbf{SQC(PAH_{\mathit{i}}) = (f_{oc}K_{oc} + f_{sc}K_{sc})\ FCV(PAH_{\mathit{i}})} \tag{2}$$

If some fraction of the PAHs are so occluded within soot so as to be practically non-exchangeable on timescales of interest, then Eq. 2 would also need to include a factor for the fraction that is available for equilibrium partitioning (AEP; ref. 2-3):

$$\mathrm{SQC}(\mathrm{PAH}_i) = \frac{(f_{oc}K_{oc} + f_{sc}K_{sc})}{\mathrm{AEP}}\ \mathrm{FCV}(\mathrm{PAH}_i) \qquad (3)$$

In either case, it appears necessary to quantify not only f_{oc}, but also f_{sc}, to derive such a first-order approximation of the exposed contaminant levels.

One further implication of the environmental soot-associated PAH speciation is that current laboratory-based practices, using liquid PAH solutions and extracts in sorption and toxicity testing, may not realistically reflect the actual availability of *in situ* PAHs to participate in such processes. To further constrain the proposed extension of the hydrophobic partitioning model to include soot-phase partitioning, K_{SC} should be evaluated under controlled conditions. This first direct investigation on the quantitative relationship between *in situ* PAH distribution and the presence of soot-phases indicates that understanding this link may prove crucial to elucidating the biogeochemical cycling of such combustion-derived compounds.

Acknowledgments

The laboratory of A. Sarofim is thanked for the first NIST-SRM 1650 split. Lorraine Eglinton is gratefully acknowledged for Argonne Standard Coal Series samples and Tim Eglinton for kerogen samples. Bernard Chien kindly donated an unused car-tire sample. Inspiring discussions with John Farrington, John Hedges, Allison MacKay, and Jean Whelan catalyzed this work. Financial support came from the Office of Naval Research (grant # NOOO14-93-1-0883), National Oceanic and Atmospheric Administration (# NA36RM044-UM-S242), National Institute of Environmental Health Sciences (# 2-P30-ESO-2109-11), and Massachusetts Water Resources Authority. F. H. and C. C. acknowledge the support of the MIT Undergraduate Research Opportunities Program. The views herein are those of the authors and do not necessarily reflect the views of NOAA or any of its subagencies.

References

1. Walters, R. W.; Luthy, R. G. *Environ. Sci. Technol.* **1984**, 18, 395.
2. McGroddy, S. E.; Farrington, J. W. *Environ. Sci. Technol.* **1995**, 29, 1542.
3. McGroddy, S. E.; Farrington, J. W.; Gschwend, P. M. *Environ. Sci. Technol.* **1996**, 30, 172.
4. Socha, S. B.; Carpenter, R. *Geochim. Cosmochim. Acta* **1987**, 51, 1273.
5. Karickhoff, S. W.; Brown, D. S.; Scott, T. A.; *Water Res.* **1979**, 13, 241.
6. Chiou, C. T.; Porter, P. E.; Schmedding, D. W. *Environ. Sci. Technol.* **1979**, 206, 831.
7. Karickhoff, S. W. *Chemosphere* **1981**, 10, 833.
8. Baker, J. E.; Eisenreich, S. J.; Eadie, B. J. *Environ. Sci. Technol.* **1991**, 25, 500.
9. Readman, J. W.; Mantoura, R. F. C.; Rhead, M. M. *Sci. Tot. Env.* **1987**, 66, 73.
10. Broman, D.; Näf, C.; Rolff, C.; Zebühr, Y. *Environ. Sci. Technol.* **1991**, 25, 1850.
11. Poster, D. L.; Baker; J. E. *Environ. Sci. Technol.* **1996**, 30, 341.
12. Miller, M. M.; Wassik, S. P.; Huang, G.-L.; Shiu, W.-Y.; Mackay, D. *Environ. Sci. Technol.* **1985**, 19, 522.
13. Yalkowsky, S. H.; Valvani, S. C. *J. Chem. Eng. Data* **1979**, 24, 127.
14. Brownawell, B. J.; Farrington, J. W. *Geochim. Cosmochim. Acta* **1986**, 50, 157.
15. Luehrs, D. C.; Hickey, J. P.; Nilsen, P. E.; Godbole, K. A.; Rogers, T. N. *Environ. Sci. Technol.* **1996**, 30, 143.
16. Ruepert, C.; Grinwis, A.; Govers, H. *Chemosphere* **1985**, 14, 279.
17. Goldberg, E. D. *Black Carbon in the Environment*; Wiley: New York, 1985.
18. Goldberg, E. D.; Hodge, V. F.; Griffin, j. J.; Koide, M.; Edgington, D. N. *Environ. Sci. Technol.* **1981**, 15, 466.
19. Griffin, J. J.; Goldberg, E. D. *Geochim. Cosmochim. Acta* **1981**, 45, 763.
20. Griffin, J. J.; Goldberg, E. D. *Environ. Sci. Technol.* **1983**, 17, 242.
21. Renberg, I.; Wik, M. *Ecol. Bull.* **1985**, 37, 53.
22. Griffin, J. J.; Goldberg, E. D. *Science* **1979**, 206, 563.
23. Wik, M; Natkanski, J. *Phil. Trans. R. Soc. Lond.* **1990**, B327, 319.
24. Broman, D.; Näf, C.; Wik, M.; Renberg, I. *Chemosphere* **1990**, 21, 69.
25. Venkataraman, C.; Friedlander, S. K. *Environ. Sci. Technol.* **1994**, 28, 563.

26. Fung, K. *Aerosol Sci. Technol.* **1990**, 12, 122.
27. Kuhlbusch, T. A. J. *Environ. Sci. Technol.* **1995**, 29, 2695.
28. Akhter, M. S.; Chughtai, A. R.; Smith, D. M. *Appl. Spectrosc.* **1985**, 39, 143.
29. Akhter, M. S.; Chughtai, A. R.; Smith, D. M. *Appl. Spectrosc.* **1985**, 39, 154.
30. Nieuwenhuize, J.; Maas, Y. E. M.; Middelburg, J. J. *Mar. Chem.* **1994**, 45, 217.
31. Hamins, A. In *Environmental Implications of Combustion Processes*; Puri, I. K., Ed.; CRC Press: Boca Raton, FL, 1993; pp 71-95.
32. Tissot, B. P.; Welte, D. H. *Petroleum Formation and Occurence.* Springer-Verlag: New York, 1978.
33. Spliethoff, H. M.; Hemond, H. F. *Environ. Sci. Technol.* **1996**, 30, 121.
34. Faegri, K.; Iversen, S. *Textbook of Pollen Analysis.* Blackwell: Oxford, 1989.
35. Orson, R. A.; Simpson, R. L.; Good, R. E. *J. Sed. Petrol.* **1990**, 60, 859.
36. Wehling, K.; Niester, Ch.; Boon, J. J.; Willemse, M. T. M.; Wiermann, R. *Planta* **1989**, 179, 376.
37. Grimmer, G.; Böhnke, H. *Cancer Lett.* **1975**, 1, 75.
38. Prahl, F. G.; Carpenter R. *Geochim. Cosmochim. Acta* **1979**, 43, 1959.
39. Hites, R. A.; LaFlamme, R. E.; Windsor Jr, J. G.; Farrington, J. W.; Deuser, W. G. *Geochim. Cosmochim. Acta* **1980**, 44, 873.
40. Gschwend, P. M.; Hites, R. A. *Geochim. Cosmochim. Acta* **1981**, 45, 2359.
41. Sporstøl, S.; Gjøs, N.; Lichtenthaler, G.; Gustavsen, K. O.; Urdal, K.; Oreld, F.; Skei, J. *Environ. Sci. Technol.* **1983**, 17, 282.
42. Youngblood, W. W.; Blumer, M. *Geochim. Cosmochim. Acta* **1975**, 39, 1303.
43. LaFlamme, R. E.; Hites, R. A. *Geochim. Cosmochim. Acta* **1978**, 42, 289.
44. Benner Jr., B. A.; Wise, S. A.; Currie, L. A.; Klouda, G. A.; Klinedinst, D. B.; Zweidinger, R. B.; Stevens, R. K.; Lewis, C. W. *Environ. Sci. Technol.* **1995**, 29, 2382.
45. Hottle, H. C.; Howard, J. B. *New Energy Technology-Some Facts and Assessments*; MIT Press: Cambridge, MA, 1971.
46. National Academy of Sciences. *Particulate Polycyclic Organic Matter*; Nat. Acad. Sci: Washington, DC., 1972.
47. Shiaris, M. P. *Appl. Environ. Microbiol.* **1989**, 55, 1391.
48. Ross, M. M.; Risby, T. H.; Steele, W. A.; Lestz, S. S.; Yasbin, R.E. *Coll. Surf.* **1982**, 5, 17.

49. Donnet, J. B.; Schultz, J.; Eckhardt, A. *Carbon* **1968**, 6, 781 (in French).
50. Lahaye, J. *Polymer Degrad. Stabil.* **1990**, 30, 111.
51. Falconer, R. L.; Bidleman, T. F.; Cotham, W. E. *Environ. Sci. Technol.* **1995**, 29, 1666.
52. Farrington, J. W.; Goldberg, E. D.; Risebrough, R. W.; Martin, J. H.; Bowen, V. T. *Environ. Sci. Technol.* **1983**, 17, 490.
53. Gustafsson, Ö.; Gschwend, P. M.; Buesseler, K. O. submitted.
54. U.S. Environmental Protection Agency *Sediment quality criteria for the protection of benthic organisms: Fluoranthene*; EPA 822-R-93-012; Offices of Water, Research, and Development and, Science and Technology; Washington, DC, 1993.

Chapter 6

Soot as a Strong Partition Medium for Polycyclic Aromatic Hydrocarbons in Aquatic Systems

Örjan Gustafsson and Philip M. Gschwend

R. M. Parsons Laboratory, MIT 48-415
Department of Civil and Environmental Engineering
Massachusetts Insitute of Technology
Cambridge, MA 02139, USA
Tel. 617-253-1638
Fax. 617-253-7395

Submitted, American Chemical Society Symposium Book "Molecular Markers in Environmental Geochemistry", R. Eganhouse (Ed.)

Abstract. The spatial distributions of polycyclic aromatic hydrocarbons (PAHs) in many aquatic environments appear to be dictated by partitioning with soot as opposed to with bulk organic matter. Recent field-observations of the solid-water distribution coefficients of members of this contaminant assemblage are consistently elevated compared to expectations from organic-matter-based partition models. Increasing hydrophobicity across the PAH assemblage is seen to affect relative distributions. Using PAHs as molecular markers of sorption suggests that an active exchange of such planar molecules between a strong sorbent, such as soot, and the surrounding water is taking place. Quantification of PAHs, organic carbon, and soot carbon in surficial continental shelf sediments off New England revealed that the distribution of PAHs was highly correlated with soot carbon. Estimates of the soot-water partition coefficient for several PAHs, assuming sorbate-soot association is thermodynamically similar to sorbate fusion, are found to agree reasonably well with published aqueous sorption constants to activated carbon.

Introduction.

Several polycyclic aromatic hydrocarbons (PAHs) are carcinogenic and have been classified by the US Environmental Protection Agency as "Priority Pollutants" (1). In fact, PAHs have been identified as the principal human cell mutagens in extracts of a particular natural sediment, clearly illustrating the need for environmental chemists to emphasize studies of this compound class (2). Furthermore, large amounts of these organic contaminants continue to be released into the environment, primarily from combustion of fossil and wood fuel, but also from direct petroleum spills.

A useful starting point for anticipating these and other chemicals' dispersal and effects in the environment is to consider their "phase"-distribution. This physico-chemical speciation largely governs the extent to which a given compound may undergo transport and transformation. PAHs are both easy to analyze and span a range of well-known thermodynamic properties, making them suitable as molecular markers of environmental partitioning. Elucidation of the behavior of a few PAHs thus affords extrapolation to many other compounds of similar structure through linear free energy relationships. Due to their high aqueous activity coefficients, PAHs and many other xenobiotic chemicals have a high affinity for solid phases. In the widely accepted solid-water partition model for such hydrophobic compounds, developed by Karickhoff and Chiou (3, 4), particulate PAH concentrations are normalized to the total organic carbon content of the solid, believed to be the sorbent property that dictates the tendencies of hydrophobic sorbates to associate with the solid. This classical organic-matter-based partition model has shown its ability to predict, from thermodynamic properties of the system, the chemical speciation in hundreds of laboratory-based sorption studies where a wide array of soils and sediments have been spiked with organic chemicals like PAHs (e.g., 5, 6).

However, many recent field observations have reported *in situ* distribution coefficients ($(K_{oc})_{obs}$) of PAHs that are orders of magnitude above the predictions of the classical model (Figure 1). These enhanced particle-associations for PAHs appear to be widespread as they have been documented in such diverse environmental compartments as surface waters of lakes (7), rivers (8), estuaries (9), and the ocean (10, 11), as well as in sediment porewater (12) and rainwater (13). In contrast, $(K_{oc})_{obs}$ of similarly hydrophobic polychlorinated biphenyls (PCBs) are typically lower and agree better with predictions from the Karickhoff-Chiou model (e.g., 13-16).

An association between PAHs and various pyrogenic carbon phases, all henceforth referred to as soot, has been previously postulated to control the distribution and bioavailability of these compounds (e.g., 9, 12, 17-25). However, only in two previous studies has a direct link between soot and particulate PAHs been examined through simultaneous quantification in natural sediments (18, 23). Broman and co-workers performed microscopy-counting of coarse (> 5-10 μm) charcoal particles in sediment-trap collected material and found a correlation between such particle counts and PAH concentrations. However, because most PAH-carrying soot particles in the atmosphere are much smaller than can be detected with optical microscopy (e.g., 26, 27), it is not possible to interpret quantitatively their results in terms of a PAH partition model. Recently, a thermal-oxidation method which determines the total mass of sedimentary soot carbon, SC, was developed (18). Our earlier work demonstrated that the vertical

Figure 1. Enhanced organic-carbon normalized *in situ* partition coefficients $(K_{oc})_{obs}$ for PAHs observed in diverse environmental regimes: surface waters of lakes (open squares = ref. 7), rivers (filled squares = ref. 8), estuaries (filled diamonds = ref. 9), and the ocean (filled circles = ref. 10; dotted open circle = ref. 11), as well as in sediment porewater (crosses = ref. 12) and rainwater (inverted open triangles = 13). K_{ow} values are from (3, 80, 81) and the model-predicted regression with K_{oc} is from (79).

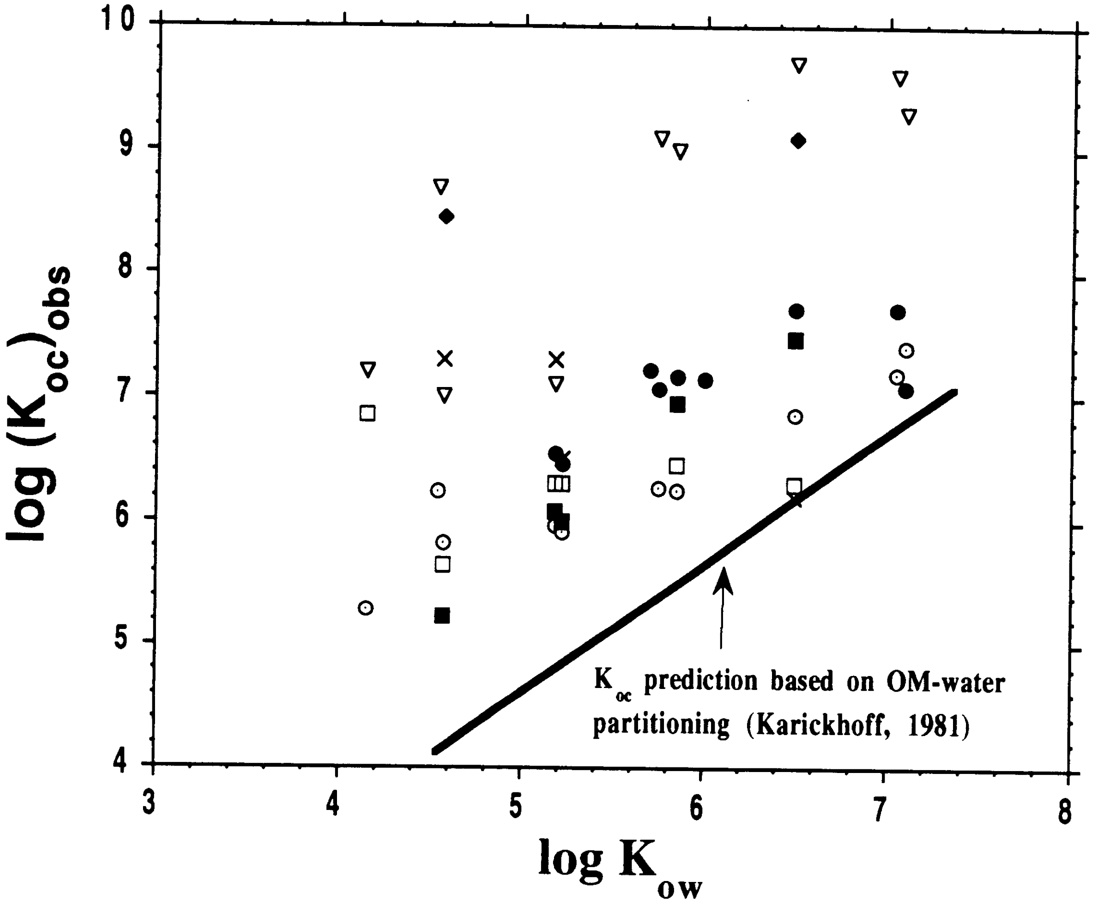
10
9
8
7
6
5
4
3
4
5
6
7
8
$\log (K_{oc})_{obs}$
$\log K_{ow}$
K_{oc} prediction based on OM-water partitioning (Karickhoff, 1981)

distribution of SC in a lacustrine core correlated with the PAH pattern, while being decoupled from the organic carbon profile. Measurements of total SC in Boston Harbor sediments of a few parts per thousand (by dry mass) were also used to rationalize previously reported (12) elevated PAH $(K_{oc})_{obs}$ in two sediment-porewater systems (18).

Obviously, inclusion of soot-bound PAHs in the quantified particulate fraction of field studies (e.g., those of Figure 1) would yield elevated $(K_{oc})_{obs}$. However, inspection of the entire contaminant assemblage exhibiting elevated distribution coefficients reveals that there is still a pronounced effect of hydrophobicity on the relative solid-solution distributions. This observation strongly suggests that an active exchange between the, presumed, soot-associated PAHs and their dissolved counterparts is taking place. Hence, a significant fraction of pyrogenic PAHs appears to be not "permanently occluded" (e.g., 9, 12, 22) but rather to partition between what seems to be a strongly sorbed state and the surrounding water (18). In the absence of controlled sorption studies in soot-water systems, we estimated PAH partition coefficients between activated carbon (as an analog for soot) and water from the linear portion of sorption isotherms developed by others (28). Such a pyrogenic phase is a significantly better sorbent than natural organic matter for PAHs on a carbon-mass basis. Such observations have lead to the hypothesis that for planar aromatic molecules such as PAHs, we need to expand the classical hydrophobic partion model to include sorption, not only into natural organic carbon, but also with soot carbon phases (18):

$$\mathbf{K_d = f_{oc}K_{oc} + f_{sc}K_{sc}} \qquad (1)$$

where f_{oc} and f_{sc} are the non-soot organic carbon and soot carbon mass-fractions of the solid matrix, respectively, and K_{oc} and K_{sc} are the organic carbon and soot carbon normalized equilibrium distribution coefficients, respectively.

The first objective of this paper is to demonstrate that the concentrations of PAHs in marine sediments are better correlated with soot carbon content (f_{sc}) than with organic carbon content (f_{oc}), implying that PAH sorption to soot controls PAH cycling and effects. We further evaluate the relevant physico-chemical sorbent properties of soot, discuss potential sorption mechanisms, and derive an estimate of the magnitudes of soot-water equilibrium partitioning (K_{sc}) for typical PAHs.

Methods.

Sediment Sampling. Large-volume box-cores were obtained from different locations in the Gulf of Maine during several cruises (Figure 2). In 1990, two stations in Boston Harbor: at the mouth of Fort Point Channel (FPC) and off Spectacle Island (SI) were cored. In May 1994, sediments in Portland Harbor (PH), outer Casco Bay (CB), and a station in the open Gulf of Maine, Wilkinson Basin (WB) were sampled, while in July 1996, sediments were collected from two sites in Cape Cod Bay (CCB1 and CCB2), Massachusetts Bay (MB), and near Stellwagen Bank (SB). All samples were taken with a Sandia-Hessler type MK3 (Ocean Instruments, San Diego, CA) corer with a 0.25 m^2 by 0.7 m deep box. Where the sediment-water interface appeared undisturbed, we used acrylic liners (ca. 13 cm diameter) to extract sub-cores. The sub-cores were immediately extruded on board and trimmed. Sections for organic compound, OC, and SC determination were stored frozen in solvent-rinsed amber glass bottles with Al-foil lined Teflon caps.

Quantification of Sedimentary Total Organic and Soot Carbon. Our analytical method for measuring OC and SC in complex sedimentary matrices has been detailed and validated elsewhere (18). Briefly, the OC+SC content of dried sediment is obtained by carbon elemental analysis (PE 2400 CHN; Perkin Elmer Corp., Norwalk, CT) after destruction of carbonates through mild acidification of the sample in Ag capsules (Elemental Microanalysis Ltd., Manchester, NH). For SC, dried sediment is thermally oxidized at 375°C for 24 h, followed by acidification and carbon elemental analysis. Concentration of OC is then calculated as the difference between OC+SC and SC.

Quantification of Sedimentary PAHs. Concentrations of PAHs in FPC and SI were taken from published estimates in the same cores (12). No PAH data exist for CCB1 and CCB2 sediments. In all other samples, about 10 g of the wet sediments were transferred to a Soxhlet extractor and spiked with four deuterated PAH recovery standards, spanning a range in aqueous solubilities. The sediments were extracted for 48 h in a 9:1 mixture of methylene chloride and methanol. Extracts were concentrated

Figure 2. Locations of sediment sampling stations in the Gulf of Maine.

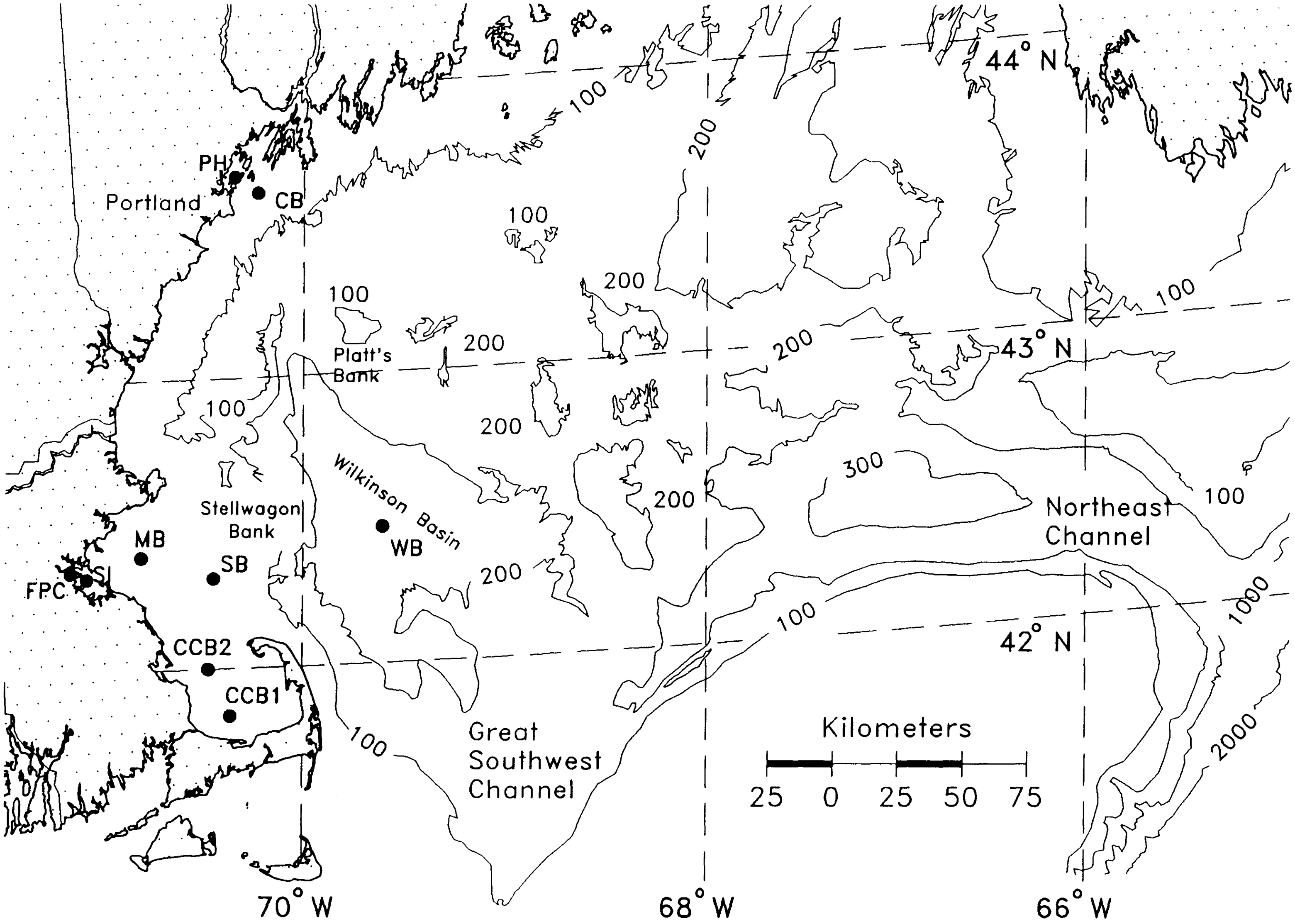
44° N
43° N
42° N
70° W
68° W
66° W
PH
CB
Portland
Platt's Bank
Stellwagon Bank
Wilkinson Basin
MB
SB
WB
SI
FPC
CCB2
CCB1
Great Southwest Channel
Northeast Channel
Kilometers
25 0 25 50 75
100
200
300
1000
2000

using Kuderna-Danish or rotary evaporation and were then charged to a fully activated silica gel gravity column containing $NaSO_4$ (anh.) and activated copper (prepared according to ref. 29) to remove residual water and elemental sulfur, respectively. The PAHs were eluted in the third fraction with 30 mL 3:1 hexane - toluene and quantified by gas chromatography - mass spectrometry (Hewlett-Packard 5995B). Recoveries of PAH internal standards for both samples and blanks were 65-95% for the entire procedure, and reported concentrations are corrected for these recoveries. PAH contents of the samples were several orders of magnitude above those of the blanks.

Results and Discussion.

Source-Diagnostic PAH Ratios. The relative abundances of alkylated-to-unsubstituted parent PAHs contain information useful in elucidating the origin of environmental PAHs (e.g., 17, 30, 31). The alkyl homolog distribution of petroleum generally exhibits an increasing abundance with increasing carbon number over the first four-six homologs (e.g., 17) while the unsubstituted congeners are the most abundant in PAH assemblages from combustion processes (e.g., 17, 32).

Since the form in which PAHs are introduced to the environment may affect their dispersal and transformations, we have consolidated source-diagnostic ratios of the 178 (phenanthrene) and 202 (pyrene) series from a large literature data set (about 20 independent studies representing over one-hundred observations: refs. 19, 21, 23-25, 32-44, Gustafsson-Gschwend *et al.*, unpublished data from Gulf of Maine) to elucidate the relative importance of petroleum and pyrogenic sources of PAHs to a variety of aquatic environments (Figure 3). The reported ratios support the contention by LaFlamme and Hites (30) that the global distribution of PAHs in contemporary aquatic environments is dominated by an input from combustion processes (Figure 3). The historical sedimentary record of PAHs follows the usage of fossil and wood fuel (e.g., 18-19, 45-48), and we may thus conclude that the predominantly pyrogenic PAHs in today's environment are from anthropogenic combustion as opposed to natural forest fires.

The Sedimentary Distribution of Organic and Soot Carbon. Examining nine sediments from diverse environments in detail, we found organic carbon concentrations ranging from 30-50 mg OC per gram dry weight sediment (gdw sed.) in rapidly accumulating harbor regimes to 10-20 mg OC/gdw sed. at offshore continental shelf locations, to a value of 1.5 mg OC/ gdw sed. at a highly winnowed site with coarse sand (Table I). The sedimentary soot carbon concentrations varied even more widely (factor of 15), decreasing with increasing distance from urban sources. SC concentrations ranged from 2-7 mg SC/gdw sed. in urban harbors to 0.1-0.7 mgSC /gdw sed. further offshore (Table I). These results suggest that 3-13% of reduced carbon in modern continental shelf sediments is anthropogenic soot, with the highest fractions being found in or near urban harbors.

Table I. Organic and Soot Carbon Concentrations in Gulf of Maine Sediments

Sample	*depth (cm)*	*Lattitude (N)*	*Longitude (W)*	*Organic Carbon (mg OC/ gdw sed.)*	*Soot Carbon (mg SC/ gdw sed.)*
FPC	7-9	42°21'22"	71°02'41"	50.9±0.7	6.61±0.84
SI	0-1	42°19'46"	70°59'34"	28.8±2.0	2.72±0.40
PH	2-3	43°39'63"	70°14'32"	37.0±4.3	1.76±0.56
CB	2-3	43°36'94"	70°09'31"	12.5±3.5	0.72±0.10
WB	2-3	42°38'00"	69°36'26"	22.5±0.5	0.71±0.30
CCB1	2-3	41°51'18"	70°17'54"	11.1±0.2	0.34±0.13
CCB2	2-3	42°03'30"	70°24'36"	13.0±0.2	0.42±0.04
MB	2-3	42°22'00"	70°54'00"	1.50±0.7	0.11±0.07
SB	2-3	42°20'33"	70°23'30"	22.3±0.4	0.75±0.01

Regression of PAHs with OC and SC. Our data indicate a significantly higher degree of correlation for PAHs with SC than with OC (Table II and Figure 4). Regressions were performed for three PAHs with 3-, 4-, and 5-ringed systems, respectively, and consequently spanning a range in hydrophobicities. In addition to higher correlation coefficients ("R^2"), a greater degree of significance for each of the PAH-soot relations was calculated ("p") (Table II). We tested the Null hypothesis that SC and PAH are not correlated and found that its probability to be valid was less than

Figure 3. The PAH source-diagnostic ratios of (a) the sum of methyl-phenanthrenes and -anthracenes to phenanthrene and (b) the methyl-pyrenes and -fluoranthenes to pyrene from a wide range of atmospheric, water-column, and sedimentary environments (19, 21, 23-25, 32-44, Gustafsson-Gschwend *et al.*, unpublished data). The solid lines refer to typical ratios found in petrogenic and pyrogenic sources of PAHs (17, 31, 32).

Diagnostic PAH Source Ratios - 178 series -

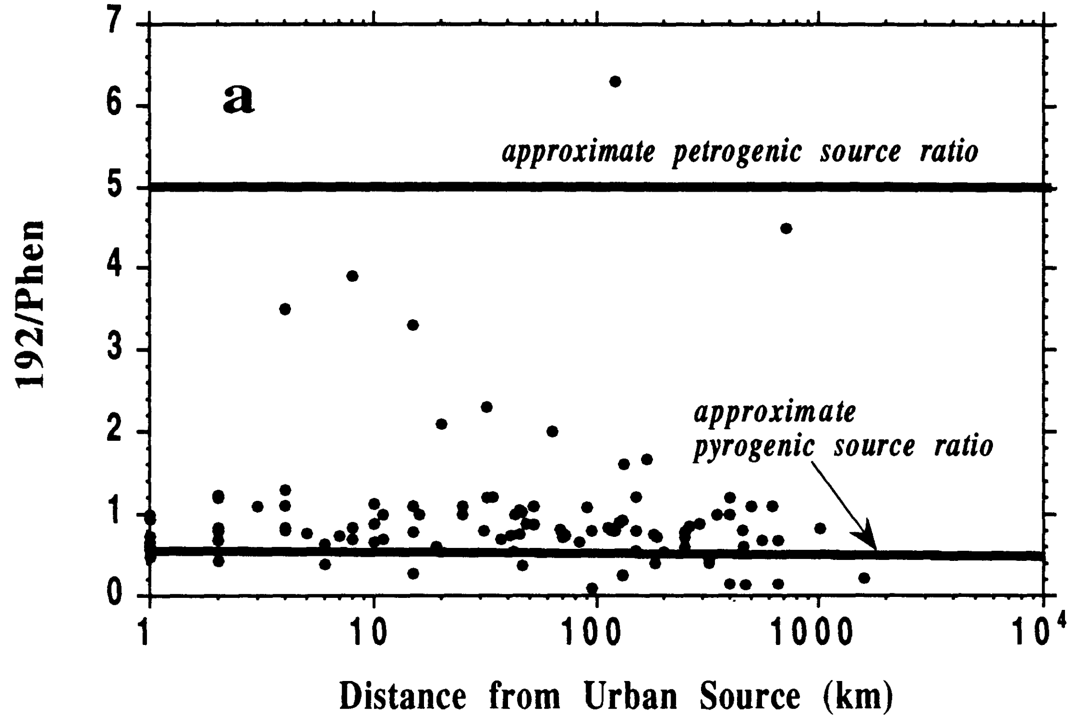

Diagnostic PAH Source Ratios - 202 series -

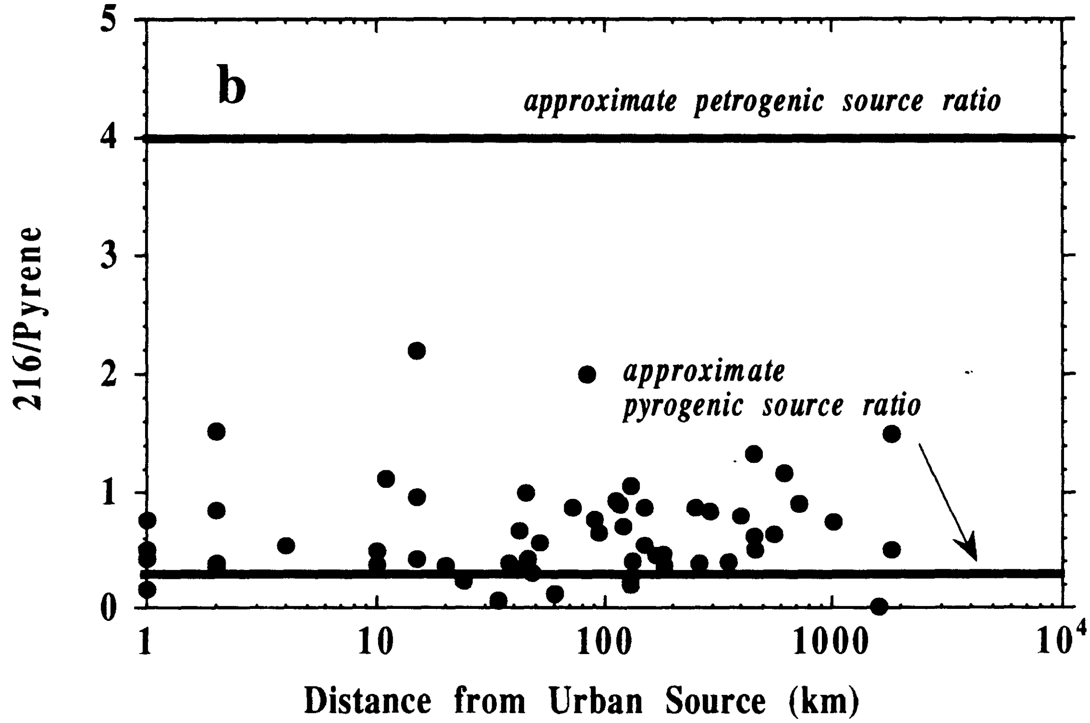

Figure 4. Regressions (n = 7) between sedimentary concentrations of benzo[a]pyrene with (a) organic carbon and (b) soot carbon, respectively, illustrating the better correlation of PAHs with soot carbon (see Table II).

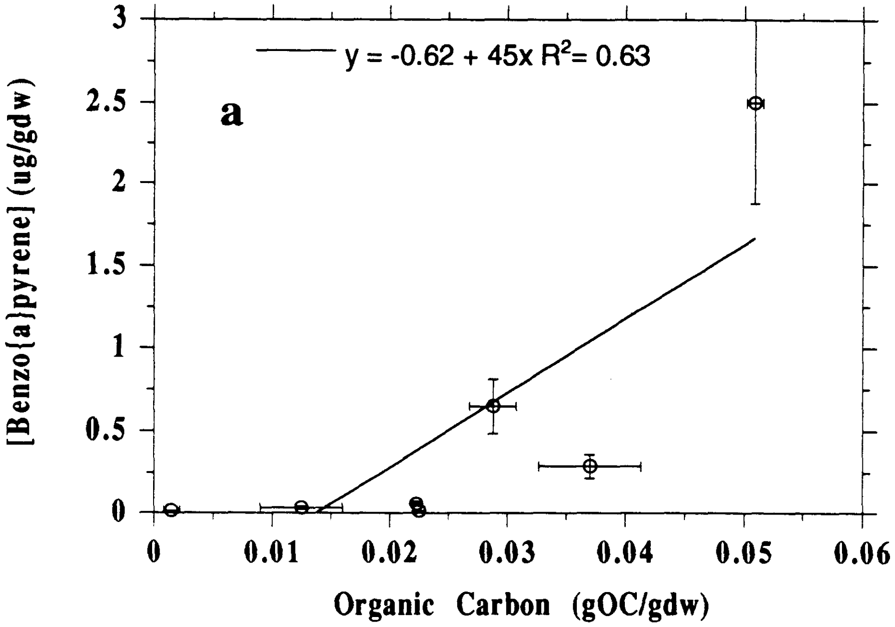
y = -0.62 + 45x R^2= 0.63
a
[Benzo{a}pyrene] (ug/gdw)
3
2.5
2
1.5
1
0.5
0
0
0.01
0.02
0.03
0.04
0.05
0.06
Organic Carbon (gOC/gdw)

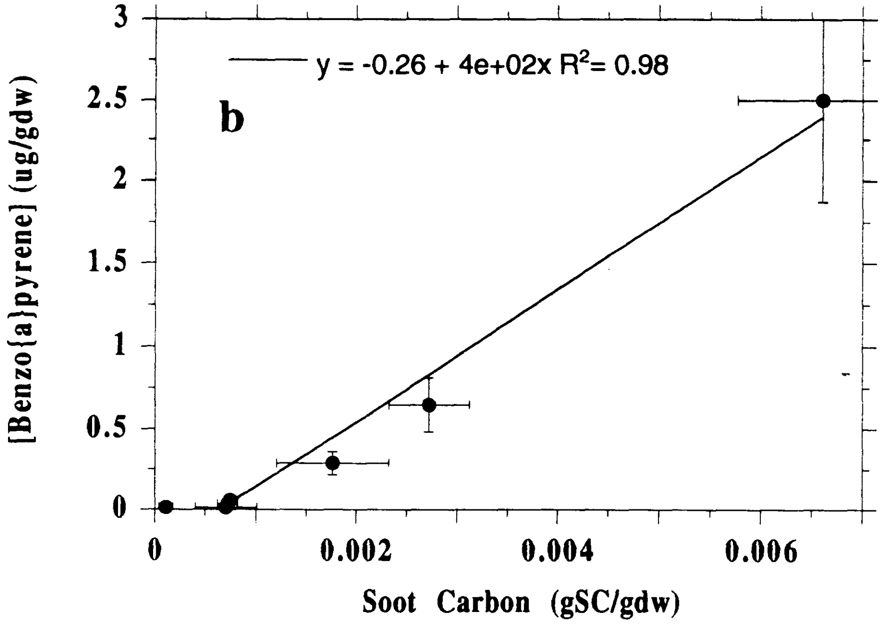
y = -0.26 + 4e+02x R^2= 0.98
b
[Benzo{a}pyrene] (ug/gdw)
3
2.5
2
1.5
1
0.5
0
0
0.002
0.004
0.006
Soot Carbon (gSC/gdw)

1%. However, the statistical analysis indicated quite significant probabilites for OC and PAH to not be correlated (Table II).

These strong correlations between field measurements of SC and PAHs lend credence to the applicability of the analytical soot carbon method. More importantly, the SC data strongly suggest that the spatial distribution of PAHs are chiefly dictated by interactions with soot as opposed to with bulk organic matter. Since both amorphous organic and soot carbon are likely to be largely associated with the "fines" fraction of accumulating sediments, some correlation between OC and SC may also be observed. However, since grain size is not the relevant intrinsic sorbent property, and since the statistical analysis yields significantly better correlation for PAHs with SC than with OC, future work on the phase-speciation of PAHs should focus on the soot carbon content of sediments. One exception is obviously near oil spills. These results suggest that it is necessary to revise the fundamental assumption of bulk organic matter partitioning currently made in fugacity and bioavailablity models when applied to ambient PAHs (49-52). A strong soot sorbent would mean significantly lower dissolved fractions and correspondingly lower predictions of bioavailabilities.

Table II. Correlations of PAHs with OC and SC in Seven Marine Sediments

Compound	*Organic Carbon*		*Soot Carbon*	
	Correlation Coefficient - R^2	*Probability Level -* p	*Correlation Coefficient* R^2	*Probability Level* p
Phenanthrene	0.74	< 0.10	0.99	< 0.01
Pyrene	0.59	< 0.10	0.97	< 0.01
Benzo[a]pyrene	0.63	> 0.50	0.98	< 0.01

Physico-Chemical Properties of Soot. To develop an understanding of the underlying mechanisms and driving force behind the association of PAHs with soot, it is helpful to consider both macroscopic features and molecular details of the soot matrix.

Soot Particles - Formation and Physical Properties. Earlier microscopy-based approaches to quantifying sedimentary soot have revealed some of the physical properties of these pyrogenic carbon phases found in aquatic environments. Grossly, soot particles may be divided into two groups, where different formation processes render distinct macroscopic properties. The few-to-tens of µm-sized coarse "charcoal" particles (e.g., 53-57), resulting from incomplete combustion of fuel particles, often occur as single spheroidal forms in sediments. The fine "soot" particles (e.g., 58), occuring as individual spheres of 3-30 nm diameter, are found aggregated into grape-like clusters. Such fine soot is formed from vapor-phase condensation processes where free-radical reactions between polyaromatic and acetylenic species play a key role during both inception and surface growth (e.g., 59-62). Hence, in addition to being a dilute fraction of the entire sedimentary matrix, the fact that soot particles may exhibit very different morphologies and span several orders of magnitude in size renders microscopy-based approaches to quantify the entire pool of PAH-carrying sedimentary soot less attractive than bulk chemical analysis (18).

However, there are physical similarities (e.g., density, surface area, and surface chemical structures) among soots from different sources whether furnace flames, diesel and gasoline engines, or by commercial processes (62, 63). Specific densities are near 1.8-2.1 g/cm^3, similar to the density of pure graphite (2.1-2.2 g/cm^3; 63, 64). Brunauer-Emmet-Teller (BET) surface areas of soot appear to be around 100 m^2/g, not much greater than two-dimensional (exterior) surface areas calculated from the SEM-derived diameters of the spheres and assuming the above density (e.g., 63-66). The similarity in three- and two-dimensional surface areas suggest that soots' pores are generally too narrow for penetration by the adsorbing species. High-resolution transmission electron microscopy (HRTEM) images have recently been presented with reported interlayer spacing for diesel soot on the order of 4 Å (67), suggesting that the pore-width is at most a few Å.

Soot Particles - Chemical Properties. Recent TEM studies, in combination with spectroscopic results, confirm the picture of soot as a multi-layered aromatic system as was hypothesized long ago (e.g., 68). Large C:H and C:O elemental ratios suggest that soot must possess a highly condensed and conjugated structure (e.g., 62, 66). The most prominent feature in FTIR spectra of soot is the absorption band at 1590 cm^{-1}, corresponding to C=C stretching mode of polyaromatic systems (66, 69). This is consistent with earlier findings of aromatic stretching modes of graphitic planes (e.g., 70, 71). Minor bands in FTIR spectra suggest the presence of some C=O and C-O bonds in soot (66). The same dominant 1590 cm^{-1} absorption band was reported also in the Raman spectrum of soot, indicating lattice vibrations of graphitic structure (i.e., crystal symmetry; ref. 66). With dimensions for crystallites of carbon black (72), Akhter and co-workers calculated that there should be nearly 30 aromatic rings per layer of this overall aromatic network (66). Cross-polarization magic-angle-spinning (CP/MAS; solid state) ^{13}C NMR results indicate that 90-100% of the total organic carbon in soot is aromatic, supporting the overall condensed backbone picture (66). Hence, soot may be thought of as particles of multi-layered macro-PAHs (conjugated blocks of about 30 rings), structurally held together with some carbon-bridges and ether-linkages, and containing some substitution of conjugated carbonyls and acid anhydrides (a hypothetical structure is shown in Fig. 16 in ref. 73).

Soot-Water Partitioning of PAHs. Strong interaction between PAH molecules and the condensed aromatic structure of soot may be anticipated. The positioning of sorbed PAHs on or in the soot matrix may have an effect on the ease whereby the molecules may exchange with the surrounding media. Urban atmospheric soot is commonly described as containing an organic film of liquid compounds (e.g., 60, 63). PAHs are often found to make up a significant fraction of the extractable fraction (e.g., 60, 74). However in aquatic environments, this liquid layer is likely to either dissolve in the surrounding water or degrade. In fact, our sedimentary PAH-SC regressions (e.g., Figure 3) suggest that the extractable PAHs contribute less than one per cent of the SC mass. Hence, in aquatic sedimentary environments, PAHs may be anticipated to interact directly with the soot backbone structure. There, the PAHs can exist, for instance, in an aromatic layer "trapped" between macro-PAH blocks. The few-Å-"thick" PAHs may also be sorbed on the exterior layer of the soot, or in the interplanar spacing between two layers.

It is easy to envision the favorable π-cloud overlap between the planar-PAHs and the flat "macro-PAH" surface of soot. This close-up contact would likely lead to greatly reduced rotational and translational freedom of the PAH molecules. This sorbed state may hence be best modeled as a fusion (solid precipitation) onto the planar soot surface. Note that the strength of dispersion forces is highly dependent on the distance of separation between the soot surface and the center of the sorbent molecule (e.g., ref.

75). As a result, other non-planar aromatic molecules, such as *ortho*-substituted PCBs, may not experience fully reduced rotation and, thus, not become "locked" in a solid-like state. It is noteworthy that non-*ortho* substituted (coplanar) PCBs exhibit enhanced affinity to urban aerosols compared to more non-planar congeners despite similar subcooled liquid vapor pressures (76), suggesting the importance of a close and favorable alignment between sorbate and soot.

Estimation of PAH Soot-Water Partitioning. To explore potential mechanisms and the physico-chemical driving forces of soot-water partitioning of PAHs, it is useful to attempt to conceptualize the process and isolate thermodynamic measures of each part's importance. We will explore the partitioning mechanism envisioned above, where PAHs are either dissolved in the aqueous phase or fused on the semi-crystalline soot surface. The latter would lead to greatly reduced rotational and translational freedom of the molecules. This sorbed state is assumed to best be modeled as a solid precipitation.

For a PAH distributing itself between the soot and the surrounding aqueous phase, at equilibrium, its fugacities (f_i) in the two media are equal:

$$f_{\text{soot-surf}} \equiv f_{\text{water}} \tag{2}$$

These fugacities may be expressed relative to the fugacities of a PAH in its pure solid and liquid forms, respectively:

$$\gamma_{\text{soot-surf}}\; x_{\text{soot-surf}}\, P_{\text{soot-surf}}(s) \;\equiv\; \gamma_w\, x_w\, P^{\circ}_w(l) \tag{3}$$

where γ, and x are the PAH activity coefficients and mole fractions on the soot surface and in the water, respectively, and P is the vapor pressure. The formulation on the left hand side follows the description for solid solutions of Prausnitz (ref. 77; p. 403), with the assumption that sorption to the surface of the soot is thermodynamically similar to sorption onto a pure PAH solid. If $P^{\circ}_w(l)$ is chosen as the reference state, one may use the Prausnitz' (ref. 77; p. 390) approximation to relate the solid vapor pressure of a compound to its subcooled liquid vapor pressure for the change in free energy associated with the phase transition (ΔG_{fusion}), and recast Equation 3:

$$\gamma_s\, x_s \exp[-(\Delta S_\phi/R)((T_m/T) - 1)]\, P^\circ_w(l) \equiv \gamma_w\, x_w\, P^\circ_w(l) \qquad (4)$$

where ΔS_ϕ is the change in entropy resulting from the phase-transition, T_m is the melting point of the solid PAH, and T is the absolute temperature of the system.

A soot-water equilibrium distribution constant (K_{sw}) may be defined as:

$$K_{sw}\ (L/m^2) \equiv \frac{C_s}{C_w} = \frac{x_s\, V_w}{A_s\, x_w} \qquad (5)$$

where C_s is the concentration of the compound on the soot surface (mol/m^2) and C_w is its concentration in the aqueous phase (mol/L). A_s is the specific area of the soot (m^2/mol) and V_w is the specific volume of the aqueous solution (L/mol); these terms are constant for dilute conditions. From above (equation 5) we now substitute for the ratio x_s/x_w:

$$K_{sw}\ (L/m^2) = \frac{\gamma_w\, V_w}{\gamma_s \exp[-(\Delta S_\phi/R)((T_m/T) - 1)]\, A_s} \qquad (6)$$

with the liquid fugacities canceling out. This equation can be manipulated to separate terms:

$$\log K_{sw} = \log \gamma_w - \log \gamma_s + \log\left(\frac{V_w}{A_s}\right) + \frac{\Delta S_\phi}{2.3\, R}\left(\frac{T_m}{T} - 1\right) \qquad (7)$$

As is apparent from Equation 7, the magnitude of K_{sw} is dependent on the relative (in)compatibilities of a PAH with the aqueous and soot phases (i.e., the aqueous and solid activity coefficients), and the free energy costs of phase transition.

If the terms in Equation 7 could be estimated, we would be able to *a priori* predict K_{sw}. We start with the first term, using anthracene to illustrate the relative magnitudes of the terms. The aqueous activity coefficient is a measure of the non-ideality of the solution (relative to pure subcooled liquid anthracene). Since the solubility of anthracene is low ($C_w^{sat} = 10^{-4.40}$ M), γ_w must be very close to γ_w^{sat}. Since the specific volume of a dilute aqueous solution is known (0.018 L/mol), γ_w may be estimated from:

$$\gamma_w \approx \gamma_w{}^{sat} = \frac{1}{x_w{}^{sat}} = \frac{1}{C_w{}^{sat}V_w} = \frac{1}{10^{-4.40}\,0.018} = 10^{6.1} \qquad (8)$$

For soot association, in the infinite dilution case (Henry's law region; where sorption isotherm is linear during initial low coverage), the same assumption of no interaction between sorbed molecules may be made. Following the above assumption that PAH sorption onto soot is thermodynamically similar to associating with a pure PAH crystal, the activity coefficient of soot-sorbed PAHs can be approximated by:

$$\gamma_s \approx \gamma_s{}^{sat} = \frac{1}{x_s{}^{sat}} = 1 \qquad (9)$$

Considering the relative interactions with the surrounding media, it is not a surprise that PAHs are much more compatible with soot than with water as these relative activity coefficients indicate. In the infinite dilution case, the surfaces of the aqueous soot particles are covered by water molecules. Hence, the specific surface of soot in an aqueous system is:

$$A_s = A_{H2O}\,N_A = 0.5\ Å^2 \text{x}\ 6.023\ 10^{23}\ \text{mol}^{-1} = 3000\ \text{m}^2/\text{mol} \qquad (10)$$

where A_{H2O} is the two-dimensional surface area of a water molecule and N_A is Avogadro's number. The entropy of liquid-solid phase transfer (ΔS_m) at the melting point for rigid molecules is relatively invariant and may be estimated from (78):

$$\Delta S_m(T_m) \approx 56.5 \qquad (\text{J/mol K}) \qquad (11)$$

The total entropy-change upon fusion of PAHs is made up of approximately 15 J/mol K due to translational restriction and 42 J/mol K due to loss of rotational freedom (78). As noted above, we suspect that interaction of PAHs with an aromatic soot surface leads to reduced rotational and translational freedom compared to the liquid state of the molecule. However, because a PAH molecule parallel to the soot plane is restricted in only one of three translational planes (orthogonal to surface), and in two of three rotational dimensions, this close-up surface interaction is likely less restricting than formation of a three-dimensional solid crystal. Given only one-third reduction in translation (1/3 x 15 J/mol K) and two-thirds reduction in rotation (2/3 x 42 J/mol K), we estimate ΔS_{Φ} of PAH soot sorption to be approximately 33 J/mol K. Since for anthracene $T_m = 489$ K,

$$\frac{\Delta S_{\phi}}{2.3\,R}\left(\frac{T_m}{T} - 1\right) \approx \frac{33}{2.3 \times 8.3}\left(\frac{489}{298} - 1\right) = 0.8 \qquad (12)$$

Substituting the estimated values of the terms making up K_{sw} back into Equation 7 results in a thermodynamically-based *a priori* estimate of the soot-water distribution for anthracene of:

$$\log K_{sw}\ (\text{anthracene}) \approx 1.7\ L_w/m^2{}_{soot} \qquad (13)$$

Since the surface area of soot particles such as diesel particulate matter, flame soot, and graphitized carbon blacks typically cluster around 10^5 m^2/kg (e.g., 63, 64, 73), the equilibrium distribution coefficient may be presented in sorbent-mass based units, fascilitating comparison:

$$\log K_{sw}\ (\text{ant}) \approx 6.7\ L_w/kg_{soot} \qquad (14)$$

This estimate may be compared to values for partitioning of anthracene in an activated-carbon - water system (log $K_{ac\text{-}w}$) of 6.5 (ref. 82) and 6.8 (calculated in ref. 18, from the Henry's law region of the sorption isotherms in ref. 28). In contrast, the organic carbon - water partition constant (log K_{oc}) for anthracene (≈ 4.1) is much smaller (e.g., 79). Theoretical K_{SW} partition coefficients were calculated for a set of PAHs and compared with measured and/or estimated partitioning to activated carbon and natural organic carbon matrices, respectively (Table III).

Table III. Comparison of Estimated K_{sw} with $K_{ac\text{-}w}$ and K_{oc} Values (L_w/kg_C)

Compound	T_m *(K)*	*log* γ_w	*log* K_{sw}	*log* $K_{ac\text{-}w}$		*log* K_{oc}
			estimated	*measured*		
	ref. 80	ref. 80		ref.28	ref.82	ref.79
Acenaphthene	369	5.59	5.8	7.2	6.2	3.5
Fluorene	389	5.86	6.2	7.1	6.3	3.8
Anthracene	489	6.14	6.7	6.8	6.5	4.1
Phenanthrene	374	6.34	6.4	7.0	6.5	4.2
Pyrene	429	6.62	7.0	7.7		4.8
Fluoranthene	384	6.78	6.9	7.8	6.9	4.8
Chrysene	528	7.52	8.2	8.5		5.4
Benz[a]anthracene	435	7.62	7.8	7.4		5.5
Benzo[a]pyrene	448	8.08	8.4		7.8	6.1
Dibenzo[a,h]anthracene	539	8.09	9.3		8.2	6.8

The good match between our theoretically deduced soot-water equilibrium distribution and empirically obtained data from an assumed related sorbent matrix (activated carbon) suggests that the conceptualized mechanism and parameterization of the physico-chemical driving forces may be representative of the actual sorption process.

Conclusions.

The dominant form of PAHs in many aquatic environments is to be associated with soot. Inspection of the entire PAH assemblage reveals the importance of hydrophobicity on the relative solid-water distributions. This characteristic implies that an active exchange between soot-associated PAHs and their dissolved counterparts is taking place, albeit on an unknown timescale. Another implication of this study is that PAHs are good markers for the presence of soot and other soot-associated contaminants.

A much better correlation for PAHs was found with soot carbon compared with bulk organic carbon, despite the fact that soot carbon is only present at a few per cent of the non-soot organic carbon levels. Soot carbon could account for 97-99% of the sedimentary distributions observed for phenanthrene, pyrene, and benzo[a]pyrene; three PAHs of quite varying physico-chemical properties, whereas there was no significant correlation between PAHs and organic carbon at the 95% confidence limit.

A thermodynamic evaluation of the soot-water partition process resulted in theoretical estimation of PAH partition coefficients which were substantially larger than traditional organic-carbon normalized partition constants, but which agreed reasonably well with results from sorption onto activated carbon. The significantly enhanced affinity to highly condensed and aromatic surfaces is suggested to be a result of geometrically efficient π-cloud overlapping.

There are far-reaching implications of soot (de)sorption of PAHs dominating the environmental phase-speciation of these, and by inference many other physico-chemically similar, contaminants. Estimated K_{SW} together with measurements of soot carbon concentrations in coastal sediments suggest that the dissolved fraction of these compounds that are available for biological uptake and homogeneous phase reactions and transport are much lower than previously thought. This insight about PAH behavior may be extrapolatable to structurally similar contaminant assemblages such as coplanar PCBs and polychlorinated dioxins, and to lesser extents also to other hydrophobic pollutants. These findings should inspire controlled soot-water sorption studies of PAHs and other contaminants to further constrain the magnitude and kinetics of this partition process, as well as elucidating what fractions of soot-associated PAHs are available for desorption on different time scales.

Acknowledgments.

The captains and crew of R/V Asterias, R/V Argo Maine, and R/V Diane G. are thanked for their assistance during sediment sampling. John Farrington is thanked for lending us his MK-3 box corer. The able coring skills of Hovey Clifford, Chris Swartz, Chris Long, John MacFarlane, and Tom Ravens are recognized. John MacFarlane, Allsion MacKay, Keong Kim, and Rachel Adams are acknowledged for support and assistance during sample analysis. Inspiring discussions with John Farrington, Bob Eganhouse, Shige Takada, Johan Axelman, Dag Broman, and Adel Sarofim contributed to this work. Shige Takada is especially thanked for contributing a pre-publication data set to Figure 1. Financial support came from the Office of Naval Research (grant # NOOO14-93-1-0883), National Oceanic and Atmospheric Administration (# NA36RM044-UM-S242), National Institute of Environmental Health Sciences (# 2-P30-ESO-2109-11), and Massachusetts Water Resources Authority. The views herein are those of the authors and do not necessarily reflect the views of NOAA or any of its subagencies.

Literature Cited.

1. *Evaluation and Estimation of Potential Carcinogenic Risks of Polynuclear Aromatic Hydrocarbons* (Office of Health and Environmental Assessment, Office of Research and Development, US Environmental Protection Agency, Washington, DC, 1985).
2. Durant, J. L.; Thilly, W. G.; Hemond, H. F.; LaFleur, A. L. *Environ. Sci. Technol.* **1994**, *28*, 2033.
3. Karickhoff, S. W.; Brown, D. S.; Scott, T. A. *Water Res.* **1979**, *13*, 241.
4. Chiou, C. T.; Porter, P. E.; Schmedding, D. W. *Environ. Sci. Technol.* **1979**, *206*, 831.
5. Schwarzenbach, R. P.; Gschwend, P. M.; Imboden, D. M. *Environmental Organic Chemistry*. Wiley-Interscience: New York, NY, 1993, 269-276.
6. Kile, D. E., Chiou, C. T.; Zhou, H.; Li, H.; Xu, O. *Environ. Sci.Technol.* **1995**, *29*, 1401.
7. Baker, J. E.; Eisenreich, S. J.; Eadie, B. J. *Environ. Sci. Technol.* **1991**, *25*, 500.
8. Takada, H.; Kumata, H.; Satoh, F. 212th American Chemical Society National Meeting. Division of Environmental Chemistry extended abstracts, pp. 295-297.
9. Readman, J. W.; Mantoura, R. F. C.; Rhead, M. M. *Sci. Tot. Env.* **1987**, *66*, 73.
10. Broman, D.; Näf, C.; Rolff, C.; Zebühr, Y. *Environ. Sci. Technol.* **1991**, *25*, 1850.
11. Ko, F.-C.; Baker, J. E. *Mar. Chem.* **1996**, *49*, 171.
12. McGroddy, S. E.; Farrington, J. W. *Environ. Sci. Technol.* **1995**, *29*, 1542
13. Poster, D. L.; Baker; J. E. *Environ. Sci. Technol.* **1996**, *30*, 341.
14. McGroddy, S. E.; Farrington, J. W.; Gschwend, P. M. *Environ. Sci. Technol.* **1996**, *30*, 172.
15. Brownawell, B. J.; Farrington, J. W. *Geochim. Cosmochim. Acta* **1986**, *50*, 157.
16. Burgess, R. M.; McKinney, R. A.; Brown, W. A. *Environ. Sci. Technol.* **1996**, *30*, 2556.
17. Youngblood, W. W.; Blumer, M. *Geochim. Cosmochim. Acta* **1975**, *39*, 1303.
18. Gustafsson, Ö.; Haghseta, F.; Chan, C.; MacFarlane, J.; Gschwend, P. *Environ. Sci. Technol.* **1997**, *31*, 203.
19. Gschwend, P. M.; Hites, R. A. *Geochim. Cosmochim. Acta* **1981**, *45*, 2359.

20. Farrington, J. W.; Goldberg, E. D.; Risebrough, R. W.; Martin, J. H.; Bowen, V. T. *Environ. Sci. Technol.* **1983**, *17*, 490.
21. Prahl, F. G.; Carpenter, R. *Geochim. Cosmochim. Acta* **1983**, *47*, 1013.
22. Jones, D. M.; Rowland, S. J.; Douglas, A. G.; Howells, S. *Intern. J. Environ. Anal. Chem.* **1986**, *24*, 227.
23. Broman, D.; Näf, C.; Wik, M.; Renberg, I. *Chemosphere* **1990**, *21*, 69.
24. Bouloubassi, I.; Saliot, A. *Oceanologica Acta* **1993**, *16*, 145.
25. Wakeham, S. G. *Mar. Chem.* **1996**, *53*, 187.
26. Venkataraman, C.; Friedlander, S. K. *Environ. Sci. Technol.* **1994**, *28*, 563.
27. Allen, J. O.; Dookeran, N. M.; Smith, K. A.; Taghizadeh, K.; Lafleur, A. L. *Environ. Sci. Technol.* **1996**, *30*, 1023.
28. Walters, R. W.; Luthy, R. G. *Environ. Sci. Technol.* **1984**, *18*, 395.
29. Blumer, M. *Anal. Chem.* **1957**, *29*, 1039.
30. LaFlamme, R. E.; Hites, R. A. *Geochim. Cosmochim. Acta* **1978**, *42*, 289.
31. Sporstøl, S.; Gjøs, N.; Lichtenthaler, G.; Gustavsen, K. O.; Urdal, K.; Oreld, F.; Skei, J. *Environ. Sci. Technol.* **1983**, *17*, 282.
32. Lee, M. L.; Prado, G. P.; Howard, J. B.; Hites, R. A. *Biomed. Mass Spectrom.* **1977**, *4*, 182.
33. Takada, H.; Farrington, J. W.; Bothner, M. H.; Johnson, C. G.; Tripp, B. W. *Environ. Sci. Technol.* **1994**, *28*, 1062.
34. Lipiatou, E.; Saliot, A. *Mar. Chem.* **1991**, *32*, 51.
35. Lipiatou, E.; Marty, J.-C.; Saliot, A. *Mar. Chem.* **1993**, *44*, 43.
36. Bates, T. S.; Hamilton, S. E.; Cline, J. D. *Environ. Sci. Technol.* **1984**, *18*, 299.
37. Broman, D.; Colmsjö, A.; Näf, C. *Bull. Environ. Contam. Toxicol.* **1987**, *38*, 1020.
38. Dachs, J.; Bayona, J. M.; Fowler, S. W.; Miquel, J.-C.; Albaigés, J. *Mar. Chem.* **1996**, *52*, 75.
39. Barrick, R. C.; Prahl, F. G. *Estuarine Coastal Shelf Sci.* **1987**, *25*, 175.
40. Windsor Jr, J. G.; Hites, R. A. *Geochim. Cosmochim. Acta* **1979**, *43*, 27.
41. Hites, R. A.; LaFlamme, R. E.; Windsor Jr, J. G. In *Petroleum in the Marine Environment*; Petrakis, L.; Weiss, F. T., Eds.; Adv. in Chem. Ser. 185; American Chemical Society: Washington, DC, 1980; pp289-311.

42. Simo, R.; Colom-Altés, M.; Grimalt, J. O.; Albaigés, J. *Atmos. Env.* **1991**, *25A*, 1463.
43. Bjørseth, A.; Lunde, G.; Lindskog, A. *Atmos. Env.* **1979**, *13*, 45.
44. Ehrhardt, M.; Petrick, G. *Mar. Chem.* **1993**, *42*, 57.
45. Grimmer, G.; Böhnke, H. *Cancer Lett.* **1975**, *1*, 75.
46. Hites, R. A.; LaFlamme, R. E.; Farrington, J. W. *Science* **1977**, *198*, 829.
47. Prahl, F. G.; Carpenter R. *Geochim. Cosmochim. Acta* **1979**, *43*, 1959.
48. Hites, R. A.; LaFlamme, R. E.; Windsor Jr, J. G.; Farrington, J. W.; Deuser, W. G. *Geochim. Cosmochim. Acta* **1980**, *44*, 873.
49. Mackay, D.; Paterson, S. *Environ. Sci. Technol.* **1981**, *15*, 1006.
50. Mackay, D.; Paterson, S. *Environ. Sci. Technol.* **1991**, *25*, 427.
52. U.S. Environmental Protection Agency *Sediment quality criteria for the protection of benthic organisms: Fluoranthene*; EPA 822-R-93-012; Offices of Water, Research, and Development and, Science and Technology; Washington, DC, 1993.
53. Griffin, J. J.; Goldberg, E. D. *Science* **1979**, *206*, 563.
54. Griffin, J. J.; Goldberg, E. D. *Geochim. Cosmochim. Acta* **1981**, *45*, 763.
55. Goldberg, E. D.; Hodge, V. F.; Griffin, j. J.; Koide, M.; Edgington, D. N. *Environ. Sci. Technol.* **1981**, *15*, 466.
56. Renberg, I.; Wik, M. *Ecol. Bull.* **1985**, *37*, 53.
57. Wik, M; Natkanski, J. *Phil. Trans. R. Soc. Lond.* **1990**, *B327*, 319.
58. Griffin, J. J.; Goldberg, E. D. *Environ. Sci. Technol.* **1983**, *17*, 244.
59. Prado, G.; Lahaye, J. In *Mobile Source Emissions Including Polycyclic Organic Species*; Rondia, D.; Cooke, M.; Haroz, R. K., Eds.; NATO Advanced Research Workshop Series; Reidel: Liege, Belgium, 1983; pp. 259-275.
60. Longwell, J. P. In *Soot in Combustion Systems and its Toxic Properties*; Lahaye, J., Prado, G., Eds.; NATO/Plenum Press: New York, 1981; pp. 37-56.
61. Lahaye, J. *Polymer Degrad. Stabil.* **1990**, *30*, 111.
62. Hamins, A. In *Environmental Implications of Combustion Processes*, Puri, I. K., Ed.; CRC Press: Boca Raton, 1993; pp 71-95.
63. Risby, T. H.; Sehnert, S. S. *Environ. Health Perspec.* **1988**, *77*, 131.
64. Ross, M. M.; Risby, T. H.; Steele, W. A.; Lestz, S. S.; Yasbin, R. E. *Colloids and Surfaces* **1982**, *5*, 17

65. Ross, M. M.; Risby, T. H.; Lestz, S. S.; Yasbin, R. E. *Environ. Sci. Technol.* **1982**, *16*, 75.

66. Akhter, M. S.; Chughtai, A. R.; Smith, D. M. *Appl. Spectrosc.* **1985**, *39*, 143.

67. Rainey, L.; Palotas, A.; Bolsaitis, P.; Vander Sande, J. B.; Sarofim, A. F. *Appl. Occup. Environ. Hyg.* **1996**, *11*, 777.

68. Donnet, J. B.; Schultz, J.; Eckhardt, A. *Carbon* **1968**, 6, 781 (in French).

69. Smith, D. M.; Griffin, J. J.; Goldberg, E. D. *Anal. Chem.* **1975**, *47*, 233.

70. Tuinstra, F.; Koenig, J. L. *J. Chem. Phys.* **1970**, *53*, 1126.

71. Friedel, R. A.; Carlson, G. L. *J. Phys. Chem.* **1971**, *75*, 1149.

72. Avgul, N. N.; Kiselev, A. V. *Chemistry and Physics of Carbon*; Dekker: New York, NY, 1970.

73. Akhter, M. S.; Chughtai, A. R.; Smith, D. M. *Appl. Spectrosc.* **1985**, *39*, 154.

74. Lee, M. L.; Bartle, K. D. In *Particulate Carbon Formation During Combustion*; Siegla, D. C.; Smith, G. W., Eds.; Plenum: New York, NY, 1981, 91-104.

75. Israelachvili, J. *Intermolecular and Surface Forces*; Academic Press: San Diego, CA; 1992, 2nd Ed.

76. Falconer, R. L.; Bidleman, T. F.; Cotham, W.E. *Environ. Sci. Technol.* **1995**, *29*, 1666.

77. Prausnitz, J. M. *Molecular Thermodynamics of Fluid-Phase Equilibria*; Prentice-Hall: Englewood Cliffs, NJ, 1969.

78. Yalkowsky, S. H.; Valvani, S. C. *J. Chem. Eng. Data* **1979**, *24*, 127.

79. Karickhoff, S. W. *Chemosphere* **1981**, *10*, 833.

80. Miller, M. M.; Wassik, S. P.; Huang, G.-L.; Shiu, W.-Y.; Mackay, D. *Environ. Sci.Technol.* **1985**, *19*, 522.

81. Ruepert, C.; Grinwis, A.; Govers, H. *Chemosphere* **1985**, 14, 279.

82. Luehrs, D. C.; Hickey, J. P.; Nilsen, P. E.; Godbole, K. A.; Rogers, T. N. *Environ. Sci. Technol.* **1996**, *30*, 143

Chapter 7

Using ^{234}Th Disequilibria to Estimate the Vertical Removal Rates of Polycyclic Aromatic Hydrocarbons from the Surface Ocean

Örjan Gustafsson[1,2], Philip M. Gschwend[1]*, and Ken O. Buesseler[2]

[1]Department of Civil and Environmental Engineering, MIT 48-415, Massachusetts Institute of Technology, Cambridge, MA 02139, USA

[2]Department of Marine Chemistry and Geochemistry, Woods Hole Oceanographic Institution, Woods Hole, MA 02543, USA

submitted
Marine Chemistry

Abstract

A novel ^{234}Th-coupled approach was employed to deduce the vertical fluxes of polycyclic aromatic hydrocarbons (PAHs) through surface waters of harbor, coastal, shelf, and pelagic regimes. We found reasonable agreement between these surface ocean fluxes, based on direct measurements of mixed layer properties, and fluxes deduced from underlying sediments where the radionuclide inventories relative to source expectations indicated minimal sediment focussing effects. Fluxes decreased exponentially away from northeastern USA, and source-diagnostic molecular ratios indicate that atmospheric fallout of combustion-derived PAHs from the continents is the dominant source. Despite higher unit area flux inshore, the open ocean represents a large and dominant integral sink for PAHs. Of the 60 metric-ton of pyrene that we estimate to annually become sequestered in the western North Atlantic, < 10% is deposited in urban and coastal waters while the remaining 90% is exported further offshore on the continental shelf and to pelagic regimes.

1. Introduction

Polycyclic aromatic hydrocarbons (PAHs) are ubiquitous and recalcitrant organic pollutants. These aromatic compounds are introduced into the environment predominantly by petroleum discharges and fuel combustion emissions. Due to their ongoing and abundant releases, resulting in wide dispersal and exposure of humans and ecosystems, the environmental fate of PAHs continues to be the focus of much attention (e.g., NRC, 1985; EPA, 1985, 1993; Durant *et al.*, 1994; Simonich and Hites, 1994). The ocean has been hypothesized as being a major global sink for PAHs and many other such hydrophobic organic contaminants, HOCs (e.g., DDT: Woodwell *et al.*, 1971; Tanabe and Tatsukawa, 1983; Iwata *et al.*, 1993; Simonich and Hites, 1995; PCBs: Harvey *et al.*, 1973; Harvey and Steinhauer, 1976; Tanabe *et al.*, 1983; Knap *et al.*, 1986; Iwata *et al.*, 1993; Simonich and Hites, 1995; PAHs: Burns and Villeneuve, 1985; NRC, 1985; Lipiatou and Albaigés, 1994; Simonich and Hites, 1994; and general HOCs: e.g, UNEP, 1995; Wania and MacKay, 1995, 1996). Researchers have long recognized the importance of quantifying the fluxes of such organic pollutants through the surface ocean in order to: (a) understand their environmental dispersal, (b) predict their longevity in sensitive regimes, and (c) formulate global mass balance fate models (Woodwell *et al.*, 1971; Tanabe and Tatsukawa, 1983; NRC, 1985; Simonich and Hites, 1995).

The existing void of upper ocean HOC inventory and flux data is largely a result of the ease of contamination of such trace-level samples and the historical lack of a method that allows direct estimation of pollutant export from the mixed surface ocean. In the particular case of PAHs, absence of direct measurements of surface ocean fluxes has caused evaluations of the ocean as a pollutant sink to be limited to indirect information from either estimated inventories of the sources of direct petroleum spillages to the sea (NRC, 1985) or data from sediment trap and dated bottom core samples (e.g., Gschwend and Hites, 1981; Broman *et al.*, 1988; Lipiatou and Saliot, 1991; Näf *et al.*, 1992; Takada *et al.*, 1994; Tolosa *et al.*, 1996; Wakeham, 1996). These latter techniques are potentially integrating over space and time scales that are different than those of the dynamic surface ocean system; and the results from both methods include the uncertain influences of processes such as particle dissolution, compound desorption and degradation, and sediment resuspension.

Here we overcome many such difficulties by coupling water column PAH inventories with the radioactive disequilibrium of two natural radionuclides (^{238}U-^{234}Th) to estimate the surface ocean fluxes of PAHs. The strength of ^{234}Th-derived upper-ocean PAH export estimates is that they are based on direct measurements of mixed layer properties. Like Th, PAHs exhibit substantial affinity towards marine particles (e.g., Windsor and Hites, 1979; Broman *et al.*, 1988; Näf *et al.*, 1992; Schwarzenbach *et al.*, 1993; Means, 1995). Settling HOC carrier-phases are largely aggregates of smaller particles, formed either by biological processes, such as fecal pellet packaging, and/or abiotic flocculation processes (e.g., Fowler and Knauer, 1986; Farley and Morel, 1986; Alldredge and Silver, 1988; Stolzenbach, 1993). Fine soot particles, demonstrated to affect the marine distribution of pyrogenic PAHs (Broman *et al.*, 1990; Gustafsson *et al.*, 1996a, b), are very likely also incorporated in such aggregates. Hence, settling ^{234}Th and PAHs are expected to belong to, and be coupled through, this same particle dynamics.

The radioactive disequilibrium between the particle-reactive ^{234}Th and its highly water-soluble radiogenic source, ^{238}U, is used to quantify such settling particle fluxes. ^{234}Th has a strong affinity for marine particles (e.g., Bhat *et al.*, 1969; Turner *et al.*, 1981), and with a half-life of 24.1 days, this isotope is an excellent tracer of upper ocean particle aggregation and sedimentation processes occuring on timescales 1-100 days. Hence, this method provides an indirect estimate of the gravitoid flux (see chapter 2). To calculate the Th flux, we assume steady-state and neglect advective and eddy diffusive transport. Our previous studies have shown that these assumptions are reasonable in continental shelf and pelagic regimes as the particle settling flux of ^{234}Th at such sites is the dominant term in the ^{234}Th activity balance (Buesseler *et al.*, 1992a, 1994). Chapter 8 of this thesis have shown that horizontal dispersion may increase the actual vertical flux of ^{234}Th by a factor of three relative to estimates from just the local disequilibrium, but only at one station within a few kilometers of the coast. This horizontal transport may be important to consider if one is interested in the exchange between a harbor and the outside bay. However, the effect of using a one-dimensional model for studying the PAH fluxes on an ocean scale is minor as will be discussed below. Combining ^{238}U-^{234}Th activities with parallel measures of the particle-associated PAH concentrations, we obtain estimates of gravitoid-mediated PAH export fluxes:

$$F_{PAH} = F_{Th} \frac{[PAH]_{part}}{[^{234}Th]_{part}} = \frac{z_{mix}\ \lambda_{Th}\ ([^{238}U]_{tot} - [^{234}Th]_{tot})\ [PAH]_{part}}{[^{234}Th]_{part}} \qquad (1)$$

where F_i is the net vertical removal flux of PAHs or ^{234}Th; [^{238}U] and [^{234}Th] are their decay activities in particulate or total phases; $[PAH]_{part}$ is the particulate PAH concentration; z_{mix} is the depth of the mixed surface layer; and λ_{Th} is the radioactive decay constant for ^{234}Th (0.0288 day^{-1}). Here we report the first quantification of one group of HOCs, the PAHs, and their vertical fluxes out of the mixed surface ocean at four distinct regimes.

2. Methods

2.1 HOC Sampling and Analysis

Our approach to minimize fractionation and contamination during sampling was to use closed *in situ* pumping through inert stainless steel materials (Gustafsson *et al.*, 1996c). A low internal volume *in situ* pump (Fultz Pumps Inc., Lewistown, PA), made of stainless steel and with a small Teflon impeller, was deployed to the middle of the mixed surface layer. Water was pumped through 1/4" (ca. 0.0063 m) inner-diameter stainless-steel tubing to a shipboard sample extraction system. For particulate samples, pre-combusted (450°C for 24 h) GF/F glass-fiber filters (approximately 1 μm cut-off; Whatman Inc.) were positioned in a 142 mm stainless steel filter holder with a Teflon O-ring (Microfiltration Systems Inc., Dublin, CA). The filter back-pressure was monitored with an on-line stainless pressure gauge (Davis Instruments, Baltimore, MD) and the filters were changed before 20 psi was reached to minimize cell breakage. The filtrate volumes were recorded using a downstream flow totalizer (ABB Water Meter, Ocala, FL). Glass-fiber filters were transferred to pre-combusted Al-foil envelopes in a ship-board laminar-flow clean hood and stored frozen. The Gulf of Maine samples were collected on the R/V Argo Maine in late May, 1994, while the Sargasso Sea sample was collected a year earlier, but in the same season, in June 1993 aboard the R/V Weatherbird.

Sediment trap subsamples and trapped total particulate mass data were provided by C. Pilskaln (U. Maine, Orono) from 14-day integrated material collected in April 1995. The Honjo-type trap (Honjo and Doherty, 1988) was deployed at the same continental shelf site (150 m depth, 125 m above bottom) as surface water and bottom sediment had been sampled in the corresponding season a year earlier.

Separate subcores for HOCs and radionuclides were obtained from a 0.25 m^2 by 0.7 m deep Sandia-Hessler MK-III box corer (Ocean Instruments, San Diego, CA) following procedures described in detail earlier (Gustafsson *et al.*, 1996b, d). HOC subcores from apparently undisturbed sediments were immediately extruded and trimmed on board using solvent-rinsed stainless steel tools. The sectioned sediment was stored frozen in solvent-rinsed amber glass bottles with Al-foil lined Teflon caps.

For PAH analysis, the filters or sediments were spiked with four PAH internal standards (d_{10}-phenanthrene, *p*-terphenyl, d_{12}-benz[a]anthracene, d_{12}-perylene) and soxhlet extracted for 48 h with a 9:1 mixture of dichloromethane-methanol (Ultra-Resi Analyzed, J. T. Baker Inc.). The concentrated extracts were further purified with a method adapted and modified from Takada and Ishiwatari (1985), employing a fully activated silica gel column. The PAH fraction from the filters was analyzed using gas chromatographic high resolution mass spectrometry. High-precision 1.0 μL cool on-column auto-injections (HP7673 autosampler) were performed onto a 30 m by 0.32 mm inside diameter (film thickness 0.25 μm) DB-5 fused silica capillary column (J&W Scientific) housed in a HP5890 Series II gas chromatograph, temperature-programmed to start at 70°C, ramp first at 20°C/minute to 180°C, and then finally ramp at 6°C/minute to a

5 minute hold at 310°C. A VG Autospec EQ hybrid mass spectrometer was operated in positive electron ionization mode (accelerating voltage 8000 V) and with a resolution of 1/7500 D. Signals were acquired in grouped selective ion recording. PAHs recovered from sediment samples were analyzed using an HP5995B benchtop gas chromatograph - mass spectrometer, also equipped with an identical DB-5 capillary column. Analytical blanks were included in every sample batch and were found to be insignificant for reported analytes. Recoveries of PAH standards for both samples and blanks were 64-93% for the entire procedure, and reported data are corrected for these internal standard yields.

Particulate organic carbon (POC) of subsampled glass-fiber filters was measured on a Perkin-Elmer 2400 CHN analyzer in Ag capsules after *in situ* removal of carbonates following the method of Gustafsson *et al.* (1996a).

2.2 ^{234}*Th and* ^{238}*U Sampling and Analysis*

^{234}Th and ^{238}U were collected simultaneously with HOCs from the surface mixed layer using a parallel system. Protocols used for water column and sediment sampling and analyses of these radionuclides have been described previously (Gustafsson *et al.*, 1996d and references therein). Briefly, a diaphragm pump was used to pump 20-30 L of seawater through plastic tubing and through deckboard 1µm-filters and MnO_2-impregnated adsorbers (Buesseler *et al.*, 1992b; Greenamoyer and Moran, 1996). Samples for salinity calibration of the CTD data, necessary for accurate ^{238}U estimation (Chen *et al.*, 1986) were collected in glass salinity bottles, stored at room temperature, and analyzed at WHOI with a salinometer (Guildline Autosal 8400A) calibrated with IAPSO Standard Sea Water.

^{234}Th filters and adsorbers were combusted, brought up in acid solution, spiked with ca. 10 dpm ^{230}Th yield monitor, purified with ion-exchange columns, and electroplated onto stainless steel planchets (Buesseler *et al.*, 1992b, Moran and Buesseler, 1993, Gustafsson *et al.*, 1996d). Following procedures outlined in the above studies, the ^{234}Th activity was measured on low background beta detectors. Recoveries of ^{230}Th internal standard were quantified by α-counting spectrometry (Buesseler *et al.*, 1992b) and were in the range 75-96%. The samples for ^{234}Th were counted 4-5 times with a weekly interval to check for background interferences and to improve precision and accuracy. Activities were decay-corrected to the mid-point of sample collection. Errors were propagated from counting statistics, based upon the fit of the raw counts to the ^{234}Th decay curves.

3. Results and Discussion

3.1 Spatial Trends in Concentrations of PAHs, ^{234}Th, and Ancillaries

Analyses of particle-bound PAHs from four ocean stations, located at logarithmically spaced distances from the North American continent, showed a decrease for prevalent individual compounds from picomolar to femtomolar concentrations with increasing distance (Table 1). We found values of $\sum$methylphenanthrenes-to-phenanthrene below 0.5, characteristic of combustion-derived and urban air PAH samples (Youngblood and Blumer, 1975; Gschwend and Hites, 1981; Sporstøl *et al.*, 1983), and this ratio decreased slightly going offshore (0.43 to 0.22). These data are consistent with atmospheric dilution and eventual fallout of land-based combustion-derived PAH-containing aerosols.

Total ^{234}Th activities increased offshore (Table 1). The relative proportion of total ^{234}Th found in the particulate fraction increased when approaching the coast (Table 1). These trends are consistent with a pattern of decreasing scavenging further away from the coast (Bhat *et al.*, 1969; Moran and Buesseler, 1993).

Total ^{238}U activities were estimated from salinity (Chen *et al.*, 1986). The assumed conservative relationship between ^{238}U and salinity has previously been confirmed in this region by direct analysis of ^{238}U from the two coastal stations (Gustafsson *et al.*, 1996d). POC levels were highest closest to the shore and decreased at each station going outward (Table 1). POC is likely a good indicator of the relative particle-mediated scavenging intensity of different sites, which is directly reflected in the spatial pattern of ^{238}U-^{234}Th disequilibrium.

3.2 PAH Fluxes

In order to use thorium to predict accurately vertical HOC transport, both the thorium and the HOCs must associate with the same settling materials. In addition to the qualitative reasons presented in the Introduction why this is likely to be true, it is important that we found a tight correlation between particle-bound ^{234}Th and POC, the sorbent property dictating the particle-association of many lipophilic compounds (e.g., Schwarzenbach *et al.*, 1993). We observed K_d(Th) to be proportional to POC (r = 0.96; n = 4). Normalizing to the POC (Table 1), we found K_{oc}(Th) to be 3 x 10^6 L/kg_{oc}. This corroborates the ^{234}Th-POC coupling found in another year-round near-coastal study (Moran and Buesseler, 1993). Thus, our presumption that thorium and hydrophobic organic compounds are coupled through the same particle cycling dynamics appears valid.

Using the ^{234}Th isotopic "clock" (Eqn. 1), we calculated substantial decreases in surface ocean fluxes of the three PAHs, pyrene, benzo[a]pyrene, and dibenz[a,c]anthracene, with increasing distance from the North American continent (Table 2 and Fig. 1). A parallell study evaluating the relative importance of nearcoastal horizontal and vertical transport (chapter 8) showed that horizontal dispersion only appears to affect the vertical flux estimates at the harbor station (factor of 2-3). Since vertical transport on an ocean scale is considered here and the harbor sink is relatively insignificant, that finding does not appreciably affect the total ocean fluxes deduced in this study. The geographical flux pattern discovered is consistent with nearshore run-off and high rates of atmospheric fall-out of PAHs close to urban sources. Long-range aeolian PAH transport on finer combustion particles appears to dominate the oceanic PAH flux.

The ^{234}Th-derived direct estimates of PAH surface ocean fluxes may be contrasted to fluxes obtained from underlying sediment traps and cores. Analyses of box cores collected at the same three Gulf of Maine sites, and on the same occasion as surface water sampling, have provided core-top PAH concentrations (Gustafsson *et al.*, 1996b) and excess ^{210}Pb inventories (Gustafsson *et al.*, 1996d). A box core collected in 1988 close to our pelagic water column site has similarly been analyzed for PAHs and excess ^{210}Pb (Σinventory: 31 dpm/cm^2, Benoit, unpublished data). For the three Gulf of Maine

Table 1. Concentrations of PAHs, ^{234}Th, ^{238}U, and POC in upper ocean regimes.

Location	particulate PAHs (fM)			^{234}Th (dpm/m^3)		^{238}U(dpm/m^3)	POC(µg/L)
(km from NE USA)	Pyrene	Benzo[a] pyrene	Dibenz[a,c] anthracene	particulate	total		
Portland Harbor, Maine (1 km)	6300±600	1100±200	94±14	334±19	504±32	1920	150
Casco Bay, Gulf of Maine (15 km)	1500±200	270±40	21±3	389±21	778±40	2040	140
Wilkinson Basin Gulf of Maine (130 km)	270±30	4.3±0.6	0.26±0.04	308±32	1689±53	2330	90
Station BATS§ North Atlantic (1600 km)	30±3	0.58±0.08	0.061±0.008	220±10	2270±130	2610	29

§Station BATS is the Bermuda Atlantic Time Series site of the Joint Global Ocean Flux Study (JGOFS).

Table 2.

Estimated upper ocean fluxes of three PAHs with increasing hydrophobicity. Uncertainties of PAH export fluxes represent the propagated analytical variability of total ^{234}Th, particulate ^{234}Th, and PAHs measured.

Location*	**surface water export flux** (pmol/m^{2}day)	sediment trap flux (pmol/m^{2}day)	bottom sediment flux (pmol/m^{2}day)
Harbor (1 km)			
Pyrene	**6200±800**		9100
Benzo[a]pyrene	**1100±200**		4000
Dibenz[a,c]anthracene	**92±16**		2500
Coastal (15 km)			
Pyrene	**2100±300**		1800
Benzo[a]pyrene	**380±60**		510
Dibenz[a,c]anthracene	**29±5**		110
Cont. Shelf (130 km)			
Pyrene	**640±100**	430	760
Benzo[a]pyrene	**10±2**	10	98
Dibenz[a,c]anthracene	**0.62±0.12**	0.49	39
Pelagic Ocean (1600 km)			
Pyrene	**38±5**		70
Benzo[a]pyrene	**0.64±0.10**		40
Dibenz[a,c]anthracene	**0.067±0.010**		not analyzed

*Length-scales in parentheses refer to distances from nearest urban PAH sources.

Figure. 1 Surface-ocean fluxes and area-integrated mass removal rates of pyrene (**a**) and benzo[a]pyrene (**b**) for four marine regimes in the western North Atlantic Ocean. Dark bars represent PAH fluxes and grey bars denote PAH sinks. The uncertainties represent one standard deviation of the propagated analytical variabilities.

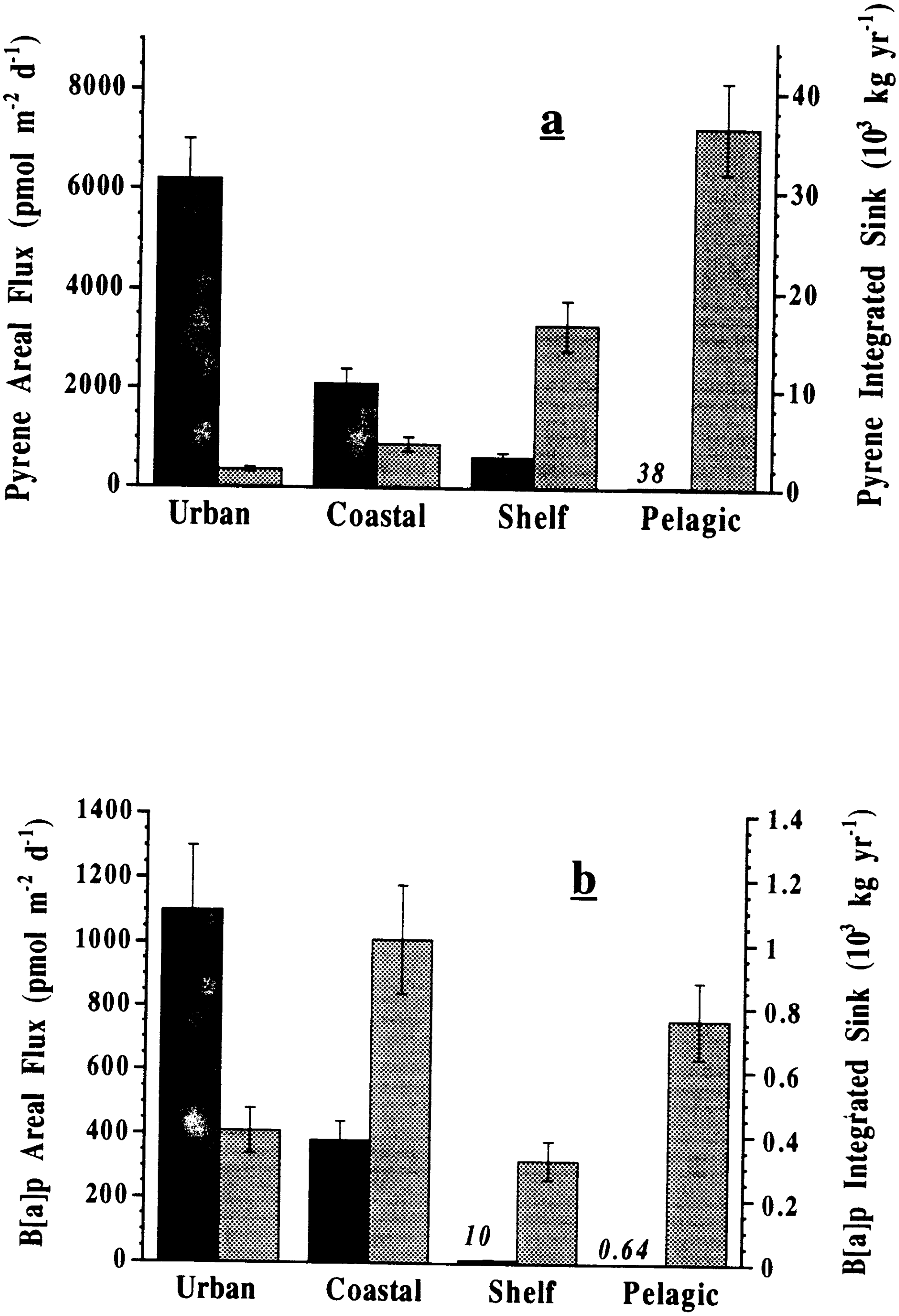
a
Pyrene Areal Flux (pmol m-2 d-1)
Pyrene Integrated Sink (103 kg yr-1)
8000
6000
4000
2000
0
40
30
20
10
0
38
Urban
Coastal
Shelf
Pelagic
b
B[a]p Areal Flux (pmol m-2 d-1)
B[a]p Integrated Sink (103 kg yr-1)
1400
1200
1000
800
600
400
200
0
1.4
1.2
1
0.8
0.6
0.4
0.2
0
10
0.64
Urban
Coastal
Shelf
Pelagic

cores, the sedimentation rates were deduced by exponentially fitting the excess ^{210}Pb profiles below the zone of bioturbation (e.g., Berner, 1980). Bottom sediment PAH accumulation fluxes for these sites were then derived by combining their sedimentation rates with core-top PAH concentrations (e.g., Gschwend and Hites, 1981). In these cores we observed no significant PAH depth gradient between the surficial and deeper sediments below the bioturbation zone, which otherwise could cause this approach to yield an underestimation of the surface sediment fluxes due to sediment mixing. In the pelagic core it was not possible to fit an excess ^{210}Pb profile due to the short half-live of ^{210}Pb compared to the slow accumulation. Following the approach of Sackett (1964), we calculated the average excess ^{210}Pb flux by multiplying the total inventory (mixed down to 3.5 cm in this core) with the mean life of ^{210}Pb (32.3 years). Pelagic sediment PAH accumulation flux was thus deduced from the relative abundance of surface layer PAH (Backhus and Gschwend, unpublished data) and excess ^{210}Pb.

Bottom sediment fluxes were within a factor of two of the Th-derived surface ocean fluxes for pyrene at all four stations (Table 2). However, larger deviations were found for the more sorptive compounds, benzo[a]pyrene (factor of 4-10) and dibenz[a,c]anthracene (factor of 4-60), at the harbor and shelf basin sites (Table 2), two stations where the sedimentary excess ^{210}Pb inventories were most enhanced relative to expected source fluxes (Gustafsson *et al.*, 1996d). The pelagic sediment flux of benzo[a]pyrene may be an overestimate as surface sediment concentrations two-to-thirtyfold times lower than ours have been reported at two nearby sites (Windsor and Hites, 1979). These results illustrate one of the limitations associated with evaluating surface ocean dynamics from bottom sediment accumulations, especially for deposits such as those on the continental shelf off northeastern USA which may be influenced by resuspension (Buesseler *et al.*, 1985/86). While we have only analyzed material from one sediment trap and thus no large conclusions can be drawn from the results, the sediment trap-derived PAH fluxes from a single (mid-shelf) station agreed remarkably well with the ^{234}Th-derived surface ocean fluxes for all three compounds (Table 2).

Combining our ocean-scale pyrene flux data with estimates from other studies, a general picture emerges for the atmospheric fallout of PAHs as a function of distance from urban centers. The pyrene fluxes observed in our study (Fig. 1) agree with previous reports of marine fluxes of pyrene at corresponding distances in the same region of the world (Table 3: Gschwend and Hites, 1981; Takada *et al.*, 1994). The rapid fall-off in fluxes that we observe over harbor, coastal, continental shelf, and open ocean distances also resembles the pattern, and absolute magnitudes, characterized in greater detail in two other regions of the ocean: the midwestern Baltic Sea (Broman *et al.*, 1988; Näf *et al.*, 1992: Table 3) and the northwestern Mediterranean Sea (e.g., Lipiatou and Saliot, 1991; Tolosa *et al.*, 1996: Table 3). In fact, we considered all ocean measurements of pyrene fluxes reported and available to us (see Table 4 for references, sites and techniques included), as a function of predominant upwind distance from nearest major urban source (Figure 2). Despite the large geographical distribution and varying techniques used to estimate the fluxes in all these studies, there appears to be considerable consistency in the pattern of oceanic PAH fluxes. This agreement suggests that the environmental dispersion processes are rather invariant and thus may lend themselves to modeling generalizations and predictions.

The spatial variation of ^{234}Th-derived surface ocean PAH fluxes is also consistent with observed bimodal size-distribution of urban aerosol PAHs (Venkataraman and Friedlander, 1994; Allen *et al.*, 1996), suggesting predominantly near-shore deposition of large particles, followed by longer-range aeolian transport and fallout of the finer combustion particles. The delivery of these dual PAH-carriers to the ocean may be expressed with a bi-exponential function:

$$F_{Pyr} = a\ e^{-bx} + c\ e^{-dx} \tag{2}$$

where F_{pyr} is the ocean flux of pyrene (pmol/m^{2}day), x is the distance (km) from the source region, and a, b, c, and d are constants. This function was fitted to our ^{234}Th-derived surface ocean pyrene flux data (Fig. 1). This fit resulted in a=6000 pmol/m^{2}day, b=0.10 km^{-1}, c=820 pmol/m^{2}day, and d=0.0019 km^{-1}. One interpretation of these length scales for PAH deposition (i.e., 7 and 400 km) is that they reflect the fates of the large and fine combustion-derived aerosols, respectively.

3.3 Residence Times of HOCs in the Surface Ocean

The coupling of HOC concentrations with ^{238}U-^{234}Th disequilibria also affords

Table 3.

Vertical pyrene fluxes in or off NE USA and in two other regions studied with high spatial sampling density.

Location of study	Ocean Pyrene Fluxes* ($pmol/m^2day$)			
and flux method	Urban	Coastal	Shelf	Pelagic
This study				
^{234}Th-derived	**6200±800**	**2100±300**	**640±100**	**38±5**
trap-derived			430	
sediment-core-derived	9100	1800	760	70
Sites off Northeastern USA (Gschwend and Hites, 1981) (sediment cores)	5000-12000		400-500	40-80
Pelagic Western North Atlantic (Takada *et al.*, 1994) (deep sediment trap)				70
Midwestern Baltic Sea (Broman *et al.*, 1988; Näf *et al.*, 1992) (shallow sediment traps)	7000-14000	1000-3000		
NW Mediterranean Sea (e.g., Lipiatou and Saliot, 1991; Tolosa *et al.*, 1996) (intermediate-deep sediment traps and cores)	7000-24000	2000-7000	200-900	20-140

*In published work where pyrene fluxes were not independently reported, the pyrene contribution of the presented "total PAH" fluxes was calculated either using the pyrene-to-"total-PAH" ratio available in the same work, or, when this was not available, assuming that pyrene was 10% of the "total PAH" (e.g., Masclet *et al.*, 1986).

Table 4.

Studies contributing pyrene flux data shown in Figure 2

Symbol	Reference	Study Region	Technique
+	Gschwend and Hites (1981)	Northeastern USA	dated cores
♦	Bates *et al.* (1984)	Puget Sound, WA	traps and dated cores
❑	Broman *et al.* (1988)	Midwestern Baltic Sea	traps
-	McVeety and Hites (1988)	Northern Lake Superior	mass balance model of air samples, dated cores
Δ	Lipiatou and Saliot (1991)	NW Mediterranean Sea	dated cores
◇	Näf *et al.* (1992)	Midwestern Baltic Sea	traps
○	Lipiatou *et al.* (1993)	NW Mediterranean Sea	traps
▲	Lipiatou and Albaigés (1994)	NW Mediterranean Sea	atmos. impactors
×	Takada *et al.* (1994)	Pelagic NW Atlantic Ocean	traps
■	Axelman *et al.* (1995)	Central Baltic Sea	dated cores
▼	Dachs *et al.* (1996)	SW. Mediterranean Sea	traps
∇	Wakeham (1996)	Western Central Black Sea	dated cores
❑	Tolosa *et al.* (1996)	NW Mediterranean Sea	dated cores
Θ	Takada *et al.* (submitted)	Honshu, Japan	atmos. impactors
●	This study	NW Atlantic Ocean	^{234}Th-coupled, traps, and dated cores

Figure 2. Literature-collated ocean pyrene fluxes as a function of upwind distance from nearest major urban source. The references of, and techniques used in, the different studies are provided in Table 4.

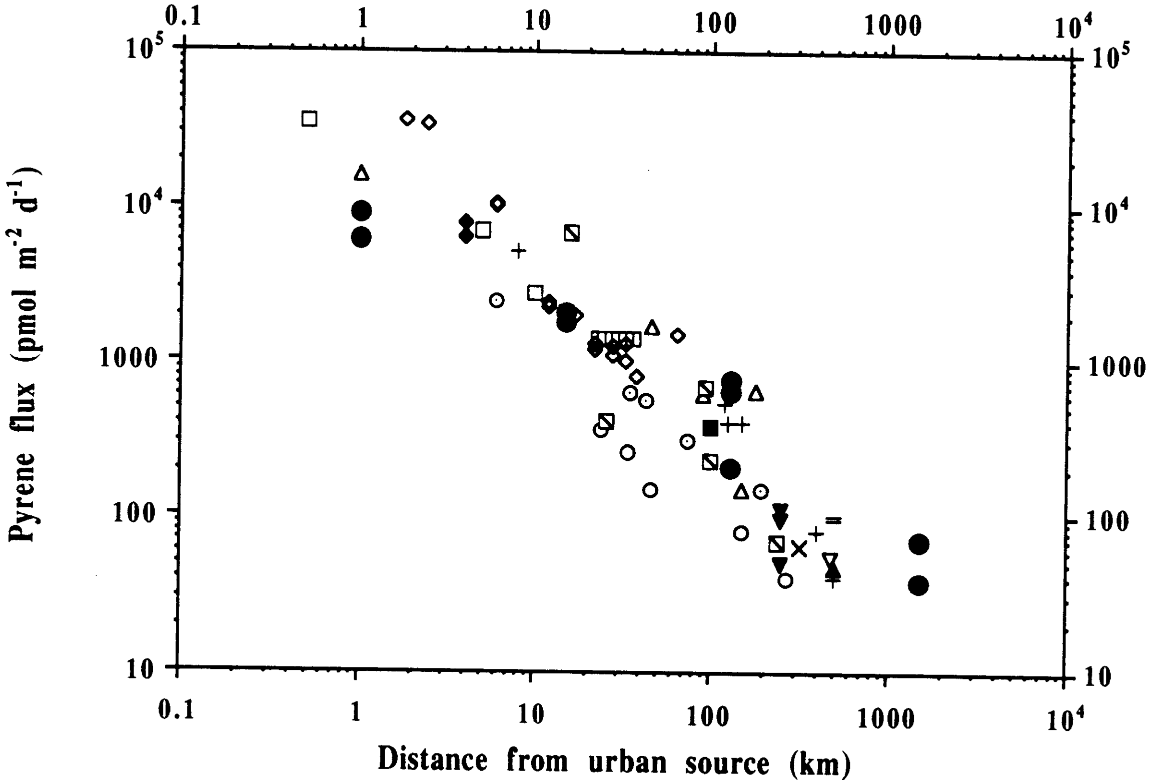
0.1
1
10
100
1000
10⁴
10⁵
10⁴
1000
100
10
Pyrene flux (pmol m⁻² d⁻¹)
Distance from urban source (km)

the possibility to estimate how long any given HOC molecule remains in the surface ocean layer. In the absence of reliable measurements of the dissolved HOC pool, the particle-seawater distribution of each compound can be estimated using POCs and K_{oc}s of individual HOCs, assuming an insignificant colloidal phase. Having measured the particulate HOC levels, and estimated their vertical removal rates, surface ocean residence times, τ, of the total concentration of individual HOCs can be derived:

$$\tau = \frac{[\mathrm{HOC}]_{tot}}{F_{HOC}/z_{mix}} = \frac{z_{mix}\,[{}^{234}\mathrm{Th}]_{part}}{F_{Th}} \frac{\mathrm{POC}\cdot K_{oc}}{1 + \mathrm{POC}\cdot K_{oc}} \tag{3}$$

where the first term on the right-hand side reflects the time-scale for the environment-specific process of particle sedimentation, as traced by ^{238}U-^{234}Th. This process has a characteristic time of days in near-coastal waters and weeks in pelagic regimes. The surface ocean residence times of HOCs are further affected by the second term on the right-hand-side of Eqn. 3, the molecule-specific fraction of its total concentration that is in the particulate pool. Combining these two specific terms to estimate surface ocean residence times of HOCs suggests that compounds with K_{oc}'s around 10^5 exhibit lifetimes of a few years in coastal surface waters (POC 0.1-0.2 mg/L) with respect to sedimentation. However, HOCs with K_{oc}'s around 10^6 may be expected to be removed on settling particles in about one month in coastal surface waters. In contrast, the same HOCs may remain in the upper pelagic ocean (POC $\approx$ 0.03 mg/L) for about a year, unless they are removed by other degradation mechanisms.

3.4 Global PAH Mass Balances

The largest limitation to developing a global mass balance of PAHs is the lack of knowledge regarding oceanic fluxes (NRC, 1985; Simonich and Hites, 1994). Our flux results provide an opportunity to estimate the magnitude of the surface ocean PAH sink in the northwestern Atlantic Ocean. Since transport on oceanic scales is considered here, the entire US northeast is treated as a line source (length of coastline is 1600 km). For the sink-estimates, the area of the near-source depositional region (5 x 10^3 km^2), harbors and urban waters, was estimated using a 3 km characteristic width based on the PAH fall-out pattern studied in detail along the Swedish east-coast (Broman *et al.*, 1988; Näf *et al.*, 1992). The next characteristic regime of PAH influence, the coastal region (3 x 10^4 km^2), was estimated similarly as extending to approximately 20 km away from the continental source (above references and Table 2). The area of the remaining northeastern US continental shelf was taken as 3.5 x 10^5 km^2 from published estimates (Buesseler *et al.*, 1985/86). The portion of the pelagic North Atlantic assumed to be influenced by emissions from USA was modeled as a sector of a circle with an angle of 160° and a radius of 3000 km (half-way across to Europe). This pelagic sector, in which our station BATS is at a representative central location, has an area of 1.3 x 10^7 km^2. While the PAH flux per area is several orders of magnitude larger in urban and coastal waters, the area-integrated total inputs to the continental shelf, and especially to the vast expanses of this portion of the open ocean, constitute equal or larger sinks than the localized PAH sequestration in the vicinity of the continental source region (Fig. 1). Based on these ^{234}Th-derived PAH fluxes, we estimate that 60 metric-ton/yr pyrene and 3 metric-ton/yr benzo[a]pyrene are entering the western portion of the North Atlantic from continental USA. Since there is an even distribution of pyrene and benzo[a]pyrene between fine and coarse particles (Allen *et al.*, 1996), the more rapid decrease in benzo[a]pyrene ocean fluxes with distance compared to pyrene is consistent with its higher lability towards photochemical and other oxidative transformations during atmospheric transport (Butler and Crossley, 1981; Masclet *et al.*, 1986; Pitts Jr. *et al.*, 1986). Based on the geographical flux pattern and the source-diagnostic molecular ratios, we believe that atmospheric deposition of combustion-derived PAHs from the eastern USA is the major source of PAHs to this region of the world ocean.

These PAH sink determinations, based on our direct measurements, may be contrasted to estimates of pyrene and benzo[a]pyrene inputs to the world ocean from petroleum discharges (National Research Council, 1985). Multiplying the NRC estimates of various global petroleum hydrocarbon discharge rates by the pyrene and benzo[a]pyrene content of crude and distilled petroleum listed in the same report (4.4 and 32 ppm for pyrene and 2.0 and 0.6 ppm for benzo[a]pyrene, in crude and distilled petroleum, respectively), one may estimate the PAH ocean input from offshore operations, marine transportation, natural seeps, and municipal-plus-industrial waste discharges (Figure 3). Our ^{234}Th-deduced input estimates of combustion-derived pyrene and benzo[a]pyrene to the North Atlantic is larger than any of their previously estimated sources to the entire global ocean. Simonich and Hites (1994) have developed a mass-

Figure 3. Comparison of our receptor-based estimates of total pyrene (a) and benzo[a]pyrene (b) import to NW Atlantic Ocean with source-based estimates of fossil-fuel derived inputs to the entire global ocean.

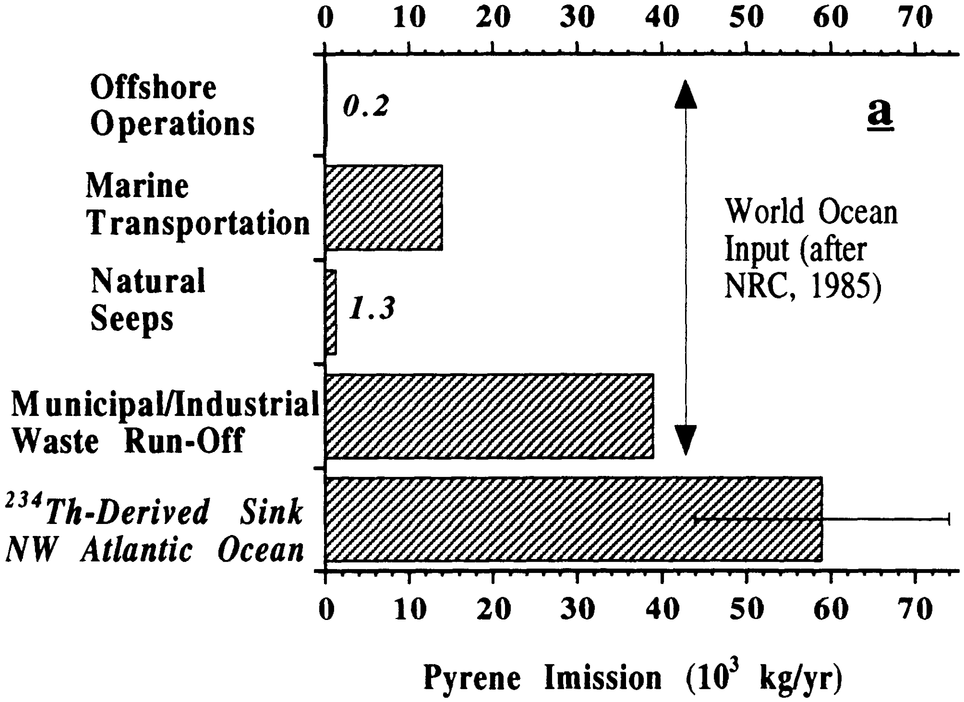
0 10 20 30 40 50 60 70
Offshore Operations
0.2
Marine Transportation
Natural Seeps
1.3
Municipal/Industrial Waste Run-Off
234Th-Derived Sink NW Atlantic Ocean
World Ocean Input (after NRC, 1985)
a
Pyrene Imission (10^3 kg/yr)

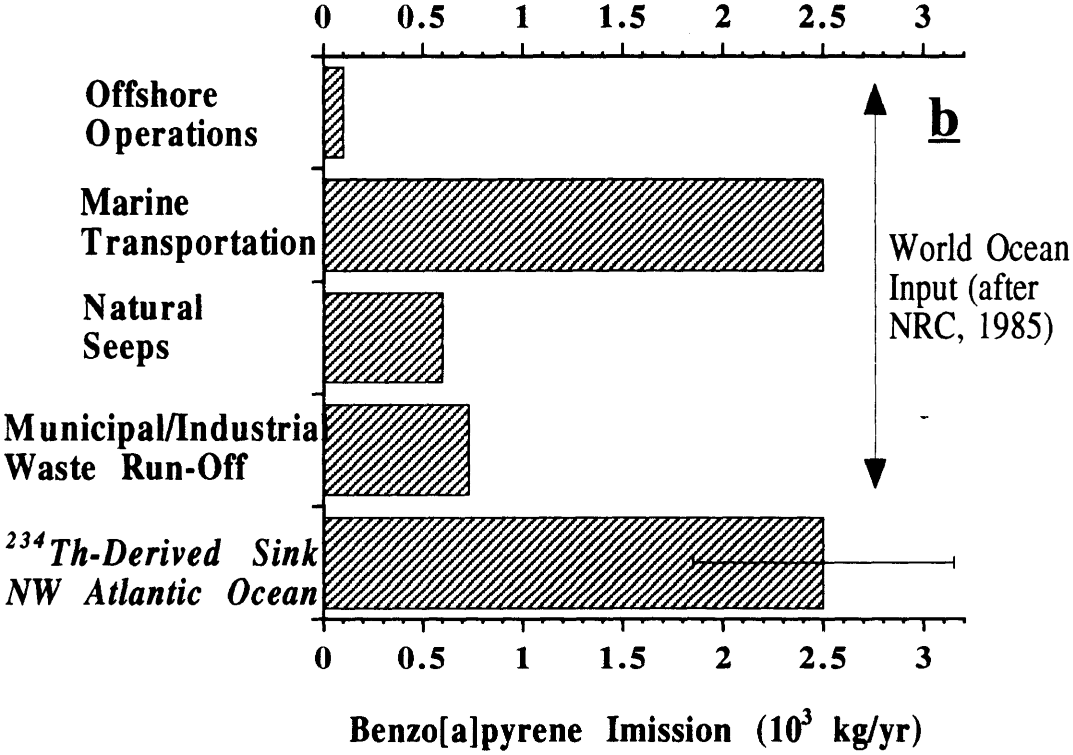
0 0.5 1 1.5 2 2.5 3
Offshore Operations
Marine Transportation
Natural Seeps
Municipal/Industria Waste Run-Off
234Th-Derived Sink NW Atlantic Ocean
World Ocean Input (after NRC, 1985)
b
Benzo[a]pyrene Imission (10^3 kg/yr)

balance for pyrene and other PAHs for the northeastern continental USA. They found that 40% of the total combustion-derived pyrene (160 metric-ton/yr) had an uncertain fate. The ocean PAH sink identified here can account for almost half of these "missing PAHs", with a significant portion of the remainder likely transformed either in the atmosphere or transported further offshore.

4. Conclusions

We have demonstrated the utility of coupling particulate HOC inventories with the surface ocean ^{234}Th deficit to derive direct estimates of surface ocean fluxes and residence times of these anthropogenic compounds. Our results suggest that the ocean is an important sink for one group of continentally-derived HOCs, the polycyclic aromatic hydrocarbons (PAHs), and this may also prove true for other HOCs as well. Our direct measurements of the composition and fluxes of PAHs through the surface ocean indicate that these first estimates of the total ocean flux of PAHs are much larger than what we could calculate from petrogenic sources. The dominant source of oceanic PAHs is very likely continental fuel combustion. These findings constitute a major advance in our understanding of the world ocean PAH budget and serve to guide international efforts to improve the health of the global oceans (NRC, 1985; GESAMP, 1993; UNEP, 1995). There is a large need for receptor-based ocean flux measurements of persistent organic pollutants to assess the importance of their oceanic sink. The thorium-coupled flux approach introduced here facilitates the development of global-scale mass-balance models of many such hydrophobic contaminants.

Acknowledgments

We appreciate the support of the crews and captains of R/V ARGO MAINE and R/V WEATHERBIRD. We gratefully acknowledge D. Backhus and G. Benoit for PAH and ^{210}Pb data from the pelagic core, J. Greenamoyer and B. Moran for ^{234}Th sampling, C. Pilskaln for a sediment trap subsample and unpublished sediment trap total particulate mass data, as well as J. MacFarlane, C. Long, C. Swartz, and J. Andrews for cruise participation. H. Takada is thanked for contributing a pre-publication data set to Fig. 2. J. Farrington and C. Cavanaugh provided enlightening discussions of an earlier draft of this paper. This study was funded by the US Office of Naval Research Contract No. NOOO14-93-1-0883 and the National Oceanic and Atmospheric Administration Contract No. NA36RM044-UM-S242. The sediment trap sample was provided through NOAA contract NA46RM0451 to C. Pilskaln. The views expressed herein are those of the authors and do not necessarily reflect the views of NOAA or any of its subagencies. This is contribution #XXXX from the Woods Hole Oceanographic Institution.

References

Alldredge, A. L. and Silver, M. W. 1988. Characteristics, dynamics and significance of marine snow. Prog. Oceanogr., 20: 41-82.

Allen, J. O., Dokeran, N. M., Smith, K. A., Sarofim, A. F., Taghizadeh, K. and Lafleur, A. L., 1996. Measurement of polycyclic aromatic hydrocarbons associated with size-segregated atmospheric aerosols in Massachusetts. Environ. Sci. Technol., 30: 1023-1031.

Axelman, J., Bandh, C., Broman, D., Carman, R., Jonsson, P., Larsson, H., Linder, H., Näf, C. and Pettersen, H., 1995. Time-trend analysis of PAH and PCB sediment fluxes in the Northern Baltic Proper using different dating methods. Mar. Freshwater Res., 46: 137-144.

Bates, T. S., Hamilton, S. E. and Cline, J. D., 1984. vertical transport and sedimentation of hydrocarbons in the central main basin of Puget Sound, Washington.. Environ. Sci. Technol., 18: 299-305.

Bhat, S. G., Lal, D., Rama and W. S. Moore., 1969. ^{234}Th/^{238}U ratios in the ocean. Earth Planet. Sci. Lett., 5: 483-491.

Broman, D., Colmsjö, A., Ganning, B. Näf, C. and Zebühr, Y., 1988. A multi-sediment-trap study on the temporal and spatial variability of polycyclic aromatic hydrocarbons and lead in an anthropogenic influenced archipelago. Environ. Sci. Technol., 22: 1219-1228.

Broman, D., Näf, C., Wik, M. and Renberg, I., 1990. The importance of spheroidal carbonaceous particles (SCPs) for the distribution of particulate polycyclic aromatic hydrocarbons (PAHs) in an estuarine-like urban coastal water area. Chemosphere, 21: 69-77.

Buesseler, K. O., Livingston, H. D. and Sholkovitz, E. R., 1985/86. ^{239,240}Pu and ^{210}Pb inventories along the shelf and slope of the northeast U.S.A. Earth Planet. Sci. Lett., 76: 10-22.

Buesseler, K. O., Cochran, J. K., Bacon, M. P., Livingston, H. D., Casso, . A., Hirschberg, D., Hartman, M. C. and Fleer, A. P., 1992b. Determination of thorium isotopes in seawater by non-destructive and radiochemical procedures. Deep-Sea Res. I., 39: 1103-1114.

Buesseler, K. O., Bacon, M. P., Cochran, J. K. and Livingston, H. D., 1992a. Carbon and nitrogen export during the JGOFS North Atlantic Bloom Experiment estimated from ^{234}Th:^{238}U.disequilibria. Deep-Sea Res. I., 39: 1115-1137.

Buesseler, K. O., Michaels, A. F., Siegel, D. A. and Knap, A. H., 1994. A three dimensional time-dependent approach to calibrating sediment trap fluxes. Global Biogeochem. Cycles, 8: 179-193.

Burns, K. A. and Villeneuve, J.-P., 1985. Biogeochemical processes affecting the distribution and vertical transport of hydrocarbon residues in the coastal Mediterranean. Geochim. Cosmochim. Acta, 47: 995-1006.

Butler, J. D. and Crossley, P., 1981. Reactivity of polycyclic aromatic hydrocarbons adsorbed on soot particles. Atmos. Envir., 15: 91-94.

Chen, J. H., Edwards, R. L. and Wasserburg, G. J., 1986. ^{238}U, ^{234}U, ^{232}Th in seawater. Earth Planet. Sci. Lett., 80: 241-251.

Dachs, J., Bayona, J. M., Fowler, S. W., Miquel, J.-C. and Albaigés, J., 1996. Vertical fluxes of polycyclic aromatic hydrocarbons and organochlorine compounds in the western Alboran Sea (southwestern Mediterranean). Mar. Chem., 52: 75-86.

Durant, J. L., Thilly, W. G., Hemond, H. F. and LaFleur, A. L., 1994. Identification of the principal human cell mutagen in an organic extract of a mutagenic sediment. Environ. Sci. Technol., 28: 2033-2044.

EPA, 1985. Evaluation and Estimation of Potential Carcinogenic Risks of Polynuclear Aromatic Hydrocarbons. Office of Health and Environmental Assessment, Office of Research and Development, US Environmental Protection Agency, Washington, DC.

EPA, 1993. Sediment Quality Criteria for the Protection of Benthic Organisms: Fluoranthene; EPA 822-R-93-012; Offices of Water, Research, and Development and, Science and Technology; U.S. Environmental Protection Agency, Washington, DC.

Farley, K. J. and Morel, F. M. M. 1986. Role of coagulation in the kinetics of sedimentation. Environ. Sci. Technol., 20: 187-195.

Fowler, S. W. and Knauer, G. A., 1986. Role of large particles in the transport of elements and organic compounds through the oceanic water column. Prog. Oceanogr., 16: 147-194.

GESAMP, 1993. Impact of Oil and and Related Chemicals and Wastes on the Marine Environment Rep. Stud. Vol. 50, IMO/FAO/UNESCO/WMO/IAEA/UNEP Joint Group of Experts on the Scientific Aspects of Marine Pollution: New York, 180 pp.

Greenamoyer, J. and Moran, S. B., 1996. Evaluation of a spiral wound cross-flow filtration system for size-fractionation of Cu, Ni, and Cd in seawater. Mar. Chem., in press.

Gschwend, P. M. and Hites, R. A., 1981. Fluxes of polycyclic aromatic hydrocarbons to marine and lacustrine sediments in the northeastern United States. Geochim. Cosmochim. Acta, 45, 2359-2367.

Gustafsson, Ö., Haghseta, F., Chan, C., MacFarlane, J. and Gschwend, P. M., 1996a. Quantification of the dilute sedimentary "soot-phase": Implications for PAH speciation and bioavailability. Environ. Sci. Technol., accepted.

Gustafsson Ö. and Gschwend, P. M., 1996b. Soot as a strong partition medium for polycyclic aromatic hydrocarbons, submitted.

Gustafsson, Ö., Buesseler, K. O. and Gschwend, P. M., 1996c. On the integrity of cross-flow filtration for collecting marine organic colloids. Mar. Chem., in press.

Gustafsson, Ö., Buesseler, K. O., Geyer, W. R., Moran, S. B. and Gschwend, P. M., 1996d. On the relative importance of horizontal and vertical transport of particle-reactive chemicals in the coastal ocean: Two-dimensional Th-234 modeling., submitted.

Harvey, G. R., Steinhauer, W. G.and Teal, J. M., 1973. Polychlorobiphenyls in North Atlantic Ocean water. Science, 180: 643-644.

Harvey, G. R., and Steinhauer, W. G., 1976. Transport pathways of polychlorinated biphenyls in Atlantic water. J. Mar. Res., 34: 561-575.

Honjo, S. and Doherty, K. W., 1988. Large aperture time-series sediment traps; design objectives, construction and application. Deep-Sea Res., 35: 135-149.

Iwata, H., Tanabe, S, Sakai, N. and Tatsukawa, R., 1993. Distribution of persistent organochlorines in tehj oceanic air and surface seawater and the role of ocean on their global transport and fate. Environ. Sci. Technol., 27: 1080-1098.

Knap, A. H., Binkley, K. S. and Deuser, W. G., 1986. Synthetic organic chemicals in the deep Sargasso Sea. Nature, 319: 572-574.

Lipiatou, E. and Saliot, A., 1991. Fluxes and transport of anthropogenic and natural polycyclic aromatic hydrocarbons in the western Mediterranean Sea. Mar. Chem., 32: 51-71.

Lipiatou, E., Marty, J. -C. and Saliot, 1993. Sediment trap fluxes of polycyclic aromatic hydrocarbons in the Mediterranean Sea. Mar. Chem., 44: 43-54.

Lipiatou, E. and Albaigés, J., 1994. Atmospheric deposition of hydrophobic organic chemicals in the northwestern Mediterranean Sea: comparison with the Rhone river input. Mar. Chem., 46: 153-164.

Masclet, P., Mouvier, G. and Nikolaou, K., 1986. Relative decay index and sources of polycyclic aromatic hydrocarbons. Atmos. Envir., 20: 439-446.

McVeety, B. D. and Hites, R. A., 1988. Atmospheric deposition of polycyclic aromatic hydrocarbons to water surfaces: A mass balance approach. Atmos. Environ., 22: 511-536.

Means, J. C., 1995. Influence of salinity upon sediment-water partitioning of aromatic hydrocarbons. Mar. Chem., 51: 3-16.

Moran, S. B. and Buesseler , K. O., 1992. Short residence time of colloids in the upper ocean estimated from ^{238}U-^{234}Th disequilibira. Nature, 359: 221-223.

Moran, S. B. and Buesseler , K. O., 1993. Size-fractionated ^{234}Th in continental shelf waters off New England: Implications for the role of colloids in oceanic trace metal scavenging. J. Mar. Res., 51: 893-922.

Näf, C., Broman, D. Pettersen, H., Rolff, C. and Zebühr, Y. 1992. Flux estimates and pattern recognition of particulate polycyclic aromatic hydrocarbons, polychlorinated dibenzo-p-dioxins, and dibenzofurans in the waters outside various emission sources on the Swedish Baltic coast. Environ. Sci. Technol., 26: 1444-1457.

NRC, 1985. Oil in the Sea: Inputs, Fates, and Effects. National Research Council, Washington, DC.

Pitts Jr, J. N., Paur, H.-R., Zielinska, B., Arey, J., Winer, A. M., Ramdahl, T. and Meija, V., 1986. Factors influencing the reactivity of polycyclic aromatic hydrocarbons adsorbed on filters and ambient POM with ozone. Chemosphere 15: 675-685.

Sackett, W. M. 1964. Measured deposition rates of marine sediments and implications for accumulation rates of extraterrestrial dust. Annals of the New York Acad. Sci., 119: 339-346.

Schwarzenbach, R. P., Gschwend, P. M. and Imboden, D. M. 1993. Environmental Organic Chemistry. Wiley, New York, 681 pp.

Simonich, S. L. and Hites, R. A., 1994. Importance of vegetation in removing polycyclic aromatic hydrocarbons from the atmosphere. Nature, 370: 49-51.

Simonich, S. L. and Hites, R. A., 1995. Global distribution of persistent organochlorine compounds. Science, 269: 1851-1854.

Sporstøl, S., Gjøs, N., Lichtenthaler, R. G., Gustavsen, K. O., Urdal, K., Oreld, F. and Skei, J., 1983. Source identification of aromatic hydrocarbons in sediments using GC/MS. Environ. Sci. Technol., 17: 282-286.

Stolzenbach, K. D. 1993. Scavenging of small particles by fast-sinking porous aggregates. Deep-Sea Res. I, 40: 359-369.

Takada, H. and Ishiwatari, R., 1985. Quantitation of long-chain alkylbenzenes in environmental samples by silica gel column chromatography and high-resolution gas chromatography. J. Chromatogr., 346: 281-290.

Takada, H., Farrington, J. W., Bothner, M. H., Johnson, C. G. and Tripp, B. W., 1994. Transport of sludge-derived organic pollutants to deep-sea sediments at Deep Water Dump Site 106. Environ. Sci. Technol., 28: 1062-1072.

Takada, H., Harada, M., Midzuno, Y., Miyake, M. and Ogura, N., 1996. Atmospheric deposition of polycyclic aromatic hydrocarbons (PAHs) in Tokyo., submitted.

Tanabe, S. and Tatsukawa, R., 1983. Vertical transport and residence time of chlorinated hydrocarbons in the open ocean water column. J. Oceanogr. Soc. Japan, 39: 53-62.

Tolosa, I., Bayona, J. M. and J. Albaigés, 1996. Aliphatic and polycyclic aromatic hydrocarbons and sulfur/oxygen derivatives in Northwestern Mediterranean sediments: Spatial, and temporal variability, fluxes, and budgets. Environ. Sci. Technol., 30: 2495-2503.

Turner, , D. R., Whitfield, M. and Dickson, A. G., 1981. The equilibrium speciation of dissolved components in freshwater and seawater at 25°C and 1 atm pressure. Geochim. Cosmochim. Acta, 45: 855-881.

UNEP, 1995. Washington Declaration on Protection of the Marine Environment from Land-Based Activities. United Nations Environment Programme: Washington, DC.

Venkataraman, C. and Friedlander, S. K., 1994. Size distribution of polycyclic aromatic hydrocarbons and elemental carbon. 2. Ambient measurements and effects of atmospheric processes. Environ. Sci. Technol., 28: 563-572.

Wania, F. and Mackay, D., 1995. A global distribution model for persistent organic chemicals. Sci. Total Environ., 161/161: 211-232.

Wania, F. and Mackay, D., 1996. Tracking the distribution of persistent organic pollutants. Environ Sci. Technol., 30: 390A-396A.

Wakeham, S. G., 1996. Aliphatic and polycyclic aromatic hydrocarbons in Black Sea sediments. Mar. Chem., 53: 187-205.

Windsor, J. G. and Hites, R. A., 1979. Polycyclic aromatic hydrocarbons in Gulf of Maine sediments and Nova Scotia soils. Geochim. Cosmochim. Acta, 43: 27-33.

Woodwell, G. M., Craig, P. P. and Johnson, H. A., 1971. DDT in the biosphere: Where does it go? Science, 174: 1101-1107.

Youngblood, W. M. and Blumer, M. 1975. Polycyclic aromatic hydrocarbons in the environment: homologous series in soils and recent marine sediments. Geochim. Cosmochim. Acta, 39: 1303-1314.

Chapter 8

On the Relative Importance of Horizontal and Vertical Transport of Particle-Reactive Chemicals in the Coastal Ocean: Two-Dimensional Th-234 Modeling

Örjan Gustafsson[1,2], Ken O. Buesseler[2], W. Rockwell Geyer[3], S. Bradley Moran[4], and Philip M. Gschwend[1*]

[1]Ralph. M. Parsons Laboratory, MIT 48-415, Department of Civil and Environmental Engineering, Massachusetts Institute of Technology, Cambridge, MA 02139. *Address correspondence to this author.
[2]Department of Marine Chemistry and Geochemistry, Woods Hole Oceanographic Institution, Woods Hole, MA 02543.
[3]Department of Applied Ocean Physics and Engineering, Woods Hole Oceanographic Institution, Woods Hole, MA 02543.
[4]Graduate School of Oceanography, University of Rhode Island, Narragansett, RI, 02882

submitted
Continental Shelf Research

ABSTRACT

Using horizontal distributions of ^{238}U-^{234}Th disequilibrium data, "particle-reactive" chemicals in coastal waters were shown to be significantly affected by both horizontal transport and vertical scavenging processes. During an intense scavenging episode in September 1993 (> 95 % ^{238}U-^{234}Th disequilibria), vertical scavenging was more important than horizontal transport in both Inner and Outer Casco Bay, Gulf of Maine. However, in May 1994, several-fold higher ^{234}Th activities, more typical of normal coastal scavenging conditions, were measured. At this time, the two-dimensional model treatment of the data suggested that onshore horizontal dispersion of ^{234}Th was substantial. Recognition of this horizontal flux required us to increase the net vertical scavenging flux in Inner Casco Bay by a factor of three over that obtained based only on the local ^{238}U-^{234}Th disequilibrium.

The radionuclide (^{210}Pb$_{xs}$, ^{234}Th$_{xs}$, ^{7}Be) record of the underlying sediments provided supporting evidence for horizontal transport of chemicals. The highest sedimentary inventories for all three radionuclides were found at the stations nearest to the coast. As anticipated from their relative particle-affinities, the "regional boundary-scavenging" indicator ^{7}Be/^{234}Th$_{xs}$ was highest at the coastal boundary.

The two-dimensional transport model was also applied to assess the distributional fate of polycyclic aromatic hydrocarbons (PAHs) in Casco Bay. Our results suggest that less than half of the pyrene and benzo[a]pyrene introduced to Portland Harbor, ME may be settling locally and that horizontal export to offshore locations is as important. Insights from this coupled transport model also helped elucidate PAH speciation and constrained the magnitudes of other PAH cycling processes.

1. INTRODUCTION

The transport of chemicals in the coastal ocean is determined both by complex coastal circulation and the compound-specific extent of vertical scavenging. In particular, many chemicals of environmental concern have a high affinity for particles (e.g., Cu, Pu, Hg, As, polychlorinated biphenyls (PCBs) and dioxins (PCDDs), polycyclic aromatic hydrocarbons (PAHs), and organochlorine pesticides). As a consequence, their fate is affected by particle-mediated transport. Geochemists, studying these chemical scavenging processes, make extensive use of the natural radionuclide ^{234}Th (e.g., Bhat *et al.*, 1969; Santschi *et al.*, 1979, 1980; Minagawa and Tsunogai, 1980; Bacon and Anderson, 1982; McKee *et al.*, 1984, 1986; Coale and Bruland, 1985, 1987; Baskaran *et al.*, 1992; Wei and Murray, 1992; Moran and Buesseler, 1992, 1993; Buesseler *et al.*, 1992a, 1995; Huh and Prahl, 1995). The use of ^{234}Th as a scavenging tracer depends on its very high particle affinity (e.g., Turner *et al.*, 1981), relative ease of analysis (Buesseler *et al.*, 1992b), well-constrained source function (produced by the conservatively dispersed ^{238}U) and suitable half-life ($t_{1/2}$= 24.1 d), making it possible to derive particle-scavenging rates acting on timescales of days to months. A one-dimensional vertical ^{234}Th scavenging model has commonly been applied to derive vertical Th removal rates:

$$\frac{\partial[^{234}\mathrm{Th}]_{\mathrm{tot}}}{\partial t} = \lambda[^{238}\mathrm{U}]_{\mathrm{tot}} - \lambda[^{234}\mathrm{Th}]_{\mathrm{tot}} - F_{\mathrm{Th}} \qquad (1)$$

where $[^{234}\mathrm{Th}]_{\mathrm{tot}}$ and $[^{238}\mathrm{U}]_{\mathrm{tot}}$ are the total ^{234}Th and ^{238}U activities (dpm kg^{-1}), respectively, λ is the decay constant of ^{234}Th (0.0288 d^{-1}), and F_{Th} (dpm kg^{-1}d^{-1}) represents the vertical scavenging flux. Assuming a steady-state and that horizontal advection and dispersion are negligible, estimates of the downward removal fluxes may be obtained. The assumption of steady-state has been shown to be reasonable based on monthly sampling at two coastal locations throughout an annual cycle (Wei and Murray, 1992; Moran and Buesseler, 1993). However, a non-steady-state treatment has been required to model short-term variations in ^{234}Th during phytoplankton blooms in both coastal (Tanaka *et al.*, 1983) and pelagic regimes (Buesseler *et al.*, 1992a).

Despite the large number of ^{234}Th studies in coastal regimes (e.g., Bhat *et al.*, 1969; Santschi *et al.*, 1979; Minagawa and Tsunogai, 1980; Tanaka *et al.*, 1983; McKee *et al.*, 1984, 1986; Coale and Bruland, 1985; Huh and Beasley, 1987; Wei and Murray, 1992; Baskaran and Santschi, 1993; Moran and Buesseler, 1993; Niven *et al.*, 1995), little effort has been directed to assessing the influence of horizontal transport on the ^{234}Th activity balance (i.e., Eqn. 1). In the two studies where the assumption of negligible horizontal transport has been tested in coastal regimes, the model-predicted vertical ^{234}Th fluxes have not been well-matched by bottom sediment inventories (McKee *et al.*, 1984) and sediment trap fluxes (Wei and Murray, 1992). McKee and co-workers, recognizing that horizontal transport was dominating the ^{234}Th budget on the Yangtze shelf, calculated from their water column and surface sediment data how large a net horizontal advective transport term would be required to balance the discrepancy in the vertical fluxes. Their calculations suggest that the horizontal flux was as large as the vertical scavenging flux at this site. Wei and Murray (1992) found that the model-predicted ^{234}Th flux (Eqn. 1), which neglected horizontal transport, was a factor of two greater than the sediment-trap measured flux in Dabob Bay. They suggested that this may be due to horizontal (boundary) scavenging. Since few chemicals have a scavenging propensity comparable to that of the highly particle-reactive ^{234}Th (e.g., Jannasch *et al.*, 1988 for trace metals; Schwarzenbach *et al.*, 1993 for organic contaminants), it may be anticipated that horizontal transport plays an even larger role in the coastal transport of less particle-reactive chemicals.

The objective of our study was to evaluate the need to consider horizontal transport processes for ^{234}Th, and by inference, for other particle-reactive constituents in coastal settings. Including horizontal transport along the offshore axis (x), the ^{234}Th mass balance of Equation 1 instead takes the form:

$$\frac{\partial[^{234}\mathrm{Th}]_{tot}}{\partial t} = \lambda\,[^{238}\mathrm{U}]_{tot} - \lambda\,[^{234}\mathrm{Th}]_{tot} - F_{Th} + \frac{\partial}{\partial x}K_x\frac{\partial[^{234}\mathrm{Th}]_{tot}}{\partial x} - u_{net}\frac{\partial[^{234}\mathrm{Th}]_{tot}}{\partial x} \qquad (2)$$

where K_x is the horizontal dispersion coefficient and u_{net} is the net offshore advection.

A two-dimensional ^{234}Th mass balance model was applied to ^{234}Th data obtained at locations in the Casco Bay region of the Gulf of Maine (Figure 1). Horizontal chemical transport was anticipated in this region since previous work has shown significant tidal flushing in Casco Bay (Parker, 1982), as well as large concentration gradients of organic contaminants both in sediments (Kennicutt *et al.*, 1994) and in the water column (Gustafsson *et al.*, 1996a). Here, we estimate the magnitudes of the transport parameters from salinity and high-resolution current data and scaling arguments applied to a physically similar site. We applied the two-dimensional model to data obtained at two different occasions, differing greatly with regard to weather. We also evaluated the underlying sedimentary isotope record for indications of horizontal transport. Finally, we applied our results to interpret the distributional fate of two PAHs, representative of hydrophobic contaminants.

2. MATERIALS AND METHODS

a. Sampling

Surface seawater and bottom sediment samples were collected on two cruises on the Gulf of Maine aboard the *R/V Argo Maine*. During gale-force winds in September 1993, stations 2, 3, 4, and 5 located in the Casco Bay region were occupied (Figure 1) and efforts were focused on water column processes. From May 1994, we report radionuclide results from stations 2, 4, and a station 1, located 130 km offshore in Wilkinson Basin. On this calm-weather cruise, surface water sampling was complemented at each station by sediment box coring.

A FloJet Duplex diaphragm pump was used to pump surface seawater (20-30 L) from a depth of 5 m through acid-cleaned, Bev-a-line tubing and through either 1 μm Microquartz (MQ) filters (September 1993) or 1 μm Whatman Capsule filters (May 1994). The filtrates were passed through two in-line polypropylene adsorbers impregnated with amorphous MnO_2 prepared following Buesseler *et al.* (1992b). ^{238}U samples were collected in polyethylene bottles directly from the Bev-a-line intake line (total) and from the retentate and permeate solutions of a downstream cross-flow filtration system described in Greenamoyer and Moran (1996). Standard hydrographic data were collected with the ship's CTD. The CTD-salinity was calibrated with independent samples collected in glass salinity bottles, stored at room temperature, and analyzed at WHOI with a salinometer (Guildline Autosal 8400A) calibrated with IAPSO Standard Sea Water.

Figure 1. Map showing sampling stations occupied during fall 1993 and spring 1994 in the Casco Bay region of the Gulf of Maine. The boundaries (bold arcs) used in the model treatment of ^{234}Th and PAH exchange, separate Inner, Outer, and Off Casco Bay, and are based on the topographic and hydrographic features (see text).

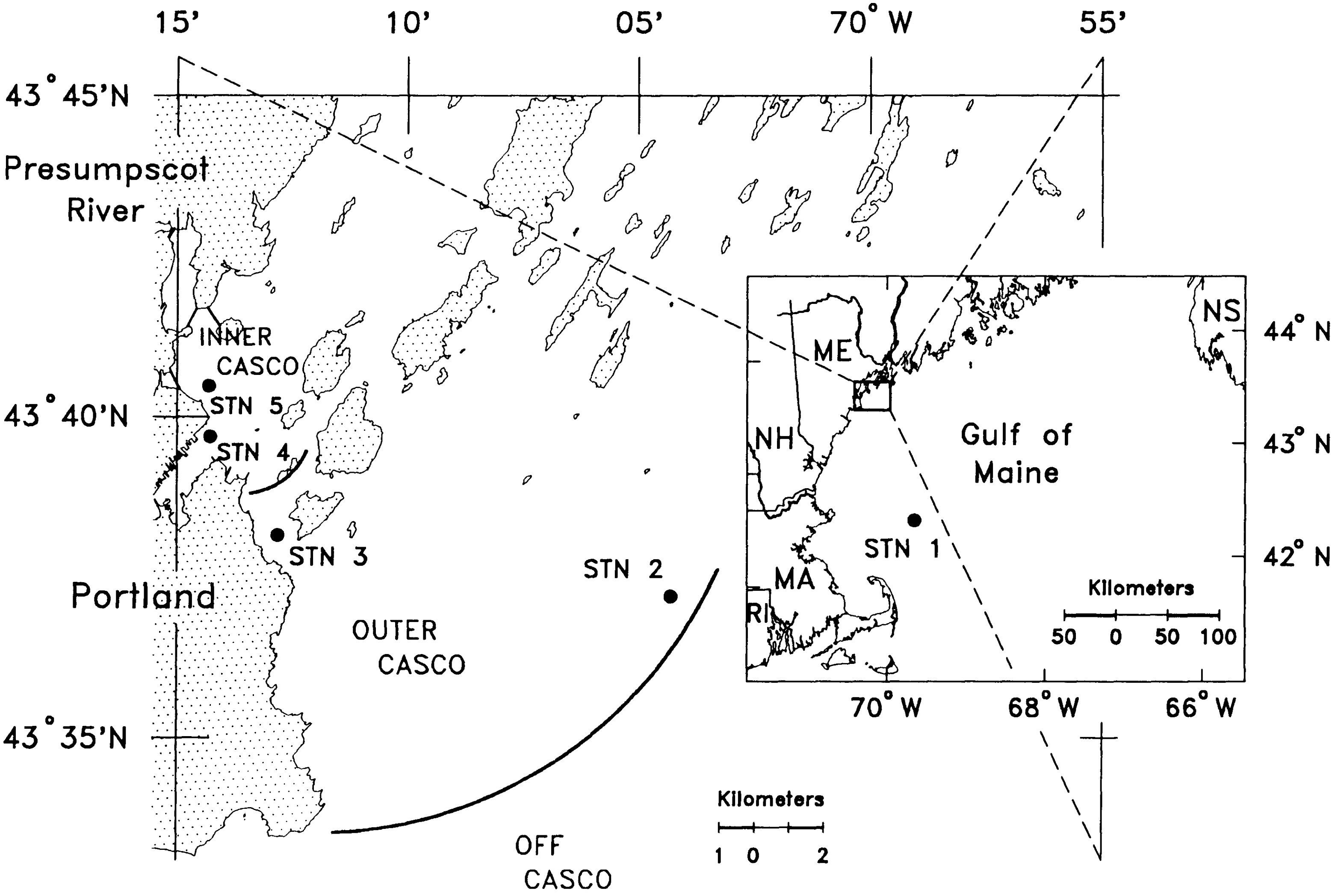
15'
10'
05'
70° W
55'
43° 45'N
Presumpscot River
INNER CASCO
STN 5
43° 40'N
STN 4
STN 3
Portland
STN 2
OUTER CASCO
43° 35'N
OFF CASCO
Kilometers
1 0 2
ME
NS
44° N
NH
43° N
Gulf of Maine
STN 1
42° N
MA
RI
Kilometers
50 0 50 100
70° W
68° W
66° W

Sediment cores were obtained with a Sandia-Hessler MK-III (Oceanic Instruments, San Diego, CA) corer with a 0.25 m^2 by 0.7 m deep box. The water overlying the sediment was siphoned off immediately after retrieval to the deck, and subsamples were collected only from cores with apparent undisturbed sediment-water interface. We used acrylic liners (ca. 13 cm diameter) to extract three separate sub-cores for radionuclides and organic compound analyses, as well as for archiving. The sub-cores were immediately extruded and trimmed on board and sections for radionuclide analysis were placed in acid-leached plastic jars.

b. Seawater ^{234}Th determination

The Whatman cartridge filters and MnO_2 adsorbers were combusted at 500°C for 12 h. To these ashed samples, and also to the MQ filters, were added approximately 75 mL 8M HNO_3 and a weighed quantity of ^{230}Th yield monitor (*ca* .12 dpm). These solutions were heated for 4 h at 90°C. After cooling, small quantities of 30% H_2O_2 were added dropwise until effervescence stopped in order to oxidize organic matter in the solution. After cooling, any solids were removed by vacuum filtration using glass fiber filters (Whatman 934AH). The solution was then purified on two ion-exchange columns following the procedure of Buesseler *et al.* (1992b). On the first column, thorium isotopes were separated from radium; on the second column, thorium was separated from uranium. The thorium-containing solutions were then prepared and electroplated onto stainless steel planchets under the conditions outlined in Moran and Buesseler (1993). Planchets were then mounted on plastic sheets and covered with layers of Al foil (9 mg cm^{-2}) to filter out low-energy beta emissions. The ^{234}Th activity was measured on low background (0.4-0.5 cpm), anticoincidence, gas-flow beta detectors by quantifying the emission of the stronger beta radiation of its immediate daughter, ^{234m}Pa (E = 2.29 MeV, $t_{1/2}$ = 1.2 min). Beta detectors were calibrated using deep ocean samples in which ^{234}Th is in secular equilibrium with ^{238}U, which in turn is conservative and may be estimated from salinity (Chen *et al.*, 1986). The samples were counted 4-5 times with a weekly interval to check for background interferences (primarily initial contamination by short-lived radium isotopes) and improve precision and accuracy. Recoveries were determined by alpha counting of the ^{230}Th yield monitor using Ortec silicon surface barrier detectors (Buesseler *et al.*, 1992b). ^{234}Th activities (dpm/kg) were decay-corrected to the mid-point of sample collection. Errors were propagated from counting statistics, based upon the fit of the raw counts to the ^{234}Th decay curves.

c. Seawater ^{238}U determination

Since there is some evidence that ^{238}U is not conservative with salinity in some coastal waters (McKee *et al.*, 1987; Carroll and Moore, 1994), we directly analyzed ^{238}U in several samples from Casco Bay. Isotope-Dilution Inductively-Coupled-Plasma Mass Spectrometry (ID-ICP-MS) was performed using a VG Instruments PlasmaQuad I ICP-MS. Seawater samples were spiked with 0.5 mL of a ^{236}U solution (6.627 dpm/mL) yielding a ^{236}U/^{238}U mass ratio near unity. Before data acquisition, each sample was used to flush the ICP-MS intake lines for 20 s. The atomic mass range 235-239 was scanned with a sweep of 600, dwell of 320 µs, acquisition time of 98.3 s, and acquiring the data in 512 channels. For mass fractionation correction, we used a 3000 m North Atlantic sample of known ^{238}U content (calculated from Chen *et al.*, 1986) spiked with a similar and known mass of ^{236}U. Instrument and method blanks were subtracted from all data. Analytical variability was calculated from triplicate analyses of each sample. ^{238}U was also determined using Thermal Ionization Mass Spectrometry (TIMS), following the procedure in Chen *et al.* (1986).

d. Sediment radionuclides determinations

Sediment radionuclides were determined with gamma spectrometry. Dried sediments were homogenized using mortar and pestle, and 31 g were transferred to 8 oz plastic counting jars with tight screw caps. Signals were acquired in 1024 channels of a Canberra multi-channel analyzer from a planar geometry low energy Ge detector (Canberra Instruments). The detector is shielded using approximately 10 cm pre-1940 lead and a 2 mm thick Cu/Al liner. Instrument electronic noise was subtracted from the signals using counts acquired in channels immediately surrounding the emission peaks. Radionuclide method blanks, from counting empty plastic counting jars, were also subtracted. Standard pitchblende (U.S. EPA Environmental Monitoring Systems Lab., Las Vegas, Nevada) was used to calibrate for U-Th series radionuclides. Standard additions of known amounts of the pitchblende were mixed into deeper sections of the sediment cores or into surficial sections after excess ^{234}Th had decayed. The calculated efficiencies thus take into account, in addition to the intrinsic detector efficiency, the branching ratios (BR: the ratio of gammas emitted to primary betas) and any self absorption factor of our constant-geometry sediment samples. ^{234}Th was quantified using its gamma emissions at 63 and 93 keV. Supported ^{234}Th was obtained by recounting after six or more half-lives had passed (>150 days). Excess ^{234}Th was obtained by subtracting the supported values and back-correcting to sampling time. Excess ^{210}Pb was obtained by subtracting supported levels (obtained from ^{214}Pb at 295 and 352 keV) from the total ^{210}Pb activities determined at 46.5 keV. ^{7}Be was quantified from its gamma emission at 475 keV (BR 10.3%), using known branching ratios and estimated intrinsic efficiencies of the bracketing peaks from ^{214}Pb (352 keV, BR 37.1%) and ^{214}Bi (609 keV, BR 46.1%) present in the pitchblende standard.

e. Estimation of Horizontal Transport Parameters

Okubo's (1971) empirical ocean mixing diagrams provide a starting point for estimating the magnitude of horizontal mixing in the coastal ocean. Beyond the outer islands (Fig. 1), using an estimated scale of 120 km, Okubo's diagrams yield a K_x of 140 m^2/s between our stations 2 and 1.

However, because of shoreline and bathymetric irregularities in the coastal waters of Inner Casco Bay, the relationship between the diffusion length scale and apparent diffusivity proposed by Okubo (1971) may underpredict significantly horizontal mixing at such sites (e.g., Fischer *et al.*, 1979; Zimmerman, 1986; Geyer and Signell, 1992). Flow separation, with accompanying high K_x, has been shown by Signell and Geyer (1990) to be a result of tidally-induced high strain rates occuring when the geographical length scale is less than or equal to the frictional and tidal excursion length scales (e.g., in coastal straits). Awaji (1982) studied mixing in a tidal strait similar in geometry but with larger tidal velocities than our site, and we estimated from his study a K_x for the straits of Casco Bay by scaling with the tidal currents (Appendix A):

$$(K_x)_{\text{Casco-Awaji}} = \left(\frac{K_x}{(U_T)^2}\right)_{\text{Awaji}} 2(u^2_{\text{rms}})_{\text{Casco}} \qquad (3)$$

where U_T is the amplitude of the tidal velocity and u_{rms} is the root-mean-square value of Eulerian tidal current measurements. From high spatial coverage southwestern Casco Bay surface current data from the same months in a previous year, taken with a tidal resolution of $\pi/3$ (Parker, 1982), we calculated a u_{rms} for our study site ranging from 0.28-0.38 m/s (corresponding to U_T = 0.4-0.5 m/s). Using Eqn. 3, to scale with Awaji's swift tidal strait transport parameters of K_x = 800 m^2/s and U_T = 2.5 m/s, yielded a $(K_x)_{\text{Casco-Awaji}}$ of 30 m^2/s around the straits in southwestern Casco Bay. This value exceeds the Okubo (1971) estimate for coastal ocean (1-10 km scales) of 0.6-8 m^2/s. However, it is only near the lower end of observed horizontal mixing coefficients in estuaries summarized by Fischer *et al.* (1979) of 50-200 m^2/s, and it thus may be a conservative estimate of the actual dispersion strength. Fischer *et al.* (1979) used scaling arguments to demonstrate that a shear dispersion mechanism alone may result in dispersion coefficients of 10-50 m^2/s for tidal velocities of 0.3-0.5 m/s. In the nearby urban estuary of Boston Harbor, Kossik (1986) used volatile halogenated organic compounds to calibrate the horizontal tidal dispersion coefficient and constrained K_x to be in the range 50-100 m^2/s in a tidal regime with similar velocities to Casco Bay (Kossik, 1986).

We estimated the net, non-tidal, advection term (u_{net}) from the local salinity field and the estimated values of K_x using the steady-state box model outlined below (see Two-Dimensional Modeling of Thorium-234).

3. WATER COLUMN RESULTS

a. Seawater ^{234}Th

While the particulate and total ^{234}Th inventories were different in the two seasons sampled, the spatial gradients exhibited similar patterns (Table 1). Total ^{234}Th activities in the fall of 1993 in Casco Bay increased unidirectionally from 0.089 dpm/kg at the innermost station (stn. 5) to 0.210 dpm/kg at the offshore station (stn. 2). These activities are extremely low relative to the parent ^{238}U activities (disequilibrium of 95% at the two innermost stations) indicating an intense scavenging period. In fact, these ^{234}Th activities are among the lowest reported anywhere (Baskaran and Santschi, 1993; Moran and Buesseler, 1993). High winds preceeding and during this cruise likely caused substantial resuspension of bed particles, resulting in efficient particle-mediated removal of ^{234}Th from the water column. In the subsequent spring cruise, 3-4 fold higher total ^{234}Th activities were found at the same stations (Table 1). A trend of increasing ^{234}Th activities away from the coast was, however, also apparent in the spring.

Table 1. Sampling dates, locations, surface water ancillary and radioisotope data for Casco Bay - Gulf of Maine cruises.

Sampling Event	Date	Lattitude (N)	Longitude (W)	Distance (km)	Depth (m)	Salinity (psu)	^{238}U-total* (dpm/kg)	^{234}Th-total (dpm/kg)	^{234}Th-particulate (dpm/kg)
93-5	9/28/93	43°40.58	70°14.38	0.9	6	30.45	2.089	0.089±0.016	0.049±0.004
93-4	9/28/93	43°39.70	70°14.33	2.4	8	31.18	2.138	0.113±0.020	0.062±0.003
93-3	9/27/93	43°38.22	70°13.12	5.7	12	31.27	2.144	0.186±0.035	0.083±0.005
93-2	9/26/93	43°37.19	70°04.32	17	32	31.70	2.174	0.210±0.035	0.149±0.006
94-4	5/20/94	43°39.63	70°14.32	2.4	8	28.66	1.965	0.491±0.032	0.325±0.019
94-2	5/21/94	43°36.94	70°09.31	12	32	29.33	2.011	0.756±0.040	0.378±0.021
94-1	5/22/94	42°38.00	69°36.26	130	295	32.90	2.256	1.688±0.053	0.299±0.032

*Calculated according to Chen *et al.* (1986): ^{238}U (dpm/kg) = 0.06857 x S‰ (psu).

b. Seawater ^{238}U

^{238}U activities were confirmed to be conservative with respect to salinity in Casco Bay (Table 2). ^{238}U activities estimated from the salinity-relationship of Chen *et al.* (1986) were indistinguishable from both ID-ICP-MS and TIMS measurements. The non-conservative behavior of uranium has been been documented in some estuaries where redox processes may result in localized removal or releases from suspended sediments or sediment pore waters (Maeda and Windom, 1982; McKee *et al.*, 1987; Carrol and Moore, 1994). These processes are apparently insignificant in most higher salinity coastal settings where the rate of mixing is high relative to the strength of diagenetic processes which can affect U geochemistry. We conclude that ^{238}U mixes conservatively in this coastal region and can thus here be predicted from salinity.

4. TWO-DIMENSIONAL MODELING OF THORIUM-234

It is informative to contrast the magnitude of the horizontal, vertical, and radioactive production and decay fluxes of ^{234}Th. To this end we used a two-dimensional box model approach to evaluate the steady-state exchange of ^{234}Th to and from the Inner and Outer regions of Casco Bay (Fig. 1). This approach assumes ^{234}Th homogeneity in the alongshore direction, which is reasonable since this radionuclide's activity is commonly correlated with suspended particle concentrations, decreasing predominantly in the offshore direction (e.g., Bhat *et al.*, 1969). Inner Casco (box I) represents the greater Portland Harbor regime, defined by the shore and a chain of islands and characterized by shallow depths of ≤10 m. Starting with the outer Portland Channel, Outer Casco (box II) comprises the water as it exits the topographically-constricted Inner region into open and deeper water. The outer boundary of Outer Casco (toward box III) was defined by offshore shoals (West Cod Ledge) and approximate location of the inner edge of the coastal boundary current. The very similar ^{234}Th activities at stns. 5 and 4 (box I), at stns. 2 and 3 (box II), and much higher activities at stn. 1 (Off Casco - Gulf of Maine Proper, box III) indicates that the defined locales represent distinct scavenging regimes. Thus, in the following model calculations, each box is represented by the mean salinity, ^{234}Th and ^{238}U values of its stations (from Table 1). The characteristic offshore

Table 2. Estimates and measurements of ^{238}U (dpm/kg) in size-fractionated Casco Bay surface waters.

Sampling Event	Sample Type	Estimate from S‰*	Measurement with ID-ICP-MS	Measurement with TIMS	ratio of ^{238}U from ICP/S‰
93-4	ultrafiltrate	2.144	2.128±0.007	2.106	0.993
93-4	retentate	2.144	2.128±0.004	2.106	0.993
93-4	total	2.144	2.103±0.008	2.106	0.981
93-2	ultrafiltrate	2.174	2.159±0.010	2.150	0.993
93-2	retentate	2.174	2.185±0.006	2.150	1.005
93-2	total	2.174	2.141±0.010	2.150	0.985

*Calculated according to Chen *et al.* (1986): ^{238}U (dpm/kg) = 0.06857 x S‰ (psu).

length scales for each box, l_I, $l_{II\text{-in}}$, $l_{II\text{-off}}$ (Table 3), were defined as the volume of the box divided by the cross-sectional area of the boundary across which exchange was considered. The characteristic gradient length scales ($l_{I\text{-}II}$ and $l_{II\text{-}III}$; Table 3) represent the distances over which the K_x's operate. In the case of $(K_x)_{\mathrm{Awaji}}$, resulting from swift tidal exchange through Portland Channel, this corresponds approximately with the distance between our stations 4 and 3 (Figure 1). An advantage of this simple box-model approach is that the mass balance may be formulated with a no-flux inner boundary condition and without having to consider the second derivative of the low-resolution ^{234}Th gradient of Eqn. 2. First, to constrain the net advection term, u, for Inner and Outer Casco at the two different occasions, we formulate the salinity balance of each box. For box I we have:

$$\frac{\partial \mathrm{Sal}_I}{\partial t} = 0 = -\frac{u_I}{l_I}\mathrm{Sal}_I + \frac{(K_x)_{\mathrm{Awaji}}}{l_{I\text{-}II}}\frac{(\mathrm{Sal}_{II} - \mathrm{Sal}_I)}{l_I} \qquad (4\text{:I})$$

and for box II:

$$\frac{\partial \mathrm{Sal}_{II}}{\partial t} = 0 = \frac{u_I}{l_{II\text{-in}}}\mathrm{Sal}_I - \frac{(K_x)_{\mathrm{Awaji}}}{l_{I\text{-}II}}\frac{(\mathrm{Sal}_{II} - \mathrm{Sal}_I)}{l_{II\text{-in}}}$$

$$-\frac{u_{II}}{l_{II\text{-off}}}\mathrm{Sal}_{II} + \frac{(K_x)_{\mathrm{Okubo}}}{l_{II\text{-}III}}\frac{(\mathrm{Sal}_{III} - \mathrm{Sal}_{II})}{l_{II\text{-off}}} \qquad (4\text{:II})$$

With other model parameters constrained (Table 3), solving the salinity distribution for "u" yields net offshore advection from box I of 17 and 18 m/d and from box II of 5 and 13 m/d during the fall and spring conditions sampled, respectively (Table 3).

Given the horizontal transport parameters, two-dimensional box models for ^{234}Th in Inner and Outer Casco Bay may similarly be described:

Table 3. Two-dimensional box model of Casco Bay.

Inner Casco Bay (box I)		
Offshore length	x_I	4100 m
Mean depth	z_I	7 m
Depth at border with Outer Casco	z_{I-II}	11 m
Characteristic length scale	$l_I = V_I/A_{I-II} = x_I\ y\ z_I\ /\ y\ z_{I-II}$	2600 m
Net offshore advection	u_I	
Fall 1993		17 m/d
Spring 1994		18 m/d
Horizontal dispersion	$(K_x)_{Awaji}$	$2.6\ 10^6\ m^2/d$
Characteristic gradient length scale (≈ stns. 4 ↔ 3)	l_{I-II}	3300 m
Dispersive "piston-velocity"	$v_{Awaji} = (K_x)_{Awaji}/l_{I-II}$	790 m/d
Outer Casco Bay (box II)		
Offshore length	x_{II}	11,000 m
Mean depth	z_{II}	20 m
Depth at border with Inner Casco	z_{I-II}	11 m
Depth at border with Off Casco	z_{II-III}	24 m
Characteristic length (Inner Casco exchange)	$l_{II\text{-}in} = V_{II}/A_{I-II} = x_{II}\ y\ z_{II}\ /\ y\ z_{I-II}$	20,000 m
Characteristic length (Off Casco exchange)	$l_{II\text{-}off} = V_{II}/A_{II-III} = x_{II}\ y\ z_{II}\ /\ y\ z_{II-III}$	9,200 m
Net offshore advection	u_{II}	
Fall 1993		5 m/d
Spring 1994		13 m/d
Horizontal dispersion	$(K_x)_{Okubo}$	$12\ 10^6\ m^2/d$
Characteristic gradient length scale (≈ stns. 2 ↔ 1)	l_{II-III}	115,000 m
Dispersive "piston-velocity"	$v_{Okubo} = (K_x)_{Okubo}/l_{II-III}$	100 m/d

$$\frac{\partial^{234}Th_I}{\partial t} = 0 = \lambda\,(^{238}U_I - {}^{234}Th_I) - F_{Th,I}$$

$$- \frac{u_I}{l_I}\,{}^{234}Th_I + \frac{(K_x)_{Awaji}}{l_{I\text{-}II}}\,\frac{(^{234}Th_{II} - {}^{234}Th_I)}{l_I} \qquad (5{:}I)$$

$$\frac{\partial^{234}Th_{II}}{\partial t} = 0 = \lambda\,(^{238}U_{II} - {}^{234}Th_{II}) - F_{Th,II}$$

$$+ \frac{u_I}{l_{II\text{-}in}}\,{}^{234}Th_I - \frac{(K_x)_{Awaji}}{l_{I\text{-}II}}\,\frac{(^{234}Th_{II} - {}^{234}Th_I)}{l_{II\text{-}in}}$$

$$- \frac{u_{II}}{l_{II\text{-}off}}\,{}^{234}Th_{II} + \frac{(K_x)_{Okubo}}{l_{II\text{-}III}}\,\frac{(^{234}Th_{III} - {}^{234}Th_{II})}{l_{II\text{-}off}} \qquad (5{:}II)$$

The relative magnitudes of the different ^{234}Th fluxes: production-minus-decay, horizontal dispersion and advection into and out from the box, as well as the resulting net vertical settling, were calculated for both the Inner and Outer Casco Bay for both 1993 and 1994 conditions. Net offshore advection of ^{234}Th is negligible ($\leq 2\%$) compared to radioactive production-minus-decay and horizontal dispersion in all four cases. Horizontal dispersion always brings ^{234}Th, from ^{234}Th-rich offshore waters, toward the coast.

Using the two-dimensional model, we found that onshore dispersion sometimes increased the estimated net vertical transport flux in Inner Casco Bay compared to scavenging predictions from the one-dimensional model (Fig. 2). During the intense scavenging period in September 1993, horizontal dispersive input resulted in a 50% elevated estimate of vertical export compared to the traditional prediction. In May 1994, when the scavenging intensity was more representative of conditions reported for other coastal regimes (e.g., Moran and Buesseler, 1993; Wei and Murray, 1993; Niven *et al.*, 1995), it was discovered that onshore dispersion of ^{234}Th increased the Inner Casco scavenging estimate by a factor of three compared to neglecting the effect of horizontal transport (Figure 2).

Figure 2. Comparison of the estimates of ^{234}Th scavenging flux using the one-dimensional (dark) and two-dimensional (light) models in Inner and Outer Casco Bay (Fig. 1) during fall (1993) and spring (1994) periods. The error bars represent propagated uncertainties from ^{234}Th counting statistics, and thus do not include an estimate of the uncertainty associated with the horizontal dispersion and net advection transport parameters.

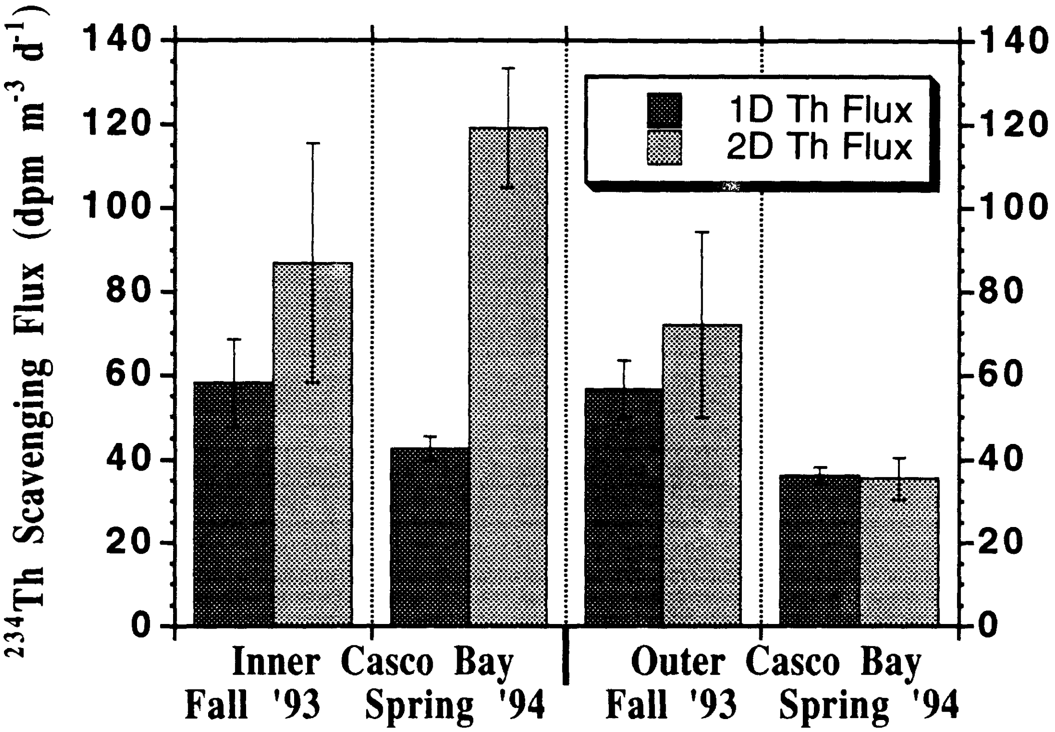

^{234}Th Scavenging Flux (dpm m^{-3} d^{-1})
140
120
100
80
60
40
20
0
1D Th Flux
2D Th Flux
Inner Casco Bay
Fall '93
Spring '94
Outer Casco Bay
Fall '93
Spring '94

In contrast, the net effect of horizontal dispersion on ^{234}Th-derived scavenging estimates is insignificant in the Outer Casco region (Fig. 2). To a large extent, this is a result of net dispersive import of ^{234}Th from box III (Off Casco) being offset by net inshore export to box I. Nevertheless, these results indicate that it may be necessary to consider horizontal dispersion in nearshore settings even for chemicals as particle-reactive as ^{234}Th, in order to better describe chemical cycling in coastal waters.

5. SEDIMENTARY RECORD OF HORIZONTAL TRANSPORT

The sedimentary record of three natural radionuclides (^{234}Th, ^{7}Be, and ^{210}Pb) provided supporting evidence for the occurence of horizontal chemical transport in the coastal ocean. Both ^{7}Be and ^{210}Pb in this coastal region have predominantly atmospheric sources, whereas ^{234}Th is produced *in situ*. ^{7}Be is formed by spallation reactions of cosmic ray particles with stratospheric nitrogen and oxygen (Lal and Peters, 1967). The atmospheric deposition rate of ^{7}Be exhibits a latitudinal and seasonal effect related to the folding of the tropopause in spring and the resulting occurence of "stratospheric overflow" (Dibb, 1989; Schuler *et al.*, 1991). However, only a weak dependence on spatial and temporal precipitation patterns have been observed (e.g., Krishnaswami *et al.*, 1980; Turekian *et al.*, 1983; Dibb, 1989; Brown *et al.*, 1989). Minor variations in atmospheric deliveries at any given site have been shown to be nearly indistinguishable in the distribution of ^{7}Be in the sediments, which is thought to be dominantly governed by local variations in particle dynamics (e.g., Canuel *et al.*, 1990). Precipitation measurements and soil profiles in the northeastern USA indicate a ^{7}Be input of 18 dpm cm^{-2} yr^{-1} (Turekian *et al.*, 1983; Olsen *et al.*, 1985; Dibb, 1989; Brown *et al.*, 1989).

The atmospheric input of ^{210}Pb originates from decay of atmospheric ^{222}Rn, emanating from soils. This source function has similarly been extensively determined in this region (e.g., Turekian *et al.*, 1983; Graustein and Turekian, 1989; Hussain *et al.*, 1990). Based on such studies, we adopted a value of 0.8 dpm cm^{-2} yr^{-1} for our study sites. Finally, as noted above, ^{234}Th in the ocean originates from the decay of highly soluble ^{238}U. The depth-integrated ^{234}Th flux represents the source function of sedimentary excess ^{234}Th (^{234}Th$_{xs}$).

The spatial distribution of the sediment inventories of ^{7}Be, ^{234}Th$_{xs}$, and ^{210}Pb$_{xs}$ were contrasted to the magnitudes of their sources (Table 4). Highest levels of all three radionuclides were found nearshore. This extra inventory must have been horizontally transported to such sedimenting coastal sites either through sediment winnowing-focusing events, or through suspended-phase surface water transport to such sites of increased scavenging intensity. We believe that runoff of terrestrially-deposited ^{7}Be and ^{210}Pb is a minor source to coastal sediments since previous studies have shown that the fluxes of ^{7}Be and ^{210}Pb in lakes and marshes, regimes with substantial terrestrial drainage areas, are in agreement with fluxes obtained from soil profiles and roof-top collectors (e.g., Olsen *et al.*, 1985; Schuler *et al.*, 1991). The ratio of the sediment inventory of ^{234}Th$_{xs}$ compared to the source was 340% in Inner Casco Bay (stn. 4), 170% at Outer Casco Bay (stn. 2), and 120% in the Wilkinson Basin of the Gulf of Maine proper (stn. 1). Thus, although individual cores may be affected by sediment focussing, our results indicate that horizontal transport significantly affects the scavenging flux of ^{234}Th; the effect becoming increasinlgy significant as one approaches the coastal boundary. Similarly, the highest sediment inventories of ^{210}Pb$_{xs}$ and ^{7}Be, relative to their sources, were found at the station closest to the shore.

While it is not possible to know from "extra" ^{234}Th$_{xs}$ inventories alone whether sediment focussing or boundary scavenging is the dominant horizontal transport process supplying ^{234}Th to a given site, using both the sedimentary inventories of ^{234}Th$_{xs}$ and ^{7}Be may resolve this issue. The approach is analogous to the successful application of the long-lived radionuclides ^{10}Be, ^{230}Th, and ^{231}Pa to elucidate ocean-basin-wide boundary scavenging (e.g., Bacon, 1988). The applicability of the ratio, ^{7}Be/^{234}Th$_{xs}$, as a boundary-scavenging indicator on scales of coastal seas is based on their different propensity for scavenging. While ^{234}Th has an operational seawater distribution coefficient, D, around 10^{6} (L/kg) (e.g., Nyffeler *et al.*, 1984; Moran and Buesseler, 1993), the lower particle-affinity of ^{7}Be ($\log D \approx 4.5$; Nyffeler *et al.*, 1984) causes it to be transported horizontally to a greater extent until it eventually decays or becomes scavenged. A virtue of the ^{7}Be/^{234}Th$_{xs}$ indicator is that it is relatively insensitive to surface sediment resuspension as this process would affect both isotopes to a similar extent. Their ratio would also be insensitive to partially missing core-tops given their similar depth distribution in sediments (which could significantly affect, for instance, the ^{210}Pb$_{xs}$/^{234}Th$_{xs}$ ratio). As expected from boundary-scavenging, ^{7}Be/^{234}Th$_{xs}$ increases

Table 4. Sediment inventories, atmospheric and water-column sources of ^{210}Pb, ^{7}Be, and ^{234}Th in the Gulf of Maine.

Sampling Event	$^{210}Pb_{xs}$ Inventories (dpm/cm^2)		^{7}Be Inventories (dpm/cm^2)		^{234}Th Inventories (dpm/cm^2)		$^{7}Be/^{234}Th_{xs}$
	measured	predicted*	measured	predicted*	measured	predicted**	measured
94-4	>110	25	3.7	3.8	4.8	1.4	0.77
94-2	38	25	1.9	3.8	7.2	4.2	0.26
94-1	64	25	0.18	3.8	3.0	2.5	0.06

* The expected inventories of these radionuclides were calculated from their measured atmospheric deliveries to the northeastern USA (^{7}Be: Turekian *et al.*, 1983; Dibb, 1989; Brown *et al.*, 1989; ^{210}Pb: Turekian *et al.*, 1983; Graustein and Turekian, 1989) given the mean life of ^{210}Pb (32 yr) and ^{7}Be (76 d).

** The water-column deficits were calculated by assuming that single depth ^{234}Th measurements were representative of the well-mixed water-column at station 4 and 2 (CTD data indicate absence of stratification) and from the similar ^{234}Th results at 5 and 30 m at station 1, where inspection of CTD data indicated a mixed-layer depth of 40 m.

from 0.06 in the open Gulf of Maine to 0.26 in Outer Casco Bay to 0.77 in the more intense scavenging regime of Inner Casco Bay (Table 4). Our sediment results suggest that boundary scavenging is dominating sediment focussing as the dominant mechanism horizontally transporting these radionuclides to coastal sediments. These results are further consistent with our two-dimensional water-column box-model which suggests that horizontal transport is more significant for less particle reactive chemicals.

6. TWO-DIMENSIONAL CONTAMINANT TRANSPORT MODEL

In principle, it should be possible to extend the two-dimensional model (Eqn. 5) to elucidate the horizontal and vertical transport of other particle-reactive chemicals, some of which may be of direct interest for the health of coastal ecosystems. Like Th, hydrophobic organic compounds, HOCs (e.g., PAHs, PCBs, polychlorinated dioxins, many pesticides), also exhibit significant affinity towards marine particles (e.g.,Tanabe and Tatsukawa, 1983; Lipiatou and Saliot, 1991; Broman *et al.*, 1991; Schulz-Bull *et al.*, 1994). Since the net-settling particulate carrier-phases are largely composed of aggregates of smaller particles, formed either by biological processes, such as fecal pellet packaging, and/or abiotic flocculation processes (e.g., Fowler and Knauer, 1986; Farley and Morel, 1986, Alldredge and Silver, 1988; Stolzenbach, 1993), ^{234}Th and HOCs are expected to belong to, and be coupled through, this same particle dynamics (Gustafsson *et al.*, 1996a). Thus, the net vertical HOC flux may be estimated from the scavenging transport of ^{234}Th (Gustafsson *et al.*, 1996a):

$$F_{HOC} = F_{Th} \frac{[HOC]_{part}}{[^{234}Th]_{part}} \qquad (6)$$

where F_{HOC} (pM/d) is the net vertical scavenging removal of HOCs, and $[HOC]_{part}$ and $[^{234}Th]_{part}$ are the particulate concentrations of HOC (pM) and ^{234}Th (dpm/kg), respectively.

Since we are interested in the overall fates of HOCs, wherein scavenging is just one process, a complete mass-balance may be formulated:

$$\frac{\partial[\mathrm{HOC}]_{\mathrm{tot}}}{\partial t} = I_{\mathrm{tot}} + k_g\left(\frac{[\mathrm{HOC}]_{\mathrm{air}}}{K_{\mathrm{Henry}}} - [\mathrm{HOC}]_{\mathrm{diss}}\right) - \sum_i k_{\mathrm{rxn}(i)}[\mathrm{HOC}]_{\mathrm{tot}(i)} - F_{\mathrm{HOC}} + \frac{\partial}{\partial x}K_x\frac{\partial[\mathrm{HOC}]_{\mathrm{tot}}}{\partial x} - u_x\frac{\partial[\mathrm{HOC}]_{\mathrm{tot}}}{\partial x} \qquad (7)$$

where I_{tot} is the chemical input function, k_g is the air-water exchange rate, K_{Henry} is the chemical's Henry's Law constant, and $\sum k_{rxn(i)}$ represents the rate of transformation reaction *i* that the chemical may undergo. For many chemicals and environmental regimes, several assumptions may be made to simplify the above expression. One of the reasons why many hydrophobic contaminants are of ecosystem concern is that they are very persistent. Thus, for such recalcitrant compounds the chemical reaction terms in Eqn. 7 may be neglected. Similarly, the partitioning of most HOCs between surface water and the overlying atmosphere is likely to be slow (of order weeks: e.g., Kossick, 1986) relative to near-coastal scavenging for most HOCs. Assuming steady-state, the balance between direct HOC input to a coastal regime such as Inner Casco Bay (i.e., box 1) and subsequent vertical and horizontal transport may be described:

$$I_{\mathrm{atm,I}} + I_{\mathrm{runoff,I}} = F_{\mathrm{Th,I}}\frac{[\mathrm{HOC}_{\mathrm{part}}]_{\mathrm{I}}}{[^{234}\mathrm{Th}_{\mathrm{part}}]_{\mathrm{I}}} + \frac{u_{\mathrm{I}}}{l_{\mathrm{I}}}[\mathrm{HOC}_{\mathrm{tot}}]_{\mathrm{I}} - \frac{(K_x)_{\mathrm{Awaji}}}{l_{\mathrm{I\text{-}II}}}\frac{([\mathrm{HOC}_{\mathrm{tot}}]_{\mathrm{II}} - [\mathrm{HOC}_{\mathrm{tot}}]_{\mathrm{I}})}{l_{\mathrm{I}}} \qquad (8)$$

where I_{atm} and I_{runoff} are the HOC inputs to the box via direct atmospheric deposition and runoff, and $[HOC_{tot}]_I$ and $[HOC_{tot}]_{II}$ are total-phase HOC concentrations in Inner and Outer Casco Bay. The relative significance of vertical and horizontal transport to the distribution of a given chemical in the coastal ocean is seen from Eqn. 8 to depend upon: (a) the relative intensity of the transport parameters, (b) concentration gradients and, importantly, (c) the fraction of the total contaminant that is particle-bound.

The remainder of this section seeks to elucidate how this compound-specific particle-affinity may affect a chemical's preferential participation in some of the outlined transport processes. To illustrate these effects, we focus on the cycling of two individual PAHs (pyrene and benzo[a]pyrene) observed during the fall 1994 Gulf of Maine cruise (Gustafsson *et al.*, 1996a). Their particulate concentrations at station 4 were 6.2±0.8 and 1.1±0.2 pM, respectively, and offshore at station 2 they had decreased to 2.1±0.3 and 0.38±0.06 pM, respectively. Since the organic-carbon normalized partition coefficients, K_{oc}'s, of these PAHs are well-known; the log K_{oc} values of pyrene and benzo[a]pyrene are 4.78 and 6.08, respectively (Karickhoff, 1981), their total-phase concentrations may be estimated (however, see discussion below) from the measured particulate HOC and POC levels:

$$[\mathrm{PAH}]_{tot} = [\mathrm{PAH}]_{part} / \frac{\mathrm{POC}\ K_{oc}}{1 + \mathrm{POC}\ K_{oc}} \tag{9}$$

We used literature information to estimate the PAH input one might anticipate at a site such as Portland Harbor/Inner Casco Bay, located in the vicinity of an intermediate-sized city. Based on many studies reporting rather similar aerosol respectively vapor PAH concentrations in populated regions (e.g., Eisenreich *et al.*, 1981; Baker and Eisenreich, 1990; Broman *et al.*, 1991b; Dickhut and Gustafson, 1995; Venkataraman *et al.*, 1995; Cotham and Bidleman, 1995), a mean harbor water column depth of 7 m, and typical estimates of atmospheric settling velocity (Eisenreich *et al.*, 1981) and washout ratios (Bidleman, 1988), we expect atmospheric fluxes of pyrene and benzo[a]pyrene into Inner Casco Bay ranging from 0.1-1 and 0.03-0.3 pM/d. The PAH runoff loadings of Portland Harbor were approximated by scaling with the Boston Harbor estimates of stormwater, combined sewage overflow, and river inputs (MWRA, 1993). A scaling factor of twenty was derived from the relative sewage flow rates of the two cities (EPA, 1988), in agreement with the relative population of the two cities, yielding best estimates of I_{runoff} for pyrene of 2 pM/d and for benzo[a]pyrene of 0.08 pM/d. Summing, these calculations suggest the sum of all sinks removing these individual PAHs from Inner Casco Bay must be near pM/d.

In light of these source estimates, and using the transport information contained in Table 3, one can start to assess the fate of PAHs introduced to Portland Harbor (Fig. 3a). In contrast to ^{234}Th, both horizontal diffusion and advection act to export PAHs to locations away from the coastal boundary. This is an outcome of the direction of their concentration gradients along a transect normal to the coastline; whereas ^{234}Th activities were increasing away from the shore, PAH concentrations and vertical fluxes fall off exponentially with increasing distance away from their land-based sources (Hites *et al.*, 1980; Broman *et al.*, 1988; Näf *et al.*, 1992; Gustafsson *et al.*, 1996a). Hence, horizontal waterborne transport of PAHs, and any other contaminants with predominantly land-based releases, will be unidirectionally outbound. The PAH fluxes to the sediments, calculated from the F_{Th} results, appear to be small relative to offshore transport.

Very interestingly, this Greater Portland Harbor box-model indicates a major imbalance in the current estimation of the PAH fluxes, with the deviation being largest for the less hydrophobic pyrene. For pyrene, this model suggests that the horizontal export is up to two orders of magnitude larger than its source inputs (Fig. 3a-top). For benzo[a]pyrene, the corresponding imbalance is a factor of three to twelve (Fig. 3a-bottom). This scenario suggests that (a) the atmospheric exchanges were negative (i.e., net flux ocean-to-air), (b) another major sink was missing, or (c) some other model assumptions were incorrect. Since it is believed that PAHs are introduced to the ocean primarily by atmospheric deposition of combustion (soot) particles (e.g., Gschwend and Hites, 1981; Sporstøl *et al.*, 1983; Broman *et al.*, 1990; Gustafsson *et al.*, 1996a, 1996b), to explain the pyrene imbalance, a gas-phase return exchange would have to be almost two orders of magnitude faster than the soot-PAH deposition and the vertical scavenging fluxes. We also doubt that photo- or biodegradation sinks were sufficient. While PAHs are known to undergo photochemical and other oxidative transformation reactions (e.g., Butler and Crossley, 1981; Behymer and Hites, 1988), it is not likely that the rates of such reactions are high enough in turbid coastal waters to account for the discovered imbalance. Thus, we are forced to reassess the assumptions made in simplifying Eq. 7 and in estimating the values of the remaining terms (Eq. 8).

The first term in Eq. 8, HOC scavenging (see also Eq. 6), only contains already evaluated parameters (i.e., K_x, u_{net}, λ) or directly measured entities (i.e., $[^{238}U_{tot}]$, $[^{234}Th_{tot}]$, $[^{234}Th_{part}]$, x, $[PAH_{part}]$). The scavenging intensity fit the ^{234}Th box-model mass-balance. Furthermore, at station 2 and 4, the water-column scavenging fluxes of pyrene were within a factor of two of the fluxes into the underlying surface sediments (Gustafsson *et al.*, 1996a), lending credence to the model-derived scavenging fluxes. The only remaining parameters not critically evaluated were the $[PAH_{tot}]$ values, which were estimated from $[PAH_{part}]$ by assuming equilibrium organic-matter partitioning (i.e., Eq. 9).

While PAHs are known to effectively partition into marine organic matter (e.g., Means *et al.*, 1980, 1995), recent field-obtained K_{oc}'s (e.g., Readman *et al.*, 1987; Broman *et al.*, 1991; McGroddy and Farrington, 1995; McGroddy *et al.*, 1996; Poster and Baker, 1996) indicate a much greater affinity for the solid-phase than predicted by organic-matter partition models (summarized in Gustafsson *et al.*, 1996b). In that work, it was demonstrated that the elevated solid affinities observed in two Boston Harbor sediments could be due to very efficient PAH partitioning to soot. Applying the relative abundance of particulate soot carbon (PSC) to POC measured by Gustafsson *et al.* (1996b) in inner and outer Boston Harbor sediments (PSC:POC ≈ 0.1) and their estimates of soot-carbon-normalized partition coefficients (K_{sc}; $10^{7.1}$ and $10^{8.0}$ for pyrene and benzo[a]pyrene), we re-estimate [PAH_{tot}] for the present study sites. Such a soot-partitioning based calculation results in much lower estimates of [PAH_{tot}] in Portland Harbor water. Also, the [PAH_{tot}] gradients are correspondingly smaller when soot-partitioning is considered, resulting in estimates of horizontal advection and diffusion of PAHs which were within a factor of three of the PAH sources and scavenging sink (Fig. 3b). Since any one of the estimated parameters (e.g., K_x, u_{net}, [PAH_{tot}], the gradients) were, at best, only known within a factor of two, this "near-closure" of a two-dimensional coastal PAH mass-balance is remarkable and does not preclude either input functions of twice the size or a transformation reaction sink of pyrene and benzo[a]pyrene. This two-dimensional chemical cycling model suggests that horizontal transport was equally or more important than vertical settling to the distribution of these hydrophobic organic contaminants in coastal waters. Furthermore, this coupled transport model of PAHs provides support for the idea that the environmental PAH speciation is commonly dominated by partitioning with a strongly-binding soot phase (McGroddy and Farrington, 1995; Gustafsson *et al.*, 1996b).

7. CONCLUSIONS

The significance of horizontal and vertical transport of particle-reactive chemicals in the coastal ocean has been assessed. Tidally-induced horizontal dispersion brings ^{234}Th-rich offshore waters toward the coastal boundary where the scavenging intensity is higher. To derive accurately vertical chemical fluxes in coastal waters, it was found necessary to apply a two-dimensional scavenging model (Eq. 5 for ^{234}Th and Eq. 6 for HOCs). For an inshore regime (i.e., Inner Casco Bay), onshore horizontal dispersion of ^{234}Th represented twice as large a contribution to the net vertical flux estimate as the

Figure 3. Two-dimensional box-models of four-ringed pyrene, and five-ringed benzo[a]pyrene in Inner Casco Bay/Portland Harbor during spring 1994. Estimates of the total-phase PAH concentrations, for horizontal transport flux calculations, were based on equilibrium organic-matter partitioning in box "a", but include partitioning to soot in box "b". Volumetric fluxes are shown in pmol L^{-1} d^{-1}.

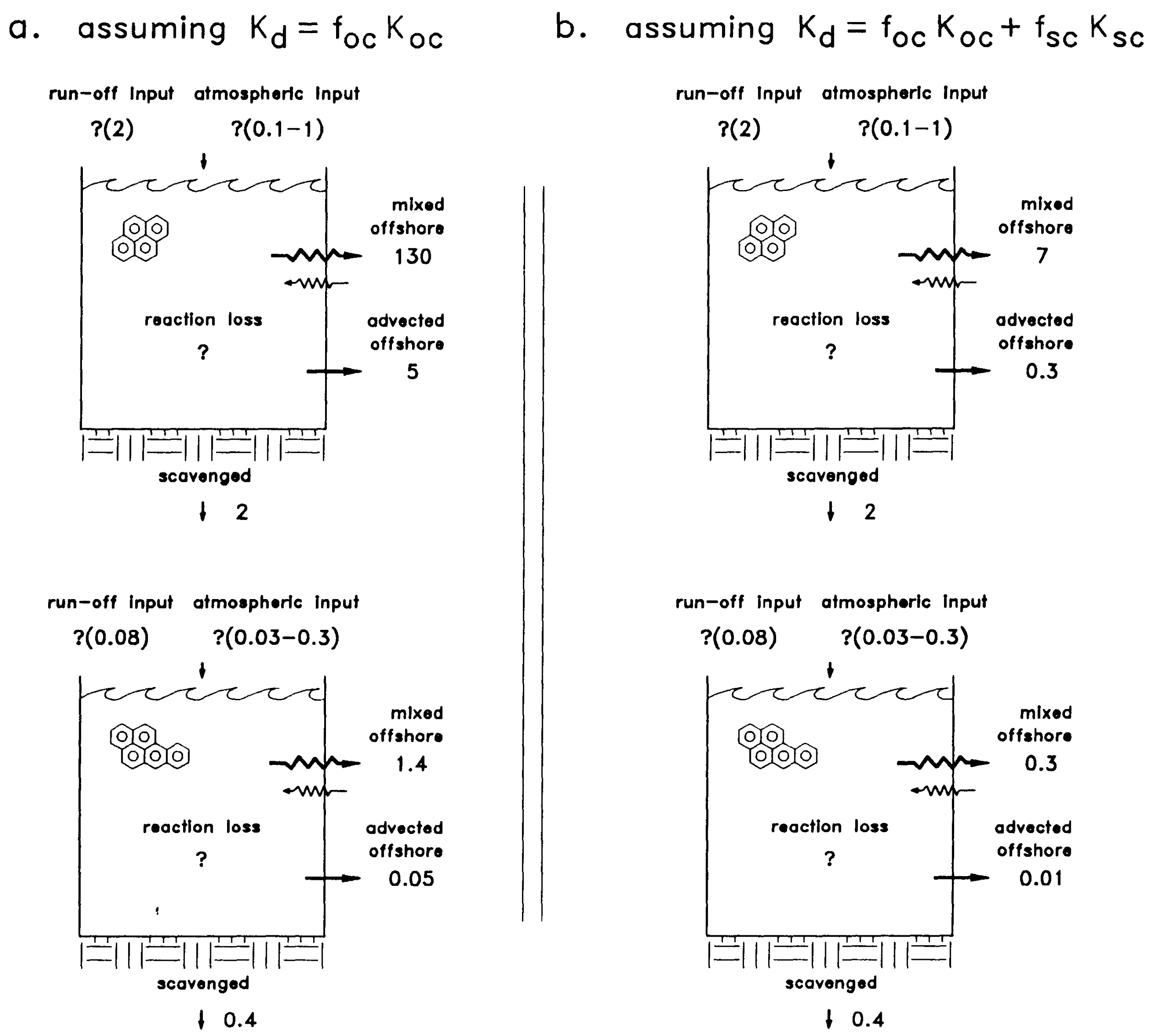
a. assuming $K_d = f_{oc} K_{oc}$
b. assuming $K_d = f_{oc} K_{oc} + f_{sc} K_{sc}$
run-off input
atmospheric input
?(2)
?(0.1-1)
mixed offshore
130
reaction loss
?
advected offshore
5
scavenged
2
run-off input
atmospheric input
?(0.08)
?(0.03-0.3)
mixed offshore
1.4
reaction loss
?
advected offshore
0.05
scavenged
0.4
run-off input
atmospheric input
?(2)
?(0.1-1)
mixed offshore
7
reaction loss
?
advected offshore
0.3
scavenged
2
run-off input
atmospheric input
?(0.08)
?(0.03-0.3)
mixed offshore
0.3
reaction loss
?
advected offshore
0.01
scavenged
0.4

production-minus-decay term. Hence, considering this horizontal transport increased the ^{234}Th-derived scavenging estimate by a factor of three relative to the traditional one-dimensional model (Eq. 1).

Supporting evidence for horizontal-transport-mediated "boundary scavenging" was found in the sedimentary radionuclide record. Sediment inventories of $^{210}Pb_{xs}$, $^{234}Th_{xs}$, and ^{7}Be were found to be greatest with respect to their vertical sources at the nearshore stations, indicating horizontal shoreward transport. Furthermore, the ratio of $^{7}Be/^{234}Th_{xs}$ was found to increase systematically when approaching the coast, and this ratio was thus suggested to be a useful indicator of "boundary scavenging" on scales of coastal seas.

The two-dimensional transport model was applied to examine the distributional fate of particle-reactive HOCs in coastal waters. It was found that at least as much of the pyrene and benzo[a]pyrene in Greater Portland Harbor was transported horizontally offshore as was settling vertically. Furthermore, the two-dimensional mass-balance model provided strong indirect evidence for the importance of pyrogenic carbon phases in the environmental PAH speciation. When this soot-like phase was considered in estimating the total-phase concentration of PAHs, the box-model sources and sinks matched within a factor of three, compared to being several orders of magnitude out of balance if organic-matter-based partitioning was used (Figure 3).

To model accurately the distributional fate and effect of chemicals in coastal waters, this work suggest that both horizontal and vertical transport need to be incorporated in mass balance models. Further progress toward a predictive understanding of the distribution of vital and toxic chemicals in dynamic coastal systems is likely to come from studies synthesizing simultaneously obtained higher-resolution information about circulation, phase-distributions, and reactions.

ACKNOWLEDGMENTS

We gratefully acknowledge the assistance of the captain and crew of R/V Argo Maine. John Farrington entrusted us with his MK-III box corer and Hovey Clifford instructed on its use. John MacFarlane, Chris Long and Chris Swartz are thanked for coring and cruise participations and John Andrews and Mary Hartman for water column ^{234}Th sampling and analysis support. Barry Grant (MIT) provided his expertise during ICP-MS measurements, and Larry Edwards group at University of Minesota gratefully performed TIMS analysis of the same ^{238}U samples. John MacFarlane also contributed his CAD expertise for two figures. Eric Adams and Melissa Bowen are recognized for helpful discussions. This work was supported by Office of Naval Research (grant# NOOO14-93-1-0883) and National Oceanic and Atmospheric Administration (#NA36RM044-UM-S242) to PMG and KOB. The views herein are those of the authors and do not necessarily reflect the views of NOAA or any of its subagencies.

APPENDIX A

Scaling Expression for Tidal Dispersion Coefficients

Based on the conceptual framework of Ketchum (1951), holding that the maximum possible extent of horizontal mixing from tides is limited to the tidal excursion distance, Arons and Stommel (1951) formulated an expression for the tidal dispersion coefficient:

$$K_x = \alpha\, U_T\, L_T \qquad (A1)$$

where U_T is the amplitude of the tidal velocity, L_T is the tidal excursion, and α is a factor that allows for a "certain vagueness about the physical processes involved". The assumption here is that α is of similar magnitude in the physically similar tidal straits of Casco Bay and Awaji's (1982) study. The tidal excursion may be defined as:

$$L_T = \int_0^{T/2} u_t\, dt \qquad (A2)$$

where u_t is the Eulerian tidal current measurements. Substituting:

$$u_t = U_T \sin\omega t \qquad (A3)$$

where ω is the radial frequency of the tide (equal to $2\pi/T$), and integrating gives the solution:

$$L_T = \frac{2\, U_T}{\omega} \qquad (A4)$$

This result may be substituted into Eqn. A1 to yield a scaling expression of K_x as a function of U_T:

$$K_x = \frac{2\alpha}{\omega}(U_T)^2 \qquad (A5)$$

Squaring and integrating Eqn. A3 over one tidal period, yields the relationship between U_T and the root-mean-square value of Eulerian tidal current measurements (u_{rms}):

$$U_T = \sqrt{2}\, u_{rms} \qquad (A6)$$

Since we have already stated the scaling requirement of physically-similar driving mechanisms, this expression may be substituted into the simplified Eqn. A5 to give:

$$(K_x)_{Casco} = \left(\frac{K_x}{U_T^2}\right)_{Awaji} 2\,(u^2_{rms})_{Casco} \qquad (A7)$$

which allows estimation of horizontal tidal dispersion based on the detailed tidal strait mixing study of Awaji (1982) and simple surface current measurements in the region under study.

REFERENCES

Alldredge, A. L. and M. W. Silver. 1988. Characteristics, dynamics and significance of marine snow. Prog. Oceanogr., *20*, 41-82.

Arons, A. B. and H. Stommel. 1951. A mixing-length theory of tidal flushing. Trans. American Geophysical Union, *32*, 419-421.

Awaji, T. 1982. Water mixing in a tidal current and the effect of turbulence on tidal exchange through a strait. J. Phys. Oceanogr., *12*, 501-514.

Bacon, M. P. 1988. Tracers of chemical scavenging in the ocean: boundary effects and large-scale chemical fractionation. Phil. Trans. Roy. Soc. Lond., *A325*, 147-160.

Bacon, M. P. and R. F. Anderson. 1982. Distribution of thorium isotopes between dissolved and particulate forms in the deep sea. J. Geophys. Res., *87*, 2045-2056.

Baker, J. E. and S. J. Eisenreich. 1990. Concentrations and fluxes of polycyclic aromatic hydrocarbons and polychlorinated biphenyls across the air-water interface of Lake Superior. Environ. Sci. Technol., *24*, 342-352.

Baskaran, M., P. H. Santschi, G. Benoit and B. D. Honeyman. 1992. Scavenging of thorium isotopes by colloids in seawater of the Gulf of Mexico. Geochim. Cosmochim. Acta, *56*, 3375-3388.

Baskaran, M. and P. H. Santschi. 1993. The role of particles and colloids in the transport of radionuclides in coastal environments of Texas. Mar. Chem., *43*, 95-114.

Behymer, T. D. and R. A. Hites. 1988. Photolysis of polycyclic aromatic hydrocarbons adsorbed on fly ash. Environ. Sci. Technol., *22*, 1311-1319.

Bidleman, T. F. 1988. Atmospheric processes. Environ. Sci. Technol., *22*, 361-367.

Bhat, S. G., S. Krishnaswami, D. Lal, Rama and W. S. Moore. 1969. ^{234}Th/^{238}U ratios in the ocean. Earth Planet. Sci. Lett., *5*, 483-491.

Broman, D., A. Colmsjö, B. Ganning, C. Näf and Y. Zebühr. 1988. A multi-sediment-trap study on the temporal and spatial variability of polycyclic aromatic hydrocarbons and lead in an anthropogenic influenced archipelago. Environ. Sci. Technol., *22*, 1219-1228.

Broman, D., C. Näf, M. Wik and I. Renberg. 1990. The importance of spheroidal carbonaceous particles (SCPs) for the distribution of particulate polycyclic aromatic hydrocarbons (PAHs) in an estuarine-like urban coastal water area. Chemosphere, *21*, 69-77.

Broman, D., Näf, C., Rolff, C. and Y. Zebühr 1991. Occurence and dynamics of polychlorinated dibenzo-*p*-dioxins and dibenzofurans and polycyclic aromatic hydrocarbons in the mixed surface layer of remote coastal and offshore waters of the Baltic. Environ. Sci. Technol., *25*, 1850-1864.

Broman, D., Näf, C. and Y. Zebühr. 1991b. Long-term high- and low-volume air sampling of polychlorinated dibenzo-p-dioxins and dibenzofurans and polycyclic aromatic hydrocarbons along a transect from urban to remote areas on the Swedish baltic coast. Environ. Sci. Technol., *25*, 1841-1850.

Brown, L., G. J. Stensland, J. Klein and R. Middleton. 1989. Atmospheric deposition of ^{7}Be and ^{10}Be. Geochim. Cosmochim. Acta, *53*, 135-142.

Buesseler, K. O., M. P. Bacon, J. K. Cochran, H. D. Livingston. 1992a. Carbon and nitrogen export during the JGOFS North Atlantic Bloom Experiment estimated from ^{234}Th:^{238}U disequilibria. Deep-Sea Res., *39*, 1115-1137.

Buesseler, K. O., J. K. Cochran, M. P. Bacon , H. D. Livingston, S. A. Casso, D. Hirschberg, M. C. Hartman and A. P. Fleer. 1992b. Determination of thorium isotopes in seawater by non-destructive and radiochemical procedures. Deep-Sea Res., *39*, 1103-1114.

Buesseler, K. O., J. A. Andrews, M. C. Hartman, R. Belastock and F. Chai. 1995. Regional estimates of the export flux of particulate organic carbon derived from thorium-234 during the JGOFS EqPac program. Deep-Sea Res. II, *42*, 777-804.

Butler, J. D. and P. Crossley. 1981. Reactivity of polycyclic aromatic hydrocarbons adsorbed on soot particles. Atmos. Environ., *15*, 91-94.

Canuel, E. A., C. S. Martens and L. K. Benninger. 1990. Seasonal variations in ^{7}Be activity in the sediments of Cape Lookout Bight, North Carolina. Geochim. Cosmochim. Acta, *54*, 237-245.

Carroll, J. and W. S. Moore. 1994. Uranium removal during low discharge in the Ganges-Brahmaputra mixing zone. Geochim. Cosmochim. Acta, *58*, 4987-4995.

Chen, J. H., R. L Edwards and G. J. Wasserburg. 1986. ^{238}U, ^{234}U and ^{232}Th in seawater. Earth Planet. Sci. Lett., *80*, 241-251.

Coale, K. H. and K. W. Bruland. 1985. ^{234}Th:^{238}U disequilibria within the California Current. Limnol. Oceanogr., *30*, 22-33.

Coale, K. H. and K. W. Bruland. 1987. Oceanic stratified euphotic zone as elucidated by ^{234}Th:^{238}U disequilibria. Limnol. Oceanogr., *32*, 189-200.

Cotham, W. E. and T. F. Bidleman. 1995. Polycyclic aromatic hydrocarbons and polychlorinated biphenyls in air at an urban and a rural site near Lake Michigan. Environ. Sci. Technol., *29*, 278-2789.

Dibb, J. E. 1989. Atmospheric Deposition of Beryllium 7 in the Chesapeake Bay region. J. Geophys. Res., *94*, 2261-2265.

Dickhut, R. M. and K. E. Gustafson. 1995. Atmospheric washout of polycyclic aromatic hydrocarbons in the southern Chesapeake Bay region. Environ. Sci. Technol., *29*, 1518-1525.

Eisenreich, S. J., B. B. Looney and J. D. Thornton. 1981. Airborne organic contaminants in the Great Lakes ecosystems. Environ. Sci. Technol., *15*, 30-38.

Environmental Protection Agency. 1988. 1988 Needs Survey Report to Congress: Assessment of Needed Publicly Owned Wastewater Treatment Facilities in the United States (EPA 430/09-89-001). EPA-Office of Water, Washington, D.C.

Farley, K. J. and F M. M. Morel. 1986. Role of coagulation in the kinetics of sedimentation. Environ. Sci. Technol., *20*, 187-195.

Fischer, H. B., E. J List, R. C. Y. Kho, J. Imberger and N. H. Brooks. 1979. Mixing in Inland and Coastal Waters, Academic Press, New York, 483 pp.

Fowler, S. W. and G. A. Knauer. 1986. Role of large particles in the transport of elements and organic compounds through the oceanic water column. Prog. Oceanogr., *16*, 147-194.

Geyer, W. R. and R. P. Signell. 1992. A reassessment of the role of tidal dispersion in estuaries and bays. Estuaries, *15*, 97-108.

Graustein, W. C. and K. K. Turekian. 1989. The effects of forests and topography on the deposition of sub-micrometer aerosols measured by lead-210 and cesium-137 in soils. Agric.and Forest Meteorol., *47*, 199-220.

Greenamoyer, J. M. and S. B. Moran. 1996. Evaluation of a spiral wound cross-flow filtration system for size-fractionation of Cu, Ni and Cd in seawater. Mar. Chem. accepted.

Gschwend, P. M. and R. A. Hites. Fluxes of polycyclic aromatic hydrocarbons to marine and lacustrine sediments in the northeastern United States. Geochim. Cosmochim. Acta, *45*, 2359-2367.

Gustafsson, Ö., P. M. Gschwend and K. O. Buesseler. 1996a. Fluxes of PAHs through the upper ocean derived from coupling with ^{238}U-^{234}Th disequilibria. submitted.

Gustafsson, Ö., F. Haghseta, C. Chan, J. MacFarlane and P. M. Gschwend. 1996b. Quantification of the dilute sedimentary "soot-phase": Implications for PAH speciation and bioavailability. accepted.

Hites, R. A., R. E. LaFlamme and J. G. Windsor Jr. 1980. Polcyclic aromatic hydrocarbons in the marine environment. *in* Hydrocarbons and Halogenated Hydrocarbons in the Aquatic Environment. B. K. Afghan and D. Mackay, eds., Plenum, 397-403.

Huh, C.-A. and T. M. Beasley. 1987. Profiles of dissolved and particulate thorium isotopes in the water column of coastal Southern California. Earth Planet. Sci. Lett., *85*, 1-10.

Huh, C.-A. and F. G. Prahl. 1995. Role of colloids in upper ocean biogeochemistry in the northeast Pacific Ocean elucidated from ^{238}U-^{234}Th disequilibria. Limnol. Oceanogr., *40*, 528-532.

Hussain, N., T. Church, R. Anderson and P. Biscaye. 1990. Radon daughters (^{210}Pb and ^{210}Po): Atmospheric fallout and oceanic removal in coastal waters of the mid-Atlantic (abstract). EOS Transactions, American Geophysical Union, *71(17)*, 537.

Jannasch, H. W., B. D. Honeyman, L. S. Ballistrieri and J. W. Murray. 1988. Kinetics of trace element uptake by marine particles. Geochim. Cosmochim. Acta, *52*, 567-577.

Karickhoff, S. W. 1981. Semi-empirical estimation of sorption of hydrophobic pollutants to sediments and soils. Chemosphere, *10*, 833-846.

Kennicutt II, M. C., T. L. Wade, B. J. Presley, A. G. Requejo, J. M. Brooks and G J Denoux. 1994. Sediment contaminants in Casco Bay, Maine: Inventories, sources, and potential for biological impact. Environ. Sci. Technol., *28*, 1-15.

Ketchum, B. 1951. The Dispersion and Fate of Pollution Discharged into Tidal Waters, and the Viability of Enteric Bacteria in the Area. WHOI Ref. No. 51-11, Woods Hole Oceanographic Institution, Woods Hole, MA, 16 pp.

Kossick, R. F.. 1986. Tracing and Modeling Pollutant Transport in Boston Harbor. M.S. Thesis, Masachusetts Institute of Technology, Cambridge, MA. 227 pp.

Krishnaswami, S., L. K. Benninger, R. C. Aller and K. L. Von Damm. 1980. Atmospherically-derived radionuclides as tracers of sediment mixing and accumulation in near-shore marine and lake sediments: Evidence from ^{7}Be, ^{210}Pb, ^{239,240}Pu. Earth Plan. Sci. Lett., *47*, 307-318.

Lal, D. and B. Peters. 1967. Cosmic-ray-produced radioactivity on the earth. Handbuch Phys., *46*, 551-612.

Lipiatou, E. and A. Saliot. 1991. Fluxes and transport of anthropogenic and natural polycyclic aromatic hydrocarbons in the western Mediterranean Sea. Mar. Chem., *32*, 51-71.

Maeda, M. and H. L. Windom. 1982. Behavior of uranium in two estuaries of the southeastern United States. Mar. Chem., *11*, 427-436.

Massachusetts Water Resources Authority. 1993. Contaminated Sedimetns in Boston Harbor, Boston. U.S. Environmental Protection Agency Region I.

McGroddy, S. E. and J. W. Farrington. 1995. Sediment porewater partitioning of polycyclic aromatic hydrocarbons in three cores from Boston Harbor, Massachussets. Environ. Sci. Technol., *29*, 1542-1550.

McGroddy, S. E., J. W. Farrington and P. M. Gschwend. 1996. Comparison of the *in situ* and desorption sediment-water partitioning of polycyclic aromatic hydrocarbons and polychlorinated biphenyls. Environ. Sci. Technol., *30*, 171-177.

McKee, B. A., D. J. DeMaster and C. A. Nittrouer. 1984. The use of ^{234}Th/^{238}U disequilibrium to examine the fate of particle-reactive species on the Yangtze continental shelf. Earth Planet. Sci. Lett., *68*, 431-442.

McKee, B. A., D. J. DeMaster and C. A. Nittrouer. 1986. Temporal variability in the partitioning of thorium between dissolved and particulate phases on the Amazon shelf: Implications for the scavenging of particle-reactive species. Cont. Shelf Res., *6*, 87-106.

McKee, B. A., D. J. DeMaster and C. A. Nittrouer. 1987. Uranium geochemistry of the Amazon shelf: Evidence for uranium release from bottom sediments. Geochim. Cosmochim. Acta, *51*, 2779-2786.

Means, J. C., S. G. Wood, J. J. Hassett and W. L. Banwart. 1980. Sorption of polynuclear aromatic hydrocarbons by sediments and soils. Environ. Sci. Technol., *14*, 1524-1528.

Means, J. C. 1995. Influence of salinity upon sediment-water partitioning of aromatic hydrocarbons. Mar. Chem., *51*, 3-16.

Minagawa, M. and S. Tsunogai. 1980. Removal of ^{234}Th from a coastal sea: Funka Bay, Japan. Earth Planet. Sci. Lett., *47*, 51-64.

Moran, S. B. and K. O. Buesseler. 1992. Short residence time of colloids in the upper ocean estimated from ^{238}U- ^{234}Th disequilibria. Nature, *359*, 221-223.

Moran, S. B. and K. O. Buesseler. 1993. Size-fractionated ^{234}Th in continental shelf waters off New England: Implications for the role of colloids in oceanic trace metal scavenging. J. Mar. Res., *51*, 893-922.

Näf, C., D. Broman, H. Pettersen, C. Roff and Y. Zebühr. 1992. Flux estimates and pattern recognition of particulate polycyclic aromatic hydrocarbons, polychlorinated dibenzo-*p*-dioxins, and dibenzofurans in the waters outside various emission sources on the Swedish Baltic Coast. Environ. Sci. Technol., *26*, 1444-1457.

Niven, S. E. H., P. E. Kepkay and A. Boraie. 1995. Colloidal organic carbon and colloidal ^{234}Th dynamics during a coastal phytoplankton bloom. Deep-Sea Res. II, *42*, 257-273.

Nyffeler, U. P., Y.-H. Li and P. H. Santschi. 1984. A kinetic approach to describe trace-element distribution between particles and solution in natural aquatic systems. Geochim. Cosmochim. Acta, *48*, 1513-1522.

Okubo, A. 1971. Oceanic diffusion diagrams. Deep-Sea Res., *18*, 789-802.

Olsen, C. R., I. L. Larsen, P. D. Lowry, N. H. cutshall, J. F Todd, G. T. F Wong and W. H. Casey. 1985. Atmospheric fluxes and marsh-soil inventories of ^{7}Be and ^{210}Pb. J. Geophys. Res., *90*, 10,487-10,495.

Parker, C. E. 1982. The Currents of Casco Bay and the Prediction of Oil Spill Trajectories, Bigelow Laboratory Tech. Rep. 28., West Boothbay Harbor, 36 pp.

Poster, D. L. and J. E. Baker 1996. Influence of submicron particles on hydrophobic organic contaminants in precipitation. 1. Concentrations and distributions of polycyclic aromatic hydrocarbons and polychlorinated biphenyls in rainwater. Environ. Sci. Technol., *30*, 341-348.

Readman, J. W., R. F. C. Mantoura and M. M. Rhead. A record of polycyclic aromatic hydrocarbon (PAH) pollution obtained from accreting sediments of the Tamar Estuary, U.K.: Evidence for non-equilibrium behavior of PAH. Sci. Tot. Env., *66*, 73-94.

Santschi, P H., Y.-H. Li and J. Bell. 1979. Natural radionuclides in the water of Narragansett Bay. Earth Planet. Sci. Lett., *45*, 201-213.

Santschi, P H., D. Adler, M. Amdurer, Y.-H. Li and J. Bell. 1980. Thorium isotopes as analogues for "particle-reactive" pollutants in coastal marine environments. Earth Planet. Sci. Lett., *47*, 327-335.

Schuler, C., E, Wieland, P. H. Santschi, M. Sturm, A. Lueck, S. Bollhalder, J. Beer, G. Bonani, H. J. Hofmann, M. Suter and W. Wolfi. 1991. A multitracer study of radionuclides in Lake Zurich, Switzerland 1. Comparison of atmospheric and sedimentary fluxes of ^{7}Be, ^{10}Be, ^{210}Pb, ^{210}Po and ^{137}Cs. J. Geophys. Res., *96*, 17051-17065.

Schulz-Bull, D. E., G. Petrick, and J. C. Duinker. 1991. Polychlorinated biphenyls in North Sea water. Mar. Chem., *36*, 365-384.

Schwarzenbach, R. P., P. M. Gschwend and D. M. Imboden. 1993. Environmental Organic Chemistry, Wiley, New York, 681 pp.

Signell, R. P. and W. R. Geyer. 1990. Numerical simulation of tidal dispersion around a coastal headland, *in* Residual Currents and Long-term Transport in Estuaries and Bays. Lecture Notes on Coastal and Estuarine Studies, No. 38, R. T. Chung, ed., Springer-Verlag, 210-222.

Sporstøl, S., N. Gjøs, G. Lichtenthaler, K. O. Gustavsen, K. Urdal, F. Oreld and J. Skei. Source identification of aromatic hydrocarbons in sediments using GC/MS. Environ. Sci. Technol, *17*, 282-286.

Stolzenbach, K. D. 1993. Scavenging of small particles by fast-sinking porous aggregates. Deep-Sea Res. I., *40*, 359-369.

Tanabe, S. and R. Tatsukawa. 1983. Vertical transport and residence time of chlorinated hydrocarbons in the open ocean water column. J. Oceanogr. Soc. Japan, *39*, 53-62.

Tanaka, N., Y. Takeda and S. Tsunogai. 1983. Biological effect on removal of Th-234, Po-210 and Pb-210 from surface water in Funka Bay, Japan. Geochim. Cosmochim. Acta, *47*, 1783-1790.

Turekian, K. K., L. K. Benninger and E. P. Dion. 1983. ^{7}Be and ^{210}Pb total deposition fluxes at New Haven, Connecticut and at Bermuda. J. Geophys. Res., *88*, 5411-5415.

Turner, D. R., M. Whitfield and A. G. Dickson. 1981. The equilibrium speciation of dissolved components n freshwater and seawater at 25°C and 1 atm pressure. Geochim. Cosmochim. Acta, *45*, 855-881.

Venkataraman, C., J. M. Lyons and S. K. Friedlander. 1994. Size distributions of polycyclic aromatic hydrocarbons and elemental carbon 1. Sampling, measurement methods, and source characterization. Environ. Sci. Technol., *28*, 555-562.

Wei, C.-L. and J. W. Murray. 1992. Temporal variations of ^{234}Th activity in the water column of Dabob Bay: Particle scavenging. Limnol. Oceanogr., *37*, 296-314.

Zimmerman, J. T. F. 1986. The tidal whirlpool: A review of horizontal dispersion by tidal and residual currents. Nether. J. Sea Res., *20*, 133-154.

Chapter 9

Thesis Distillation and a Look to the Future

General Conclusions

The physico-chemical speciation of organic pollutants (or contaminants; terms used interchangeably throughout this thesis) largely governs their fate and effects. To develop a general understanding of the phase-distribution of PAHs in natural waters, this thesis has assessed PAH partitioning both with pyrogenic carbon phases (soot) and with seawater colloids. The speciation-dependent transport of PAHs was approached along offshoreward transects through coupling the particulate PAH inventories with information of particle export rates deduced from surface ocean ^{238}U-^{234}Th disequilibria. Comprehending the processes that govern the molecular and macroscopic distribution of individual compounds will ultimately enable prediction of exposure fields for directly bioavailable forms of xenobiotic chemicals in terms of the physico-chemical properties of the molecules and the environmental systems of concern.

Integrity studies of the ability of a spiral-wound cross-flow filtration system with polysulfone membranes to collect marine organic colloids for organic chemical speciation studies raised serious concerns for this technique as a viable option. Realistic levels of individual macromolecules added to seawater were seen to be affected by compound-class specific interactions with the large volume of polysulfone ultrafiltration membrane present in commercially-available instruments employed throughout the marine research community. An equation suitable for *a priori* prediction of concentration polarization in the CFF was forwarded along with solubility parameter arguments of the sorbent tendency of different membrane materials to assist in optimization of design and operation of these systems in dilute colloidal suspensions such as seawater.

The ability of macromolecular seawater colloids to sorb PAHs was instead assessed using a less invasive, time-resolved, fluorescence quenching technique. The kinetics of PAH sorption to dispersed colloids in filtered coastal seawater was rapid. Equilbrium colloid-water distribution of a highly fluorescent methylperylene probe was attained in about one minute. The organic-carbon normalized partition coefficient was a factor of five to ten lower than predicted from the aqueous activity coefficient and literature-based predictions from studies of sorption with sediments, soils, and porewater colloids. This translated into the prediction of just 3% of pyrene and 20% of benzo[a]pyrene in the GF/F filtrate of Inner Casco Bay seawater being associated with colloids. The low sorption efficiency of colloidal organic matter present in surface seawater must be related to its composition and structure and hence ability to intermolecularly accomodate PAHs. Freshly biosynthesized organic matter in the surface ocean is rich in carbohydrates relative to its sedimentary counterpart (Benner *et al*, 1992). Extended tertiary configuration of relatively polar carbohydrate macromolecules may not provide an interior phase for HOC partitioning as succinctly illustrated by the very poor ability of cellulose to sorb low molecular weight chlorinated compounds (Garbarini and Lion, 1986). Also, seawater humics are known to be less aromatic than freshwater counterparts and may thus be anticipated to exhibit a correspondingly lower sorbent efficiency.

Elevated *in situ* solid-water distribution coefficients of PAHs, not explainable by existing hydrophobic partition models, have been suggested to be a result of PAH association with the inferred presence of soot (e.g., McGroddy and Farrington, 1995). The development of a method to quantify the dilute fraction of the total sedimentary carbon that is of pyrogenic origin allowed evaluation of this hypothesis. The concentrations of individual PAHs in seven surface sediments from the New England continental shelf were highly correlated with soot carbon ($r^2 = 0.97$-0.99) while they were not correlated with organic carbon at the 95% confidence level. Estimates of the soot-water partition coefficient for several PAHs, assuming sorbate-soot association is thermodynamically similar to sorbate fusion, were found to agree reasonably well with the published aqueous sorption constants to activated carbon. These soot-water partition constants were combined with measures of the soot content in two sediment-porewater systems where elevated *n situ* K_d's have previously been reported (McGroddy and Farrington, 1995). The elevated PAH K_d's observed at these sites can now be explained in terms of partitioning with soot. Based on these studies it may be concluded that a significant portion of the total PAH concentration is partitioning between soot and the surrounding water. On an organic-carbon basis, the highly condensed soot matrix may be a factor of 100 better sorbent than natural organic matter. The presence of approximately 10% of the total organic carbon as soot carbon in coastal and shelf sediments results in the marine PAH speciation being dominated by the soot-associated species. This thesis concludes that partitioning with seawater colloids only has a minor effect on the directly bioavailable, truly dissolved, PAH concentrations, wheras partitioning with soot attenuates the exposed levels typically by an order of magnitude or more. Neither partitioning with seawater colloids nor with soot particles may be predicted from organic-carbon based regressions available in litterature (e.g., Karickhoff, 1981).

^{234}Th-derived surface ocean fluxes of PAHs were demonstrated along a transect from nearshore to the open ocean. While reasonable agreement with fluxes into sediment traps and underlying sediments was obtained, the strength of ^{234}Th-derived upper-ocean PAH export estimates is that they are based on direct measurements of mixed layer properties. A biexponential decrease in fluxes away from northeastern USA, and source-diagnostic molecular ratios, indicate that atmosperic fallout of PAHs associated with fine and coarse soot particles is the dominant source. The characteristic length scales of PAH deposition appears to be on the order of 7 km (coarse mode soot) and 400 km (fine mode soot). While much higher fluxes were estimated nearshore, the open ocean represents a larger integral sink for PAHs. Of the 60 metric-ton of pyrene that we estimate to annually become sequestered in the western North Atlantic, < 10% is deposited in urban and coastal waters. The Western North Atlantic Ocean sink of pyrene corresponds to about 20% of all pyrene estimated to be released into the atmosphere annually from the northeastern USA (50% if consider only coastal states) (Simonich and Hites, 1994).

Finally, the process-insight developed regarding speciation (colloid and soot sorption) and vertical transport (^{234}Th-coupled flux estimates) were combined with estimates of horizontal dispersion and local source functions for PAHs to develop a two-dimensional box model for pyrene and benzo[a]pyrene in Portland Harbor - Casco Bay. The model results suggested that less than half of the pyrene and benzo[a]pyrene introduced to Portland Harbor may be settling locally, with export to the offshore being as important.

Future Work

Each portion of this work leads to myriad paths for further inquiry. In an effort to leave the trails open, I will only highlight a few of the most pressing and intriguing ideas for future investigations. Most of these ideas are not unique to, or have even originated from, this researcher and all have been generated or further developed through fruitful interactions with advisors and colleagues at MIT and WHOI as well as beyond.

We are still not able to firmly predict the phase speciation of PAHs (or any other hydrophobic compounds) in the marine environment. In this regard, the importance of the soot phase, which has been explicitly demonstrated through this thesis, requires further investigation. The soot-water equilibrium partition constant should be determined under well-controlled and relevant conditions. More measurement of particulate soot and particulate and dissolved PAHs in the field, particularly in the water column, is required to further verify the soot-partitioning concept.

Of importance to all speciation studies is the ability to obtain the truly dissolved concentration of individual compounds. Scaled up versions of reverse-phase extraction columns (e.g., Landrum *et al.*, 1984), designed to have column capacities in excess of 1000 L seawater and with column residence times of only several seconds are required to collect enough material for non-contaminated analysis and to ensure that colloid desorption in the column is not taking place. An alternative technique is time-averaging deployment of semipermeable membrane devices (e.g., Lebo *et al.*, 1995), containing a lipohilic phase that the dissolved components may diffuse into to establish equilibria. *A priori* knowledge of the membrane-water partition constants would then allow estimation of the truly dissolved concentrations.

Time-resolved fluorescence quenching techniques provide an entire new window of analytical opportunities for marine environmental chemistry. In addition to multiple possibilities to obtain colloid-water partition coefficients (quenching of steady state intensity, changes in fluorescence lifetimes and polarization moments, relative shifts in emission maxima and magnitudes), this technique offers the opportunity for kinetic studies of sorption and photochemical reactions. A PAH in an nonpolar micoenvironment "inside" a humic acid is likely to be exposed to, and to absorb, different wavelengths than a water-solubilized molecule. Furthermore, a colloid-sorbed PAH is likely to be surrounded by a different set of potential reactants (e.g., $^1O_2$, $^3DOM^*$, ROO·, HO·). Given the high electron density of its structure, it seems probable that colloid-mediated PAHs undergo different photochemical reactions, and/or with different rates than their truly dissolved counterparts. Similarly, photochemical reactions of PAHs adsorbed to the surface of soot may be an important sink. In fact, evaluation of the relative abundance of several isomer-pairs of very similar hydrophobicities as a function of offshore distance indicated preferential removal of the most photolytically active isomers with increasing exposure times (offshore distance).

The mass balance of contaminants in harbors is an issue of great societal relevance. It seems important that further studies follow up on the two-dimensional contaminant exchange model derived for Portland Harbor - Outer Casco Bay. For example, it should be possible to elucidate how large a fraction of a chemical with a given solid-solution distribution constant is deposited in Boston Harbor as opposed to being exported to Massachusetts Bay and beyond.

There is currently a large interest in developing global mass balances of persistent organic pollutants (e.g., Simonich and Hites, 1994, 1995; Wania and Mackay, 1996). Since many such compounds are hydrophobic and since the ocean covers 70% of the earth's surface, it may be anticipated that particle-mediated export into the deep ocean is a significant sink. The analytical ability to perform "trace-organic-clean" sampling and quantification of such individual components now appears feasible (e.g., Petrick *et al.*, 1996). Coupling such information with high-throughput techniques for ^{234}Th measurements (e.g., Buesseler *et al.*, 1992) should afford an estimate of the ocean sink.

References

Benner, R., Pakulski, D.J., McCarthy, M., Hedges, J.I. and Hatcher, P.G., 1992. Science, 255: 1561-1564.

Buesseler, K. O., J. K. Cochran, M. P. Bacon, H. D. Livingston, S. A. Casso, D. Hirschberg, M. C. Hartman and A. P. Fleer. 1992. Deep-Sea Res., 39, 1103-1114.

Garbarini, D. R., and L. W. Lion. 1986. Environ. Sci. Technol. 20: 1263-1269.

Karickhoff, S. W. 1981. Chemosphere, 10, 833-841.

Lebo, J. A., R. W. Gale, J. D. Pitts, D. E. Tillit, J. N. Huckins, J. C. Meadows, C. E. Orazio, K. R. Echols, D. J. Schroeder, and C. E. Inmon. 1995. Environ. Sci. Technol., 29, 2886-2892.

McGroddy, S. E. and J. W. Farrington, 1995. Environ. Sci. Technol., 29, 1542-1550.

Petrick, G., D. E. Schulz-Bull, V. Martens, K. Scholz, and J. C. Duinker. 1996. Mar. Chem., 54, 97-105.

Simonich, S. L. and R. A. Hites. 1994. Nature, 370, 49-51.

Simonich, S. L. and R. A. Hites. 1995. Science, 269, 1851-1854.

Wania, F.and D. Mackay. 1996. Environ. Sci. Technol., 30, 390A-396A.